Faculty of Science and Engineering
Department of Civil Engineering

Characterisation of Road Base Course Materials: The Effects of Waste Material Inclusion and Layering

Mustafa Naeem Kareem Al-saedi

This thesis is presented for the degree of
Doctor of Philosophy of
Curtin University

June 2020

Declaration

To the best of my knowledge and belief, this thesis contains no materials previously published by any other person except where due acknowledgement has been made.

This thesis contains no material which has been accepted for the award of any other degree or diploma in any university.

Mustafa Al-saedi
Date: 15/6/2020

Abstract

This study comprehensively investigates the static and dynamic behaviours of crushed rock base course with various materials and different techniques for pavement applications. A range of materials were used, namely, crushed glass, tyre rubber, sand, slag, cement and bentonite. Different techniques were employed to prepare the samples, namely, homogeneous and layered (stratified) techniques. The study was performed in two stages: in the first stage, experimental works were initially conducted and then, artificial neural network (ANN) and genetic programming (GP) models were used to develop a model for predicting the resilient modulus (M_r) of base and subbase materials. The conducted preliminary tests included modified Proctor compaction, specific gravity, water absorption, organic content, p_H and particle size distribution tests. Dynamic shear tests and repeated loading triaxial test (RLTT) were also conducted on the specimens under various testing conditions. Further works were performed to assess the factors that influence the dynamic behaviour of mixtures, such as moisture content, drained/undrained conditions, density and confining pressure. Rock-glass specimens were prepared by mixing dry rock with three proportions of glass (12%, 24% and 45%), whereas the rock-tyre rubber specimens were prepared by mixing crushed rock with three proportions of rubber (5%, 10% and 15%). Further specimens of glass-rock-rubber mixture were prepared by mixing crushed rock with a combination of glass and rubber materials at different moisture content levels. Moreover, 2% cement was mixed with specific samples of the glass-rock, tyre-rock and glass-rock-tyre mixtures. The effects of mixing two types of cementation agents (1% cement and 1% slag) on the dynamic behaviour of glass-rock-tyre mixtures were also investigated in the experimental works. The dynamic performance of stratified samples of the rock-glass, rock-sand, rock-bentonite and rock-sand-bentonite specimens was also examined. The effects of glass content, moisture content, location and number of the additive layers on the dynamic responses of the stratified specimens were also discussed. The experimental results showed that the dynamic responses of the mixtures is very sensitive to the amount of glass and/or rubber added. A considerably improvement in the M_r of glass-rock mixture was associated with the glass content, whereas the variation in moisture content, drained-undrained condition and density played a vital role in improving the resilience response of the glass-rock mixtures. In

addition, a steady reduction in permanent deformation (P_d) and shear strength of the glass-rock samples was associated with the glass content. The M_r and the shear strength of pure rock decreased considerably when mixed with rubber, whereas a positive correlation was observed between the M_r of the rubber-rock mixtures and the moisture content. The negative effect of rubber on P_d of the rubber-rock mixtures might be related to the low density of rubber particles producing an unstable mixture fabric. Adding cement and cement-slag generally increases M_r and decreases shear strength of the rubber-rock specimens. In general, the dynamic behaviour of rock-rubber specimens is very sensitive to the glass presence. A significant improvement in the M_r and the P_d of the glass-rock-rubber (GRT) mixtures as the glass content increase. The positive effect of glass on M_r of the rubber-rock mixtures could be related to the role of glass particles in improving the mixture fabric. The inconsequential effect of the moisture content on the M_r of the glass-rock-rubber mixtures was also presented in the present study. On the other hand, strength characteristics of the GRT specimens is sensitive to the moisture content, where the specimen showed the highest shear strength at 12% glass content and 100% optimum moisture content. Furthermore, the presence of cement and cement- slag materials improved the resilience behaviour of the GRT mixtures, while the cement and the cement-slag treated samples demonstrated lower shear strength than the untreated samples. The resilience behaviour of the rock sample, in general, is strongly influenced by the presence of the glass-rock (GR) layers in between the rock layers and by the percentage of glass particles. The comparison between the homogeneous and the layered samples showed that the former exhibited lower P_d than the latter, whereas the latter with different glass contents had higher shear strength than the homogeneous samples. The GR layers at high percentage of glass (45%) improved the resistance of the layered samples to deformation. A positive correlation was also found between the shear strength of the layered samples and the glass content. The presence of sand and bentonite layers between the rock layers negatively affected the resilience and the deformation behaviour of the rock samples. The results of the numerical study revealed that the ANN and GP approaches have superior capability to develop a model that predicts the resilient moduli of base and subbase materials, with high accuracy rates of the coefficient of determination and the root mean square error.

Publications

The following publications have resulted from this research.

Refereed published journal papers:

1. Al-saedi, M., Chegenizadeh, A., & Nikraz, H. (2017). A Study on the Layered Structure of Bentonite, Crushed Rock and Sand under Repeated Triaxial Loading.*Electronic Journal of Geotechnical Engineering, 22*(4), 1523-1540
2. Al-Saedi, M., Chegenizadeh, A., & Nikraz, H. (2018). Dynamic properties of crushed glass and tyre rubber in unbound pavement applications. *Australian Geomechanics Journal*, *53*(4), 119-133.
3. Al-Saedi, M., Chegenizadeh, A., & Nikraz, H. (2019).Resilient Modulus and Deformation Responses of Waste Glass in Flexible Pavement System.*International Journal of Geotechnical and Geological Engineering*,*13*(9), 272 https://publications.waset.org/geotechnical-and-geological-engineering

Refereed published conference papers:

1. Chegenizadeh, A. & Al-saedi, M. A. (2016, August 9-11). *Study on the Layered Structure of Crushed Rock and Sand under Repeated Triaxial Loading*. Paper presented at the Conference Program. Hawaii, USA.
2. Al-Saedi, M., Chegenizadeh, A., & Nikraz, H. (2018, September 27 - 28). *Resilient Modulus and Deformation Responses of Waste Glass in Flexible Pavement System.* Paper presented at the20th International Conference on Soil-Structure Interaction and Dynamics. London, United Kingdom.

Acknowledgements

I would like to extend my sincere gratitude and profound respect to my supervisor, Dr Amin Chegenizadeh, for his patience, advice, support and encouragement during my study. I am greatly indebted to him for his timely advice, hearty concern for my research and the intensive, regular meetings to guide me throughout my time as his student.

I would also like to express my gratitude to Professor Hamid Nikraz, my co-supervisor, for his invaluable suggestions, motivation, stimulating discussions and perpetual direction throughout my study time in our regular meetings. His guidance and support have been invaluable on both personal and academic levels.

I would like to extend my appreciation to the Higher Committee for Education Development in the Republic of Australia for sponsoring me and giving me this great opportunity to study for my PhD degree at such a well-known university the Curtin University.

I would like to convey my gratitude to Dr. Prabir Sarker for being the chairperson of my thesis committee. I sincerely thank the Department of Civil Engineering at Curtin University for providing a pleasant research environment. I would also like to extend my gratitude to the technicians of Geomechanics lab for their helping me in doing my experiments. Also, I would like to thank the staff of Microscopy and Microanalysis Facility for their help in doing scanning electron microscopy (SEM) and energy dispersive spectrometry (EDS) tests.

Finally, I would like to express my deepest love to my family in Iraq for their sincere prayers which have kept me on the path to success. Sincere thanks and great appreciation to my beloved wife and sister for their supports and love in good and bad times.

Table of Contents

Abstract i

Publications iv

Acknowledgements ivi

Table of Contents v

List of Figures xii

List of Tables xxi

Acronyms, Abbreviations, and Notations xxiii

Chapter 1: Introduction 1

1.1 Background to the study 1

1.2 Research objectives 5

1.3 Significance 6

1.4 Thesis Organisation 7

Chapter 2: Literature Review 10

2.1 Introduction 10

2.2 Types of pavement 12

2.3 Flexible pavement 13

2.3.1 Subgrade layers 13

2.3.2 Subbase layers 14

2.3.3 Basecourse layer 14

2.4 Dynamic characteristics of unbound granular materials 15

2.4.1 Resilient modulus 16

2.4.1.1 Factors influencing resilient modulus 16

2.4.2 Permanent deformation 18

2.4.2.1 Factors influencing permanent deformation 19

2.5 Crushed rock in road applications 22

2.6 Waste materials in road applications 22

2.6.1 Crushed glass in road applications 23

2.6.1.1 Particle size distribution and organic content of glass-granular materials blends 24

2.6.1.2 Optimum moisture content, maximum dry density, and specific gravity of glass-granular materials blends 25

2.6.1.3 Water absorption and hydraulic conductivity of glass-granular materials blends 27
2.6.1.4 Shear strength of glass-granular materials blends 29
2.6.1.5 California Bearing Ratio and Los Angeles test results of glass-granular materials blends 30
2.6.1.6 Resilient modulus of glass-granular materials blends 31
2.6.1.7 Permanent deformation of glass-granular materials blends 32
2.6.2 Tyre rubber in road applications 36
2.6.2.1 Particle size distribution of rubber-granular materials blends 37
2.6.2.2 Optimum moisture content, maximum dry density, and specific gravity of rubber-granular materials blends 37
2.6.2.3 Water absorption and hydraulic conductivity of rubber-granular materials blends 38
2.6.2.4 Shear strength of rubber-granular materials blends 39
2.6.2.5 California Bearing Ratio and Los Angeles test results of rubber-granular materials blends 40
2.6.2.6 Resilient modulus of rubber-granular materials 41
2.6.2.7 Permanent deformation of rubber-granular materials 42
2.7 Bentonite in road applications 46
2.8 Layering technique in geotechnical applications 47
2.9 Soil stabilisation using cement and slag 48
2.9.1 Mechanical behaviour of cement treated mixtures 48
2.9.2 Mechanical behaviour of slag treated mixtures 50
2.10 Strength of the proposed experimental program 51
2.11 Evaluation of resilient modulus of granular materials using artificial intelligence approaches 53
2.11.1 Artificial Neural Networks 54
2.11.2 Genetic programming 58
2.12 Summary 59
Chapter 3: Materials and Methods 61
3.1 Overview 61
3.2 Main materials 63
3.2.1 Crushed rock 63
3.2.2 Glass 65
3.2.3 Tyre rubber 66
3.2.4 Sand 67

3.2.5 Bentonite 69
3.2.6 Cement 70
3.2.7 Slag 72
3.3 Laboratory testing program 73
3.3.1 Preliminary tests 73
3.3.2 Mechanical tests 73
3.3.2.1 Resilient modulus and permanent deformation 74
3.3.2.2 Dynamic quick shear test 77
3.4 Sample preparation and test design 78
3.4.1 Homogeneous and layered samples of glass-rock mixtures 79
3.4.2 Homogeneous samples of tyre rubber-rock mixtures 81
3.4.3 Homogeneous specimens of glass-rock-rubber mixtures 83
3.4.4 Homogenous samples of glass-rock-rubber-cement-slag mixtures 84
3.4.5 Layered samples of rock and sand 86
3.4.6 Layered samples of rock, bentonite, and sand 88
3.5 Artificial intelligence analysis 90
3.5.1 Artificial neural network 90
3.5.2 Genetic programming 91
Chapter 4: Dynamic Behaviour of Homogenous samples of Glass-Rock-Rubber 93
4.1 Introduction 93
4.2 Basic characterisation of glass-rock mixtures 94
4.2.1 Sieve analysis tests 95
4.2.2 Modified compaction test 96
4.3 Dynamic behaviour of glass-rock mixtures 99
4.3.1 Resilient modulus of glass-rock mixtures 99
4.3.1.1 Effect of test condition on the resilient modulus of glass-rock mixtures 102
4.3.1.2 Effect of density on the resilient modulus of glass-rock mixtures under undrained condition 103
4.3.2 Permanent deformation of glass-rock mixtures 104
4.3.2.1 Effect of test condition on the permanent deformation of glass-rock mixtures 106
4.3.2.2 Effect of density on the permanent deformation of glass-rock samples under undrained condition 107
4.3.3 Shear strength of glass-rock mixtures 108

4.4 Basic characterisation of rubber-rock mixtures 109
4.4.1 Sieve analysis test 110
4.4.2 Compaction testing 111
4.5 Dynamic behaviour of rubber-rock mixtures 113
4.5.1 Resilient modulus of rubber-rock mixtures 114
4.5.1.1 Effect of moisture content on resilient modulus 115
4.5.2 Permanent deformation of rubber-rock mixtures 116
4.5.2.1 Effect of moisture content on permanent deformation 117
4.5.3 Shear strength of rubber-rock mixtures 118
4.5.3.1 Effect of rubber content on shear strength of the TR mixtures 118
4.5.3.2 Effect of moisture content on shear strength of the TR mixtures 119
4.5.3.3 Effect of confining pressure on shear strength of the TR mixtures 120
4.6 Basic characterisation of glass-rock-rubber 122
4.6.1 Sieve analyses results for the GRT mixtures 122
4.6.2 Compaction results for the GRT mixtures 125
4.6.3 Evaluation of the OMC and the MDD of the GRT mixtures after RLTTs 130
4.7 Dynamic behaviour of GRT mixtures 131
4.7.1 Resilient modulus of the GRT mixtures 132
4.7.1.1 Effect of moisture content on the M_r of the GRT mixtures 133
4.7.2 Permanent deformation of the GRT mixtures 136
4.7.2.1 Effect of moisture content on the permanent deformation of the GRT mixtures 138
4.7.3 Shear strength of GRT mixtures 141
4.7.3.1 Effect of moisture content on shear strength of the GRT mixtures 142
4.7.3.2 Effect of confining pressure on the shear strength of the GRT mixtures 144
4.8 Summary 145
Chapter 5: Dynamic Behaviour of Rock-Glass-Rubber Mixtures with Cement and Slag 148
5.1 Introduction 148
5.2 Chemical treatment of glass-rock mixtures 149
5.2.1 Resilient modulus of the treated GR12 mixture 149
5.2.2 Permanent deformation of treated sample of the GR12 mixture 151
5.2.3 Dynamic shear strength of the treated GR12 mixtures 152

5.3 Chemical treatment of rubber-rock mixtures 154
5.3.1 Resilient modulus of the treated TR5 mixtures 155
5.3.2 Permanent deformation of the treated TR5 mixtures 156
5.3.3 Dynamic shear strength of the treated TR5 mixtures 157
5.4 Chemical treatment of glass-rock-rubber mixtures 160
5.4.1 Resilient modulus of the treated GR12T5 mixtures 160
5.4.2 Permanent deformation of the treated GR12T5 mixtures 161
5.4.3 Dynamic shear strength of the treated GR12T5 mixtures 162
5.5 Comparison of the dynamic characteristics of treated and untreated GR12, TR5 and GR12T5 mixtures 164
5.6 Summary 170
Chapter 6: Dynamic Behaviour of Layered Samples of Rock, Glass, Sand and Bentonite:Layered Technique 172
6.1 Introduction 172
6.2 Resilient modulus of layered samples of rock and glass 173
6.2.1 Effect of the glass content on resilient modulus of layered samples 173
6.2.3 Effect of the GR layer location on resilient modulus of layered samples 177
6.2.4 Effect of moisture content on resilient modulus of layered samples 178
6.3 Permanent deformation of layered samples of rock and glass 179
6.3.1 Effect of glass content on permanent deformation 179
6.3.2 Effect of the GR layer location on permanent deformation of layered samples 182
6.3.4 Effect of moisture content on the permanent deformation of R+GR samples 182
6.4 Shear strength of layered samples of rock and glass 184
6.4.1 Effect of glass content on shear strength of R+GR samples 184
6.4.2 Effect of the GR layer thickness on shear strength of layered samples 186
6.4.3 Effect of moisture content on shear strength of layered samples 187
6.4.4 Comparison of layered and homogenous structures 188
6.5 Resilient modulus of layered rock-sand samples 191
6.5.1 Effect of the sand layer location on the M_r of layered R-S samples for 100 loading cycles per path 192
6.5.2 Effect of the number of sand layers on resilient modulus of the rock-sand sample for 100 loading cycles per path 193
6.5.3 Effect of the sand layer location on the resilient modulus of rock-sand samples for 10,000 loading cycles per path 194

6.5.4 Effect of the number of sand layers on the resilient modulus of rock-sand samples for 10,000 loading cycles per path 195

6.6 Permanent deformation of layered rock-sand 196

6.6.1 Effect of the sand layer location on the permanent deformation of rock-sand samples for 100 loading cycles per path 199

6.6.2 Effect of the sand layer location on the permanent deformation of rock-sand samples tested for 10,000 loading cycles per path 201

6.6.3 Effect of the number of sand layer on the permanent deformation of rock-sand sample tested for 100 loading cycles per path 204

6.6.4 Effect of the number of sand layers on permanent deformation of rock-sand samples tested for 10000 cycles/path 204

6.7 Resilient modulus of layered samples of rock-bentonite and rock-bentonite-sand materials tested for 100 cycles per path 206

6.7.1 Effect of the location of bentonite layer on resilient modulus of the rock-bentonite samples 207

6.7.2 Effect of the number of bentonite layer on the resilient modulus of rock-bentonite samples 208

6.7.3 Effect of replacing sand and bentonite layers with rock layers on the resilient modulus of rock-bentonite and rock-sand samples 209

6.7.4 Effect of sand and bentonite layers on the resilient modulus of rock-sand-bentonite samples 210

6.8 Permanent deformation of layered samples of rock-bentonite and rock-bentonite-sand materials tested for 100 cycles per path 211

6.8.1 Effect of the location of bentonite layer on the permanent deformation of rock-bentonite samples 211

6.8.2 Effect of the number of bentonite layers on the deformation of rock-bentonite samples 212

6.8.3 Effect of replacing sand with bentonite layer on the permanent deformation of rock-bentonite-sand samples 214

6.8.4 Effect of the sand and bentonite layers locationon the permanent deformation of the rock-bentonite-sand samples 214

6.9 Summary 216
Chapter 7: Modelling Resilience Susceptibility Using Artificial Intelligence 218
7.1 Introduction 218
7.2 Artificial neural networks 218
7.3 Genetic programming 232
7.4 Summary 236
Chapter 8: Conclusions and Recommendations 238
8.1 Introduction 238
8.2 Conclusions 238
8.2.1 Characterisations of glass-rock mixtures 238
8.2.2 Characterisations of tyres rubber-rock mixtures 240
8.2.3 Characterisations of glass-rock-rubber mixtures 241
8.2.4 Characterisation of glass-rock-cement and the glass-rock-cement-slag mixtures 242
8.2.5 Characterisations of rubber-rock-cement mixtures (TR5C2-7) and rubber-rock-cement-slag mixtures (TR5C1S-7) 242
8.2.6 Characterisations of different samples of the GR12T5C2-7 and the GR12T5C1S-7 mixtures 243
8.2.7 Dynamic evaluation of layered glass-rock samples 244
8.2.8 Dynamic evaluation of layered rock-sand samples 245
8.2.9 Dynamic evaluation of layered rock-bentonite-sand samples 246
8.2.10 Artificial intelligence approaches: modelling of resilient modulus 246
8.3 Recommendations 247
References 249
Appendixes: 269
Laboratory data 269
Co-author attribution approval statement 273

List of Figures

Figure 1.1 Roman pavement structure 1

Figure 1.2 An overview of the thesis arrangement 9

Figure 2.1 An overview of the literature review chapter 11

Figure 2.2 Typical section of rigid pavement 12

Figure 2.3 Typical section of flexible pavement 14

Figure 2.4 Typical behaviour of granular materials during the repeated load cycle (Lekarp et al., 2000) 15

Figure 2.5 Characteristics of resilient strain (εr) and permanent strain (εp) (De Vos, 2006) 19

Figure 2.6 Permanent deformation of a glass-concrete aggregate mixture at different moisture content with loading cycles (Arulrajah et al., 2014) 20

Figure 2.7 Triaxial results for glass-dredged blends (Grubb et al., 2006) 30

Figure 2.8 Permanent deformation of glass-aggregate blends (Arnold et al., 2008) 32

Figure 2.9 Effect of rubber content on the permanent deformation of rubber-subballast mixtures (Signes et al., 2016) 43

Figure 2.10 Tailings specimens for triaxial shear tests: a) course tailings specimen b) fine tailings specimen c) layered structure specimen (Zhang et al., 2015) 48

Figure 2.11 Resilient modulus of treated crushed rock with loading sequence (Siripun, Jitsangiam and Nikraz, 2009) 50

Figure 2.12 Effect of cement content on permanent deformation of pure crushed rock (Siripun, Jitsangiam and Nikraz, 2009) 50

Figure 2.13 Effects of slag and fly ash on the resilient modulus value of different waste materials (Mohammadinia et al., 2016) 51

Figure 2.14 Simple structure of ANN 57

Figure 3.1 Overall plan of the present study 62

Figure 3.2 a) dry rock, b) wet rock, c) SEM image, and d) EDS spectrum of rock 64

Figure 3.3 a) stockpiles of crushed glass, b) large tray used to mix the materials, c) dry sample of crushed glass, and d) wet glass-rock mixture 66

Figure 3.4 a) stockpiles of tyre rubber, b) dry specimen of rubber-rock mixture, c) wet specimen of rubber-rock mixture, and d) failure sample of rubber-rock mixture 67

Figure 3.5 a) stockpile of sand, b) wet sand, c) SEM image, and d) EDS spectrum of sand 68

Figure 3.6 a) dry sample of bentonite, b) wet sample of bentonite, c) SEM image, and d) EDS spectrum of bentonite 70

Figure 3.7 a) typical cement bags, b) dry sample, c)SEM image and, and d) EDS spectrum 71
Figure 3.8 a) dry sample of slag, b) wet sample of slag, c) SEM image, and d) EDS spectrum of slag 72
Figure 3.9 Stresses applied in the RLTT 74
Figure 3.10 Vertical force waveform(De Vos, 2006) 74
Figure 3.11 Stress regimes of base materials (De Vos, 2006) 75
Figure 3.12 Charted results on the personal computer screen (De Vos, 2006) 76
Figure 3.13 Overall view of the hardware and loading system of the RLTT device 76
Figure 3.14 Overall view of LVDTs and other RLTT‟s cell parts 77
Figure 3.15 Input parameters of the quick shear test (De Vos, 2006) 78
Figure 3.16 Computer screen during dynamic shear testing (the main window of the PC) 78
Figure 3.17 Sample preparation: a) trays of crushed rock and glass, b) checking the weight of each layer, c) checking the thickness of each compacted layer, and d) a fully assembled sample of glass-rock 81
Figure 3.18 Sample preparation: a) a tray of rubber and crushed rock, b) a homogenous wet mixture of tyre rubber and crushed rock, c) full sample inside the RLTT apparatus and d) blended sample after the RLTT 82
Figure 3.19 Sample preparation: a) a tray of rubber and crushed rock, b) a tray of glass-rock-rubber, c) putting O-rings around the top loading cup d) a full sample inside the RLTT cell 84
Figure 3.20 Preparation stages: a) a tray of glass-rock-cement, b) a tray of glass-rock-cement slag, c) tray of rubber-rock-cement-slag d) tray of glass-rock-rubber-cement-slag e) plastic sheet covering the mixture and f) plastic bag sealing the covered tray 86
Figure 3.21 Sample preparation: a) trays of rock and sand, b) weighing each layer, c) compaction stage and d) final layout of the specimen before the RLTT 87
Figure 3.22 Sample preparation: a) trays of bentonite, crushed rock and sand, b)preparation of each layer for the compaction stage, c) checking the thickness of each layer and d) fully assembled sample of rock-bentonite-sand 89
Figure 3.23 Screenshot of the HeuristicLab software program (the main window of the PC) 91
Figure 3.24 Line charts of training and test datasets (the main window of the PC) 92
Figure 3.25 Measured vs. predicted values (the main window of the PC) 92
Figure 4.1 Overall plan of Chapter 4 94
Figure 4.2 Gradation curves of pure rock, VicRoads limits and the glass-rock mixtures before compaction 95
Figure 4.3 Gradation curves of pure rock, VicRoads limits and the glass-rock mixtures after compaction 96
Figure 4.4 Compaction curves for rock and mixed glass-rock samples 97

Figure 4.5 Effect of glass content on the OMC and the MDD of the glass-rock mixtures 98
Figure 4.6 Resilience behaviour of pure rock sample 100
Figure 4.7 Resilience behaviour of pure rock, and GR12, GR24& GR45 mixtures 101
Figure 4.8 Variation in the resilience behaviour of rock with different glass content 101
Figure 4.9 Comparison of the resilience behaviour of the GR12 mixture under drained-undrained conditions 103
Figure 4.10 Effect of density on the resilience behaviour of the GR12 mixture under undrained condition 104
Figure 4.11 Permanent deformation of the pure rock sample 104
Figure 4.12 Deformation behaviour of the rock, GR12, GR24 and GR45 samples 105
Figure 4.13 Variation in the permanent deformation of glass-rock mixtures with different glass content 106
Figure 4.14 Comparison of the permanent deformation of GR12 sample under drained-undrained conditions 107
Figure 4.15 Effect of density on the permanent deformation of GR12 sample under undrained condition 107
Figure 4.16 Stress-strain behaviour of the pure rock sample 108
Figure 4.17 Stress-strain curves for the pure rock, GR12, GR24 and GR45 samples 109
Figure 4.18 Particles size distribution curves for pure rock, VicRoad limits, TR5, TR10 and TR15 before compaction 110
Figure 4.19 Particles size distribution curves for pure rock VicRoad limits, TR5, TR10 and TR15after compaction 111
Figure 4.20 Compaction curves of pure rock and TR mixtures containing5%, 10% and 15% rubber contents 112
Figure 4.21 Variations in the resilient moduli of pure rock with various rubber or glass contents 115
Figure 4.22 Resilient modulus-rubber content curve of TR mixtures 115
Figure 4.23 Effect of moisture content on the resilient modulus of TR5, TR10 and TR15 mixtures 116
Figure 4.24 Variation in permanent deformation of the GR and the TR mixtures according to their rubber and glass contents 117
Figure 4.25 Variation in the permanent deformation of TR mixtures with different rubber content 117
Figure 4.26 Effect of moisture content on the Pd of the TR mixtures 118
Figure 4.27 Stress-strain curves for the pure rock, TR5, TR10, and TR15 samples 119
Figure 4.28 Stress-strain curves for the pure rock, TR5, TR10 and TR15 samples according to their moisture contents 120
Figure 4.29 Effect of confining pressure on dynamic shear strength of the TR5 sample 121
Figure 4.30 Effect of confining pressure on dynamic shear strength of the TR10 sample 121

Figure 4.31 Effect of confining pressure on dynamic shear strength of TR15 sample 121
Figure 4.32 Particles size distribution curves for VicRoads limits, GR12T5, GR24T5, GR45T5 mixtures before compaction 122
Figure 4.33 Particles size distribution curves for VicRoads limits, andGR12T10, GR24T10 GR45T10 mixtures before compaction 123
Figure 4.34 Particles size distribution curves for VicRoads limits, andGR12T15, GR24T15 and GR45T15 mixtures before compaction 123
Figure 4.35 Particles size distribution curves for VicRoads limits, and the GR12T5, GR24T5 and GR45T5 mixtures after compaction 124
Figure 4.36 Particles size distribution curves for VicRoads limits, andGR12T10, GR24T10 and GR45T10 mixtures after compaction 124
Figure 4.37 Particles size distribution curves for VicRoads limits, andGR12T15, GR24T15 and GR45T15 mixtures after compaction 124
Figure 4.38 Effect of glass and rubber contents on compaction curves of pure rock..... 125
Figure 4.39 AMC/IMC ratio of pure rock, the GR, TR and GRT mixtures according to the glass and rubber contents after RLTTs..... 130
Figure 4.40 Achieved dry densities of pure rock, and the GR, TR and GRT mixtures according to the glass and rubber contents after RLTTs..... 131
Figure 4.41 Resilience behaviour of pure rock, TR5, GR12T5, GR24T5 and GR45T5 mixtures..... 132
Figure 4.42 Resilience behaviour of pure rock, TR10, GR12T10, GR24T10 and GR45T10 mixtures..... 133
Figure 4.43 Resilience behaviour of pure rock, TR15, GR12T15, GR24T15 and GR45T15 mixtures..... 133
Figure 4.44 Effect of moisture content on the resilient moduli of the GR12T5, GR24T5 and GR45T5mixtures..... 134
Figure 4.45 Effect of moisture content on the resilient moduli of the GR12T10, GR24T10 and GR45T10 mixtures..... 135
Figure 4.46 Effect of moisture content on the resilient moduli of the GR12T15, GR24T15 and GR45T15 mixtures..... 135
Figure 4.47 Effect of moisture content on the resilient moduli of pure rock, and the GR, TR and GRT mixtures containing different glass and rubber contents..... 136
Figure 4.48 Variation in the permanent deformation of pure rock, TR5, and the GRT mixtures containing 5% rubber with 12%, 24% and 45% glass content..... 137
Figure 4.49 Variation in the permanent deformation of pure rock, TR10, and the GRT mixtures containing 10% rubber with 12%, 24% and 45% glass content..... 138
Figure 4.50 Variation in the permanent deformation of pure rock, TR15, and the GRT mixtures containing 15% rubber with 12%, 24% and 45% glass content..... 138
Figure 4.51 Effect of moisture content on the permanent deformation of the GR12T5, GR24T5 and GR45T5 mixtures..... 139

Figure 4.52 Effect of moisture content on the permanent deformation of the GR12T10, GR24T10 and GR45T10 mixtures 139
Figure 4.53 Effect of moisture content on the permanent deformation of the GR12T15, GR24T15 and GR45T15 mixtures 140
Figure 4.54 Effect of moisture content on the permanent deformation of pure rock, GR, TR and GRT mixtures containing different glass and rubber contents 141
Figure 4.55 Variation in the shear behaviour of pure rock, TR5, GR12T5, GR24T5 and GR45T5 mixtures 142
Figure 4.56 Effect of moisture content on the shear strength of the GR12T5 mixture 143
Figure 4.57 Effect of moisture content on the shear strength of the GR24T5 mixture 143
Figure 4.58 Effect of moisture content on the shear strength of the GR45T5mixture 143
Figure 4.59 Shear stress-strain curves of the GR12T5 mixtures at various confining pressures 144
Figure 4.60 Shear stress-strain curves of the GR24T5 mixtures at various confining pressures 145
Figure 4.61 Shear stress-strain curves of the GR45T5 mixtures at various confining pressures 145
Figure 5.1 Effect of the glass, glass-cement and glass-cement-slag contents on resilience behaviour of pure rock after seven days 151
Figure 5.2 Effect of the glass, glass-cement and glass-cement-slag contents on permanent deformation of pure rock after seven days 152
Figure 5.3 Effect of glass, glass-cement, and glass-cement-slag contents on dynamic shear strength of pure rock after seven days 153
Figure 5.4 Failure patterns observed after RLTTs of GR12 mixtures: a) cement treated sample (GR12C2-7), b) cement-slag treated sample (GR12C1S-7), and c) untreated sample 154
Figure 5.5 Effect of rubber, rubber-cement and rubber-cement-slag contents on the resilience behaviour of pure rock after seven days 156
Figure 5.6 Effect of rubber, rubber-cement and rubber-cement-slag contents on permanent deformation of pure rock after seven days 157
Figure 5.7 Effect of rubber, rubber-cement and rubber-cement-slag contents on the shear strength for the pure rock after seven days 159
Figure 5.8 Failure patterns observed after RLTTs of TR5 samples: a) cement treated sample, b) cement-slag treated sample 159
Figure 5.9 Effect of glass-rubber, glass-rubber-cement and glass-rubber-cement-slag contents on the resilience behaviour of pure rock after seven days 161
Figure 5.10 Effect of glass-rubber-cement and glass-rubber-cement-slag contents on the permanent deformation of pure rock after seven days 162
Figure 5.11 Effect of glass-rubber and glass-rubber-cement contents on the shear strength of pure rock after seven days 163

Figure 5.12 Effect of cement-slag contents on the shear strength of the GR12T5C2-7 mixture after seven days 163
Figure 5.13 Failure patterns observed after RLTTs of the GR12T5 samples: a) cement-slag treated sample and b) cement treated sample 164
Figure 5.14 The resilient modulus of cement treated, cement-slag treated and untreated samples of the GR12, TR5 and GR12T5 mixtures 165
Figure 5.15 The permanent deformation of cement treated, cement-slag treated and untreated samples of the GR12, TR5 and GR12T5 mixtures..... 166
Figure 5.16 Shear stress-strain curves of cement treated, and cement-slag treated samples of the GR12, TR5 and GR12T5 mixtures 167
Figure 5.17 The resilient modulus of pure rock, cement treated, cement-slag treated and untreated samples of the GR12, TR5, GR12T5 mixtures 168
Figure 5.18 The permanent deformation of pure rock, cement treated, cement-slag treated and untreated samples of the GR12, TR5 and GR12T5 mixtures..... 169
Figure 5.19 The ultimate shear strength of pure rock, cement treated, cement-slag treated and untreated samples of the GR12, TR5 and GR12T5 mixtures..... 170
Figure 6.1 Effects of the glass content and the layer thickness on the resilient modulus of pure rock sample 175
Figure 6.2 Fully-assembled of R+GR samples a) the 4R+4GR layered sample, and b) the 2R+2GR layered sample..... 175
Figure 6.3 Effect of the GR24 layer thickness on the resilient modulus of the pure rock sample..... 176
Figure 6.4 Effect of the GR45 layer thickness on the resilient modulus of the pure rock sample..... 177
Figure 6.5 Effect of the GR24 and GR45 layer locations on the resilience behaviour of the 4R+4GR24 and the 4GR+4R45samples..... 178
Figure 6.6 Effect of moisture content on the resilient modulus of R+GR24 sample 179
Figure 6.7 Effects of glass content and the layer thickness on the permanent deformation of pure rock sample 180
Figure 6.8 Effect of the GR24 layer thickness on the permanent deformation of pure rock specimen..... 181
Figure 6.9 Effect of the GR45 layer thickness on the permanent deformation of pure rock specimen..... 181
Figure 6.10 Effect of the GR24 and GR45 location on permanent deformation of the 4R+4GR24 and 4R+4GR45 samples 182
Figure 6.11 Effect of moisture content on the permanent deformation of R+GR24 specimen..... 183
Figure 6.12 Effect of glass content on permanent deformation of the GR, R+GR, 2R+2GR and 4R+4GR groups 184
Figure 6.13 Stress-strain curves of the R, R+GR12, R+GR24, and R+GR45 samples..... 185

Figure 6.14 Stress-strain curves for the R, 2R+2GR12, 2R+2GR24 and 2R+2GR45 samples 187
Figure 6.15 Effect of the GR24 layer thickness on shear strength of R+GR24 sample 187
Figure 6.16 Effect of moisture content on shear strength of the R+GR24 sample 188
Figure 6.17 Resilient modulus of the homogenous and the layered GR samples containing 12%, 24% and 45% glass contents 189
Figure 6.18 Permanent deformation of the homogenous and the layered GR samples containing 12%, 24% and 45% glass contents 189
Figure 6.19 Shear stress-strain curves of the layered and the homogenous GR samples containing: (a) 12% glass content, (b) 24% glass content, and (a) 45% glass content 190
Figure 6.20 Failure patterns observed after RLTT of a 4R+4GR45sample 191
Figure 6.21 Effect of the sand layer location on the resilient modulus of rock-sand samples for 100 loading cycles /path 193
Figure 6.22 Effect of the number of sand layers on the resilient modulus of the rock-sand sample for 100 loading cycles /path 194
Figure 6.23 Effect of the sand layer location on the resilient modulus of the rock-sand samples for 10000 loading cycles /path 195
Figure 6.24 Effect of the sand layer number on the M_r of the rock-sands samples for 10000 loading cycles /path 196
Figure 6.25 Maximum deviatoric stress vs. permanent deformation for pure rock sample 197
Figure 6.26 Maximum deviatoric stress vs. permanent deformation for rock sample for 100 and 10000 loading cycles during the first stage of the RLTT (20 kPa confining pressure) 197
Figure 6.27 Maximum deviatoric stress vs. permanent deformation for rock sample for 100 and 10000 loading cycles during the all stages of the RLTT (20, 35, 50, 70 and 100 kPa confining pressure) 198
Figure 6.28 Number of loading cycles vs. permanent deformation for rock samples tested for 100 and 10,000 loading cycles/path 198
Figure 6.29 Maximum deviator stress vs. permanent deformation for rock-sand samples with sand layers in different locations tested for 100 cycles/path during the all stages of the RLTT (20, 35, 50, 70 and 100 kPa confining pressure) 200
Figure 6.30 Effect of the sand layer location on the permanent deformation of rock-sand specimens tested for 100 cycles/path 200
Figure 6.31 Effect of the sand layer location on the failure patterns of rock-sand samples after RLTTs: a) 6R+S+R(100), b) 4R+S+3R(100) and c) R+S+6R(100) samples 201
Figure 6.32 Effect of the sand layer location on the permanent deformation of sand-rock specimens tested for 10000 cycles/path during the all stages of the RLTT (20, 35, 50, 70 and 100 kPa confining pressure) 202
Figure 6.33 Effect of the sand layer location on the permanent deformation of sand-rock samples tested for 10,000 cycles/path 203

Figure 6.34 Permanent deformation of the sand-rock samples tested under 100 and 10000 cycles/path 203
Figure 6.35 Effect of the number of sand layers on permanent deformation of the rock-sand specimens tested for 100 cycles/path 204
Figure 6.36 Effect of the number of sand layers on the permanent deformation of rock-sand samples tested for 10000 cycles/path 205
Figure 6.37 Failure pattern of 2R+S+R+S+R+S+R(100) sample after completion the RLTT 206
Figure 6.38 Effect of the bentonite layer location on the resilient modulus of R-BE samples tested for 100 cycles/path 208
Figure 6.39 Effect of the sand and bentonite layers locations on the resilient modulus of rock samples tested for 100 (cycles/path) 208
Figure 6.40 Effect of the number of bentonite layers on the resilient modulus of the rock-bentonite sample tested for 100 cycles/path 209
Figure 6.41 Resilience behaviour of rock-sand and rock-bentonite layered samples tested for 100 loading cycles/path 210
Figure 6.42 Effect of the sand and the bentonite layer locations on the resilience behaviour of the 2R+BE+R+S+3R sample tested for 100 loading cycles/path 210
Figure 6.43 Effect of the location bentonite layer on the permanent deformation of rock-bentonite samples tested for 100 loading cycles/path 212
Figure 6.44 Permanent deformation of rock-sand and rock-bentonite samples tested for 100 loading cycles/path 212
Figure 6.45 Effect of the number of bentonite layers on the permanent deformation of rock-bentonite samples tested for 100 loading cycles/path 213
Figure 6.46 Locations of failure zones and failure patterns of 2R+BE+R+BE+3R (100) sample after RLTT 213
Figure 6.47 Effect of replacing sand with bentonite layer on the permanent deformation of rock-bentonite-sand samples tested for 100 loading cycles/path 214
Figure 6.48 Effect of the sand and bentonite layer locations on the permanent deformation of the 2R+BE+R+S+3R sample tested for 100 loading cycles/path 215
Figure 6.49 Locations of failure zones and failure pattern of 2R+S+R+BE+3R(100) sample after RLTT 216
Figure 7.1 Schematic representation of artificial neural networks 222
Figure 7.2 Measured vs. Prediction resilient modulus for ANN model 1 223
Figure 7.3 Accuracy assessment of model 1: a) training, b) validation, c) testing, and d) overall sets 224
Figure 7.4 Measured vs. predicted resilient moduli for ANN model 2 225
Figure 7.5 Accuracy assessment of model 2: a) training, b) validation, c) testing, and d) overall sets 226

Figure 7.6 Measured vs. Prediction resilient moduli for ANN model 3 227
Figure 7.7 Accuracy assessment of model 3: a) training, b) validation, c) testing, and d) overall sets 228
Figure 7.8 Measured vs. Prediction resilient moduli for ANN model 4 229
Figure 7.9 Accuracy assessment of model 4: a) training, b) validation, c) testing, and d) overall sets 229
Figure 7.10 Measured vs. Prediction resilient moduli for ANN model 5 230
Figure 7.11 Accuracy assessment of model 5: a) training, b) validation, c) testing, and d) overall sets 231
Figure 7.12 Measured vs. Prediction resilient moduli for all ANN models 232
Figure 7.13 Tree of the GP model 235
Figure 7.14 Measured values of resilient modulus vs. those predicted by the GP model 236
Figure 7.15 Line charts of training and test datasets of the GP model (a comparison between the resilient modulus of the training-testing sets and the estimated resilient modulus) 236

List of Tables

Table 2.1 Studies investigating the influences of waste glass on unbound materials' properties 34
Table 2.2 Studies investigating the influences of waste rubber on unbound materials' properties 44
Table 2.3 A review of the previous works and the proposed experimental program regarding the effects of waste materials inclusion and layering on the unbound material characteristics 52
Table 3.1 Crushed rock properties 64
Table 3.2 Specifications for crushed rock base course 65
Table 3.3 Crushed glass properties 65
Table 3.4 Tyre rubber properties 67
Table 3.5 Pure sand properties 68
Table 3.6 Bentonite properties 69
Table 3.7 Specifications of cement 71
Table 3.8 Specifications of slag 72
Table 3.9 Preliminary tests and the related standards 73
Table 3.10 Stress path applied to each sample (AASHTO T 307) 80
Table 3.11 Structure design of glass-rock specimens 80
Table 3.12 Structure design of tyre rubber-rock mixtures 82
Table 3.13 Structural design of glass-rock-rubber mixtures 83
Table 3.14 Structural design of the cement and cement-slag treated samples 85
Table 3.15 Stress path applied to each sample 87
Table 3.16 Structural design of the layered samples of rock and sand 88
Table 3.17 Structural design of the layered samples of rock-bentonite and rock-bentonite-sand 89
Table 4.1 Geotechnical properties of mixed glass-rock samples 99
Table 4.2 Geotechnical properties of rubber-rock mixtures with different rubber content 113
Table 4.3 Geotechnical properties of the GR12T5, GR24T5 and GR45T5 mixtures before and after compaction 127
Table 4.4 Geotechnical properties of the GR12T10, GR24T10 and GR45T10 mixtures before and after compaction 128
Table 4.5 Geotechnical properties of the GR12T15, GR24T15 and GR45T15 mixtures before and after compaction 129
Table 7.1 Properties of base course materials 221
Table 7.2 Statistical distribution of each parameter in the normalisation database 221

Table 7.3 Details of the performance of model 1……..223
Table 7.4 Details of the performance of model 2…….…....225
Table 7.5 Details of the performance of model 3……..227
Table 7.6 Details of the performance of model 4……..228
Table 7.7 Details of the performance of model 5 ……..……230
Table 7.8 Symbolic regression parameters……..…233
Table 7.9 Coefficients of Equation (7.2) ……..…….233
Table 7.10 Performance of the resilient modulus model for the training and testing datasets…….……....234

Acronyms, Abbreviations, and Notations

[CBR]	[California bearing ratio]
[M_r]	[Resilient modulus]
[$_{Pd}$]	[Permanent deformation]
[ABS]	[Australian Bureau of Statistics]
[GR]	[Glass-rock mixtures]
[TR]	[Tyre-rock mixtures]
[GRT]	[Glass-rock-rubber mixtures]
[R]	[Rock]
[BE]	[Bentonite]
[ANN]	[Artificial neural network]
[GP]	[Genetic programming]
[RLTTs]	[Repeated loading triaxial tests]
[AI]	[Artificial intelligence]
[σ_1]	[Primary principal or axial stress]
[σ_3]	[Minor principal or confining stress]
[σ_d]	[Deviator stress]
[ε_r]	[Axial resilient strain]
[RCA]	[Recycled concrete aggregate]
[UGM]	[Unbound granular material]
[RG]	[Recycled glass]
[CR]	[Crushed rock]
[SP-SM]	[Poorly graded sand with silt material]
[WR]	[Waste rock]
[p_H]	[Power of hydrogen]
[LA]	[Los Angeles]
[AASHTO]	[American Association of State Highway and Transportation Officials]
[LBR]	[Limerock bearing ratio]
[OMC]	[Optimum moisture content]
[UCS]	[Unconfined compressive strength tests]
[w_c]	[Water content]

[θ]	[Bulk stress]
[SM]	[Silty sand soil]
[GM]	[Well-graded gravel]
[GW]	[Fine to course gravel]
[GC]	[Clayey gravel]
[GP]	[Poorly graded gravel]
[S'_r]	[Degree of saturation]
[D_r]	[Degree of compaction]
[Ii]	[First stress invariant]
[k'_s]	[The material constants]
[q_u]	[Unconfined compressive value]
[G]	[Glass]
[S]	[Sand]
[SL]	[Slag]
[C]	[Cement]
[SEM]	[Scanning Electron Microscopy test]
[K]	[Potassium]
[O]	[Oxygen]
[Fe]	[Iron]
[Na]	[Sodium]
[Mg]	[Magnesium]
[Si]	[Silicon]
[Al]	[Aluminium]
[Ti]	[Titanium]
[Gs]	[Specific gravity]
[ASTM]	[American Society for Testing Materials]
[Ca]	[Coliseum]
[SiO_2]	[Silicon dioxide]
[Al_2O_3]	[Aluminume oxide]
[TiO2]	[Titanume dioxide]
[Fe_2O_3]	[Iron Oxide]
[CaO]	[Calciume Oxide]
[Na_2O]	[Sodium Oxide]
[MgO]	[Magnesium Oxide]

[K_2O]	[Potassium Oxide]
[GP]	[General purpose cement (GP)]
[SO_3]	[Sulfur trioxide]
[GBFS]	[Granulated blast furnace slag]
[ε_p]	[Permanent strain]
[CDAS]	[Control and Data Acquisition System]
[PC]	[Personal computer]
[UTS]	[Universal Testing System]
[LVDT]	[Linear variable differential transformer]
[UTS]	[Universal Testing System]
[GR12]	[Glass-rock mixture at 12% glass]
[GR24]	[Glass-rock mixture at 24% glass]
[GR45]	[Glass-rock mixture at 45% glass]
[R+GR12]	[Layered sample of glass-rock mixture at 12% glass]
[R+GR24]	[Layered sample of glass-rock mixture at 24% glass]
[R+GR45]	[Layered sample of glass-rock mixture at 45% glass]
[TR5]	[Rubber-rock mixture at 5% rubber]
[TR10]	[Rubber-rock mixture at 10% rubber]
[TR15]	[Rubber-rock mixture at 15% rubber]
[GR12T5]	[Glass-rock-rubber mixture at 12% glass and 5% rubber]
[GR24T5]	[Glass-rock-rubber mixture at 24% glass and 5% rubber]
[GR45T5]	[Glass-rock-rubber mixture at 45% glass and 5% rubber]
[GR12T10]	[Glass-rock-rubber mixture at 12% glass and 10% rubber]
[GR24T10]	[Glass-rock-rubber mixture at 24% glass and 10% rubber]
[GR45T10]	[Glass-rock-rubber mixture at 45% glass and 10% rubber]
[GR12T15]	[Glass-rock-rubber mixture at 12% glass and 15% rubber]
[GR24T15]	[Glass-rock-rubber mixture at 24% glass and 15% rubber]
[GR45T15]	[Glass-rock-rubber mixture at 45% glass and 15% rubber]
[MRWA]	[Main Roads Western Australia]
[γ_d]	[Dry density]
[γ_c]	[Confining pressure]
[σ_d]	[Deviator stress]
[D_{50}]	[Mean diameter]
[C_c]	[Coefficient of curvature]

[C_u]	[Coefficient of uniformity]
[LMA]	[Levenberg–Marquardt back-propagation algorithm]
[R^2]	[Coefficient of determination]
[D_{10}]	[Effective size, Particle size at 10% passing]
[D_{30}]	[Particle size at 30% passing]
[D_{60}]	[Particle size at 60% passing]
[ACSS]	[Australian Soil Classification System]
[AMC]	[Actual moisture content]
[AD]	[Achieved density]
[R-BE]	[Rock-bentonite sample]
[R-BE-S]	[Rock-bentonite-sand sample]
[R-S]	[Rock-sand sample]
[M_c]	[Moisture content]
[RMSE]	[Root mean square error]
[PI]	[Plasticity index]
[LL]	[Liquid limit]
[σ_c]	[Confining pressure]

Chapter 1: Introduction

1.1 Background to the study

The history of roads began in the ancient city of Ur, Iraq, in approximately 4000 BC. Here, the ancient Sumerian civilisation of southern Mesopotamia made the first steps in road construction. In that period, road networks consisted of stone materials, which were used to pave city streets (Adams, 1972). According to the earlier report published by Collins and Hart (1936), the Romans eventually decided to construct layered roads for military purposes near Radstock, England around AD 406. The multilayered road system of Roman was approximately 0.9 m thick and 4.3 m wide. Road system consisted of a top surface layer lime grouted polygonal slabs (100 mm), a base layer of fine stone and lime (250 mm), a subbase layer of course local stone (400 mm) and at the bottom, a 150 mm layer of flat stones. Figure 1.1 shows a typical section of Roman pavement structure.

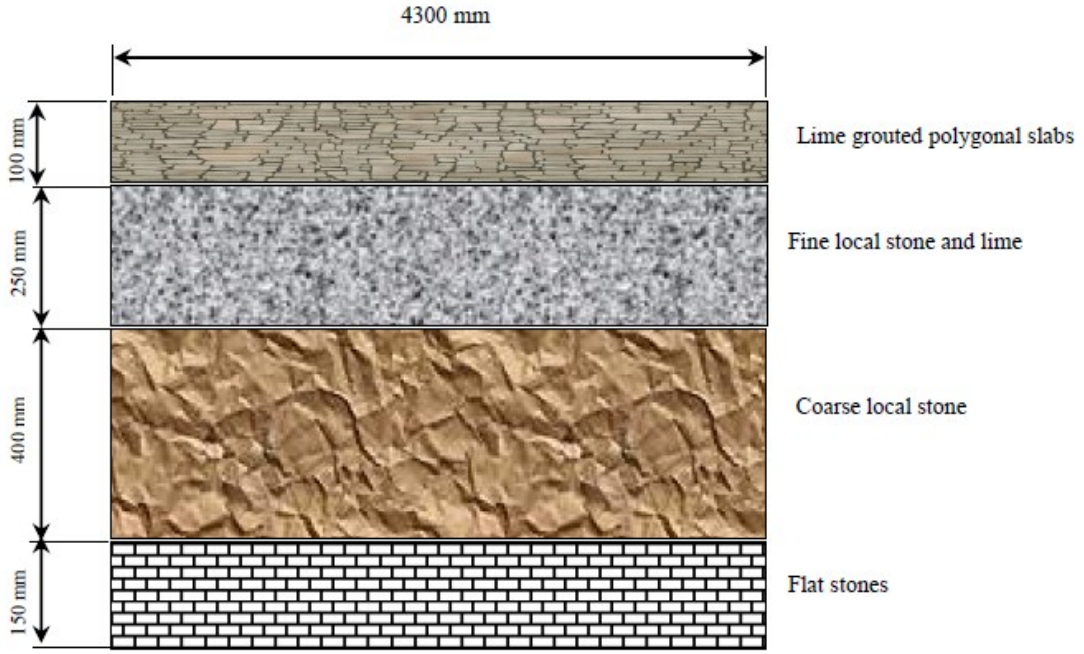

Figure 1.1 Roman pavement structure

In the recent decades, the increase in the industrial and commercial activities around the world requires an increase in road networks and therefore, the previous pavement structures are no longer suitable for the requirements of modern networks.The pavement structure is constantly evolving but the flexible, rigid and combined

pavements are the commonly used as multilayered pavement system during recent years. Flexible pavement consists of treated granular materials between the surface (typically bituminous) and the natural subgrade layer. In Australia, the most common type of pavement structure is the flexible pavement which comprises of subbase, base layers, and a thin service layer of bitumen on top. In flexible pavement system, the performance of granular materials is dependent on their deformation and strength criteria under the dynamic traffic loads which transmitted directly from the bitumen layer to the base and subbase layers underneath. It is important to mention that any deformation occurring in the base or subbase layers can cause dangerous cracks or ruts in asphalt pavement so it is important to assess the dynamic behaviour of the granular materials under dynamic loads. To attain this assessment, tests such as the California bearing ratio (CBR) test and the repeated loading triaxial test (RLTT) test should be conducted. Recently, the RLTT is the most tests widely conducted to evaluate the permanent deformation and the resilient modulus of granular materials under the repeated load impacts. The M_r can be defined as the correlation between deviator stress and recovered strain under dynamic loads, and considered as a fundamental parameter in pavement design. The term M_r was initially used by Seed, Chan and Lee (1962) to explain the resilience behaviour of soils, and there was strong evidence that the results of resilient deflection gained from a California deflection device are more accurate than the results of total pavement deflection. In 1995, a development has occurred on the term M_r where defined as the ratio of subjected deviatoric stress to recovered strain (Witczak & Mirza, 1995). After that, Senol et al. (2002) concluded that the M_r is one of the major factors influencing pavement design. Thus, this study will mainly dependent on the RLTT to assess the resilience, deformation, and dynamic shear behaviour of granular materials under repeated loads.

According to Australian Bureau of Statistics (ABS, 2017), the average Australian produces about 1.5 tonnes of waste materials per year including plastic, paper, food and glass. In addition, Australia produces about 1.36 MT of waste glass per year including bottles, jars and glass containers. It is important to mention that the waste glass is not recycled locally in Western Australia. Furthermore, about 52.5 million tyres are disposed of each year with only 13% being recycled, creating a serious environmental issue in Australia when stored it. All this waste of glass and tyre

rubber can be classified as hazardous to health and the environment (Australian Government, Department of Environment and Energy, 2016). When referring to granular materials in Western Australia, we should mentioned that their main source is the natural rock which is the most common granular materials used as base and subbase layers in Western Australia. Also, an extensive quantity of crushed rock is needed to cover the more than 300,000 km of roads existing in Australia and thus, the utilisation of waste materials as a substitute for crushed rock has significant environmental and economic benefits. Furthermore, the behaviour of crushed glass is identical to that of natural unbound soils and therefore, the presence of glass in different paving layers could potentially satisfy the mixture requirements in road applications. Thus, many previous studies had a role in understanding the dynamic behaviour of glass-soil mixtures. The effect of glass on the static and dynamic performance of soils has been considered in earlier studies. Wartman, Grubb and Nasim (2004); and Ali et al. (2011) investigated the static and dynamic characteristics of glass-soil mixtures. In addition, the RLTTs have been performed by Arulrajah, Ali, Disfani and Horpibulsuk (2014) to assess the resilience performance of rock-glass mixtures. The results concluded that the rock-glass mixtures failed at low cycle numbers, and the crushed rock with 20% glass content showed the highest shear strength compared to other mixtures. These results were attributed to the low cohesion of glass particles.

Tyre rubber-soil mixtures have been widely used in civil engineering and hence, the dynamic behaviour of tyre rubber-soil has been assessed over the past few decades. A positive correlation was found between the permanent deformations (P_d) of soil-rubber mixtures and the rubber content when subjected to shaking loads (Humphrey, Sandford, Cribbs, & Manion, 1992; Hazarika, Yasuhara, Karmokar, & Mitarai, 2007). Recently, cyclic triaxial tests were conducted by Nakhaei, Marandi, Kermani, and Bagheripour (2012) to investigate the suitability of using an unbound material-rubber mixture in pavement applications. A negative correlation was found between the shear strength of the mixture and the rubber content. Different samples of tyre rubber-subgrade mixtures were employed in experimental studies conducted by Cosentino, Bleakley, Armstrong, Misilo and Sajjadi (2014) to evaluate the resilience behaviour of the mixtures under the RLTT. The research on the effect of rubber and glass on the dynamic behaviour of crushed rock material is limited. To address this

gap, this research will extend the experimental work on the RLTT on different samples of glass-rock-rubber mixtures. Moreover, the use of cementation agents to improve the dynamic responses of base and subbase materials has been less extensive and therefore, the effect of chemical treatments on the P_d and M_r of rock material has been considered in several studies. For example, improving the physical characterises of soil has been an essential objective for many investigations in road applications, such as Senol et al. (2002) and Arora and Aydilek (2005). According to their conclusions, the static and the dynamic characteristics of soils were improved when mixed with different additives, such as cement and slag. The research on the effect of a layered technique on the dynamic behaviour of soils is also limited and thus, there has been considerable interest in a layered technique in recent years. However, little studies have been published on single-layer rock structures, for example, Babiker, Smith, Gilbert and Ashby (2014) addressed the problem of the specimens failure under loading stages using the layered samples. At the same time, Gravanis, Pantelidis and Griffiths (2014) studied the stability of the single-stratified structure of the rock sample. By the same approach, Zhu and Tang (2006); Ma, Liu, Wang, Xu, Hua, Fan and Yi (2013); Zhou, Cao and Ye (2014); and Momeni, Karakus, Khanlari and Heidari (2015) sought to address the static and dynamic performances of the single-stratified sample of rock. Moreover, Excessive consumption of natural resources, such as unbound aggregate materials, has encouraged research workers to find alternative waste materials, such as fine materials, to use in geotechnical applications. Regarding the effect of fine materials on unbound materials properties, most previous studies on the effects of fine materials on the static and dynamic characteristics of unbound materials have mainly focused on the blending technique (partially substitution of fine materials with soils). However, few studies are available on the effect of a whole layer of fine materials on the static and dynamic behaviours of unbound soils. More precisely, the study on the effect of bound layers as bentonite on the dynamic behaviour of unbound aggregate materials (rocky soils) is limited. Bentonite is one of the suitable binding materials in geotechnical engineering applications; it has received considerable attention in many studies. Depending on the findings of Zhang, Yin, Wei, Fan, Wang and Nie (2015) who reported that the presence of a layer of fine materials can positively affect the shear strength of course-fine samples, this research will extend experimental works

to study the dynamic behaviour of pure rock samples with different layers of bentonite.

1.2 Research objectives

The main objective of this research is to identify an alternative material to crushed rock for road applications. Crushed rock, waste glass, tyre rubber, bentonite and sand are investigated in this dissertation. Moreover, cement and slag materials are used as binding materials to stabilise the waste material/rock samples. Furthermore, a stratified technique will be used instead of a homogeneous technique to prepare different samples. An assessment of the new technique and a comparison between both techniques will be performed. Various approaches have been used to obtain the above objectives.

1. Assess the suitability of using different homogenous mixtures of glass-rock (GR), tyre rubber-rock (TR) and glass-rock-tyre rubber (GRT) in road applications, as specified below.
    - Basic properties: Assess the specific gravity, water absorption, density and acidity or alkalinity of the new mixtures.
    - Geotechnical engineering properties: Assess the resilient modulus (M_r), permanent deformation (P_d), dynamic shear strength, maximum dry density, optimum moisture content and gradation.
2. Investigate the effect of binding materials, such as cement, on the M_r, P_d and dynamic shear behaviour of the homogenous samples of GR, TR and GRT mixtures under different test conditions.
3. Study the effect of combination of two types of cementation material (cement and slag) on the dynamic responses of the homogenous mixtures of GR, TR and GRT.
4. Employ a layered technique to examine the dynamic behaviour of different rock-GR samples under different conditions of moisture content, the layer location and the number of layers.
5. Evaluate the results of the stratified technique through a series of comparison between the dynamic behaviour of the stratified and the homogenous samples of glass-rock mixtures.

6. Study the dynamic response of different layered samples of rock (R), bentonite (BE), and/or sand (S) layers with variations in cycles number, the layer location, the number of layers, and the stress level.
7. Employ data from previous experimental studies in artificial neural network (ANN) and genetic programming (GP) models to predict the resilient modulus of base and subbase materials.

1.3 Significance

The findings of this study will improve the understanding the effects of waste material inclusion and layering on the characterisation of road base course materials. It will examine some critical points:

1. This study provide extra investigations concerning the effect of waste glass and tyre rubber on the dynamic behaviour of road base course materials, where previous investigations have illustrated inconsistent results.
2. A new understanding of the dynamic behaviour of glass-rock-rubber blends under repeated loading triaxial tests, the findings will help to clarify the influence of blending pure rock with different types of waste materials (glass, tyres rubber and slag) on dynamic behaviour.
3. The results of this research will provide initial information on the influences of cement and cement-slag mixtures on the dynamic behaviour of GR, TR and GRT mixtures.
4. The research will also provide an initial impression of the influence of replacing cement with a waste fine material of slag on the dynamic behaviour of GR, TR and GRT mixtures.
5. This research will offer an alternative method instead of the homogeneous technique to consume waste materials and provide a new understanding of the dynamic responses of layered samples of rock-(glass-rock), rock-bentonite and rock-bentonite-sand materials.
6. The consumption of waste materials such as tyre rubber, crushed glass, slag and bentonite in road applications will reduce the cost of base and subbase materials, which contribute to boosting the economic. Also, recycling and storing or transferring waste materials to other places are harmful to health and

environment and thus, consuming the waste materials as construction materials in road applications can reduce the health hazards of these materials.

7. This study will produce an alternative way to minimise the consumption of natural resources (crushed rock) by using slag, bentonite, and two of the major waste materials in Australia (glass and tyre rubber) in road applications.
8. This research will also provide a modified model for predicting the M_r of base and subbase materials used in pavement applications.

1.4 Thesis Organisation

This thesis is divided into eight chapters. To establish the research objectives, Chapters 2 to 8 are briefly outlined below and Figure 1.2 presents a diagram of the thesis chapters which explains the stages conducted to achieve the objectives of this thesis.

Chapter 2 presents the first stage of the research: a detailed review of the general characteristics of pure crushed rock, glass-soil, rubber-soil and glass-soil-rubber blends. The structures of pavement layers of rigid and flexible pavements are also presented. In addition, the factors affecting the dynamic behaviour of unbound materials in road applications are discussed. The static, dynamic and chemical characteristics of crushed rock with waste materials are described in Chapter 2. The use of different waste materials, such as crushed glass, tyre rubber, slag and bentonite in road applications, is also discussed in Chapter 2. Moreover, brief reviews of using the layered technique, cement, bentonite, and slag in geotechnical applications are presented in that chapter. Finally, a summary of the numerical study conducted by previous sttudies to develop models for predicting different geotechnical properties of soils was also described in the review chapter.

Chapter 3 presents the materials used in the experiment program and their basic parameters: rock, glass, rubber, cement, slag, bentonite, sand, and the glass-rock, rubber-rock, glass-rock-rubber mixtures. This part also presents the test apparatuses, sample preparation methods and samples design.

In Chapter 4, samples are prepared with different percentages of glass 12%, 24% and 45% of the total dry weights of the rock samples. A wide range of tyre rubber contents (5% to 15%) in crushed rock samples is also considered in this section. A

combination of glass and rubber with crushed rock is investigated. Therefore, the samples of GRT mixtures were preparedat different glass:rock:rubber ratios then a group of static and dynamic tests were conducted on the modified mixtures. The preliminary tests include modified Proctor compaction, specific gravity, water absorption, organic content, p_H and particle size distribution tests (before and after compaction) of the GR, TR and GRT mixtures.The resilient modulus, permanent deformation and shear strength of the mixtures are attained. Further investigations were performed to assess the factors that influence the dynamic behaviour of the GR, TR, and GRT mixtures such as moisture content, drained-undrained conditions, density and confining pressure.

Chapter 5 presents the results of mixing two types of cementation agent (cement and slag) on the dynamic behaviours of GR, TR and GRT mixtures. In the first section of this chapter, 2% cement was mixed with specific samples of GR, TR and GRT materials, then the RLTT was conducted after a seven-day hydration period. Further investigation of the samples was conducted to discover the effect of 1% cement with 1% slag on the resilient modulus and shear strength of the pure rock sample.

Chapter 6 presents the dynamic responses of stratified samples of glass-rock, sand-rock and rock-sand-bentonite samples under RLTTs. Further studies were conducted to investigate the effects of the glass content, location and number of the addition layers. The effect of moisture content on the dynamic characteristics of GR layers is also investigated in this part of the study. A comparison between the dynamic responses of the homogenous and the layered techniques is presented in this chapter.

Chapter 7 presents numerical works conducted to develop a model for predicting the resilient modulus of granular materials. The works employ different preliminary parameters and AI models to develop a numerical model. Firstly, the ANN was employed in this study to build a new model using a wide range of basic parameters selected from previous studies on base and subbase materials. Based on the first stage results, the GP was employed to develop a theoretical model to predict resilient modulus of base and subbase materials.

In final stage of this thesis, Chapter 8 provides a brief summary of the conclusions drawn from the experimental and the empirical results. Some limitations and recommendations for future study also presents in Chapter 8.

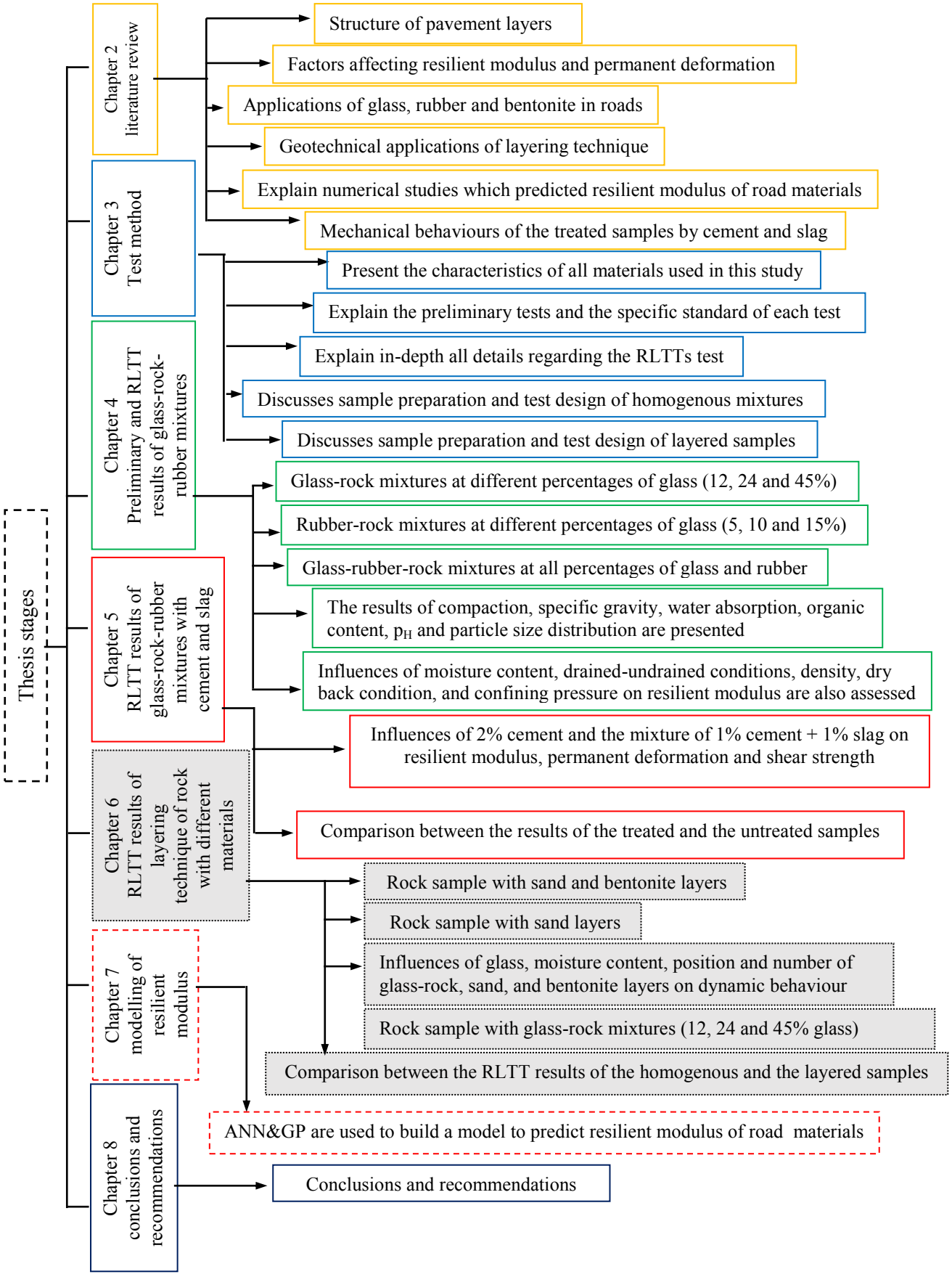

Figure 1.2 An overview of the thesis arrangement

Chapter 2: Literature Review

2.1 Introduction

The primary purpose of this chapter is to review recent research into the preliminary and dynamic characteristics of unbound granular materials mixed with different waste materials in road applications. The first part begins by describing pavement types and the benefits of using multiple layers in road construction. The next section describes in greater details the flexible pavement layers, their engineering characteristics and elastic-deformation behaviour under dynamic impacts. It also explains the factors influencing resilient modulus (M_r) and permanent deformation (P_d) such as moisture content, density, gradation, shape, fine material and stress. Also, a brief review of using natural crushed rock in road applications is summarised. Attention is then drawn to the development of using waste materials such as glass and rubber as alternative materials in road applications. The section that follows will focus on layering techniques in geotechnical applications. A brief report will outline some applications of layered techniques, such as single-layered and multilayered techniques. These applications have been used to solve critical issues in geotechnical applications in recent years. Another section of the existing study discusses the possibility of using bentonite material as a binder material with soils during previous studies.

By reviewing previous studies, the stabilisation of road materials is discussed in this chapter. Fine cementitious materials, such as cement and slag, have been commonly used in stabilising the granular materials in Western Australia. Thus, a review of experimental works assessing the dynamic behaviour of crushed rock with various percentages of cement is presented. The next section reviews different studies used slag and fly ash to improve the soil characteristics in road applications. The final two sections of this chapter provide details of the proposed research program strength, and the previous studies that have used artificial neural network (ANN) and genetic programming (GP) models in recent engineering applications. Figure 2.1 illustrates the structure of Chapter 2.

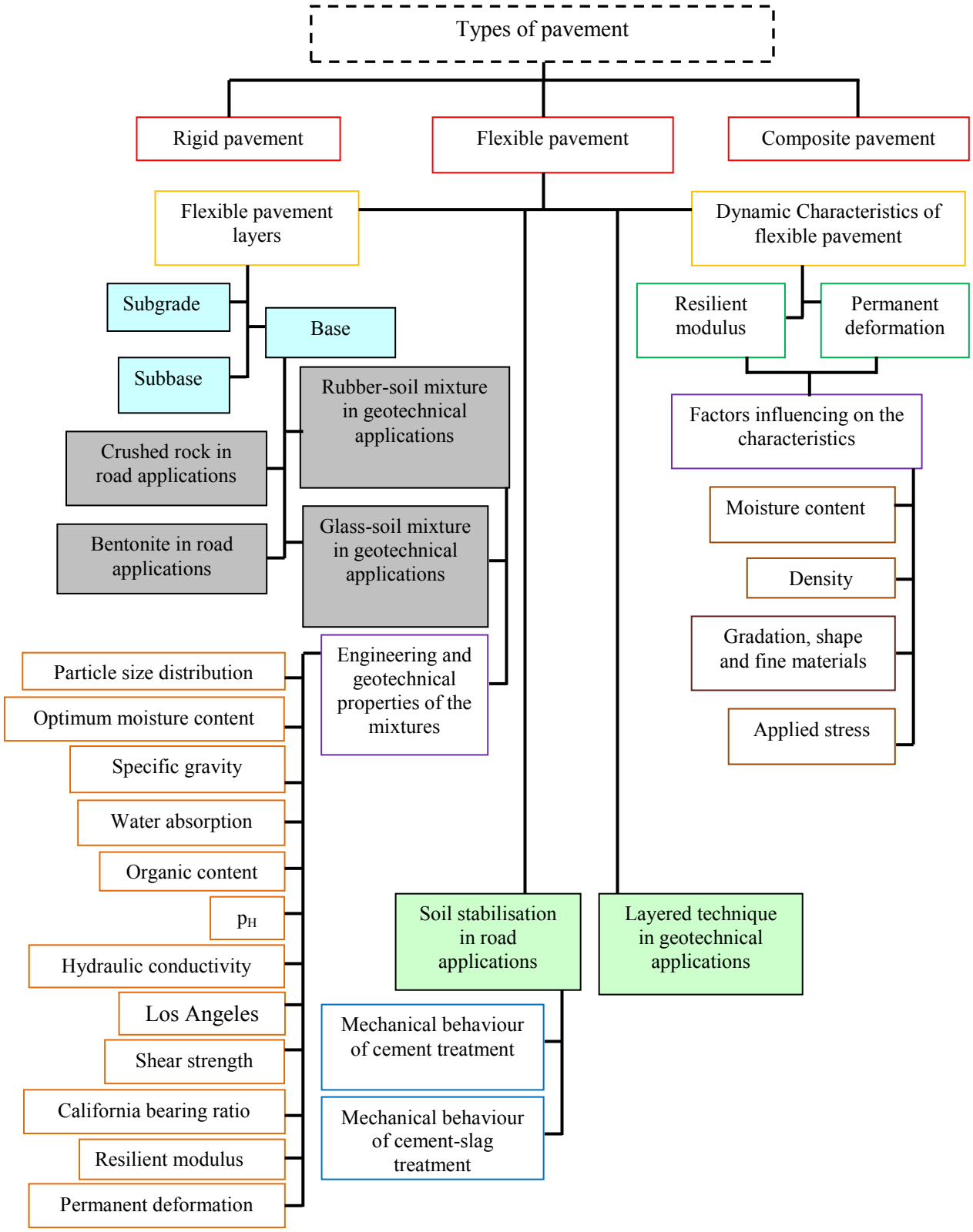

Figure 2.1 An overview of the literature review chapter

2.2 Types of pavement

The function of a multilayered pavement system is to distribute the load of the vehicle from the surface layer to the natural layer underneath. The multilayered pavement can be classified into three main types: rigid, composite, and flexible pavement. In general, the structure of the rigid pavement is designed to improve the road performance under dynamic and environmental impacts. According to American Foundrymen's Society (2004), the structure of rigid pavement consists of different soil layers underneath its surface. The first layer is the concrete layer, which has direct contact with vehicle loads and should has the highest strength resistance and the minimal deflection under repeated loads, whereas the lower layer consists of a prepared subgrade layer with or without subbase or base layers. Figure 2.2 details a typical section of rigid pavement. The second type of multilayered pavement is the composite pavement, which typically consists of a hard asphalt layer over a plain concrete base layer. No further discussion of the rigid or the composite pavements is made in this study, because that is beyond the scope of this research. Flexible pavement is the third type of the multilayered pavement and in general, this type consists of several layers of granular materials located between the surface and the subgrade layers. The typical structure and materials of the flexible pavement and a review of relevant literature are presented in the next sections.

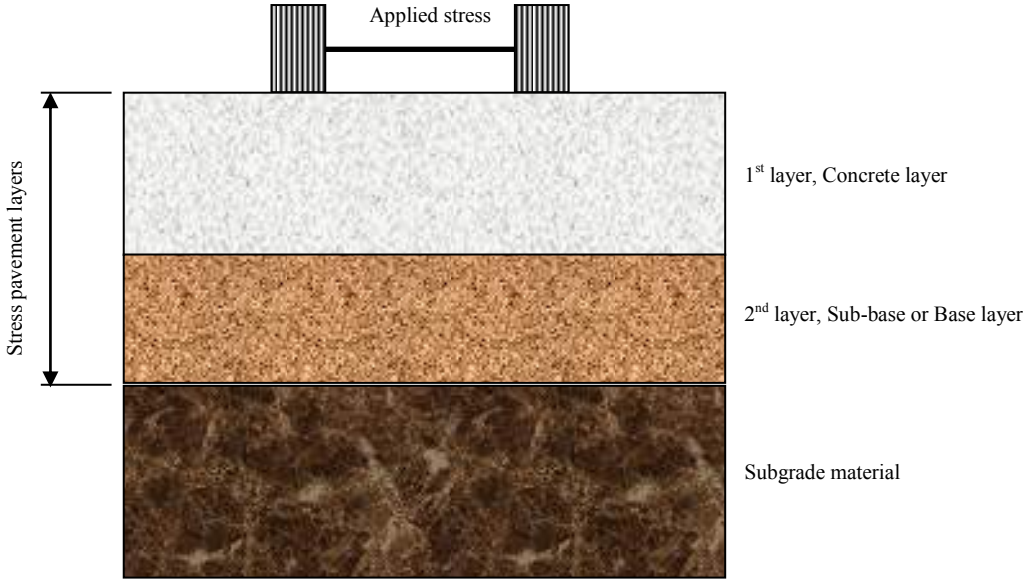

Figure 2.2 Typical section of rigid pavement

2.3 Flexible pavement

Since the 1920s, flexible pavement has been used in a wide range of highway engineering projects as a multilayered system. Before explaining the construction system of flexible pavement, it is necessary discussed the mechanism of the vehicle load distribution. As explained in section 2.1, wheel loads are distributed from the surface layer through granular materials to the natural soil underneath. The surface layer is exposed to heavy repeated loads from vehicles and to different environmental impacts which can cause cracks or deep potholes in the surface. Thus, regular maintenance and repairs for the surface are required during the pavement's life which can be expensive. Despite its regular maintenance and the initial construction costs, flexible pavement is still less expensive than other types of pavement. In detail, flexible pavement is a combination of several layers laid down on the subgrade layer (natural ground); the task of these layers is transmitting the vehicle loads from the road surface to the natural layers safely, and providing a comfortable service for the road users. Based on the specific road design requirements (American Foundry men's Society, 2004), the flexible pavement layers consist of different materials have unique physical, mechanical and chemical properties. Before proceeding to describe flexible granular materials, it is necessary to clarify exactly how pavement layers are ordered. The layers are sorted according to their resistance to vehicle stress and therefore, the materials which have the highest resistance should located on the top, while the lowest resistance should located at the bottom. More details about this system will be discussed in next section. A classic example of flexible pavement layers is presented in Figure 2.3.

2.3.1 Subgrade layers

A subgrade layer is a foundation of natural soil or prepared materials compacted above the natural soil (Sharp, 2005). It is difficult for subgrade materials to endure repeated traffic loadings and thus, this issue has received considerable research attention. Many techniques have been employed to solve this issue and the multiple-layer system is one of these techniques, where the road stresses are transmitted through the base and subbase layers until reaching the subgrade layer. Hence, different layers are paved between the subgrade layer and the road surface. Soil stabilisation technique is also a practical way to improve the dynamic behaviour of

subgrade layer and that could provide further support to pavement layers and undoubtedly reduce the subbase layer thickness (Nikraz, 2004).

2.3.2 Subbase layers

Usually, a subbase layer consists of granular materials paved between the subgrade and base layers. Although it cost more, subbase materials have higher stiffness, strength, and more resistant to deformation than the subgrade materials. There are also some differences between base and subbase materials; subbase materials have less stiffness and resistance than base materials but it is cheaper. In fact that the traffic pressure spreads over a wider area than the contact area between the tyre and the pavement surface and therefore, the designers sometimes construct more than one layer of subbase materials to provide extra resistance against wheel stresses.

2.3.3 Basecourse layer

A base layer is a layer of unbound material located beneath the surface layer. Since the base layer is close to the surface, it normally supports the asphalt surface layer and carries most of the wheel loadings. Therefore, it plays a crucial role in reducing the effects of tensile and surface deformation. Special specifications and high requirements that must be followed before proceeding to design the base layer (Sharp, 2005), and a wide range of high-quality materials can be used to construct the base layer such as natural crushed rock, crushed aggregate, stabilised soils, cemented unbound materials and broken stone.

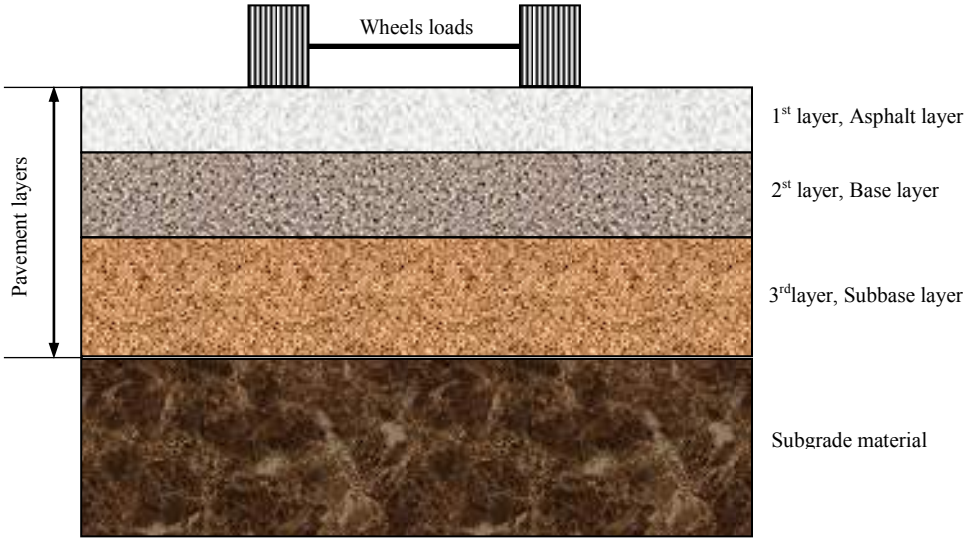

Figure 2.3 Typical section of flexible pavement

2.4 Dynamic characteristics of unbound granular materials

Before proceeding to construct any paved road, design of the pavement layers is required, considering things such as thickness and type of materials used. One of the main important aspects in flexible pavement design is the resilient modulus (M_r) and therefore, this section describes the philosophy of the resilience behaviour of granular materials. It is important to note that different tests are employed to assess the dynamic characteristics of granular materials. One of these tests, which can evaluate the dynamic behaviour of different materials under wheel loads, is repeated loading triaxial test (RLTT). The test is among the most widely used to measure the permanent deformation (P_d) and M_r of different soils in road applications. In general, RLTT is conducted under different axial and confining pressure conditions (Jameson, 2010). Recently, Nowamooz, Ho, Chazallon and Hornych (2013) employed the RLTT to assess the dynamic behaviour of granular materials by estimating the M_r and P_d values. One of the most important parameters of the RLTT is the recoverable deformation which is a temporary change in the dimensions of the unbound granular materials after removing the applied loads. It is important to know that the resilience behaviour of the granular materials depends on the loading conditions. For example, if the strength of the granular materials is greater than the applied load, the soil can be considered undergo elastic deformation and the shape is wholly or partially recoverable, whereas non-recoverable deformation occurs when the applied load is greater than the strength of the material. More detail about the material behaviour during a cycle of repeated loadings is presented in Figure 2.4.

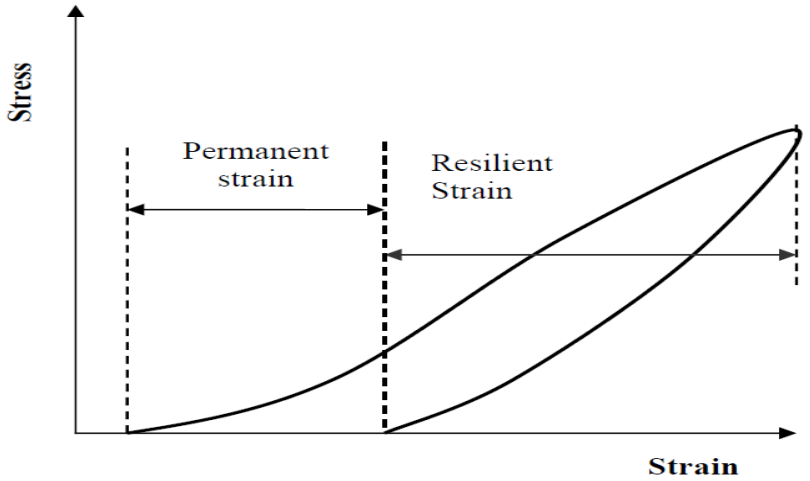

Figure 2.4 Typical behaviour of granular materials during the repeated load cycle (Lekarp et al., 2000)

2.4.1 Resilient modulus

Resilient modulus (M_r) is a critical parameter in the dynamic performance of granular materials under repeated loading triaxial test (RLTT); it has been identified as a major contributing factor in pavement design over past decades. M_r is a function of the stiffness of a material and it is important to note that the first systematic study of M_r was by Seed, Chan and Lee (1962). The authors reported that the M_r is equal to the applied deviator stress divided by the recoverable strain for rapid loading. Based on RLLT, the stress-strain correlation can be expressed according to Equation 2.1:

$$M_r = \frac{(\sigma_1 - \sigma_3)}{\varepsilon_r} \quad or \quad M_r = \frac{\sigma_d}{\varepsilon_r} \tag{2.1}$$

Where:

M_r =Resilient modulus

σ_1 = Primary principal or axial stress

σ_3= Minor principal or confining stress

σ_d = Deviator stress

ε_r= Axial resilient strain

In addition, Seed, Chan and Lee (1962) also provided strong experimental evidence that the outputs of the RLTT can be successfully employed in pavement design. Moreover, Senol et al. (2002) confirmed that M_r is the most crucial factor in pavement design in terms of pavement design and elastic responses of granular materials under repeated loads.

2.4.1.1 Factors influencing resilient modulus

The following sections summarise the main factors that influence the M_r of unbound materials. These factors have been explored by previous studies and considered the most important factors to characterise the resilience behaviour of unbound granular materials. An early study of Lekarp and Dawson (1998) explored the influences of stress, density, moisture content, fine materials content, gradation, number of load cycles, stress history, load duration, frequency and load sequence on the M_r value. Further explanations of the most essential factors are described below:

Moisture content plays a vital role in the dynamic performance and elastic response of granular materials. Many previous studies have investigated the relation between

moisture content and the M_r value. Early investigations were carried out by Johnson (1974), and Yoder and Witczak (1975). An inverse correlation was noticable between the M_r and the moisture content of granular materials. More recent evidence of that correlation was found by Rahman and Erlingsson (2016), who concluded that soil with the lowest moisture content has the highest M_r. They reported that the increase in moisture content caused an increase in pore-water pressure and thus, decreased the effective stress and consequently decreased the M_r value of unbound materials.

Throughout history of pavement materials, density of is one of the most important factors affecting the M_r value. It can positively affect the resilience behaviour of unbounded materials (Levey & Barenberg, 1970; Smith & Nair, 1973; Kalcheff & Hicks, 1973. In contrast to earlier conclusions, density was considered to have an inconsequential influence on M_r (Thom & Brown, 1988). Following this, Barskale and Itani (1989) and Vuong (1992) substantiated previous findings that there is a remarkable positive correlation between density and M_r. When applied load is transmitted through particles, the contact and the interlocking between the particles are the optimum in the dense state which resulted in minimal deformation and thus, high M_r.

Moreover, a considerable number of studies have been published on the effects of the gradation, shape, and fine mateials on the M_r of granular materials. A positive correlation was reported by Pappin (1979) and Thom and Brown (1988) between M_r and well-graded materials. The small and fine particles of well-graded materials fill the voids between the course particles resulting in high density and consequently, high M_r. Also, Barskale and Itani (1989) and Arnold (2004) investigated the effect of particle shape on M_r. Their findings reported that the shape of particles played a significant role in the evaluation of the M_r of unbound materilas. They also concluded that the effect of shape on the M_r was more significant in granular materials than that in other soils, and the angular aggregates showed higher M_r than the rounded particles. In contrast to the above conclusions, granular gravel showed higher modulus than the crushed one (Lekarp, Isacsson & Dawson, 2000). The presence of fine materials as a result of crushing processes affected the grain size distribution and the stability of the aggregate fabric, and that could be the reason for the conflicting results. Several studies have been investigated the effect of fines on the resilince behaviour of granular materials. After a series of repeated loading tests

performed by Hicks and Monosmith (1971) on crushed aggregate samples, a remarkable reduction in the M_r was associated with the fine materials increase. In contrast, Kalcheff (1974) and Chou (1976) found that the fine materials do not affect M_r of granular materials. The contrasting results in the previouse studies could be related to the role of shape and the ratio of the fine materials in enhancing the soil fabric. Several years later, the correlation between M_r and the grain size was comprehensively investigated by Rada and Witczak (1981), who concluded that course materials reported higher M_r than fine materials.

The effect of stress on the M_r of the unbound materials is well understood from the previous research studies. Many studies have investigated the effects of stress level on the resilience behaviour of granular materials (Lekarp et al., 2000; Van Niekerk, Molenaar & Houben, 2002). Morgan (1966) and Hicks and Monismith (1971) reported that granular materials with low levels of mean stress showed higher M_r than that with high stress levels. The influence of the shape and the duration of the stress pulses on M_r have also been highlighted by Monismith, Seed, Mitry and Chan (1967), Monismith, Hicks and Salam (1971) and Mohammad (1994). They stated that there was an insignificant effect of the duration of the stress pulses on the M_r value. After that, Maher et al. (2000) investigated the effects of principal stresses on M_r of granular materials. Their findings concluded that there was a positive correlation between the stress and the M_r value. The positive correlation could be attributed to role of the stress increase in enhancing the stability of the soil fabric. In another case of investigation, Lekarp et al. (2000) and Kim and Tutumluer (2006) studied the effect of stress history on resilience behaviour of granular materials. The results illustrated that the preloaded samples showed higher M_r than those with no loading history.

2.4.2 Permanent deformation

Permanent deformation (P_d) is the strain remaining after the unloading stage; it is considered one of the most crucial parameter in the dynamic responses of granular materials. Figure 2.5 illustrates the responses of resilience strain and permanent strain to cyclic loading. Basically, P_d provides valuable insights into the elastic-plastic correlation of soils during loading stages.

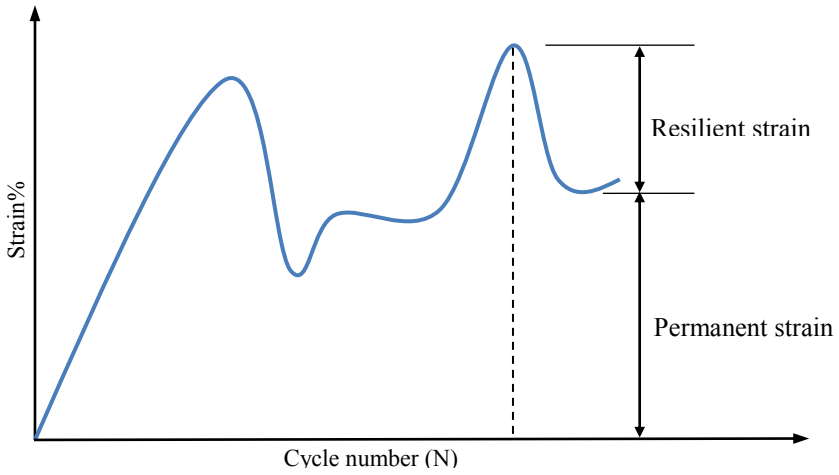

Figure 2.5 Characteristics of resilient strain (ε_r) and permanent strain (ε_p) (De Vos, 2006)

2.4.2.1 Factors influencing permanent deformation

This section will focus on reviewing the main factors affecting the P_d of granular materials. Barskale and Itani (1989) and Lekarp (1999) explored various influences such as stress, density, moisture content, fine content, grading size, stress history, load duration, frequency and load sequence. More details on these factors will be described below:

Throughout the history of granular materials, moisture content has been identified as a critical influence on P_d. Vuong (1992) concluded that a sample with the lowest moisture content showed less P_d than those with the higher contents. Subsequently, Gidel et al. (2001) and Khogali and Mohamed (2004) studied the effect of moisture content on the P_d of granular materials. The results demonstrated a positive correlation between the moisture content and the P_d. The degree of saturation has also been highlighted in many studies. Based on the dynamic responses of granular materials, the relation between the degree of saturation and the P_d has been widely investigated by Thom and Brown (1987), and Bejarano and Harvey (2002). These studies reported a positive correlation between the P_d and the moisture content. Arulrajah et al. (2014) also supported the above conclusion that the moisture content is a potentially important factor influencing the P_d. Figure 2.6 shows the correlation between the optimum moisture content (OMC) and the P_d of fine recycled glass/recycled concrete aggregate mixture at a 15% glass content. The permanent strain value decreased when the moisture content decreased from 81% (OMC) to

74% (OMC), and then increased with decreasing the moisture content to 68% (OMC).

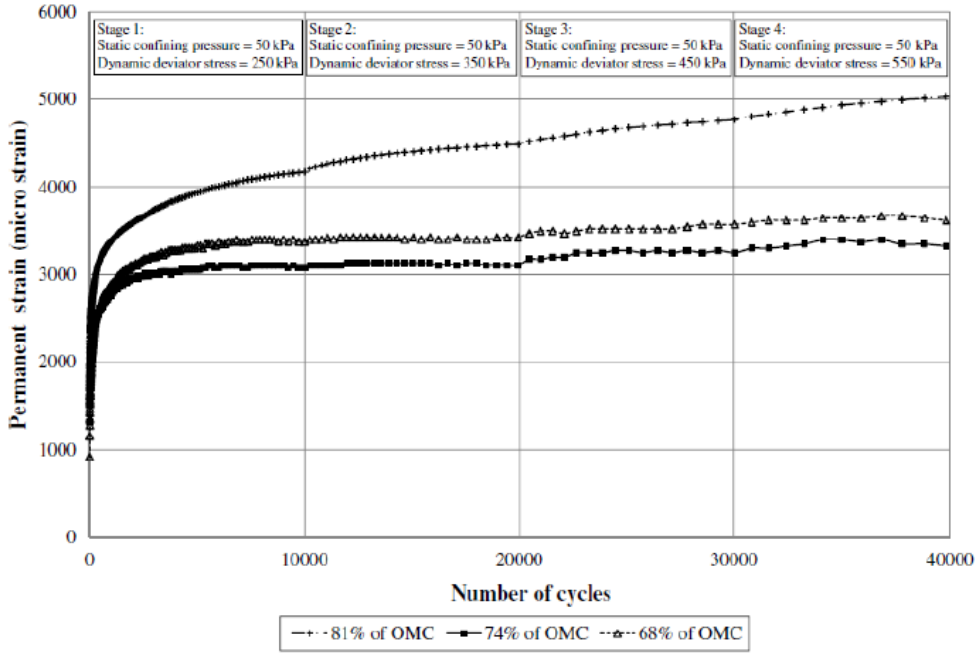

Figure 2.6 Permanent deformation of a glass-concrete aggregate mixture at different moisture content with loading cycles (Arulrajah et al., 2014)

Several important studies have indicated that P_d was influenced by the density of unbound materials (Thom & Brown, 1988; Theyse, 2002b). Lekarp et al. (2000) and Cheung and Dawson (2002) attempted to study the correlation between density and the P_d of granular materials. Their conclusions were indicated that the densest materials showed the lowest deformation. Other studies have considered the correlation between the compaction degree and the P_d of granular materials (Van Niekerk et al., 2002; Magnusdottir & Erlingsson, 2002), who stated that the degree of compaction can play a remarkable role in the P_d, where a positive correlation was noticeable between the degree of compaction and the resistance of materials against deformation. The positive effect of density on the resistance of granular materials could be related to the role of density in reducing the compressibility of soil and consequently, lower P_d.

Physical properties of the soil grains such as shape, gradation, and the surface roughness are other main influences on dynamic characteristics of pavement materials. The loads in granular materials are transmitted from a grain to another by contact. Thus, the strength required to withstand these loads is directly dependent on

the physical properties of the soil grains. High levels of interlocking are achieved if the surface is rough and the shape is angular. Otherwise, smooth-surfaced and rounded shapes produce low levels of interlocking. Lekarp et al. (1996) found that the soil gradation has notably more influence than the compaction. Van Niekerk et al. (2002) confirmed what Thom and Brown (1988) concluded concerning the importance of gradation on the P_d of granular materials. Some of the previous studies reported that the well graded materials showed less P_d than the uniform materials (Lekarp et al., 2000; Núñez et al., 2004). Based on the parameters influencing deformation of gravel, Lekarp et al. (2000) focused on the shape parameter. Their results indicated that the angular gravels showed more resistance to deform than the rounded gravels. These results were consistent with Huurman and Molenaar (2006) who also focused on the influence of particle shape of angular aggregates on P_d. Their findings concluded that the angular aggregates reported lower P_d than the rounded ones. This behaviour was attributed to the role of angular shape in enhancing the stability and the interlocking of aggregate and consequently, low P_d. In addition, Cheung and Dawson (2002) conducted a series of dynamic tests on granular materials and highlighted the importance of particles shape on P_d. According to their results, the particles roughness and the surface friction play significant roles in the materials response against P_d. The effect of fine materials on the granular materials deformation has been reported in many previous experimental studies. Magnusdottir and Erlingsson (2002) concluded that a specific percentage of fine materials can be considered as a critical factor in P_d. They also concluded that 9% fine materials content is required to improve the P_d resistance of granular soils.

Stress is another factor influencing the mechanical characteristics of pavement materials. The findings of Wolff and Visser (1994) and Lekarp et al. (1996) concluded that the stress increase from low to high level caused in changing the P_d state from elastic to plastic. These findings were consistent with the other following results which confirmed the key role of stress on P_d, where the rate of P_d directly increased with the stress increase (Lekarp et al., 2000; Van Niekerk et al., 2002). Whereas, the investigation of Werkmeister et al. (2003b) concluded that the granular materials underneath the asphalt layer are in a critical state when exposed to high levels of repeated stresses. The conditions which clarify the effects of confining pressure and shear stress on the P_d have been explored by many previous studies (Khogali & Mohamed, 2004; Huurman & Molenaar, 2006), who stated that the

effects of confining pressure and shear stress on P_d were significant. More work on the influence of the loading history state of soils was performed by Lekarp et al. (2000) and Kim and Tutumluer (2006). The results of repeated loading triaxial tests showed that the preloaded soil showed less P_d than the soil without a stress history.

2.5 Crushed rock in road applications

This section provides a brief review of using crushed rock as a base or subbase material in road applications. Base and subbase materials are the most-used groups of granular materials in road applications and they have also been extensively used in pavement layers around the world. Even though the asphalt industry has reached an advanced stage of development, the foundation layers and their components such as base and subbase materials are still essential components in base and subbase layers and play key roles in pavement systems. Many types of natural materials such as gravel, crushed waste rock, and broken stone are used as foundation materials in pavement layers (Nikraz, 2004). In general, the foundation material is a type of construction material that transmits traffic loads directly from the surface to the layers underneath. Around Australia, one of the essential natural materials commonly used underneath the pavement surface is the crushed rock. The crushed rock aggregate is different from other construction aggregates such as gravel, which usually have roundly shapes produced by the natural processes of weathering. The crushed rock is produced through manufacturing processes including mining, breaking and crushing and consequently, a deep understanding of the behaviour of crushed rock is essential in the design and analysis of pavement layers (Watson, 1995; Molenaar, 2005).

2.6 Waste materials in road applications

The purpose of this section is to review the literature on waste material groups used in geotechnical applications. Waste materials are usually referred to as any materials that are discarded after use in commercial, industrial and human activities. According to the Australian Bureau of Statistics (2016), 1.5 tonnes of waste materials are produced per year per capita, including food, paper and glass and thus, the consumption of waste materials as a substitute for natural substances in immense quantities will result in significant environmental and economic benefits. There are

many types of waste materials used in road construction, such as glass, tyre rubber, crushed concrete, roofing shingles and slag.

2.6.1 Crushed glass in road applications

Waste glass is one of the most widely used groups of waste materials in road applications. Recycling waste glass is less expensive than using natural sand in glass industry but separating glass according to colours is a marked obstacle and therefore, recycling waste glass is considered economically inefficient. If waste glass were to be used in roadway construction, colors separation will not be necessary and could be crushed and used directly. From this perspective, consumption of thirty-six million tons of waste glass in Australia per year in road applications could make a significant improvement in health, environment and economics.The suitability of glass-rock mixtures has been previously investigated through different assessments. Concerning the assessment of using different colours of crushed glass with granular materials, Wartman et al. (2004) and Ali et al. (2011) did not identify any significant differences between the results of the mixtures containing different colours of glass. On the other hands, different limitations and recommendations were recorded in the previous studies related to the glass-granular materials mixtures containing high percentages of glass (Viswanathan, 1996). A general assessment of glass-rock mixtures was performed by Ali et al. (2011), different laboratory tests on glass-rock mixtures were conducted to estimate particle size distribution, specific gravity, workability, hydraulic conductivity and shear strength of the glass-rock mixtures. The results showed a positive correlation between glass content and the workability and hydraulic conductivity of the new mixtures. A significant increase was also found in water absorption and consolidation due to the fine materials content increase, while a significant reduction in M_r and P_d was associated with the fine materials increase. Based on the physical and the mechanical characteristics of glass-aggregate mixtures, Disfani et al.(2011) found many similar characteristics between crushed glass and crushed aggregates. Recently, Gischig et al.(2015) assessed the effect of glass content on shear strength of the base course materials. The results of assessment illustrated a negative correlation between shear strength and glass content. They also indicated that a glass-rock mixture containing 15% of glass with a maximum size 4.75mm showed good workability and satisfied the rock sample requirements for shear strength. Different studies have also focused on the influence

of crushed glass on basic and geotechnical characteristics of different granular materials,as summarised below.

2.6.1.1 Particle size distribution and organic content of glass-granular materials blends

Many previous studies have focused mainly on the effect of waste glass on granular materials classification before the compaction efforts. However, few studies are available on the effect of waste glass on classification of granular materials before and after compaction. The effect of glass content on the grain size distribution curves of limestone before compaction was investigated by Viswanathan (1996). A wide range of glass contents were employed to prepare different glass-limestone mixtures containing 5%, 10%, 20% and 50% glass by total weight of the limestone sample. The results indicated that the glass-limestone mixtures with 5% and 10% glass satisfied the specifications of the base materials. On the basis of the glass-soil mixture classification, several studies have conducted a series of sieve analysis test before and after the compaction effort. The findings of these studies performed a preliminary judgment on the suitability of using the mixtures in road construction. In this case, Ali et al. (2011) have investigated the effect of glass on the pure rock classification. A wide range of glass contents with a maximum size of 4.75 mm was mixed with natural rock with a maximum size of 20 mm. The gradation curves of the new mixtures before and after compaction were compared with the upper and the lower limits of VicRoads (road authority of Victoria, Australia). Research findings concluded that the gradation curves of the glass-rock mixtures before compaction almost satisfied the subbase material limits. Even the rock sample with 40% and 50% glass contents did not satisfy the upper limits set after compaction effort; all mixtures were considered to be well graded and suitable for road applications. An increasing amount of waste materials has encouraged Arulrajah et al. (2014) to study the suitability of reusing two types of waste materials in pavement layers.The results of USCS classification before and after the compaction effort indicated that the new mixtures of waste glass-recycled concrete aggregate and waste glass-crushed rock were classified as poorly graded sand with silt material (SP-SM). One of the most significant findings of the research is that the addition of waste glass resulted in a slight divergence of the gradation curves with the upper and the lower limits of base course materials of the aggregate and rock soils.

The presence of organic materials play a significant role in the stability of soils under dynamic loadings (Reinhard & Drefahl, 1999) and therefore, backfill materials or pavement layers should be free of or at the minimal organic materials. A series of organic content tests were conducted on samples prepared by mixing crushed rock materials with different waste glass contents to examine the influence of waste glass on the organic content of the glass-rock mixture. Despite there was a wide range of debris in waste glass, a significant reduction in organic content of the waste glass-crushed rock mixtures was associated with the glass content (Ali et al., 2011). The findings of this study also reported that the organic content of waste glass and crushed rock is below 1% which indicates negligible organic levels. The above findings are consistent with the findings of Arulrajah et al. (2014) who examined the effect of the fine glass content on the organic content of waste rock and recycled concrete aggregate materials. The findings of this study concluded that the organic content of the aggregate reduced from 3% to 2.84%, 2.65%, 1.95%, 1.71%, 1.54, and 1.41% when mixed with 10%, 15%, 20%, 30%, 40% and 50% glass, respectively.

2.6.1.2 Optimum moisture content, maximum dry density, and specific gravity of glass-granular materials blends

The optimum moisture content (OMC) and the maximum dry density (MDD) played a substantial role in dynamic behaviour of granular materials. The presence of glass might affect the moisture-density correlation of granular materials because of the fact that the glass particles have zero water absorption. Hence, the literature on the moisture-density correlation of glass-soil blends was highlighted in many previous studies. Senadheera, Nash and Rana (1995) conducted a modified Proctor compaction test on glass-caliche blends to investigate the effects of waste glass on the OMC and the MDD of the blends. The research findings pointed that the OMC decreased with increasing glass content. Viswanathan (1996) investigated the effect of the glass presence on the OMC and MDD of the limestone material. The overall results indicated that the presence of glass had a considerable effect on the compaction curves of limestone at all glass percentages. Basically, pure glass particles have low density compared to those of aggregate or limestone material; therefore, a considerable reduction was noticeable in the MDD of glass-limestone mixture with further glass content. The findings also illustrated a negative correlation between the OMC of the glass-limestone mixtures and the glass content. This result

was consistent with the findings of Ali et al. (2011), who reported that the MDD of rock material decreased with the glass content increase, and the compaction curves of the glass-rock mixtures showed less curvature than those of the natural rock. The reason for this behaviour might be related to the glass material itself, where the glass particles are less sensitive to water than the natural soil. In addition, the OMC of pure rock material increased when the glass content increased up to 30% and then decreased when the glass content increased to 50%. The different results that have been reached by studies have made the influence of glass on the OMC of natural soils a controversial topic. On this topic, a series of laboratory tests was conducted by Arulrajah et al. (2014) on fine recycled glass with waste rock and recycled concrete aggregate to assess their suitability as base and subbase materials. Different fine glass contents (10%, 15%, 20%, 30%, 40% and 50%) were mixed with waste rock and with recycled concrete aggregate. The density of fine glass is less than the waste rock density, and this could be the reason of decreasing the MDD values of the crushed rock sample when mixed with 10%, 15%, 20%, 30%, 40%, and 50% fine glass. Regarding the effect of fine glass on MDD, the behaviour of recycled concrete aggregate was the same as that of waste rock when mixed with the same proportions of fine glass. There are more variations in this study regarding the dry density-moisture correlation. For example, the OMC values of waste rock decreased significantly from 9.25% to 8.25% when waste rock was mixed with 10% fine glass, and then increased to 8.6%, 9.1% and 9.3% when mixed with 15%, 20% and 30% fine glass, respectively. After that, a steady reduction in the OMC occurred after mixing with high percentages of glass (40% and 50%). In the case of concrete aggregate-fine glass mixtures, an extensive variation in the OMC of the mixtures was associated with the glass presence. The OMC values of recycled concrete aggregate decreased steadily from 12.3% to 11.5% when recycled concrete aggregate mixed with 10% and 15% of fine glass, respectively; while the values increased directly to 11.7% and 11.8% when the aggregate mixed with 20% and 30% of glass, respectively. With high ratios of glass/aggregate (50%), the OMC of the mixtures decreased to 11%.The variation in the MDD and the OMC values reported in the study could be attributed to the various particle sizes of the new mixtures, where the smaller particles fill up the voids between the course particles, causing an increase in the dry density of the mixture. Furthermore, the angular shape, the smooth surfaces,

and the low sensitivity of the fine glass particles directly influenced the OMC and the MDD of the rounded aggregate particles.

The specific gravity of soil is defined as the ratio of the unit weight of a material in air to the unit weight of distilled water at 4°c. In general, the specific gravity of glass is about 10% lower than that of the natural aggregate (Das, 2007). It was therefore expected that the specific gravity of glass-natural aggregate blends would be lower than the specific gravity and the dry density of natural aggregate.This fact was consistent with the findings of Ali et al. (2011), who reported that the specific gravity value of waste glass approximately 15% lower than the natural aggregate and therefore, a sharp reduction in specific gravity of the natural aggregate occurred with the glass presence. The influence of glass on specific gravity of the unbound materials was an area of uncertainty because of the divergent results in the previous studies. The above differing results are consistent with the findings of Arulrajah et al. (2014), who reported that the fine glass particles causing an increase in the specific gravity of the recycled concrete aggregate and the waste rock soils, despite the specific gravity of glass was lower than that of recycled concrete aggregate and the waste rock materials.

2.6.1.3 Water absorption and hydraulic conductivity of glass-granular materials blends

Water absorption is the amount of water that is absorbed by particle surfaces. Several critical factors can influence the absorption of granular materials; one of these factors is the nature of the particle's surfaces. It is important to know that the glass particles have low ability to absorb water (pure glass has zero water absorption), while the fine materials absorb more water than the course ones. Ali et al. (2011) studied the effect of glass on water absorption of the glass-rock mixture. The findings of this study concluded that a clear reduction in water absorption of the mixtures was associated with the glass increase. The smooth surfaces of the glass and its specific fabric are the main reason for reducing the ability of the rock-glass mixtures to absorb water.

Regarding the effects of the size and shape of glass particles on the water absorption of glass-soil blends, a series of absorption test was conducted by Arulrajah et al. (2014) on both course and fine glass aggregates. The findings reported insignificant differences between water absorption of the course glass-aggregate mixtures and the aggregate. In fine glass case, the absorption of fine glass-aggregate mixture at 10%,

15% and 20% of fine glass was higher than the aggregate material, while the addition of glass (30%, 40% and 50%) resulted in a rapid reduction in the absorption of aggregate. It is important to know that the lack of course particles (larger than 4.75mm) and existence a wide range of paper, plastic and food in waste glass could be the main reason for the varied results of water absorption of glass-granular materials that discussed in this section.

The hydraulic conductivity refers to the flow of soil water, which depends on the soil type. According to the findings of Terzaghi, Peck and Mesri (1996), waste glass-unbound material mixtures are classified as low-permeability materials, as natural aggregates. While the findings of Arulrajah et al. (2012) reported that the hydraulic conductivity of fine recycled glass to be a high permeability material similar to sand.The different results that have been concluded by many previous studies have made the hydraulic conductivity of glass-unbound material mixtures a controversial topic. Viswanathan (1996) performed a series of laboratory investigations to assess the suitability of using glass-limestone mixtures in pavement works. The results of hydraulic studies showed that the average hydraulic conductivity of a 50:50 glass: lime stone mixture was about 0.011 cm/sec, while the hydraulic conductivity of pure limestone was 0.051 cm/sec. Consequently, the hydraulic conductivity of limestone decreased with the glass content increase. These results are similar to those of Poon and Chan (2006), who reported a steady increase in hydraulic conductivity of the glass-rock mixture with the glass content increase. Arulrajah et al. (2014) also performed hydraulic conductivity tests on two types of mixtures, fine glass-recycled cement aggregate and fine glass-crushed rock mixtures. The blends were prepared and mixed at the OMC, then compacted to 98% of the MDD. The constant head method was used to determine the hydraulic conductivity of the mixtures. In general, the aggregate and rock were considered low permeability materials when mixed with different glass contents. The findings of this research also concluded that an increase in the permeability value of the aggregate and the rock was occurred when mixed with 10%, 15%, 20% and 30% of glass, this finding was consistent with the findings of Viswanathan (1996) and Poon and Chan (2006). Unexpected results were informed by Arulrajah et al. (2014), a gradual decrease in permeability of both the aggregate and the rock was associated with an increase in the glass content to 40% and 50%. Several factors can explain these discrepancies in the results above. The differences in particle size distribution, shape, gradation, suppliers have been

considered to be the primary factors affecting the hydraulic conductivity of granular materials, whereas the permeability of unbound-glass mixtures is affected by the glass sources and the amount of debris. In addition, waste glass is quite sensitive to the crushing process and therefore, the particle size distribution, shape, and gradation of crushed glass may be exposed to the conversion as a result of crushing and compacting impacts. Consequently, the same crushed glass can show different geotechnical properties when mixed with granular materials, and that could explain the contradicting results reported in the previous works.

2.6.1.4 Shear strength of glass-granular materials blends

Shear strength is the most important parameter in the assessment of granular materials behaviour under static and dynamic loads (Clean Washington Center, 1998). The effects of the glass on shear strength characteristics of granular materials were investigated widely in the previous studies. In 2008, Das reported that the internal friction angle of waste glass is similar to that of angular grains of dense sand. Based on the effect of glass content on shear strength of subbase materials, Viswanathan (1996) concluded that the glass content exerted a remarkable impact on the shear strength of glass-limestone mixtures. The findings of the study indicated that shear strength of the glass-aggregate mixtures decreased as the glass content increase, and the shear strength of the mixture is similar to that of the natural aggregate. Later, Grubb et al. (2006) performed a series of triaxial shear tests to evaluate the suitability of glass-dredged mixtures for road applications. The new mixtures were compacted to at least 95% of the MDD. Mohr circles were drawn, and the internal friction angle values obtained. The results concluded that the internal friction angle of dredged material increased from 34° to 39° as a result of increasing the glass content from 0% to 80%, as shown in Figure 2.7. In general, this result provided strong evidence that granular materials can be substituted with waste glass in road applications and pavement layers.

Some features such as the grains size, shape, and gradation have an important influence on shear strength of granular materials. Disfani et al. (2011) used different sizes of glass, course, medium and fine glass to prepare different samples of rock-glass mixtures. The findings reported an improvement in internal friction angle of the mixtures occurred when using course and medium sizes rather than the fine glass. In addition, the sample of glass-rock mixtures with 20% glass was considered suitable

for pavement applications. In general, the shear strength of the rock-glass mixtures showed very similar to that of the raw materials. Disfani et al. (2012) conducted a series of triaxial loading tests to assess the strength behaviour of different waste mixtures. The findings concluded that using high quality aggregate or using another additive to improve the shear strength behaviour of glass-aggregate blends was highly recommended when used in pavement layers. Recently, an investigation was conducted by Arulrajah et al. (2014) to evaluate the effect of glass content on shear strength of two waste materials, waste rock and recycled concrete aggregate. Their results concluded that the presence of glass can have a negative effect on the cohesion and the internal friction angle of both mixtures.

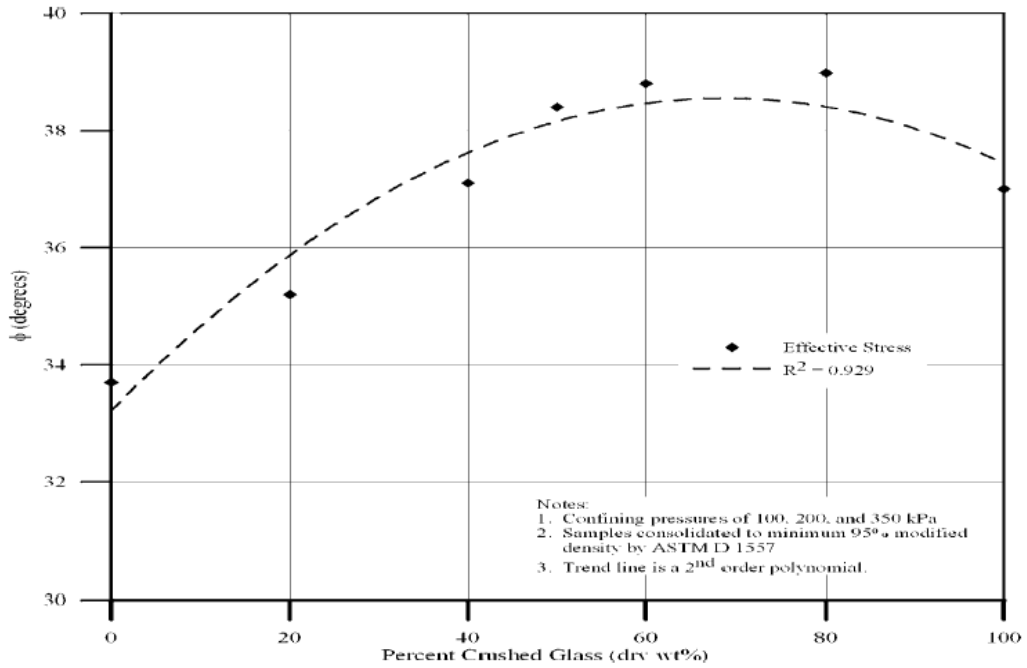

Figure 2.7 Triaxial results for glass-dredged blends (Grubb et al., 2006)

2.6.1.5 California Bearing Ratio and Los Angeles test results of glass-granular materials blends

Some investigations have focused on the mechanical behaviour of glass-aggregate mixtures. Ali et al. (2011) examined the effect of glass content on California bearing ratio (CBR) of different glass-rock mixtures. The results indicated that the mixtures with 10% to 50% glass contents satisfied the VicRoads requirement for subbase materials. Arulrajah et al. (2014) also performed CBR tests on two types of mixtures: waste rock-glass and recycled concrete aggregate-glass. Waste materials were mixed with different percentages of glass (10%, 15%, 20%, 30%, 40% and 50%). As a

result of increasing the glass content from zero to 50%, the CBR values of the waste rock-glass and the recycled aggregate-glass mixtures reduced from 181% to 121% and from 211% to 98%, respectively.

Los Angeles (LA) test or the abrasion ratio is a function of material durability and hardness under the crushing impacts. The previous results indicated that the abrasion ratio of the glass-rock mixtures increased slightly with the glass content increase (Ali et al., 2011). Arulrajah et al. (2014) conducted LA test on different samples of fine glass-waste rock mixtures. The abrasion ratios of the mixtures ranged between 25% and 23%, while those of the fine glass-recycled concrete aggregate mixtures ranged between 27% and 24%. One of the most significant findings of this research is that the mixture with 15% glass content showed the lowest abrasion ratio, and there was an indication that all mixtures were satisfied the maximum LA value for base materials (35%).

2.6.1.6 Resilient modulus of glass-granular materials blends

A considerable amount of literature has been published on the M_r of glass-soil mixtures. The Clean Washington Center (1993) followed the procedure of AASHTO T 294 to investigate the resilience behaviour of glass-rock blends under repeated loads. A significant reduction was found in M_r of the glass-rock blends as the glass inclusion. Senadheera et al. (1995) conducted repeated loading triaxial tests on different samples of glass-subbase mixtures to investigate the possibility of using waste glass in pavement layers. A wide range of glass (20% to 50%) in two different sizes (¼ and ¾ inch) was mixed with subbase material (caliche). Their results concluded that the M_r values of the glass-caliche blends decreased by 15% with the addition of 50% of ¼-inch glass. While the M_r value of glass-caliche blends decreased by 23% with the addition of 50% of ¾-inch glass, where the particle sizes of waste glass played a vital role in the resilience behaviour of the glass-caliche mixtures. In general, a significant reduction in M_r of the glass-caliche mixtures was associated with the glass increase. Rana (2004) performed a series of triaxial tests on different samples of glass-caliche mixtures to assess their stiffness responses. Subbase material (caliche) with a wide range of glass was used to prepare the new mixtures. With up to 30% glass content, M_r of the new mixtures was significantly higher than those of pure caliche. Similar to the conclusions of Rana (2004), Ali et al. (2011) found that a sample of the glass-rock mixture with 30% glass content

appears suitable for use in road layers as subbase materials. An investigation was also conducted by Arulrajah et al. (2014) to assess the effects of glass on the M_r values of glass-rock and glass-recycled concrete aggregate mixtures. A noticeable reduction in M_r of the mixtures was observed with the glass increase. In the main, the results showed that all mixtures satisfied the requirements of subbase material.

2.6.1.7 Permanent deformation of glass-granular materials blends

Based on AASHTO T294-94 procedure, Rana (2004) conducted repeated loading triaxial tests (RLTTs) on glass-caliche mixtures to evaluate their deformation behaviour under repeated loadings impacts. The results concluded that the P_d of the modified mixtures was increased as the addition of glass. Later, Arnold et al. (2008) conducted a series of RLTT to assess the deformation behaviour of glass-aggregate mixtures under repeated loads; Figure 2.8 illustrates the correlation between P_d and the number of load cycles. The P_d of pure aggregate increased with 10% of glass and then decreased with 20% glass. Moreover, a significant reduction in the P_d of aggregate was associated with increasing the glass content to 50%. In general, the glass presence inversely affected the P_d of pure aggregate. This behaviour might be attributed to the role of glass in impairing the stability of the glass-aggregate mixture fabric of and thus, high P_d.

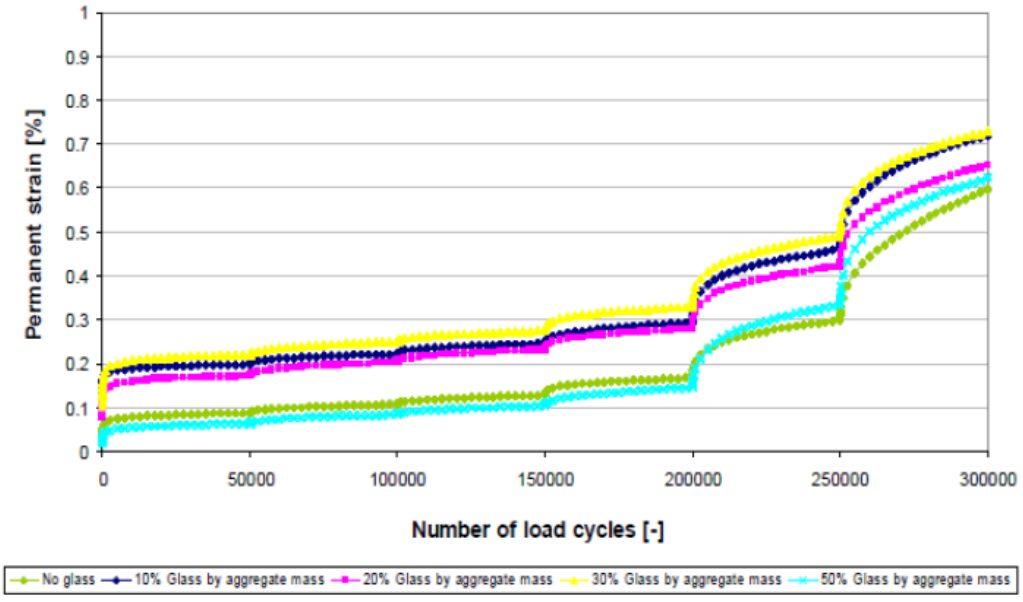

Figure 2.8 Permanent deformation of glass-aggregate blends (Arnold et al., 2008)

After that, a series of RLTTs was performed by Disfani et al. (2011) on different glass-subbase mixtures to investigate the effect of glass content on the P_d of pure rock samples. The glass-rock mixture containing 15% glass in a maximum size of 4.75 mm was considered suitable as a subbase material. In the process of assessing the suitability of waste glass for use in road applications, Arulrajah et al. (2014) investigated the deformation behaviour of glass-aggregate mixtures under RLTTs. The results illustrated a marked decrease in the P_d of the aggregate as the glass content increase.

A summary of many important investigations demonstrating the effects of waste glass on static and dynamic characterisations of different types of unbound materials are summarised in Table 2.1. Many previous studies focused on using specific sizes to investigate the suitability of waste glass as unbound materials, while the existing study used the waste glass source gradation for a comprehensive study. Note that there is many variations in these studies in terms of the replacement ratio of glass, but the common value of glass in the literature ranged between 10% and 50%, as shown in Table 2.1.

Table 2.1 Studies investigating the influences of waste glass on unbound materials' properties

Study	Recycled materials	Mix design	Laboratory tests	Major findings
Senadheera, Nash and Rana (1995)	Glass cullet in two different sizes (¼ and ¾ inch)	Granular material (caliche) replaced by 20 to 50% of Glass cullet	Resilient modulus	The resilient modulus of the glass-caliche blends decreased by 15% with the addition of 50% of ¼-inch glass, while the M_r value of glass-caliche blends decreased by 23% with the addition of 50% of ¾-inch glass. The particle sizes of waste glass played a vital role in the resilience behaviour of the glass-caliche mixtures. In addition, the M_r of glass cullet-caliche mixtures at higher stress levels decreased with further glass content. While the modified mixtures showed higher moduli than the granular material at low stress levels.
Viswanathan (1996)	Glass cullet	Five different replacement ratios of glass to granular material (caliche) were adopted, namely 5, 10, 20, 50, and 100%	Particle size analysis, compaction test, triaxial test, constant head permeability test	Up to 20% glass, insignificant effect of glass on the optimum moisture content and the dry density of the glass-caliche mixture. The caliche with 20% glass did not seem affecting the shear strength, while increasing the replacement ratio of glass resulted in lower quality of the strength. The permeability of the mixtures positively affected by the increase of the replacement ratio and the caliche with 50% glass can be used as a filter material for underdrains.
Rana (2004)	Glass cullet	20, 30, and 50% of granular material (caliche) used in pavement subbase layers replaced by glass cullet respectively	Particle size analysis, modified Proctor compaction test, resilient modulus	An increase in the glass cullet from zero to 20, 30, and 50% led to a decrease in the OMC from 14.75 to 11.5, 9, and 8%, and lower the MDD from 118.2 to 112.5, 110.0, and 97.50 Ib/m^3, respectively. Up to 30% glass, the resilient modulus of the caliche-glass mixture increased with the glass content increase. While permanent deformation is negatively affected by the increase of the replacement ratio, where the deformation of pure caliche increased about 66% as the glass content increased to 20%.
Grubb et al. (2006)	Crushed glass sized 9.5mm	Aggregate (dredged) material replaced by 20, 40, 50, 60, and 80% of crushed glass	Compaction test, compressibility, hydraulic conductivity, triaxial shear tests	An increase in the glass content led to an increase in the dry density and a decrease in the OMC of the glass-dredged mixture. Both the compressibility and the hydraulic conductivity are negatively affected by the increase of the glass ratio. The internal friction angle of dredged material increased from 34° to 39° as a result of increasing the glass content from 0% to 80%.
Arnold et al. (2008)	Crushed glass sized 9.5mm	Aggregate (dredged) material replaced by 10, 20, 30, and 50% of crushed glass	Particle size analysis, permanent deformation	The 10 and 20% of glass-aggregate mixture has a grading being inside the limits. An increase in the glass content from 0% to 50% led to a decrease in the dry density from 2.34 to 2.21. The permanent deformation of the aggregate increased with 10% of glass and then decreased with 20% and 50%.
Ali et al. (2011)	Glass cullet with the	10, 15, 20, 25, 30, 40 and 50% of crushed	Particle size analysis, modified compaction, specific	Even the rock sample with 40 and 50% glass contents did not satisfy the upper limits set after the compaction effort, all mixtures were considered to be well graded and suitable for road applications.

	maximum particle size of 4.75 mm	rock as road pavement subbase lyres replaced by glass cullet, respectively. .	gravity, water absorption, organic content, pH, California Bearing Ratio (CBR), Los Angeles abrasion test (LA)	Specific gravity, water absorption, organic content, fines content, and MDD of the waste glass-crushed rock mixtures are negatively affected by the increase of the replacement ratio of glass. Note that the compaction curves of the glass-rock mixtures showed less curvature than those of the natural rock. Increasing the replacement ratio to 30% glass to rock resulted in lower OMC compared to pure rock, and then increased upon the addition of glass. The replacement of glass to rock did not seem affecting the abrasion ratio and the pH values of the glass-rock mixtures. An increase in the glass content from zero to 50% led to a reduce in the CBR of the crushed rock from 181 to 121%.
Disfani et al. (2009)	Fine recycled glass	10, 20, 30, 40, 50, 60, 70, 80, and 90% of glass was used to replace biosolids in road embankment applications	Particle size analysis, modified compaction, CBR, and direct shear test	The particle size distribution of the glass became finer with the biosolids content increase. The MDD values of the biosolids-glass mixture were increased and the OMC values were decreased as the glass content increase. Biosolids with different glass content exhibited low CBR values compared to the pure biosolids. But the internal friction angle of the mixture increased from 10º to 43º as increasing the glass content from zero to 50%.
Disfani et al. (2011)	Coarse, medium and fine sized of recycled glass	Use as natural aggregates in road application	Particle size analysis, modified compaction, specific gravity, hydraulic conductivity ,water absorption, organic content, pH, LA, CBR, direct shear test, triaxial shear test	The fine and medium recycled glass were classified SW-SM while coarse glass was classified GP. The specific gravity of glass was found to be about 10% lower than the value of natural aggregate. The medium re size of glass showed a higher MDD than the fine, while the medium glass showed a lower OMC than the fine glass. The LA of fine and medium glass is approximately equal to those of demolition material. While the medium glass reported higher CBR and internal friction angle than the fine glass. In general, coarse glass was found to be unsuitable for geotechnical engineering applications.
Arulrajah et al. (2014)	Fine recycled glass, recycled concrete aggregate, and waste rock	Recycled concrete aggregate and waste rock were mixed with different percentages of glass (10, 15, 20, 30, 40 and 50%) for using in pavement base applications	Particle size distribution, water absorption, modified compaction, LA, flakiness index, hydraulic conductivity, CBR, and repeated loading triaxial tests.	The new mixtures of waste glass-recycled concrete aggregate and waste glass-crushed rock were classified as poorly graded sand with silt material (SP-SM), and the addition of glass resulted in a slight divergence of the gradation curves with the upper and the lower limits of base course materials. Up to 20% of glass, the absorption of fine glass-aggregate mixture was higher than the aggregate material, while a rapid reduction in the absorption was noticeable with further glass. The OMC values of waste rock decreased significantly when mixed with 10% fine glass, and then increased with 15, 20 and 30% but a steady reduction in the OMC occurred with 40 and 50% of glass. The results also indicated that an increase in the fine glass led to a reduction in the MDD, specific gravity, organic content, and the permeability of both recycled concrete aggregate and the waste rock soils. The presence of 50% of glass led to a reduction in CBR values of the waste rock and the recycled aggregate from 181% to 121% and from 211% to 98%, respectively. In addition, the presence of glass can have negative effects on the cohesion and the internal friction angle of both mixtures. A noticeable reduction in the M_r and P_d of the mixtures was observed with the glass increase. In general, all mixtures were satisfied the maximum LA value for base materials (35%) and the requirements of subbase material.

2.6.2 Tyre rubber in road applications

Increased road traffic in developing countries has led to an increase in the number of tyres and consequently, increasing the waste tyre stockpiles which causing potential environmental problems and damage in human health. In Australia, 51 million tyres are disposed of annually (Australian Government, Department of Environmental and Energy, 2016). With these huge stockpiles, using the waste tyres in construction and geotechnical applications plays a significant role in minimising the consumption of strategic inventories of natural resources. Whole tyres have been widely used in landfill works and in soil supporting works where tyres are stacked vertically to construct retaining walls. However, the quantities of used tyres in construction are not commensurate with the increasing of the waste tyres stockpiles and therefore, the existing studies have attempted to use different process techniques to accommodate the generated quantities of waste tyres which probably led to minimise the stockpiles and conserve the natural resources. Engineering properties of rubber-soil mixtures are affected by the variationof the tyre processing. Based on this process, different types of waste tyre aggregatecan are produced, such as tyre shreds, tyre crumb, tyre chips, and tyre buffings. These types of tyre aggregate are widely used in the geotechnical applications as a mixture with different soils or separately. Based on the process used to produce the retreated tyres, the consumed surfaces of used tyres are stripped off and then coated with new rubber surface.Tyre buffings are one of the waste tyre aggregate types which can defined as a by-product of the strapping process; it comes in small sizes, fabric shapes, and free wires parts. As a result, tyre buffing generally used as additives or in soil stabilisation applications (Edinçliler et al., 2004). Shredded and crumbed tyres are other types of waste tyre aggregate that previous studies used as reinforcement materials with sand and gravel in construction and pavement applications (Foose, Benson & Bosscher, 1996; Lee et al., 1999; Feng & Sutter, 2000; Edinçliler, Baykal & Dengili, 2004; Hataf & Rahimi, 2005; Edeskär, 2006). Depending on the shredding machine, different shapes and sizes of tyre shreds are available; the normal size of tyre shreds around 50 to 300mm. This product has many distinctive properties where it can be used as a mixture or separately. It is distinguished by its light unit weight and therefore, this product is suitable to use as lightweight materials. Tyre shreds are considered as an open drain material, and that could be a useful characteristic when used in the embankment works (Salgado and

Yoon, 2003). Tyre crumbs are another type of waste tyre aggregate, which characterized by a variety of sizes, shapes, and free of wires. These characteristics have made this product suitable in a number of geotechnical applications such as use it as lightweight aggregate. Tyre chips are another type of waste tyre aggregate, which completely wire-free and have specific shapes, rectangular and square. Several characteristics may be mentioned regarding this type of product to use in geotechnical engineering, light weight, high thermal, and low cost compared to other types of the waste tyre aggregate (Humphrey, 1999). A considerable amount of literature has been published on the rubber-soil mixtures characteristics. Some authors concluded that granulated or shredded tyre rubber exhibits frictional behaviour, low unit weight, low bulk density, high permeability and high levels of deformation (Hall, 1991; Manion, 1992; Humphrey et al., 1992; Edil & Bosscher, 1994). More explanations concerning the effect of tyre rubber on the static and dynamic behavior of granular materials are provided in the review below.

2.6.2.1 Particle size distribution of rubber-granular materials blends

The particle size distribution of rubber-aggregate mixtures was studied by Signes et al. (2015). The findings of this study concluded that all mixtures were within the required gradation curves of the subballast material. Note that it can produce any size gradation required by sieving rubber to different sizes and mix as required with other material. Therefore, it is not necessary to review in depth the previous results of particle size distribution of rubber-soil mixtures in this section.

2.6.2.2 Optimum moisture content, maximum dry density, and specific gravity of rubber-granular materials blends

Compaction parameters are essential characteristics of rubber-unbounded mixtures and play critical roles in road materials. Speir and Witczak (1996) conducted a laboratory program to investigate the maximum dry density (MDD) and optimum moisture content (OMC) of aggregate-rubber mixtures. The compaction results of the aggregates-shredded rubber mixtures indicated that the MDD of the mixtures decreased with the addition of rubber. Conversely, the OMC increased with the rubber increase. Other studies have investigated the correlation between rubber content and the density of granular materials. The results of these studies reported a clear reduction in the MDD of the materials with the rubber presence (Papp, Maher

& Baker, 1997; and Signes et al., 2016). Further laboratory investigations have assessed the behaviour of sand-rubber mixtures under the compaction impacts (Ghazavi, 2004). Rubber-sand mixtures showed a significant reduction in density with the rubber increase, where the MDD of sand reduced from 14kN to 8kN when mixed with 70% rubber. In 2009, Subramanian and Jeyapriya confirmed the inverse effects of rubber on the MDD of granular materials (Subramanian and Jeyapriya, 2009). Cosentino et al. (2014) also studied the effect of rubber on the compaction curves of lime rock aggregate. The shape of the compaction curve was mostly independent of the rock-rubber ratio. Two major points can be concluded through the above studies. The first is the inverse effect of the rubber on the MDD of the rubber-soil mixtures which could be attributed to the light weight of rubber particles, and the second is the effect of low sensitivity of rubber grains to water which played a major role in influencing the OMC of the mixtures.

The specific gravity of granular materials is very dependent on the rubber content (Parakh et al., 2016), where specific gravity of rubber-aggregate mixtures decreased from 2.83% to 2.33% due to the addition of 15% rubber. Similarly, Signes et al. (2016) reported a sharp reduction in the specific gravity of aggregate due to the addition of rubber content. These studies provide an evidence that the physical properties of rubber-soil mixtures such as specific gravity might be affected by the light weight, size, and shape of the rubber particles.

2.6.2.3 Water absorption and hydraulic conductivity of rubber-granular materials blends

A series of experimental tests were carried out by Signes et al. (2016) to estimate the physical properties of various rubber-aggregate mixtures. The absorption values of aggregate increased by 5% with the addition of rubber. This finding corroborates the conclusions of Hidalgo et al. (2015), where a positive correlation was reported between rubber content and the absorption of rubber-aggregate mixtures. This positive correlation could be attributed to the difference in water absorption between rubber (5%) and the aggregate particles (0.71%).

A series of laboratory tests were conducted by Speir and Witczak (1996) to establish the hydraulic conductivity of rubber- granular material mixtures. Two types of granular materials were mixed with 7.7% and 15% shredded rubber to investigate the

suitability of using the mixtures as base or subbase materials. The results indicated that the coefficient of permeability of the mixtures increased with rubber content increase. Rubber-soil mixtures were also considered as an open drain material which is useful in the embankment applications (Salgado and Yoon, 2003). This view was supported by Cosentino et al. (2014), who reported a steady increase in the permeability of the rubber-soil mixtures with rubber content increase.

2.6.2.4 Shear strength of rubber-granular materials blends

Shear strength of rubber-soil blends has received considerable attention among geotechnical research works, and a considerable amount of previous research have been conducted to characterise the effect of rubber on shear strength of granular materials. Ghazavi (2004) conducted a laboratory program to examine the shear response of sand-rubber mixtures. Sand was mixed with 10%, 15%, 20%, 50%, 70% and 100% waste rubber of garden hose. The rubber grains were mostly bigger than 0.9mm and smaller than 8mm. In loose and dense conditions, insignificant variations in shear strength of sand when mixed with 10% rubber. Sand grains at this low ratio of rubber endured most of the shear force and therefore, insignificant difference in the strength of the rubber-sand mixture and the strength of pure sand sample. In the dense conditions, the value of internal friction angle of the mixture increased from 37° to 37.6° when the rubber content increased from 10% to 15%, while it increased from 31.2° to 35.3° in the loose conditions. The positive effect of the rubber on internal friction angle was attributed by Ghazavi (2004) to the role of a 15% rubber in enhancing the fabric stability of the mixture, as the sand particles filling the voids between the rubber particles, causing an increase internal friction between sand and rubber particles. The findings of this research also concluded that the 20% of rubber reduced the internal friction of the mixtures. This behaviour was attributed to the effect of voids between the rubber and the sand particles, which were partially filled by sand and affected on the soil fabric stability. Consequently, shear resistance of the mixture then became completely dependent on the rubber particles.

Attom (2006) conducted a series of direct shear test to assess the strength behaviour of different samples of tyre rubber-sand mixtures. Three types of sand were mixed with different proportions of tyre rubber almost smaller than 4.76mm. Both the internal friction angle and the shear strength of pure sand increased with the tyre rubber increase. Note that these findings did not fully support the conclusions of

Ghazavi (2004). The significant differences in fabric, shapes and sizes between the tyre rubber and the waste garden rubber could be attributed to the results diverse above. A series of direct shear test were carried out by Prasad and Raju (2009) to investigate the suitability of tyre rubber as an alternative to gravel subbase materials. Gravel materials were mixed with a range of tyre chips (0.5% to 7%) passing through 4.75mm sieve. The findings concluded that the shear parameters of subbase increased with an increase in the tyre rubber from 0.5% to 5% and thereafter decreased. These findings are somewhat consistent with the findings of Ghazavi (2004) that the presence of 1% to 5% rubber caused in decrease the voids between the rubber and the aggregate particles and consequently, high friction forces between the different particles, where further rubber inversely affected the shear strength of the rubber-aggregate mixtures. Recently, Cabalar (2011) investigated the stress-strain behaviour of rubber-sand mixtures. Two types of sand were mixed separately with 5%, 10%, 20% and 50% of rubber. The results showed that both internal friction and shear strength of course sand decreased with the rubber content increase, while both the internal friction and shear strength of fine sand decreased when mixed with 5% and 10% of rubber and then levelled off with further addition.

2.6.2.5 California Bearing Ratio and Los Angeles test results of rubber-granular materials blends

An investigation into the effect of rubber inclusion on California bearing ratio (CBR) rubber-granular materials was performed by Speir and Witczak (1996). The results showed a significant reduction in CBR values associated with the rubber content increase. Papp et al. (1997) confirmed the previous findings and contributed additional evidence that aggregate samples which mixed with shredded rubber showed lower CBR values than those without rubber. Subramanian and Jeyapriya (2009) conducted soaked and unsoaked CBR tests on rubber-subbase mixtures to investigate the bearing behaviour of the modified blends. In contrast to earlier findings, an improvement in the unsoaked CBR values of the rubber-subbase mixtures was associated with the tyre rubber increase, whereas an insignificant effect of rubber content on soaked CBR values was noticeable in this study. With more focus on soaked conditions, Prasad and Raju (2009) carried out CBR tests to evaluate the bearing behaviour of waste tyre rubber-gravel mixtures. The results indicated that the mixture with 5% rubber showed higher CBR value than that of pure aggregate

sample. Beyond that ratio, a sharp reduction in the CBR values of the mixtures was associated with the rubber content increase. Similarly, Signes et al. (2015) reported a steady reduction in the CBR values of aggregate because of the rubber presence. The discrepancy in the values of CBR concluded in the previous work could be attributed to the variation in the rubber size, fabric characteristics and shape in different mixtures which could influence the stability of the mixtures fabric. Soaked and unsoaked conditions might also influence the CBR values. The probable reason for the inverse effect of the soaked condition is the loose of interlocking between rubber surface and soil when submerged the samples in water which produced unstable fabric and then, low CBR.

Los Angeles (LA) tests were carried out by Signes et al. (2015) on rubber-aggregate mixtures to assess their responses to the crushing forces.The findings reported that a 20% reduction in the LA values of aggregate was associated when mixed 10% rubber. However, the rubber-aggregate mixtures were suitable in road construction instead of the raw material. Parakh et al. (2016) investigated the possibility replacing course aggregate with rubber in road application . A wide range of rubber contents (5%, 10% and 15%) were mixed with aggregate to assess the LA of the modified mixtures. A steady reductions in the LA values of the aggregate-rubber mixtures was associated with the rubber content increase. The positive role of rubber in enhancing the LA of granular materials could be attributed to the high capability of the rubber particles (an uncrushable and high compressibility material) to decrease their volume under the crushing forces.

2.6.2.6 Resilient modulus of rubber-granular materials

Resilient modulus (M_r) has been identified as a central part of the pavement design process over past decades. Many studies have investigated the correlation between rubber content and the M_r of different soils (Humphrey & Sandford, 1993; Humphrey et al., 1993; Warith & Rao, 2006; Hazarika et al., 2007). Speir and Witczak (1996) identified a steady reduction in M_r of granular materials associated with the tyre rubber increase. Papp et al. (1997) conducted a series of repeated loading tests on different samples of shredded tyre chips-subbase mixtures to assess their resilience behaviours. A steady reduction in the M_r of the modified mixtures was noticeable with the rubber increase. This view was not supported by Wang et al. (2006), who reported a positive correlation between the tyre rubber and the elastic

moduli of gravel material. With greater focus on the M_r of rubber-subballast materials, further study was undertaken by Signes et al. (2016). Subballast material was mixed with different proportions of tyre rubber (1%, 2.5% and 5%) to investigate the resilience behaviour of the rubber-subballast mixtures. There were similarities between the results of this study and those described by Estevez (2009) who reported that the rubber presence can improve the resilience behaviour of subballast material. The reason for the discrepancy mentioned in the previous studies could be attributed to the difference in physical characteristics of rubber or the variation in rubber:soil ratios, where the physical properties and the mixing ratios played a significant role in the stability of mixture fabric. For example, the high compressibility of rubber could play a substantial role in increasing voids between the particles when subjected to repeated loads and then decreased the stability of the mixture fabric and consequently, lower M_r.

2.6.2.7 Permanent deformation of rubber-granular materials

Based on the deformation behaviour of rubber-gravel mixtures, Prasad and Raju (2009) investigated the suitability of using waste rubber instead of gravel in road applications. The findings concluded that the gravel-rubber mixture showed less deformation than the untreated gravel. Signes et al. (2016) conducted a series of RLTT on different samples of the rubber-subballast mixtures to assess the deformation responses of the mixtures. A significant increase in permanent deformation of the mixture was associated with the rubber increase. After 30000 cycles, the permanent deformation increased about 300% when rubber content increased from 1% to 5%, as shown in Figure 2.9.

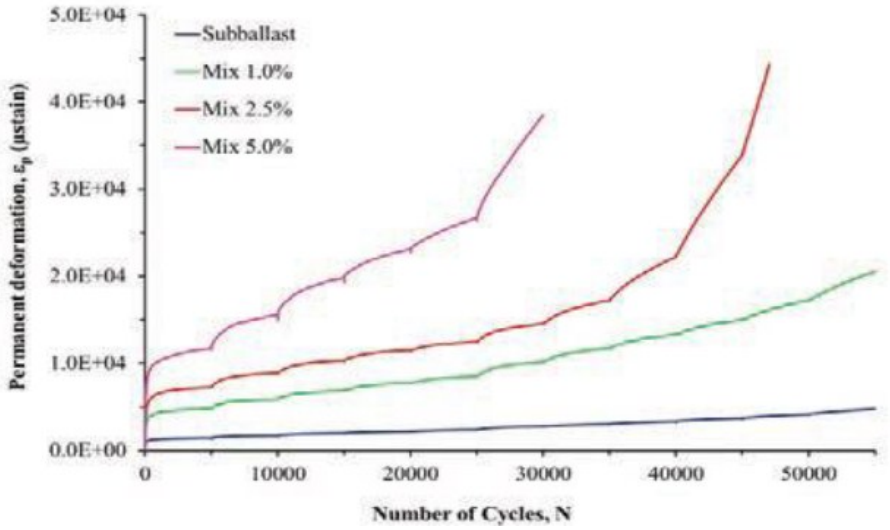

Figure 2.9 Effect of rubber content on the permanent deformation of rubber-subballast mixtures (Signes et al., 2016)

A summary of important investigations demonstrating the effects of waste tires on basic and dynamic properties of unbound materials is presented in Table 2.2. Many previous studies discussed the effects of specific sizes of tire pieces on different properties of aggregate-rubber mixtures, while the existing study used the waste tire source gradation for a comprehensive study. The variations in the static and dynamic behavior of rubber-soil mixtures could be attributed to the variations in the rubber grains properties and the replacement ratios. Note that the common replacement ratio of the rubber-coarse aggregate in the literature ranged between 5% and 15%, as shown in Table 2.2.

Table 2.2 Studies investigating the influences of waste rubber on unbound materials' properties

Study	Recycled materials	Mix design	Laboratory tests	Major findings
Speir and Witczak (1996)	Shredded rubber retained on a 9.5mm sieve	5 to 15% of rubber was used to replace aggregate	Modified Proctor, CBR, and resilient modulus tests.	Increasing the replacement ratio of shredded rubber resulted in a significant increase in the OMC and a clear reduction in the MDD of the rock-aggregate mixtures. In addition, increasing the replacement ratio of rubber to aggregate resulted in lower quantities of CBR and M_r compared to pure aggregate.
Ghazavi (2004)	Waste hose grains sized 0.9 to 8mm	10, 15, 20, 50, 70, and 100% of waste hose particles was used to replace sand.	Grain size distribution and small direct shear test.	In general, an increase in the rubber content led to an increase in cohesion of the sand-rubber mixture. Up to 15% of rubber, the initial friction of the dense sand-rubber increased from 37 to 37.6; while the initial friction of the loose sand-rubber mixture increased from 31.2 to 35.3 by adding 15% rubber.
Subramanian and Jeyapriya (2009)	Square and rectangular shapes of tractor tyres sized 20-25mm Crumb tyres scrapped of light motor vehicle tyres sized 2.36mm	Crumb tyre was added to the subbase in proportions of 2.5, 5, 7.5, and 10% Partially replaced waste tyre pieces in proportions of 2.5, 5, 7.5, 10, and 12.5%.	Modified proctor compaction, unconfined compressive strength, CBR tests in soaked and unsoaked condition, and abrasion test.	The OMC of tyre-subbase mixture generally increased and the MDD decreased with increase in percentage of tyre rubber. In addition, an inverse correlation was reported between the CBR of the mixture and the rubber content. An improvement in the unsoaked CBR value of the mixture was associated with the tyre rubber increase and the optimum value of the tyre content was found to be 7.5%. Whereas an insignificant effect of rubber content on CBR of the mixture was noticeable in soaked condition. The aggregate crushing and the abrasion value of aggregate generally decreased as the replacement ratio of rubber increased.
Prasad and Raju (2009)	Waste tyre rubber chips passing through 4.75 mm sieve	0.5, 1, 2.5, 5, 6, and 7% of rubber chips was used to replace gravel subbase.	Direct shear, cyclic load and CBR tests.	Shear parameters of gravel increased with an increase in the tyre rubber from 0.5% to 5% and thereafter decreased. Up to 5% of rubber, the CBR value of the gravel-rubber mixtures increased directly as the rubber content increased. Note that all mixtures showed lower deformation under cyclic impacts than the pure aggregate.
Cabalar (2011)	Waste tires	5, 10, 20, 50% of waste tires material was used to replace two different	Direct shear test	Shear parameters of granular material negatively affected by the increase of the replacement ratio of waste tires, where increasing the replacement ratio resulted in lower qualities of the angle of internal friction and the

		gradations and shapes of sand.		shear strength.
Hidalgo et al. (2015)	Rubber particles come from scrap tyres with the maximum particle size of 2mm	1, 2.5, 5, and 10% of tyre rubber was used to replace aggregate.	Particle size analysis, modified compaction, CBR, LA, and repeated load triaxial test.	The LA and the CBR values of aggregate generally decreased respectively from 24.9 to 20 and from 154 to 17 as the replacement ratio of rubber increased from 0 to 10%. Moreover, an addition of 10% rubber caused a significant reduction in M_r of rubber-aggregate from 250 MPa to 92.8MPa.
Signes et al. (2015)	Rubber particles from shredded tyres in three different sizes (1, 2, and 20mm).	Rubber used to replace aggregate (subballast) at different replacement rates, including 1, 2.5, 5, and 10%.	Particle size analysis, modified compaction, specific gravity, water absorption, organic content, California bearing ratio (CBR), Los Angeles abrasion test (LA), direct shear test, triaxial compression test, cyclic load triaxial test	All mixtures were within the required gradation curves of the subballast material, and adding 1 to 10% of rubber to aggregate could improve the LA values. On the other hand, the rubber presence decreased both density and bearing capacity of subballast. The CBR values of the mixtures decreased as the rubber content increase, but it was over the minimum limit of subballast materials (20). Up to 5% of rubber, the rubber-subballast mixtures in acceptable levels in terms of resilient modulus.
Cabalar and Karabash (2015)	Tire buffings falling between 1 to 12.5mm	5, 10, and 15 % tire buffings and 1, 3, and 5 % cement were used to replace crushed rock	Modified compaction and CBR tests	The OMC and the MDD of the crushed rock decreased as the tire content increase. Crushed rock-tire-cement mixture at 3% cement and 5 % tire, and 5 % cement and 5, 10, and 15 % tire showed higher CBR values than the pure crushed rock.
Parakh et al. (2016)	Coarse waste tyre rubber and powdered waste glass	5, 10 and 15% of waste tyre rubber was used to replace coarse aggregate.	Water absorption, specific gravity, LA, crushing test.	The specific gravity of rubber-aggregate mixtures decreased from 2.83% to 2.33% due to the addition of 15% rubber. In addition, replacement of coarse aggregates by tire rubber led to decrease the aggregate impact value and improved the physical properties of aggregate. A decrease in LA was observed when replacement of rubber with coarse aggregate.
Signes et al. (2016)	Free of metallic wires of rubber particles in three different sizes (1mm, 2mm, and 20mm).	Three different replacement ratios of rubber to aggregate (subballast) were adopted, namely 1, 2.5, and 5%.	Repeated load triaxial test.	Increasing the replacement ratio of rubber to aggregate resulted in lower M_r and P_d of rubber-subballat mixtures compared to the pure material. The mixtures with 1 and 2.5% rubber reported M_r higher than the acceptable level for subballast layers.

2.7 Bentonite in road applications

As one of the waste fine bound materials, Bentonite has received considerable attention in many previous studies in geotechnical engineering applications, even though some studies have reported insignificant effects of fine materials on the resilience behaviour of soils. However, the results of experimental works by Babiker et al. (2014) revealed that fine materials (passing a no. 200 sieve) can influence the dynamic behaviour of granular materials. In addition, many previous studies have reported that fine materials play a significant role in the dynamic behaviour of unbound-bound mixtures in pavement applications (Perlea, 2000; Perlea, Koester & Prakash, 1999). Because of the increasing population density, geotechnical engineers are required to contend with sensitive and difficult soils such as clay. As mentioned before, the unbound materials layers sit on a subgrade layer, which usually consists of natural soil or fill materials (Moayedi, Kazemian, Prasad & Huat, 2009; Khabiri, 2010; Tchemo et al., 2011; Chegenizadeh, Keramatikerman & Nikraz, 2016a). Therefore, pavement designers have employed the RLTT to evaluate the dynamic characteristics of different types of subgrade materials. On this topic, a series of investigations were performed by Drumm, Boateng and Johnson (1990) and Drumm et al. (1997) to assess the effect of moisture content on the M_r of clay. The results indicated that the M_r of clay decreased with the water content increase. As a part of a research program on subgrade soil, Fleming et al. (1998) conducted a group of investigations to study the M_r and permanent deformation (P_d) of bentonite in road applications. It is important to mention that remixing the bentonite samples was not recommended when studying the effect of moisture content on dynamic behaviour of soils. Like the above results, negative relation was found between the moisture content and the both of M_r and deformation resistance (Azam & Cameron, 2012). In the same vein, Babiker et al. (2014) concluded that the P_d of waste clay-waste aggregate mixtures increases with increasing deviator stress, while the M_r of the mixtures reached a minimum value at the highest level of deviator stress. Also, a positive correlation was found between P_d and the moisture content.

Moreover, most previous studies have primarily studied the effects of partial substitution of fine materials on static and dynamic characteristics of unbound materials. However, few studies are available on the influence of whole layer of fine bound materials on dynamic behaviour of the unbound material sample, where the

findings of Zhang et al. (2015) informed that the presence of a single layer of fine materials can have a positive effect on shear strength of the layered sample of course-fine soil. Consequently, further experimental study is required to assess the effects of bentonite on dynamic behaviour of granular materials.

2.8 Layering technique in geotechnical applications

Previous studies have only used homogenised models for their experimental samples. Thus, it would be interesting to understand the dynamic behaviour of layered structures in geotechnical applications. A brief overview of the history of research into layering techniques in geotechnical applications is presented in this section. In recent years, there has been an increasing amount of literature on layering techniques in dynamic applications. Nagase and Kenji (1987) investigated the cyclical behaviour of a single layer of sand. After that, a considerable amount of literature was published on rock layers. Babiker et al. (2014) applied limit analysis to the toppling-sliding failure of the rock. These studies worked on different failure types of a single layer of rock material. Other studies have investigated the slope stability of a single layer of rock space (Gravanis et al., 2014; Gischig et al., 2015). The effect of loading types has also been considered in the literature. Based on dynamic and static loading conditions, some studies have focused on a single layer of rocky space (Zhu & Tang, 2006; Ma et al., 2013; Zhouet et al., 2014; Momeni et al., 2015). It is understandable that many cases and projects deal with layered structures rather than a single layer of soil or rock and thus, multilayered structures have been found to be important when considering land subsidence. Layered techniques have also been performed in terms of excavation stability and slope failure by Pujades et al. (2014) and Zeng, Jimenez and Jurado (2015). A multi-layering technique was also used in Taiwan on a multilayered aquifer system by Lin et al. (2015). In addition, layered structures can be very important when tailing dams for mining waste are constructed. A series of geological studies were conducted by Zhang et al. (2015) on tailing materials to investigate the static and dynamic characteristics of the materials in tailing dams. As shown in Figure 2.10 (a, b and c), three types of sample were employed to assess the static and dynamic behaviours of layered techniques: course tailings sample, fine tailings sample and a layered course-fine tailings sample. The layered samples of course-fine tailings showed lower shear strength and internal friction angle than the course and fine tailings samples. Moreover, the upper layer of the layered specimens

showed more P_d than the lower layer, and the interface layer between the course and fine layers had more P_d than other points. Lack of the layered technique applications in previous studies encouraged many current studies to search in comprehensive applications for this technique, which is one of these study objectives.

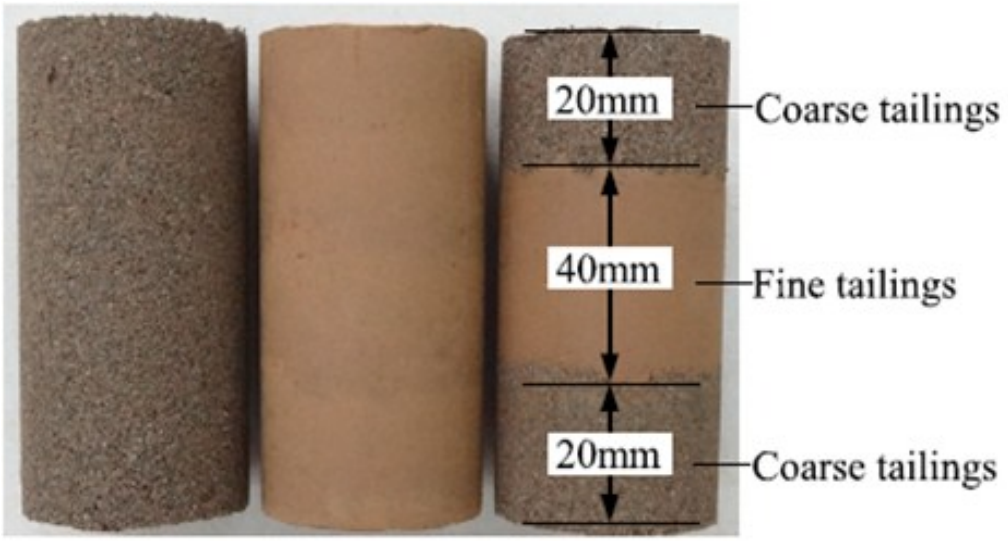

(a) (b) (c)

Figure 2.10 Tailings specimens for triaxial shear tests: a) course tailings specimen b) fine tailings specimen c) layered structure specimen (Zhang et al., 2015)

2.9 Soil stabilisation using cement and slag

The stabilisation topic, which means trying to improve the physical and chemical specifications of different materials, has been studied in several previous studies. According to the findings of the studies, fine materials could improve the performances of soils against static and dynamic impacts (Senol et al., 2002; Arora & Aydilek, 2005), where fine materials could improve many parameters such as workability, plasticity, permeability, shear strength, permanent deformation (P_d) and resilient modulus (M_r). To understand the dynamic performance of the cement and the cement-slag treated granular materials, the next sections will give a brief overview of some studies that recently investigated the effect of different additives on dynamic behaviour of different soils.

2.9.1 Mechanical behaviour of cement treated mixtures

Cement is a binder used alone in construction or adheres many soils together, such as sand, gravel and rock. In the recent decades, cement has attracted considerable

research attention in the geotechnical applications because of its effectiveness in improving the mechanical performance of different granular materials. Recently, cement has been used in many investigational studies of road applications (Du, Li & Hayashi, 1999; Du et al., 2013b and Jitsangiam & Nikraz, 2009). The findings reported that a sample of unbound materials at different cement content showed better dynamic behaviour than the untreated samole. The study of Siripun, Jitsangiam and Nikraz (2009) highlighted on stabilising base materials with 2% cement. The compaction test was conducted to determine the optimum moisture content and the maximum dry density of cemented mixtures. The mixtures were kept in plastic bags for 7, 14 and 28 days before test time to investigate the hydration time factor. This study has listed many factors affecting the dynamic behavioure of cement-crushed rock samples included hydration period and moisture content. The results of basic parameter concluded that cement with individual particles can change the fabric structure of crushed rock. The results of repeated loading triaxial test conducted on different cement-treated samples are presented in Figures 2.11 and 2.12. In Figure 2.11, the reilient modulus of the treated sample is about three times more than that of the untreated sample, whereas the factor of hydration period had a negative contribution on the resilient modulus of the cement-rock mixture. This response was attributed to the remixing and the compaction process after the hydration period, as the cementitious bonds between the rock and cement particles might be broken during the remixing and the compaction process. Figure 2.11 also shows that the reduction in moisture content had a positive contribution on the resilience behaviour of the mixtures. In Figure 2.12, the results show that 2% cement can improve the deformation resistance of pure crushed rock, and the reduction in moisture content had a positive contribution on P_d of the cement-rock mixture. On the other side, a significant increase in P_d of the mixture was associated with the hydration period increase. The findings of this study also reported that 2% cement can improve the shear strength characteristics of pure crushed rock, where the cohesion of pure rock increased from 32kPa to 168kPa when mixed with 2% cement. While a reduction in the internal friction angle from 59° to 43° was associated with the cement presence.

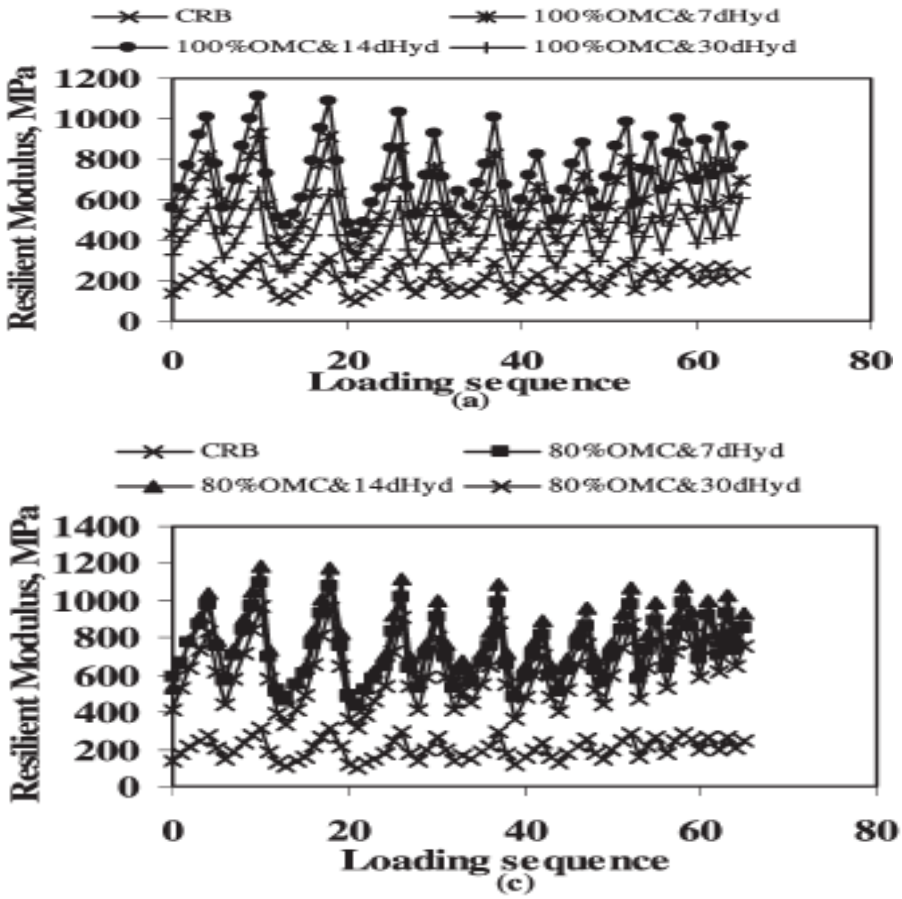

Figure 2.11 Resilient modulus of treated crushed rock with loading sequence (Siripun et al., 2009)

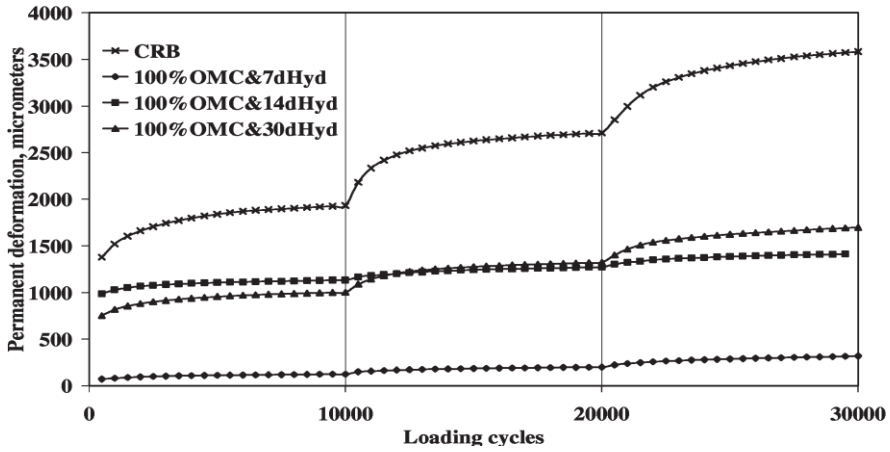

Figure 2.12 Effect of cement content on permanent deformation of pure crushed rock (Siripun et al., 2009)

2.9.2 Mechanical behaviour of slag treated mixtures

Waste materials have been widely used as base or subbase materials in pavement applications. One of the waste materials is slag which left over after iron production. A considerable amount of literature has been published on slag-soil mixture,

Mohammadinia et al. (2016) conducted an experimental investigation to stabilise crushed bricks with two stabilisers, slag and fly ash. Unconfined compressive strength tests (UCS) and repeated loadings triaxial tests were carried out to assess the dynamic responses of the treated mixtures after seven days. The findings indicated that 2% of slag could improve the behaviour of mixtures under UCS impacts. Also, the slag treated sample reported significantly higher M_r than the fly ash treated sample as shown in Figure 2.13.

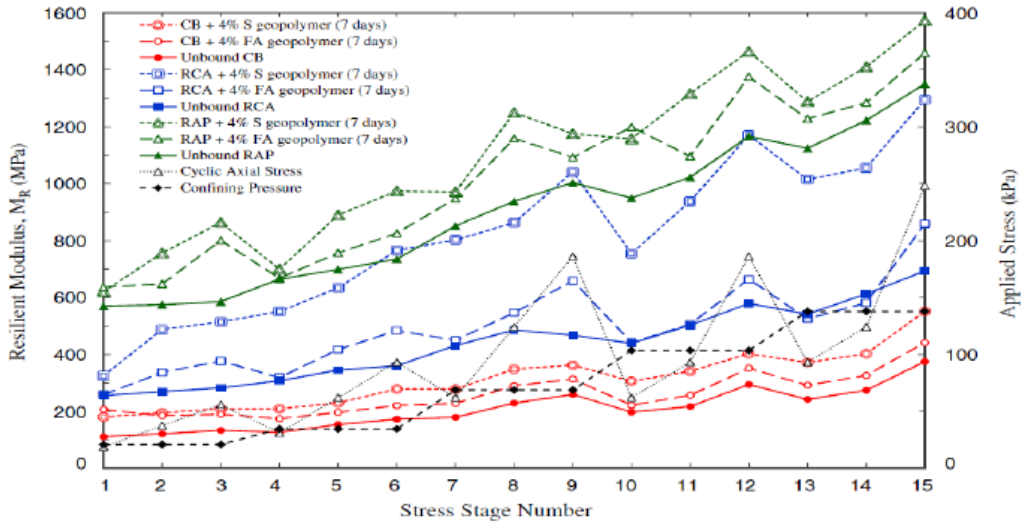

Figure 2.13 Effects of slag and fly ash on the resilient modulus value of different waste materials (Mohammadinia et al., 2016)

2.10 Strength of the proposed experimental program

Concerning the effects of different waste materials inclusion and layering on the unbound granular material characteristics, Table 2.3 presents an overview of the previous experimental works, including materials as well as the sample structure. A presentation of the proposed experimental works of this study is also detailed in the table. The proposed experimental program allows us to expand the current state of knowledge by submitting further details about the effect of waste materials on the dynamic behaviour of base and subbase materials. Note that additional materials, including waste, cementation and fine materials will be used to accomplish the investigation related the objectives of this study. An integrated study on layered structure will also highlight in the proposal works, as detailed in Table 2.3.

Table 2.3 A review of the previous works and the proposed experimental program regarding the effects of waste materials inclusion and layering on the unbound material characteristics

Previous experimental works		Proposed experimental program	
Material	Sample structure	Material	Sample structure
Rock-glass	Homogenous	Rock-glass	Layered
Rock-Rubber	Homogenous	Rock-rubber-glass	Homogenous
Soil-Bentonite	Homogenous	Rock-bentonite	Layered
		Rock-bentonite-sand	Layered
Rock-cement	Homogenous	Rock-glass-cement	Homogenous
		Rock-rubber-cement	Homogenous
		Rock-glass-rubber-cement	Homogenous
Soil-slag	Homogenous	Rock-glass-slag-cement	Homogenous
		Rock-rubber-slag-cement	Homogenous
		Rock-glass-rubber-slag-cement	Homogenous
Course-fine	layered	Rock-sand	Layered

Based on the literature review sections discussed in this chapter and despite a vast amount of experimental work on the effects of glass on static and dynamic behaviour of different granular materials over the past few decades, the behaviour of the soil-glass mixture under repeated loads remains somewhat contradictory and needs a considerable attention. In addition, the previous studies have focused in their investigations on the homogeneous soil-glass mixtures, while using these mixtures as separated layers with natural soil layers (layered technique) has not been given considerable attention in the past, which will be addressed in the proposed program. There is also a vast amount of experimental studies about the effect of tyre rubber on the dynamic responses of base and subbase materials, but very little attention has been paid to investigate the effects of a combination of glass and rubber on the dynamic behaviour of base course material, which is also need more experimental works. Furthermore, using these mixtures of glass-rock-rubber in the layered technique is one of the proposed work objectives because it was not addressed previously. Despite a significant number of the previous studies have assessed the influence of fine materials such as cement and slag on the dynamic behaviour of base

and subbase materials, lack of these studies fought in the influence of cement, slag, and cement-slag on dynamic characteristics of glass-rock-rubber mixtures. Thus, different mixtures of glass-rock-rubber-slag-cement materials will prepare in the proposed program of this study. Furthermore, notable positive results have been appeared through published studies regarding the layered technique, which used to prepare different layered samples of fine-course materials instead of being used as a homogeneous sample. Thus, the layered technique will be used to prepare different samples of crushed rock (unbound material) by replacing rock layers with other of bentonite, which is considered as bound and fine waste material. In addition, bentonite layers will also be replaced with sand ones to increase our knowledge about the effect of bound materials on the dynamic behaviour of unbound rock base material.

2.11 Evaluation of resilient modulus of granular materials using artificial intelligence approaches

In some countries, it is not easy to provide the equipment necessary to perform repeated loading triaxial test (RLTT) and accurately accounting the resilient modulus (M_r) of granular materials in the laboratory. Even if the laboratory results are available, they lack sufficient accuracy to be adopted at the site due to the differences between natural soils and the laboratory samples. These and other reasons, such as the high price of the RLTT and the long period to obtaining the results, led to an expanded the role of analytical, theoretical and empirical methods in many civil engineering applications to solve many complex problems. Despite the theoretical and analytical methods still can analyse and solve a large number of geotechnical engineering problems, these methods need a wide range of soil parameters to perform its mission (Das, 2013). Therefore, many studies have been employed artificial intelligence (AI) approaches to predict the dynamic performance of pavement layers under traffic loadings (Montoya, 2015). Artificial neural networks (ANN) and genetic programming (GP) are two of the AI approaches which have been widely used to assess different composite problems in geotechnical engineering in the last two decades. The following two sections will discuss the previous studies which used ANN and GP models to analyse and solve different soil problems.

2.11.1 Artificial Neural Networks

Theoretical, numerical and analytical methods were used by many studies to solve complex problems in geotechnical engineering. Evaluating the use of the empirical, artificial neural networks for prediction the resilient modulus (M_r) of different soils was performed by a vast amount of studies. The suitability of using one variable to predict M_r of soils was investigated by many studies. Sukumaran, Kyatham et al.(2002) performed a mathematical study to assess the suitability of using California bearing ratio (CBR) to predict M_r. Another numerical study was employed two basic variables to predict the M_r of subgrade soil, Drumm et al. (1990) used the soil index and the unconfined compressive (q_u) to predict M_r of subgrade soil. The theoretical results illustrated that q_u parameter played a vital role in the M_r prediction. Other theoretical and empirical studies used a group of soil properties to predict M_r of different soils. For example, regression equations were developed by Thompson and Robnett (1976) to estimate M_r of subgrade soil based on its basic characteristics. Basic and complex correlations between the M_r and different soil properties such as the results of unified soil classification, water content, bulk stress, and stress conditions were developed by Carmichael and Stuart (1985) as shown in Equation 2.2, which describes the general correlation between the M_r and water content (wc%), bulk stress (θ) and soil classification.

$$\text{Log Mr} = 0.523 - 0.025(\text{wc}) + 0.544\ (\log \theta) + 0.173(\text{SM}) + 0.197(\text{GR}) \qquad (2.2)$$

Where:

SM= 1 for Silty sand soils; = 0 otherwise

GR= 1 for silty gravel, well-graded gravel, fine to course gravel, clayey gravel, or poorly graded gravel (GP); = 0 otherwise

Other factors such as the degree of saturation can influence the resilience behaviour of granular materials. A group of laboratory tests was conducted by Rada and Witczak (1981) on granular materials to develop a theoretical model of M_r. The findings of the theoretical study concluded that the stress condition, degree of saturation and density are the main factors influenced the M_r value of the granular materials, as shown in Equation 2.3.

$$Mr = k_1 + k_2.S'r + k_3.Dr + k_4.\log(I_1) \quad (2.3)$$

Where:

S'_r: the degree of saturation

D_r: the degree of compaction

I_1: the first stress invariant

k'_s: the material constants

There are many reasons behind using AI approaches instead of other methods such as statistical methods and finite element methods to evaluate many complex problems in geotechnical engineering: the complex nature of the theoretical methods required a large number of soil parameters to result accurate findings, and the difficulty of developing these methods and keeping abreast of the geotechnical engineering developments. The above reasons led to a growth the AI applications within a short period to solve complex geotechnical problems with high accuracy. ANN is one of the AI approaches has received considerable attention from many research works because of its developed computational methods. Yang and Rosenbaum (2002); Xiangjun and Zhanfeng (2007); Farrokhzad, Choobbasti and Barari (2010) ; Sabbar, Chegenizadeh and Nikraz (2016) employed a set of soil properties to solve different types of geotechnical problems and develop models to predict complex parameters. One of the complex parameters of soils is the M_r which has received considerable attention by Najjar, Basheer, Ali and McReynolds (2000); Shahin, Maier and Jaksa (2004); Figueroa and Thompson (1980); Farrar and Turner (1991); Li and Selig (1994); Lekarp et al. (2000), who employed the ANN model in their studies to predict M_r of different soils. Furtheremore, a wide range of variables such as deviator stresses, confining pressure, moisture content and compaction parameters was used as input data in ANN model. Park, Kweon and Lee (2009) used the ANN with a wide range of parameters, included unconfined compression strength, optimum moisture content, plasticity index, liquid limit and percentage passing #200, to predict the M_r for subgrade and subbase materials. In addition, the findings of Nazzal and Tatari (2013) concluded that the results of ANN had more dependable than the empirical method results when used the soil index properties to predict the M_r of subgrade soil. Recently, Mosa (2017) used ANN to develop a model in the domain of resilience behaviour of base material.

Moreover, the variation in base and subbase materials encouraged some studies to develop a model for predicting the resilient modulus of base and subbase materials. Ibrahim, Kadhim and Othman (2017) performed a comparison in predicting the M_r of subgrade soil between the ANN model and extreme learning machine. Index properties of subgrade soil and the back-propagation were employed in the ANN model. The finding concluded that the ANN model reported the best prediction results, as compared to extreme learning machine. Regarding the use of waste materials in pavement layers, another study used ANN model to predict the elastic moduli of base and subbase materials containing different type of waste materials. Kim, Labuz and Dai (2007) adopted ANN model to predict the M_r of base material containing different ratios of recycled asphalt pavement.

ANN consists of several processed components known as neurons which have unique features likeness to the biological neurons. Through neurons and as in human brain, ANN can receive a lot of parameters, analysing the input data, solving and comparing different transfers functions net (Adhikary and Mutsuyoshi, 2004). The number of neurons in ANN is a few hundreds, whereas hundred or less of the neurons are required for the evaluation of the ANN performance in geotechnical engineering (Das, 2013). In general, the ANN structure is considered as a fully interconnected feed-forward multi-layer perceptron. According to the architectural structure, ANNs can be classified into several categories: back-propagation neural networks (BPNNs), categorical learning networks, and probabilistic neural networks (Hagan, Demuth & Beale, 2002). Many studies recommended to use the BPNNs for geotechnical applications (Das, 2013). A typical structure of ANN consists of different number of nodes set out in layers: input layer, hidden layer, and output layer, as shown in figure 2.14. The input layer receives the input data as external information, send for analysing and processing in the hidden layer and then the results of processing stage are sent to the output layer. One or two hidden layers are highly effective to analyse and process different problems (Goh, 1994). For example, one-layer ANN architecture was adopted by Coleri et al. (2010) to predict M_r of the subgrade soil. In addition, the architecture of the ANN was consisted of seven parameters (nodes) lined up in the input layer, one parameter (M_r) in the output layer and six nodes in hidden layer. It is important to know that the number of hidden layers was influenced by the nature of problem itself, while the number of nodes in a hidden layer is equal to half the total number of output and input nodes.

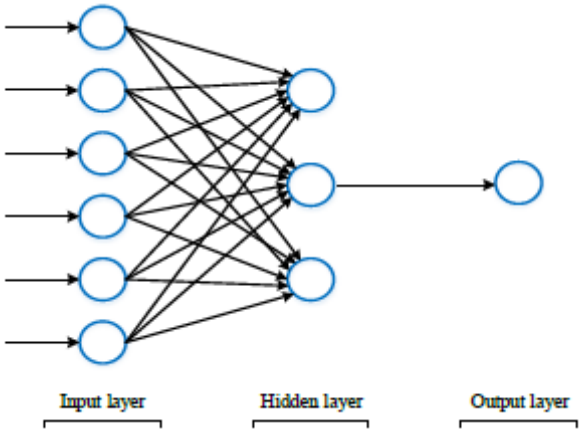

Figure 2.14 Simple structure of ANN

The information in feed-forward networks travels only forward through the input nodes, hidden nodes and, finally, the output nodes. A feed-forward network is the most straight forward type of the ANN networks therefore, Zurada (1992); Fausett (1994); Hill, Lewicki and Lewicki (2006); Ripley (2007) recommended to use the feed-forward network in geotechnical applications. Adjustment weights process of the input data continues inside the hidden layer until the slightest differences are achieved between the predicted and the actual outputs. The input data used in the ANN are divided into training, validation and testing groups, where most of the data are employed to train the network. According to many previous studies, the percentages of training, testing and validation were 70%, 15%, and 15%, respectively, while the percentages of training, testing and validation in another study were 80%, 10% and 10%, respectively (Nazzal & Tatari, 2013). It is worth mentioning that the responsibility of training group is adjusting the connection weights and the training stops when one of the following conditions is met: the maximum number of iterations is reached; the performance gradient falls below a minimal value; or the performance reaches the required value.The testing is responsible for averting the over-fitting case, while the validation is employed to assess the capability of the ANN model for estimating the accurate predictions. If the test set showed perfect performance, minimal number of hidden neurons and good training, testing and validation performances, the ANN model can be considered as an optimal model.

Depending on equations 2.4 and 2.5, the correlation between the predicted and the

measured results is assessed by Root Mean Square Error (RMSE) and the coefficient of determination (R^2). The trial and error method is also employed in ANN which is an important technique of problem solving, where the repeated attempts are continued until reach an R^2 value around 90%. The accuracy of the model results is tested after training and testing.

$$\text{RMSE} = \sqrt{(\frac{1}{N}\sum_{i=1}^{N}(yi - xi)^2)} \quad (2.4)$$

$$R^2 = \left\{ \frac{\sum_{i=1}^{n}(xi-\bar{x})(yi-\bar{y})}{\sqrt{\sum_{i=1}^{n}(xi-\bar{x})^2 \sum_{i=1}^{n}(yi-\bar{y})^2}} \right\}^2 \quad (2.5)$$

Where:

xi: the input data

yi: the model estimated

n: the number of data points

$\bar{x}$ and $\bar{y}$: the mean values of the observed data model estimation

2.11.2 Genetic programming

The next generation of AI is genetic programming (GP) which is a model of a computer program designed to develop solutions for high level problems. In GP, the computing search tries to simulate the principle of biologic evolution in nature to solve the problems. GP contributes to the mathematical algorithms development to create unique and unexpected analytical models and formulas through multiple and branching paths as a tree. In recent years, The GP provided an excellent solution for different geotechnical problems. Sabbar et al. (2017) employed the ANN and the GP with a wide range of data collected from previous experimental results to predict the liquefaction value of sand-fine materials mixtures. The results illustrated a good indication concern the prediction of the liquefaction characteristics of the granular materials. Furthermore, the previous analytical studies concluded that the GP model reported high performance when used in simulating and predicting M_r of different soils. With regards to this subject, Nazzal and Tatari (2013) used the ANN and the GP approaches in developing a model to predict M_r of subgrade soil depending on the soil index properties. The findings of the study concluded that ANN showed higher accuracy in the M_r prediction than the regression models when the GP

selected the input data of the ANN model. Depending on triaxial test parameters, the GP and the ANN was employed by Coleri et al. (2010) for developing a model to predict M_r value. The analytic results indicated that the efficiency for the M_r prediction of the GP and the ANN was 14% higher than that of the Uzan model.

2.12 Summary

A highlighted review of the experimental and the numerical published studies was undertaken concerning the static and dynamic behaviour of the raw unbound material with a wide range of glass and rubber content. An overview of the pavement types and the dynamic behaviour of granular materials under repeated loadings was presented in Chapter 2. More details of the M_r and permanent deformation (P_d) of granular materials were also reviewed. The factors influencing the resilience and the P_d of granular materials such as moisture content, density, gradation, shape, fine materials, and stress were also viewed in this chapter. In summary, there is a positive correlation between the M_r value of granular materials and some properties such as density, well-graded distribution, angular shape, course size and level of stress. In addition, a sample of granular materials, which was prepared at the lowest moisture content showed the best resilience performance. Moreover, different factors that influenced P_d of the materials were discussed. A negative correlation was found between the P_d and some parameters such as density, compaction, well-graded material, angular particles, preloading condition, and stress levels. It is important to know that, a group of studies indicated that up to 9% fine materials could improve the soil resistance against the P_d. Moreover, a positive correlation was noticable between water content and the P_d. Thus, water content can be concerned as a vital factor in P_d of soils.

A review of experimental studies on crushed rock and bentonite in road applications was also analysed, while more details on the waste-soil mixtures topic were discussed in this section. Different properties of waste glass-soil and waste rubber-soil mixtures were studied in the literature to examine the suitability of glass and rubber as base and subbase materials. Despite there were limitations of using waste glass and waste rubber as base or subbase materials, previous results presented different satisfactory specifications of the new mixtures to use in road construction. These specifications included particle size distribution, optimum moisture content,

density, organic content, p_H, hydraulic conductivity, Los Angeles test results, shear strength, CBR, M_r, and P_d.

The review of the previous investigations which explained the layered technique in their studies was also presented in this chapter.The result of the review reported significant characteristics of the layered technique in different geotechnical applications, but further investigation is needed on the layered technique. Despite many previous published investigations on cement treated roads, only a small number of studies investigated the dynamic behaviour of waste materials-rock-cement mixtures in road applications. Thus, the effect of cement on glass-rock-rubber mixtures will be investigated in this thesis. Moreover, most previous studies have focused on using one type of cementation agent. Therefore, the effects of mixing two types of agents (cement and slag) on the dynamic behaviour of the glass-rock-rubber mixtures will paid more attention in this study.

Based on the previous analytical studies, developing a model for predicting M_r of granular materials still needs more attention. Thus, the use of ANN and GP with a wide range of soil parameters to develop a model is one of this study objectives. Despite extensive research works have been assessed the glass and rubber presence in road applications, there has been little quantitative studies tried to combine between glass-rock-rubber materials in the same sample. Also, no research has been tried to use cement or cement-slag to stabilise glass-rock-rubber mixtures. Also, a few studies have employed the layered technique in geotechnical and road applications. However, the layered technique is still poorly understood. After all, further works and additional laboratory investigations are required to establish all the above topics.

Chapter 3: Materials and Methods

3.1 Overview

This chapter describes the apparatus, materials and methodology employed in this study. A mixed methodology is used based on the tests and techniques followed to reach the main objectives. One of the main objectives of this thesis is to evaluate the possibility of using different types of waste materials, such as crushed glass and tyre rubber, with crushed rock in pavement applications. Investigation of mixing rock with different waste materials to assess the dynamic behaviour of layered structures and explore the suitability of using these materials in road applications is also an objective of this study. It is important to know that the research program is divided into several parts, as detailed in Figure 3.1.

The overall research plan can be also divided into five sections, as follows.

• The preliminary and geotechnical characterisations of different homogeneous samples of glass-rock (GR), tyre rubber-rock (TR), and glass-rock-tyre rubber (GRT) mixtures are investigated in this section.

• Examination of the resilience characteristics of GR, TR and GRT mixtures with different cementation materials (cement and slag) and discussion of homogenous techniques.

• Conduction of an experiment program to evaluate the dynamic behaviour of different mixtures of glass-rock, sand-rock and sand-rock-bentonite under different conditions, and discussion of layering techniques.

• Development of predictive models of resilient modulus ($M_{r)}$ using artificial intelligence (AI) approaches.

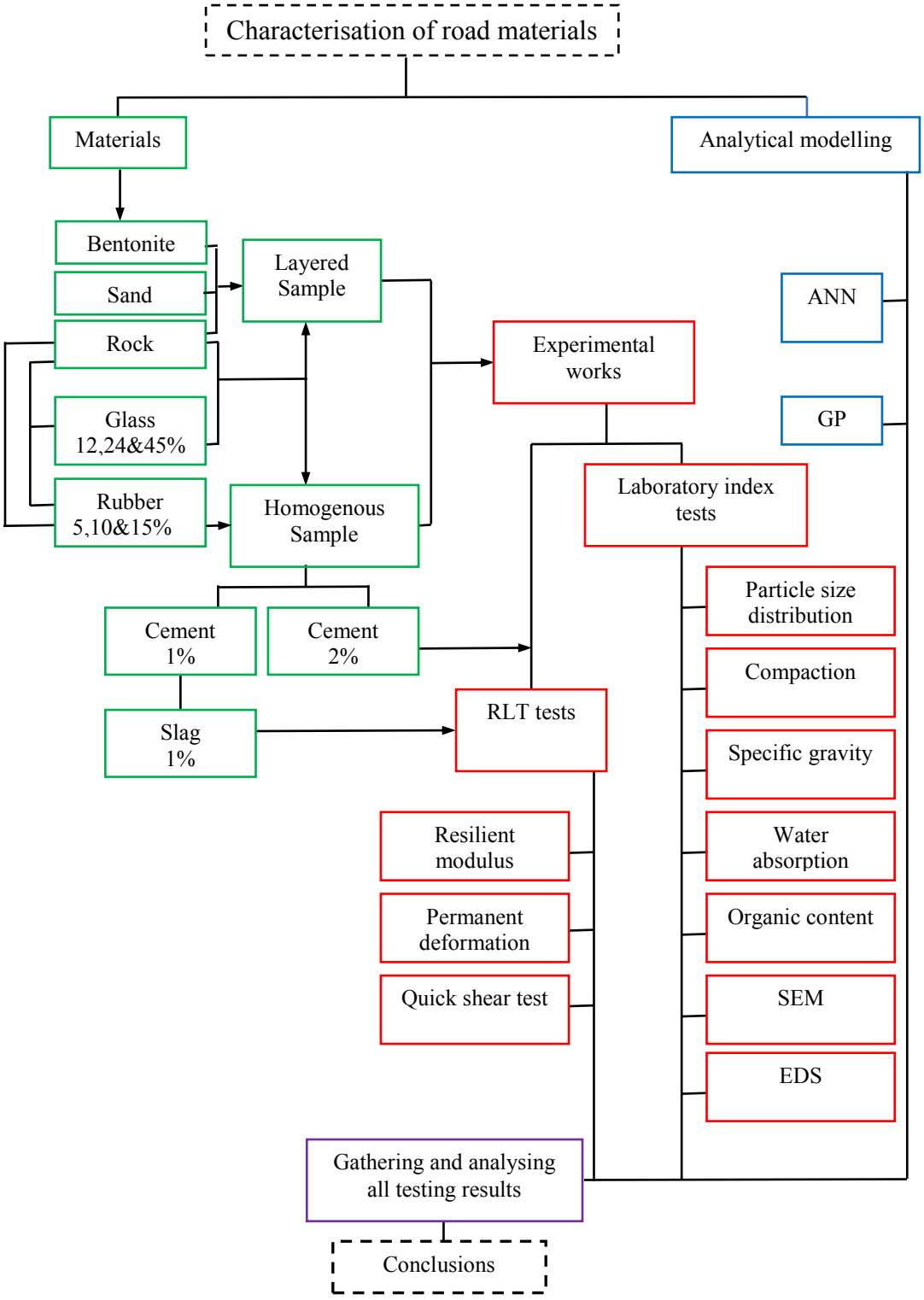

Figure 3.1 Overall plan of the present study

3.2 Main materials

The materials are explained in detail, including their sources, procedure for transport and storage, the specifications of each material. Two types of raw material were used: crushed rock (R) and pure sand. Waste materials were also used in this program: crushed glass (G) and tyre rubber (T). Three types of fine materials were also used: cement (C), slag (S) and bentonite (BE). Most of the materials were collected from Perth in Western Australia and stored in the soil mechanics laboratory at Curtin University of Technology. More details of the materials are detailed below.

3.2.1 Crushed rock

Base and subbase materials are the most widely used groups of granular materials in road applications and have been extensively used to construct multilayered flexible pavements. Around Australia, one of the essential materials commonly used as an unbound material is crushed rock (R). Figure 3.2 (a) and (b) shows samples of dry crushed rock and wet crushed rock, respectively. Figures 3.2 (c) and (d) present the results of scanning electron microscopy (SEM) and energy dispersive spectrometry (EDS) tests of pure rock material. The crushed rock was collected from Gosnells Quarry in Western Australia and supplied by Holcim Quarries Pty. Ltd. According to ASTM, rock samples were collected from the stockpiles and all necessary procedures were applied. The samples were kept in plastic bags and stored in the laboratory following the method of Disfani et al. (2009). According to the specifications of Holcim (2013), the properties of the rock can be found in Table 3.1. According to the requirements of Main Roads Western Australia, Figure 3.2 details the specifications of crushed rock base course materials. As can be seen, the significant elements are potassium (K), oxygen (O), iron (Fe), sodium (Na), magnesium (Mg), silicon (Si), aluminium (Al) and titanium (Ti).

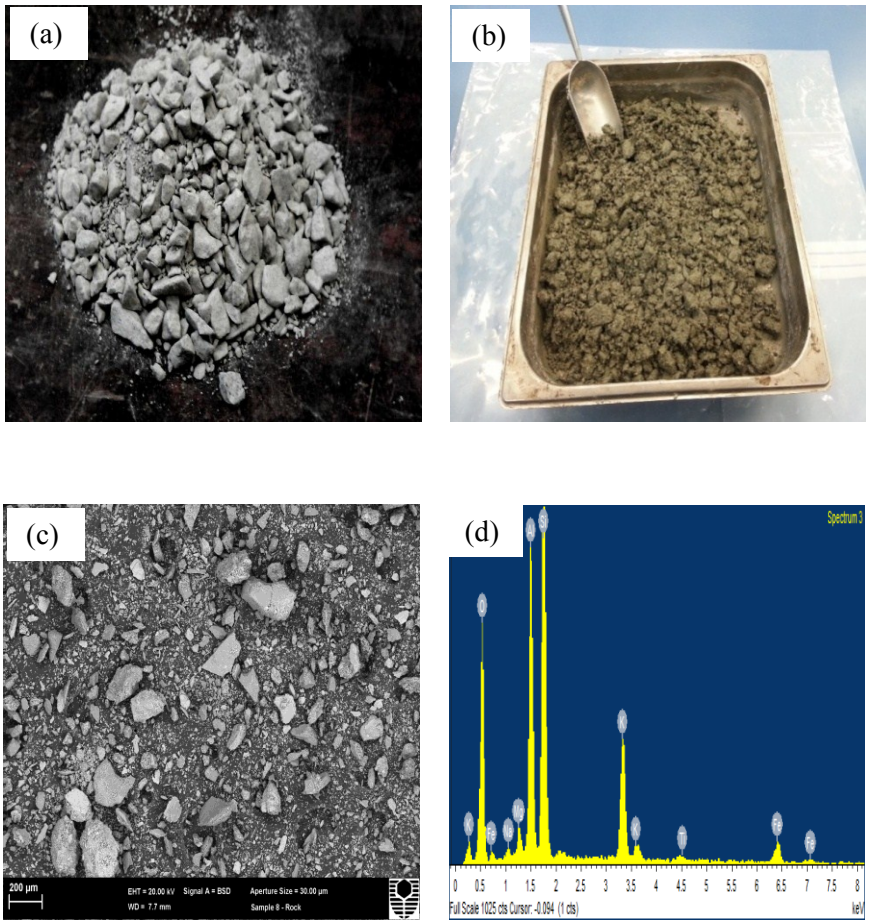

Figure 3.2 a) dry rock, b) wet rock, c) SEM image, and d) EDS spectrum of rock

Table 3.1 Crushed rock properties

Test*	Unit	Value
Particle shape (Flakiness)	%	25
Specific gravity (G_s)	%	2.96
Bulk Density	t/m^3	1.82
Liquid Limit	%	22
Linear Shrinkage	%	1.4
Organic Content	%	0.47
p_H		8.16
Water absorption	%	7.9
Los Angeles	%	20
Maximum dry density	t/m^3	2.4
Optimum moisture content	%	6
California Bearing Ratio	%	198

* Test methods in accordance with MRWA Test Method (MAIN ROADS Western Australia 2006

Table 3.2 Specifications for crushed rock base course

Test*	Limits
Liquid Limit	25.0%
Linear Shrinkage	2.0% Max / 0.4% Min
Flakiness Index	30% Max
Los Angeles Abrasion Value	35% Max
Maximum Dry Compressive Strength	1.7 MPa Min
California Bearing Ratio at 99 % MDD	100 % Min
Wet/Dry Strength Variation	35% Max
Secondary mineral content in basic igneous rock	25% Max
Accelerated soundness index by reflux	94% Min

* Test methods in accordance with MRWA Test Method (MAIN ROADS Western Australia 2006)

3.2.2 Glass

Glass with a maximum particle size of 4.75 mm was collected from Perth Bin Hire located in Duffy Street, Bayswater, Western Australia, then stored in plastic bags inside the soil mechanics laboratory at Curtin University of Technology. More characteristics of crushed glass are illustrated in Table 3.3. A stockpile of crushed glass and a big tray of glass used to mix the samples are shown in Figure 3.3 (a) and (b), respectively. A clear dry sample of crushed glass and a wet sample of crushed glass-crushed rock mixture are illustrated in Figures 3.3 (d) and (c), respectively.

Table 3.3 Crushed glass properties

Test	Unit	Value
Specific gravity	%	2.28
Bulk Density	t/m^3	1.37
Organic Content	%	0.98
p_H		9.73
Water absorption	%	0.4
Los Angeles	%	25
Maximum dry density	t/m^3	1.77
Optimum moisture content	%	1.8
California Bearing Ratio	%	41

Figure 3.3 a) stockpiles of crushed glass, b) large tray used to mix the materials, c) dry sample of crushed glass, and d) wet glass-rock mixture

3.2.3 Tyre rubber

Tyre rubber was obtained from Tyrecycle Pty. Ltd., Somerton, Victoria. According to the American Society for Testing Materials (ASTM), the samples were collected from the stockpiles and then stored in plastic bags in the soil laboratory at Curtin University. Table 3.4 illustrates the main characteristics of the tyre rubber. Figures 3.4 (a), (b) and (c) show a stockpile of whole tyres in storage, and crushed rock-tyre rubber mixtures in dry and wet conditions, respectively. Failure sample of the rubber-rock sample after the repeated loading triaxial test (RLTT) is shown in Figure 3.4 (d).

Table 3.4 Tyre rubber properties

Test	Unit	Value
Specific gravity	%	1.1
Bulk Density	t/m^3	1.153–1.198
Liquid Limit	%	Not applicable
Linear Shrinkage	%	Not applicable
Organic Content	%	0.25
p_H		7.64
Water absorption	%	0.957
Maximum Dry Density	kg/m^3	0.618 to 0.642

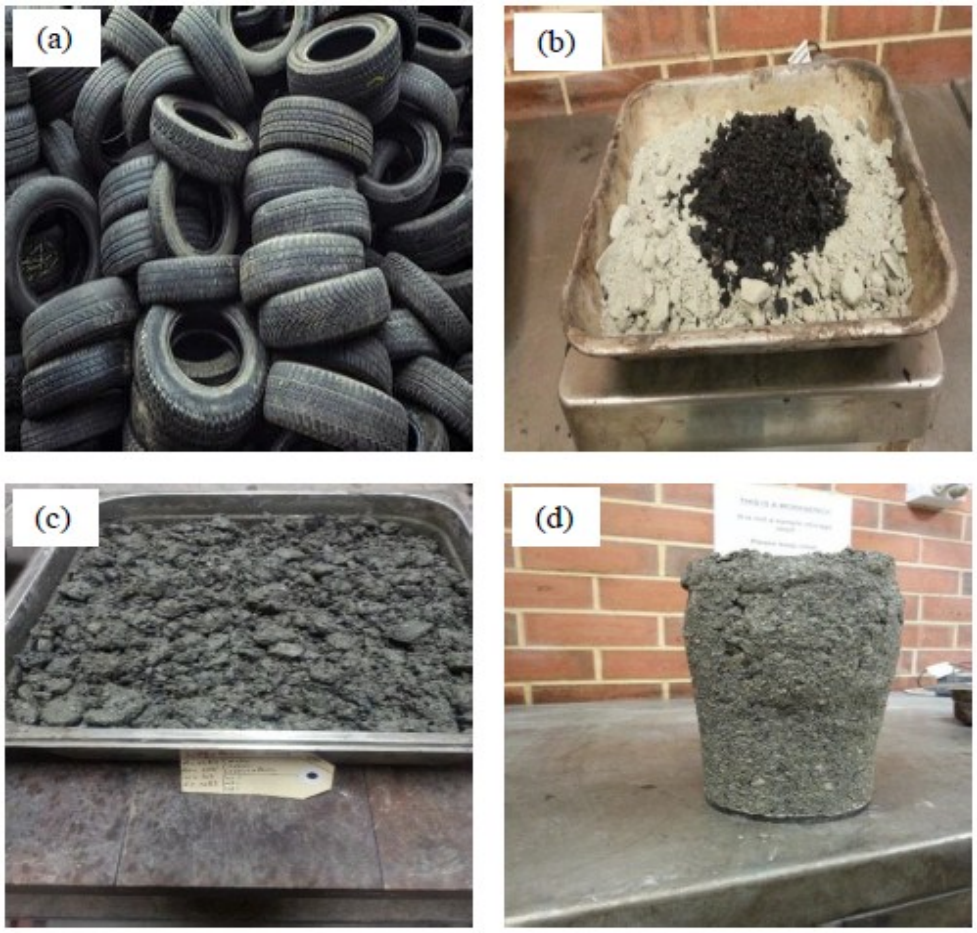

Figure 3.4 a) stockpiles of tyre rubber, b) dry specimen of rubber-rockmixture, c) wet specimen of rubber-rockmixture, and d) failure sample of rubber-rockmixture

3.2.4 Sand

The sand utilised in this research was obtained from Rocla Quarry Products, Perth, Western Australia, its main characteristics are listed in Table 3.5. Figures 3.5 (a) and (b) show dry and wet samples of sand, respectively. Figures 3.5 (c) and (d) present the results of SEM and EDS tests of a pure sand sample. The size of each particle can

be seen in Figure 3.5(c). The range of particles varied from 144 micrometres to 534 micrometres. EDS results of the utilised sand and its elements are presented in Figure 3.5(d). As can be seen, the elements of sand are silicon (Si), aluminium (Al), oxygen (O) and calcium (Ca).

Table 3.5 Pure sand properties

Test	Unit	Value
Specific gravity	%	2.58
Bulk Density	t/m^3	1.54
Chlorine (Cl)	%	0.2
Sulphate	%	<0.01
Sodium Sulphate Soundness	%	0.1
Organic Content	%	0.03
Water absorption	%	0.8
Clay & Fine Silt	%	3
Maximum dry density	t/m^3	1.67
Optimum moisture content	%	12

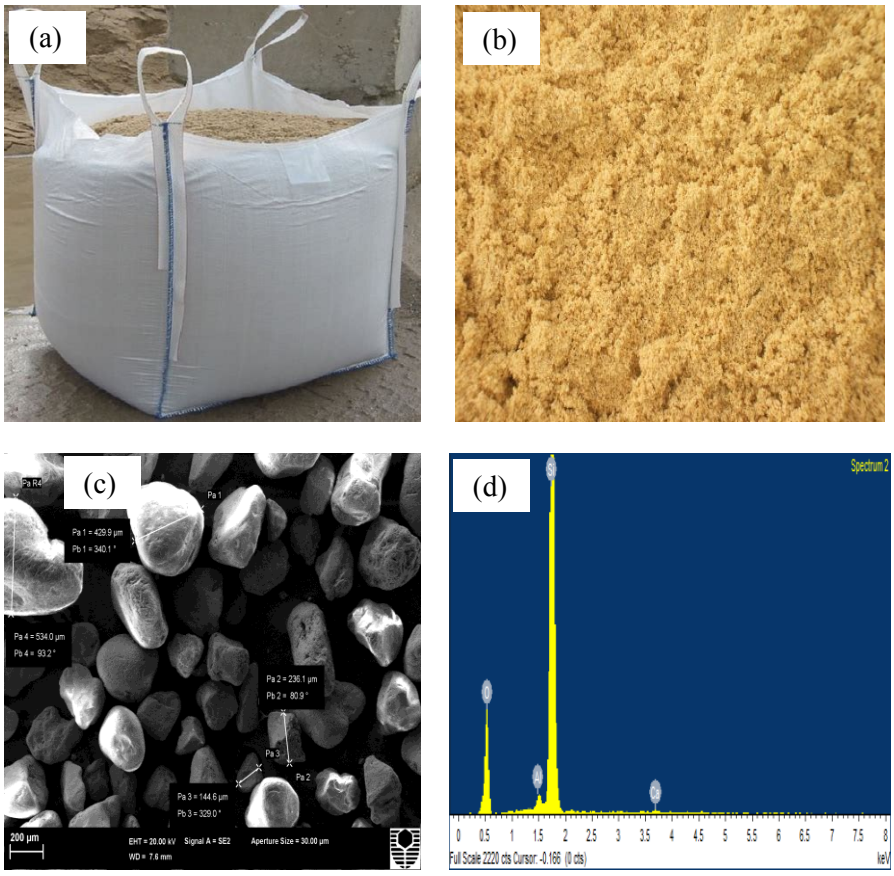

Figure 3.5 a) stockpile of sand, b) wet sand, c) SEM image, and d) EDS spectrum of sand

3.2.5 Bentonite

It is important to know that there are many types of bentonite (BE) that have been used in many experimental works recently. In the present work, the experimental works used powdered sodium-based bentonite containing a high proportion of the active mineral species montmorillonite, which is a product of Unimin Australia Ltd., Queensland, and was found in the geotechnical laboratory store at Curtin University. The main characteristics of the utilised bentonite are illustrated in Table 3.6. Figure 3.6 (a) and (b) shows dry and wet samples of the bentonite, respectively. In-depth microscopic analyses, SEM and EDS tests were conducted on pure bentonite. Figure 3.6 (c) presents the results of the SEM and EDS test. The range of particles sizes varied from 51.48 micrometres to 4.51 micrometres. EDS results of the utilised sand and its elements are presented in Figure 3.6 (d). As can be seen, the significant elements of bentonite are silicon (Si), aluminium (Al), magnesium (Mg), sodium (Na), iron (Fe) and oxygen (O).

Table 3.6 Bentonite properties

Chemical analatic data	%	Physiacle properities	Value
Silicon dioxide (SiO_2)	63.6	Water absorption (ml/g^3)	625
Aluminum oxide (Al_2O_3)	14.6	Bulk density (t/m^3)	1.0
Titanume dioxide (TiO_2)	0.4	Apparent Viscosity	6
Iron Oxide (Fe_2O_3)	2.8	Pastic viscosity	5
Calciume Oxide (CaO)	0.3	Filtrate loss (ml)	18
Sodium Oxide(Na_2O)	1.3	p_H	7
Magnesium Oxide(MgO)	2		
Potassium Oxide(K_2O)	0.5		
Loss in Ignition(1000 c°)	14.5		
Dry Screen(%passing 75 Microons)	78		
Wet Screen (%Retaned 75 microns)	2		
Bulk density (t/M^3)	1		
Optimum Mousture Content(%)	43		

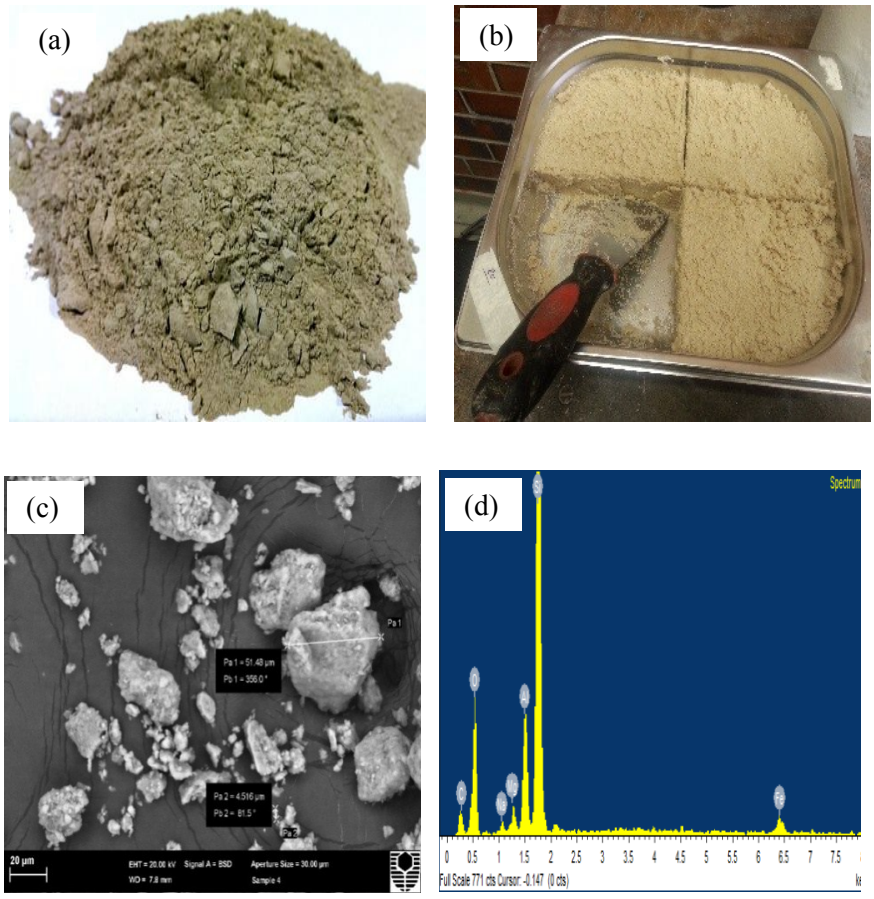

Figure 3.6 a) dry sample of bentonite, b) wet sample of bentonite, c) SEM image, and d) EDS spectrum of bentonite

3.2.6 Cement

Cement is one of the most critical fine materials used as a binding agent in road applications. Cement is produced by a series of chemical processes that combine calcium, silicon, aluminium, iron and other ingredients. General purpose cement (GP) was collected from Kwinana in Western Australia. The general specifications of this cement are shown in Table 3.7. Figures 3.7 (a) and (b) illustrate the typical cement bags and dry sample used in this investigation, respectively. Figures 3.7 (c) and (d) present the results of SEM and EDS tests of pure cement.

Table 3.7 Specifications of cement

Component	%	AS3972
Portland cement	>95%	>92.5
Limestone	>7	<7.5
Minor additional constituents	<1	<7.5

Parameter		Units	Minimum	Typical	Maximum	AS3972 limit	Test method
Setting time	Initial	Min	80	110	140	>45	AS2350.4
	Final	Min	140	170	200	>360	AS2350.4
Soundness		Mim	0	1	3	<5	AS2350.5
Compressive Strength	3 day	MPa	35	38	42		AS2350.11
	7 day	MPa	46	50	54	>35	AS2350.11
	28	MPa	58	63	69	>45	AS2350.11
Fineness		m^2/kg	350	370	390		AS2350.8
CaO		%	63.1	63.7	64.4		AS2350.2
SiO_2		%	20	20.4	20.8		AS2350.2
Al_2O_3		%	5.1	5.4	5.8		AS2350.2
Fe_2O_3		%	2.6	2.8	3		AS2350.2
MgO		%	1.1	1.3	1.5		AS2350.2
Sulfur trioxide (SO_3)		%	2.3	2.7	3	<3.5	AS2350.2
Na_2O equivalent		%	0.4	0.5	0.6		AS2350.2
Chloride		%	0	0.01	0.04	<0.1	AS2350.2
Loss on ignition		%	1.5	2.2	2.7		AS2350.2

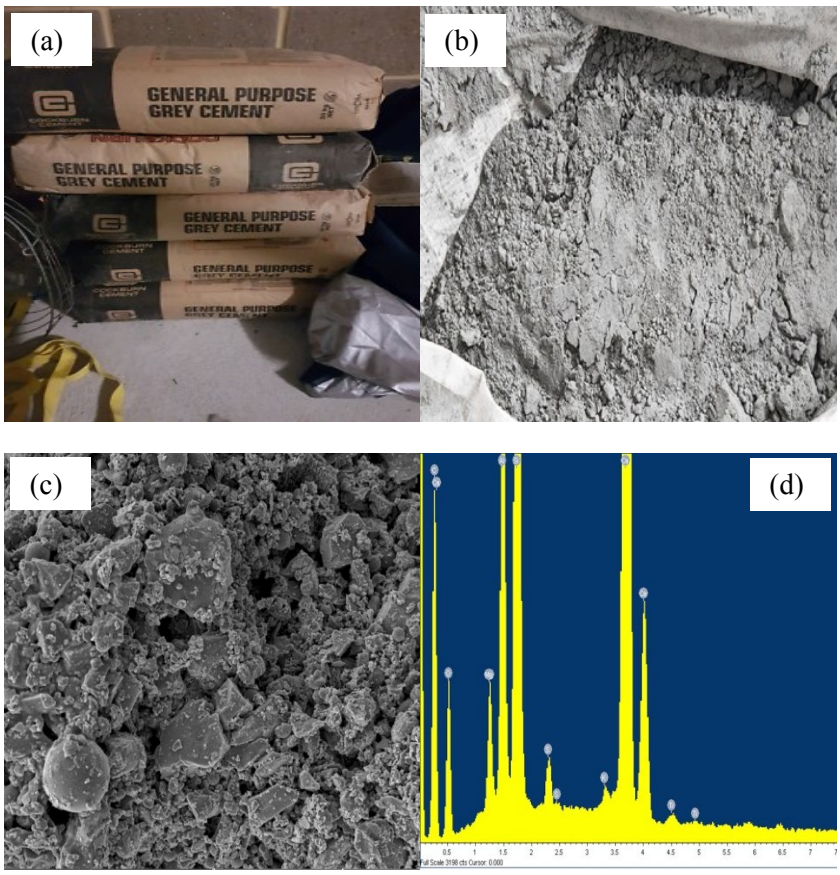

Figure 3.7 a) typical cement bags, b) dry sample, c) SEM imageand, and d) EDS spectrum

3.2.7 Slag

Slag is a waste material left over from iron production. According to the iron production technique, different types of slag are produced. Granulated blast furnace slag (GBFS) was collected from BGCS cement in Western Australia. Its specifications are listed in Table 3.8. Figures 3.8 (a) and (b) show a slag bag and dry sample, respectively. SEM and EDS images of the slag material are presented respectively in Figures 3.8 (c) and (d). As can be seen, the significant elements in slag are silicon (Si), calcium (Ca), aluminium (Al), magnesium (Mg), titanium (Ti), carbon (C), sulphur (S) and oxygen (O).

Table 3.8 Specifications of slag

Chemical components	Range	Physical properties	Details
Coliseum oxide CaO	30-50	Colour	Offwhite
Sulphur	<5	Bulk density (t/m^3)	1-1.1
Silica amorphous	35-40	Relative density	2.28-2.95
Aluminium oxide (Al_2O_3)	5-15	Surface area (m^2/kg)	400-600

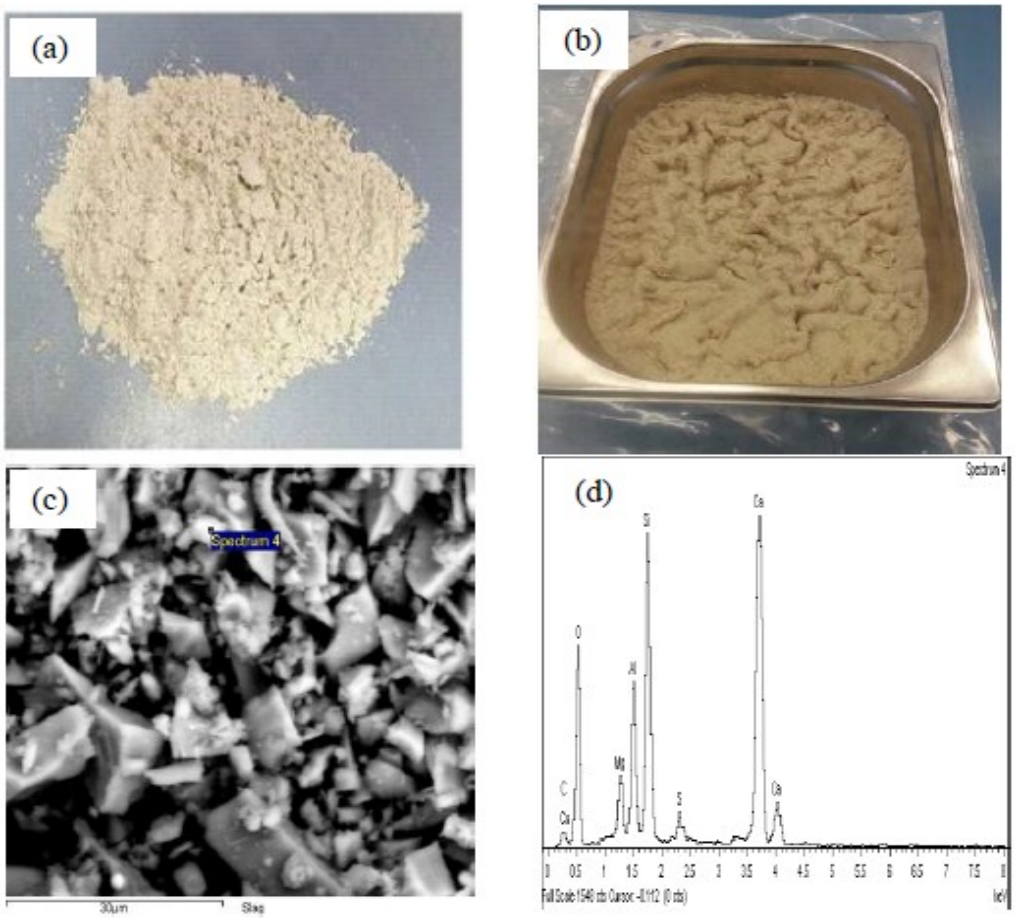

Figure 3.8 a) dry sample of slag, b) wet sample of slag, c) SEM image, and d) EDS spectrum of slag

3.3 Laboratory testing program

Laboratory tests were conducted on different samples of waste-rock mixtures to assess the suitability of using such modified mixtures in road applications. This section includes a sequence of steps taken to develop the appropriate tools and techniques needed to accomplish our goals. All experimental works were conducted at the geotechnical engineering laboratory at Curtin University in Perth, Western Australia. The laboratory tests can be classified into preliminary and mechanical tests, as below.

3.3.1 Preliminary tests

The standards and benefits of preliminary laboratory tests are summarised in Table 3.9, the sample preparation and test conditions for the preliminary tests are performed in section 4.2.

Table 3.9 Preliminary tests and the related standards

Laboratory test	Test standards	test benefits
Sieve analysis	Australian Soil Classification System ASCS (AS 1726-1993)	A series of sieves using to determine the gradation curve which is the vital component for analysing the results.
Modified compaction	Australian Standard AS (1289.5.1.1,2003)	Determine the optimum moisture content and maximum dry density which are employed to assess many of the mechanical prosperities of different materials.
Specific gravity	Standards Australia (1289.3.5.2, 1995a)	Use to estimate the porosity or the void ratio of the materials commonly used in road applications.
p_H	Standards Australia (1997a)	Determine the acidity and the alkalinity of soils which can influence the performance of cement.
Organic content	ASTM (2007a)	Organic content can individually influence the properties of soils and can affect on stabilising soil matters.

3.3.2 Mechanical tests

RLTTs were conducted on a wide range of materials and mixtures to establish the resilient modulus (M_r), Permanent deformation (P_d) and shear strength of the new mixtures. These tests can simulate the actual behaviour of foundation layers under repeated vehicle loads. Previously, the California bearing ratio (CBR) was considered a critical parameter for estimating the resilience characteristics of granular materials. Recently, pavement designers have employed RLTTs, which can provide a realistic picture of soil responses to dynamic impacts, in road design, rather than CBR parameters. The main outputs of the RLTT are M_r, P_d and dynamic shear

strength during thousands of load cycles under different conditions. $M_r$is considered a significant parameter for assessing the resilience and actual behaviour of granular materials.

3.3.2.1 Resilient modulus and permanent deformation

In the laboratory, the M_r and the P_d are estimated through the RLTT. During the test, a repeated axial cyclic stress (σ_1) and confining pressures (σ_3) are subjected to a cylindrical sample of soil as detailed in Figure 3.9. The loading-unloading phases were applied on a specimen of unbound material till fails or exceed the P_d limitations, as detailed in Figure 3.10.

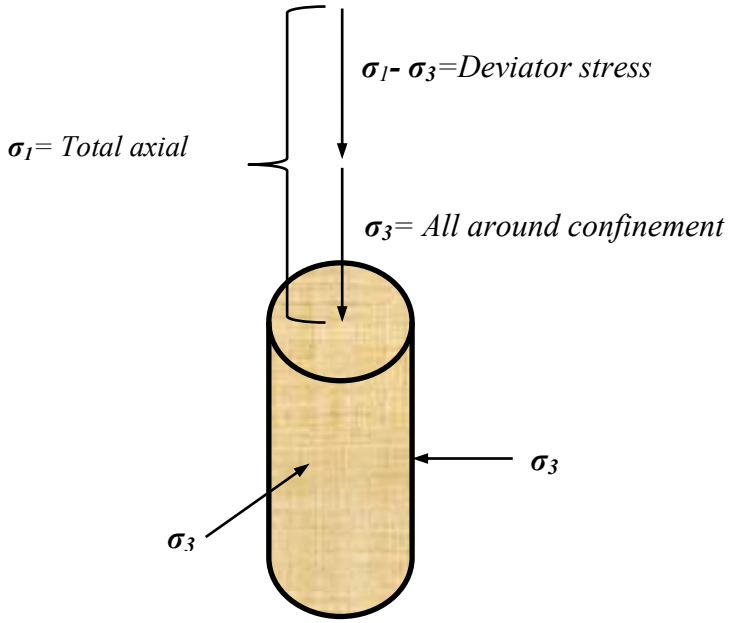

Figure 3.9 Stresses applied in the RLTT

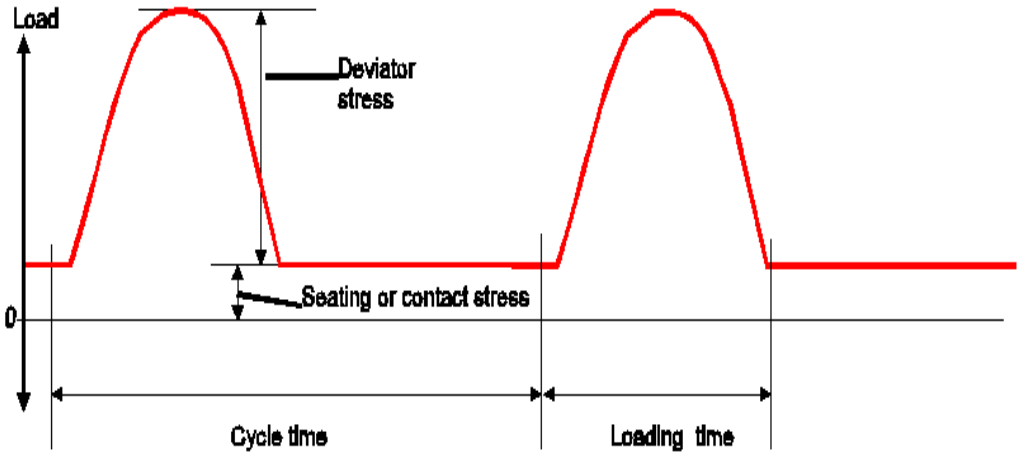

Figure 3.10 Vertical force waveform (De Vos, 2006)

The Universal Testing System (UTS) consisted of:

- A hydraulic or pneumatic axial stress loading system and a pneumatic confining stress loading system.
- Control and data acquisition system (CDAS).
- Personal computer (PC) with Microsoft Windows operating system.
- A suite of universal testing system (UTS) software applications and support files were employed to support the overall system.

Within each stress regime, the specimen is cyclically loaded with axial deviatoric stress while static confining stress is simultaneously applied. Axial loading within each stress regime is repeated for many cycles. Loading stresses together with data from axial and optional radial displacement transducers are gathered during the last five loading cycles of each stress regime so that the M_r and other material parameters may be determined. Stress regimes are selectable from a user-defined list or from a set of predefined lists described by the American Association of State Highways and Transportation Officials (AASHTO) under the designations T292-91, T294-94, TP46-94 and T307-99, as shown in Figure 3.11. On conclusion of testing, a printed report of the test was produced, and tabulated results were exported to a text file suitable for input to a spread sheet program. Figure 3.12 shows example of the charted results.

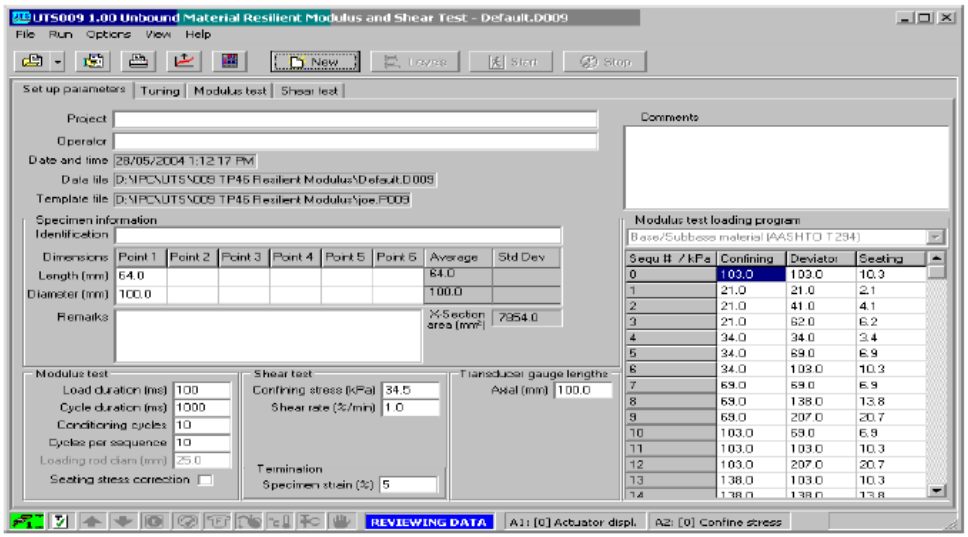

Figure 3.11 Stress regimes of base materials (De Vos, 2006)

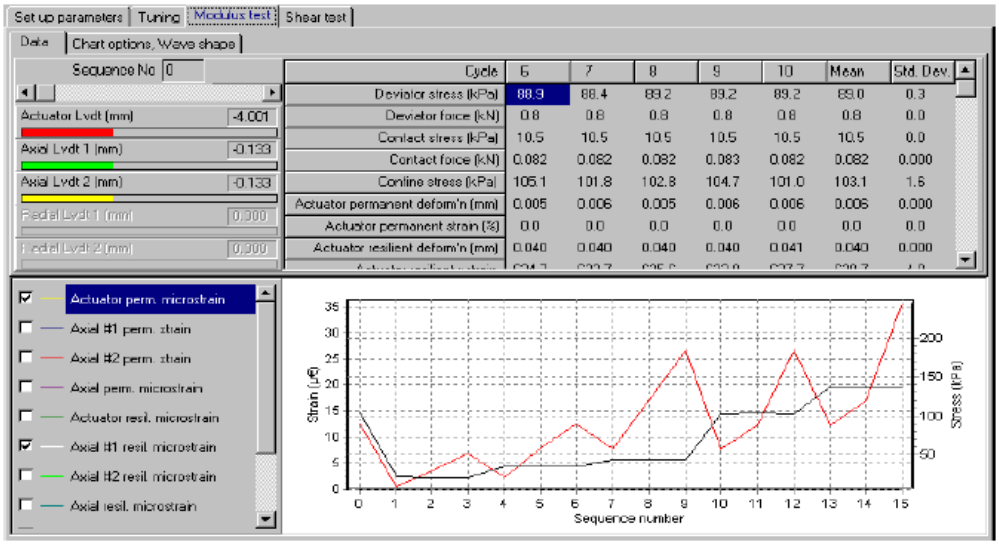

Figure 3.12 Charted results on the personal computer screen (De Vos, 2006)

Many parameters were set out to control the test's operation and data processing included load duration, cycle duration, conditioning cycles, cycles per sequence, loading rod diameter, seating stress correction, and hardware and loading system. Stress is measured by a load cell connected to the actuator. A displacement transducer attached to the actuator ram measures displacement and hence, specimen strain. Figures 3.13 and 3.14 show an overall view of the RLTT device's hardware and loading system. Additionally, two axial and two radial transducers may be optionally used for either on-or off-specimen-mounted displacement measurements. Confining stress was created by servo-controlling compressed air with air/liquid interface to the confining cell. The confining stress was measured by a pressure gauge mounted on the confining cell that was electrically connected to the CDAS.

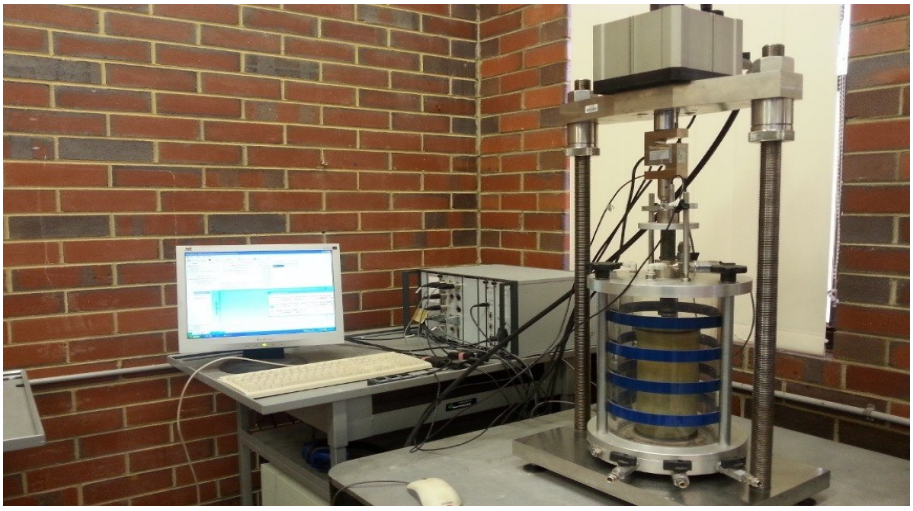

Figure 3.13 Overall views of the hardware and loading system of the RLTT device

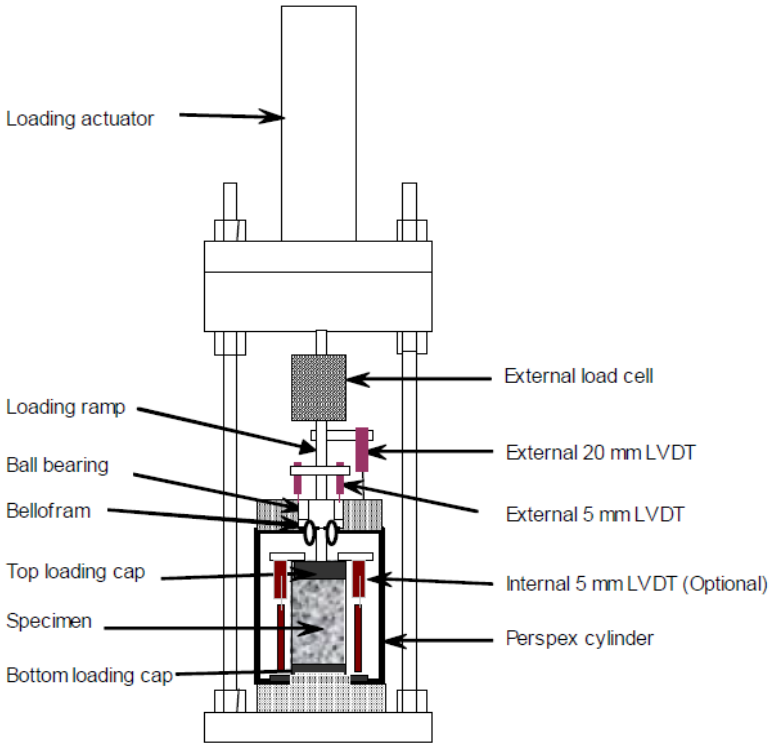

Figure 3.14 Overall view of LVDTs and other RLTT's cell parts

3.3.2.2 Dynamic quick shear test

Further investigations were conducted to assess the shear strength characteristics of the updated mixtures. After the M_r tests finished; quick shear tests were carefully conducted on the specimens. After the modulus tests, a quick shear loading test may optionally be performed to estimate the specimen's strength. If the total accumulated specimen strain (as measured by the actuator LVDT) has not reached the termination strain parameter value, then deviator stresses are no longer applied but the confining and seating stresses are maintained. The operator is presented with the following dialogue and may choose to proceed with a quick shear test. The quick shear test follows the following steps:

- Confining stresses are applied on the specimen as specified by the setup parameter, and axial stress is applied at the specified strain rate.
- The shear test cannot be initiated if the total accumulated permanent strain during the test exceeds the termination strain setup parameter. During the shear test, an axial loading strain rate is applied to the specimen while frequent sampling of all transducers occurs. The shear test continues until it is manually stopped or when

the permanent accumulated strain reaches the present termination strain value. An example of input parameters of quick shear, such as specimen information, loading duration, cycle duration, confining stress, shear rate and termination specimen strain, are detailed in Figure 3.15. A full image of the computer's screen during quick shear testing is illustrated in Figure 3.16. The stress-strain curve of the tested material and the peak strain corresponding to the stress level are detailed in the figure.

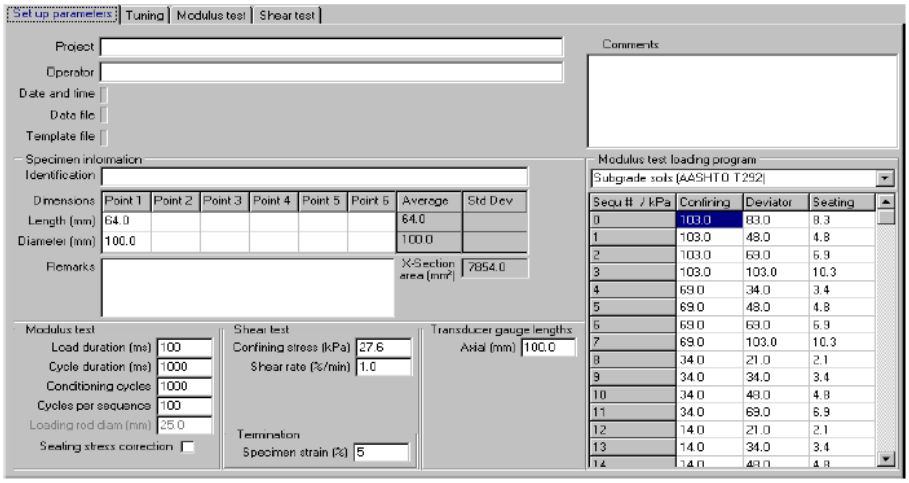

Figure 3.15 Input parameters of the quick shear test (De Vos, 2006)

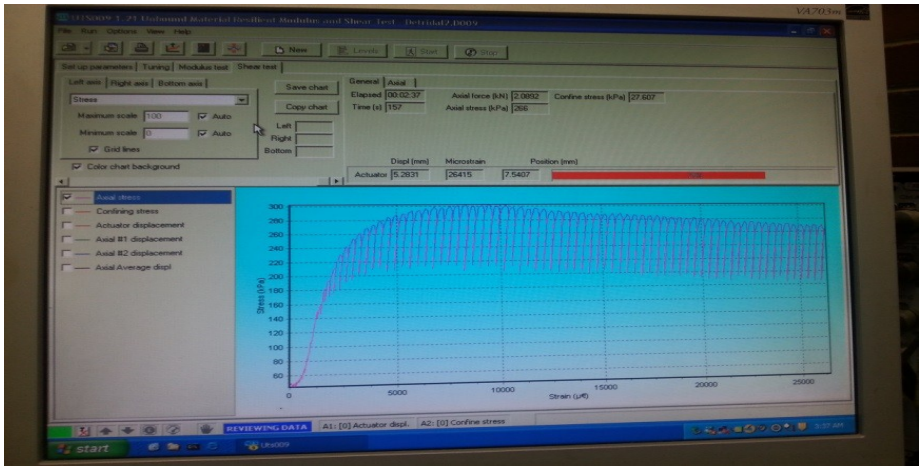

Figure 3.16 Computer screen during dynamic shear testing (the main window of the PC)

3.4 Sample preparation and test design

The dimensions of each sample were 100 × 200mm and most were prepared at the Optimum moisture content (OMC) and the maximum dry density (MDD). According to AS 1289.5.2.1, the high of each sample was divided into eight layers and the mass of each layer was determined. Each layer was compacted to the required thickness

(25mm) according to the material density by uniformly distributed blows of a hammer falling freely from a specified high. It is critical to check the accumulated layer thickness to ensure that it does not vary by more than 2mm from the target accumulative layer thickness. The top of each layer was scarified before placing more material for the next layer (Vuong & Brimble, 2000).

In the present study, the RLTTs were conducted on different samples containing a variety of materials as listed below:

- Glass-rock samples
- Tyre rubber-rock samples
- Glass-rock-rubber samples
- Glass-rock, rubber-rock, and glass rock-rubber mixtures with cement and cement-slag
- Rock-sand samples
- Rock-sand-bentonite samples

3.4.1 Homogeneous and layered samples of glass-rock mixtures

A series of RLTT was conducted on homogenous samples of glass-rock (GR) mixtures to identify their dynamic performance under repeated loads. A further study was performed on layered samples of rock-(glass-rock) materials (R+GR) to evaluate the dynamic behaviour of layered samplles under repeated loading impacts. A wide range of glass (10% to 50%) has been utilised in many previous studies (Senadheera et al., 1995; Ellis & Lowe, 2008; Ali et al., 2011; Arulrajah et al., 2014). Based on these studies, different ratios of crushed glass (12%, 24% and 45%) were mixed with pure rock materials and labelled as GR12, GR24, and GR45, respectively. Figure 3.17(a, b, c and d) presents the materials and the structural design of the glass-rock specimens. Based on MDD value, each layer was adjusted and then compacted until it approximately reached the specified height (Gabr et al., 2013). Other specimens were prepared at different moisture contents to assess the effect of the moisture variation and to simulate field conditions (VicRoads, 2010). According to AASHTO T 307, and depending on the stress path design presented in Table 3.10, the actuator applied axial stress when the confining pressure reached the required value. The structural design of the RLTT specimens are shown in Table 3.11. These particular layered configurations are chosen to explore best structure of the GR-rock specimen

by considering the RLTT and dynamic shear strength test. It is noted that the full height has been divided into eight layers and each time the rock layer has been replaced by a different number of GR layer(s) in different locations, top, middle and bottom. A further description of the homogenous and layered samples is also presented in Table 3.11.

Table 3.10 Stress path applied to each sample (AASHTO T 307)

Sequence #	Confining pressure (kPa)	Deviator pressure (kPa)	Cycles
Conditioning	103.4	93.1	1000
1	20.7	18.6	100
2	20.7	37.3	100
3	20.7	55.9	100
4	34.5	31	100
5	34.5	62	100
6	34.5	93.1	100
7	68.9	62	100
8	68.9	93.1	100
9	68.9	62	100
10	103.4	124.1	100
11	103.4	186.1	100
12	103.4	62	100
13	137.9	93.1	100
14	137.9	124.1	100
15	137.9	248.2	100

Table 3.11 Structure design of glass-rock specimens

Symbol	R	GR12	GR24	GR45	R+GR12	R+GR24	4GR45+4R
Specimen	100% Rock	88 % Rock 12% Glass	76 % Rock 24% Glass	55 % Rock 45% Glass	GR12 R GR12 R GR12 R GR12 R	GR24 R GR24 R GR246 R GR24 R	R R R R GR45 GR45 GR45 GR45

Symbol	R+GR45	2R+2GR12	2R+2GR24	2R+2GR45	4GR24+4R	4R+4GR24	4R+4GR45	R+GR12 +70% OMC
Specimen	GR45 R GR45 R GR45 R GR45 R	GR12 GR12 R R GR12 GR12 R R	GR24 GR24 R R GR24 GR24 R R	GR45 GR45 R R GR45 GR45 R R	R R R R GR24 GR24 GR24 GR24	GR24 GR24 GR24 GR24 R R R R	GR45 GR45 GR45 GR45 R R R R	GR12+0.7 OMC R+0.7 OMC GR12+0.7 OMC R+0.7 OMC GR12+0.7 OMC R+0.7 OMC GR12+0.7 OMC R+0.7 OMC

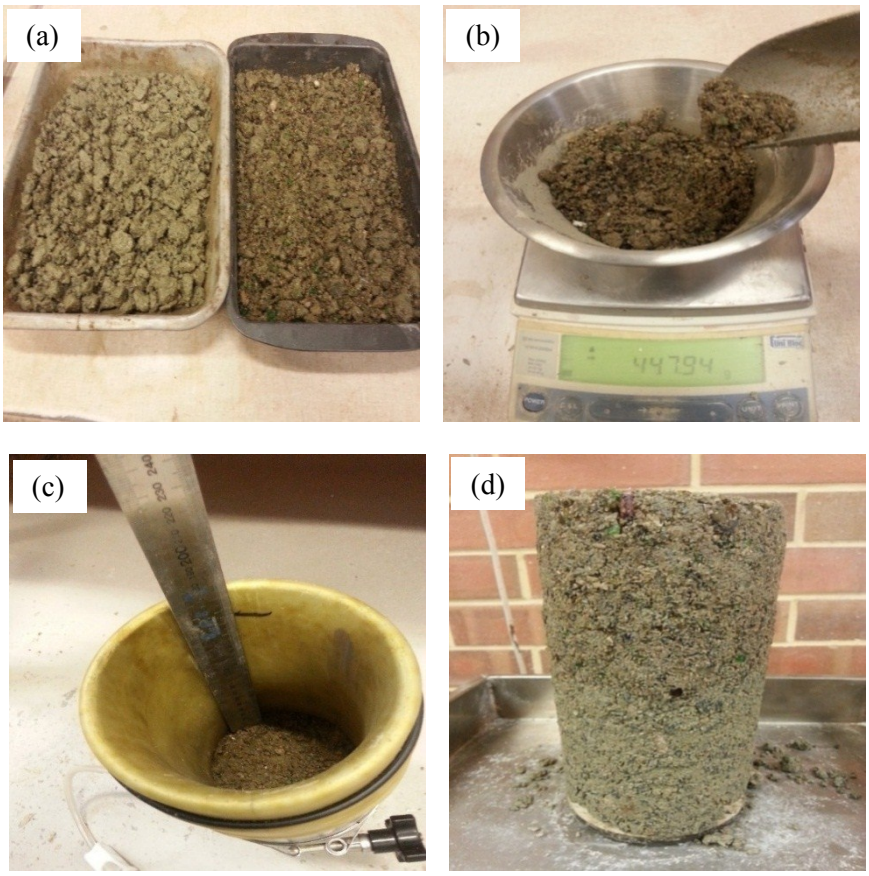

Figure 3.17 Sample preparation: a) trays of crushed rock and glass, b) checking the weight of each layer, c) checking the thickness of each compacted layer, and d) a fully assembled sample of glass-rock

3.4.2 Homogeneous samples of tyre rubber-rock mixtures

The current part of the study has examined homogenous samples of tyre rubber-rock mixtures (TR). Wide differences in surface textures, shape and density were noticeable between the crushed rock and tyre rubber particles, and that could cause to components segregation when different particles are mixed together (Ottino & Khakhar, 2000). Different steps were performed in this section to minimise the segregation between the rubber and the rock particles including: ensure homogeneity of the mixture before adding water, divided the mixture of each sample into four parts before adding water, used water spray and mixed each part gently to prevent separating the fine materials out, minimised the mixture vibration and maintaining its humidity during preparation stage, and lowered free-fall of each layer during the compaction stages. Except that, the preparation process proceeded similarly to that in section 3.4.1. A wide range of rubber (5% to 15%) has been utilised in many published studies (Speir & Witczak, 1996; Parakh et al., 2016). Therefore, different

ratios of tyre rubber, 5%, 10%, and 15% were mixed with pure rock materials in this experimental study and labelled as TR5, TR10, and TR15, respectively. Figure 3.18 details the materials and the preparation stages of the TR samples. It is important to mention that layered technique will not be used for specimens containing rubber in this study because of the negative effects of rubber-rock mixtures on the homogeneous specimens by considering the results of RLTT and dynamic shear test. A further study was conducted on the TR mixtures to assess the effect of moisture content on their resilience behaviour, more specimens were prepared at 100% and 70% OMCs. The preparation process used for all samples was followed the structural design detailed in Table 3.12.

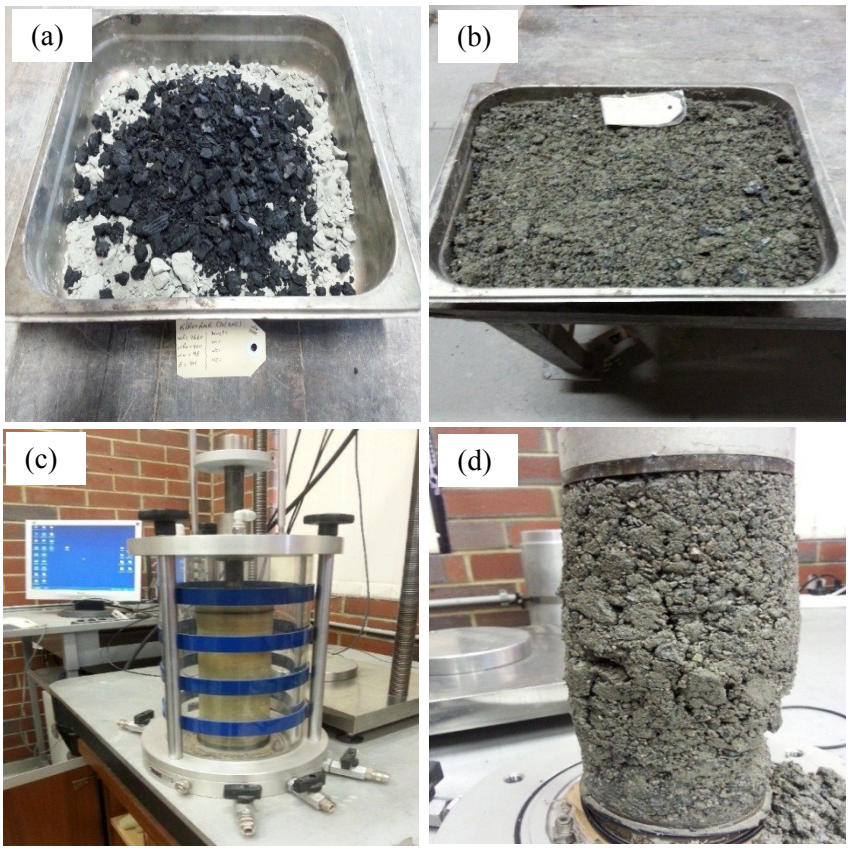

Figure 3.18 Sample preparation: a) a tray of rubber and crushed rock, b) a homogenous wet mixture of tyre rubber and crushed rock, c) full sample inside the RLTT apparatus and d) blended sample after the RLTT

Table 3.12 Structure design of tyre rubber-rock mixtures

Symbol	TR5	TR5+0.7 OMC	TR10	TR10+0.7 OMC	TR15	TR15+0.7 OMC
Specimen	95% Rock 5% Rubber	95% Rock 5% Rubber +70% OMC	90% Rock 10% Rubber	90% Rock 10% Rubber +70% OMC	85% Rock 15% Rubber	85% Rock 15% Rubber +7 0%OMC

3.4.3 Homogeneous specimens of glass-rock-rubber mixtures

Despite many studies have investigated using waste materials in road applications, few have employed a combination of glass and tyre rubber in the same specimen. It would be interesting to use the present set of analyses in a further study to assess the effects of mixing glass and rubber with crushed rock on dynamic behaviour of glass-rock-rubber mixtures (GRT). According to the mixture design presented in Table 3.13, a wide range of glass, rubber and rock was gently mixed. Based on the stress path design presented in Table 3.10, the repeated loadings were applied on each sample as soon as the preparation step compleated. Further investigation into the effect of the moisture variations were performed in this section, where dry mixtures were mixed with different moisture contents (100% and 70% OMC). On completion of the mixture preparation, the compaction stage is carried out as shown in Figure 3.19.

Table 3.13 Structural design of glass-rock-rubber mixtures

Symbol	GR12T5	GR12T5 0.7OMC	GR24T5	GR24T5 0.7 OMC	GR45T5	GR45T5 0.7 OMC
Specimen						
Symbol	GR12T10	GR12T10 70%OMC	GR24T10	GR24T10 70% OMC	GR45T10	GR45T10 70% OMC
Specimen						
Symbol	GR12T15	GR12T15 70%OMC	GR24T15	GR24T15 70% OMC	GR45T15	GR45 T15 70% OMC
Specimen						

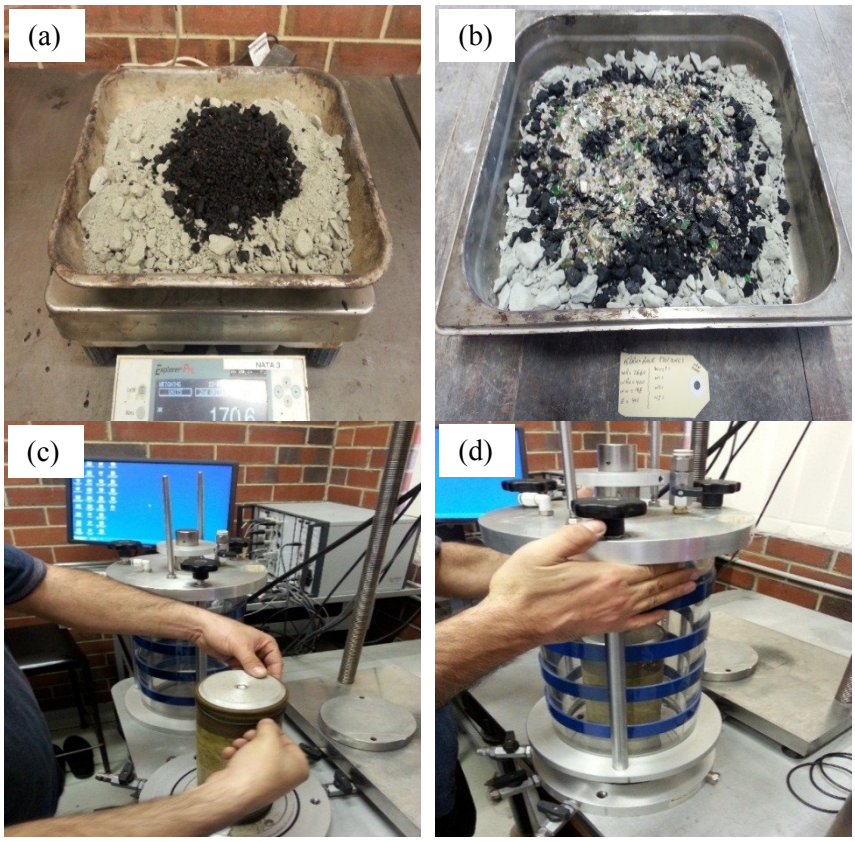

Figure 3.19 Sample preparation: a) a tray of rubber and crushed rock, b) a tray of glass-rock-rubber, c) putting O-rings around the top loading cup d) a full sample inside the RLTT cell

3.4.4 Homogenous samples of glass-rock-rubber-cement-slag mixtures

Chemical treatment of road materials is common in Australia. Based on the previous work in Chapter 2, cementation agents may improve the resilience behaviour of soils. According to Main Roads Western Australia (MRWA), base course materials can be treated by cement alone or with cement-slag or cement-fly ash mixtures. Depending on this, the dynamic behaviour of glass-rubber-rock-cement-slag mixtures was assessed in this study. Two types of agents were used in the chemical treatment process, cement and slag. Cement is the most common agent used with road materials; it can be used alone or in combination with another agent. Slag was also employed with cement in this study as a stabilise material with glass-rock-rubber mixtures. The methodological approach taken in this study is based on that of Main Roads WA (2006). AustRoads (2008) and Siripun et al. (2009) recommend mixing 2% cement with base and subbase materials. All mixtures and the structural design of the treated samples of GR, TR, and GRT are detailed in Table 3.14. Each preparation

stage started with mixing the dry materials with the cementation agent. For example, glass, crushed rock, rubber, and cement were mixed gently in a dry condition. After that, the dry mixture was gently mixed with the OMC of the GRT mixture (collected from Tables 4.3, 4.4, and 4.5) at the room temperature, as described by the MRWA test method (2007). The wet mixture was then mixed in a mixing machine for about 10 minutes and then kept in a sealed chamber and plastic bags for seven days. According to the stress path design presented in Table 3.10, the actuator applied axial stress when the confining pressure reached the required value. Further investigations were also conducted on GRT mixtures with a combination of cement and slag materials to assess the resilience behaviour of the modified mixtures. Figure 3.20 details the process of preparing the treated samples used in this study.

Table 3.14 Structural design of the cement and cement-slag treated samples

Symbol	GR12C2-7	GR12CS-7	TR5C2-7	TR5C1S-7	GR12T5C2-7
Specimen	12%Glass 88% Rock 2% Cement 7 days	12%Glass 88% Rock 1% Cement 1% Slag 7 days	5%Rubber 95 % Rock 2% Cement 7 days	5%Rubber 95 % Rock 1% Cement 1% Slag 7 days	*12% Glass* *5%Rubber* *83 % Rock* *2% Cement* *7 days*
Symbol	GR12T5C1S-7	GR12C2-14	GR12T5C2-14	GR12T5C1S-14	
Specimen	12% Glass 5%Rubber 83 % Rock 1% Cement 1% Slag 7 days	12%Glass 88% Rock 2% Cement 14 days	12% Glass 5%Rubber 83 % Rock 2% Cement 14 days	12% Glass 5%Rubber 83 % Rock 1% Cement 1% Slag 14 days	

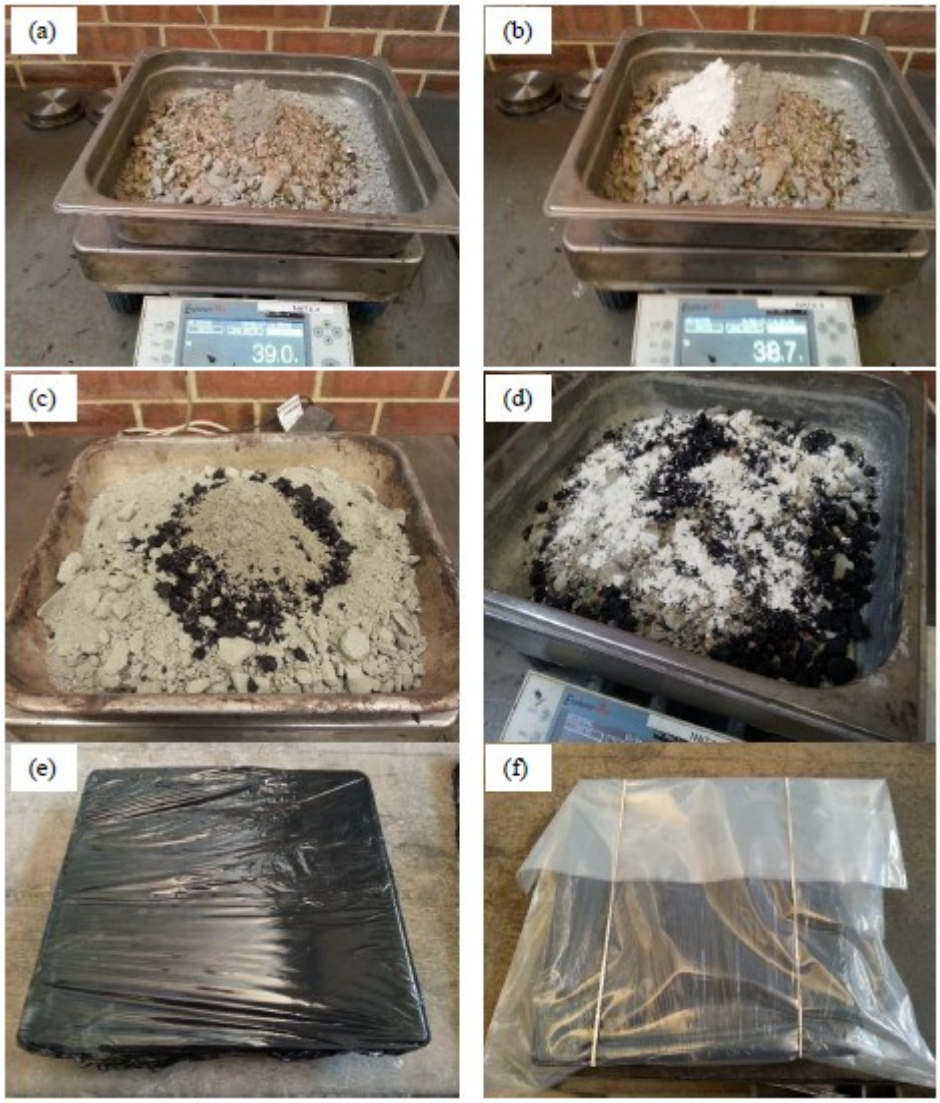

Figure 3.20 Preparation stages: a) a tray of glass-rock-cement, b)a tray of glass-rock-cement slag, c) tray of rubber-rock-cement-slag d) tray of glass-rock-rubber-cement-slag e) plastic sheet covering the mixture and f) plastic bag sealing the covered tray

3.4.5 Layered samples of rock and sand

According to British Standard BS. EN 13286-7:2004, a series of RLLTs were conducted on samples of rock-sand materials (R-S) to evaluate the dynamic behaviour of layered specimens under repeated load impacts. The number of cycles were changed (i.e. 100 and 10000) as presented in Table 3.15. The samples were prepared according to the layering technique and the structural design reported in Table 3.16. These particular layered configurations are chosen in this study to achieve optimal configuration of the R-S sample by considering the RLTT. It is noted that the number and the location of the sand layers were changed, where the sand layers were placed close to the top, bottom and middle of the rock samples, as

detailed in the table. The steps used to construct the eight layered samples of R-S are shown in Figure 3.21. Before each test, the actuator and linear variable differential transformers (LVDTs) were calibrated. After that, the test was run and each sample was subjected to an initial conditioning stress path to minimise the effect of the initial contact between the cap and the base. After the conditioning stage, the stress paths (including the confining and deviator pressures) were applied. More details about the stress path states and the way that loading was applied in each stress path are shown in Table 3.15.

Table 3.15 Stress path applied to each sample

Stress Path no.	Confining pressure (kPa)	Deviator stress (kPa)
Conditioning	70	200
From 1 to 4	20	20, 35, 50 & 70
From 5 to 9	35	35, 50, 70, 90 & 120
From10 to 14	50	50, 70, 90,120 & 160
From 15 to 19	70	70, 90,120,160 & 200
From 20 to 24	100	90, 120, 160, 200 & 240
From 25 to 29	150	120, 150, 200, 240 & 300

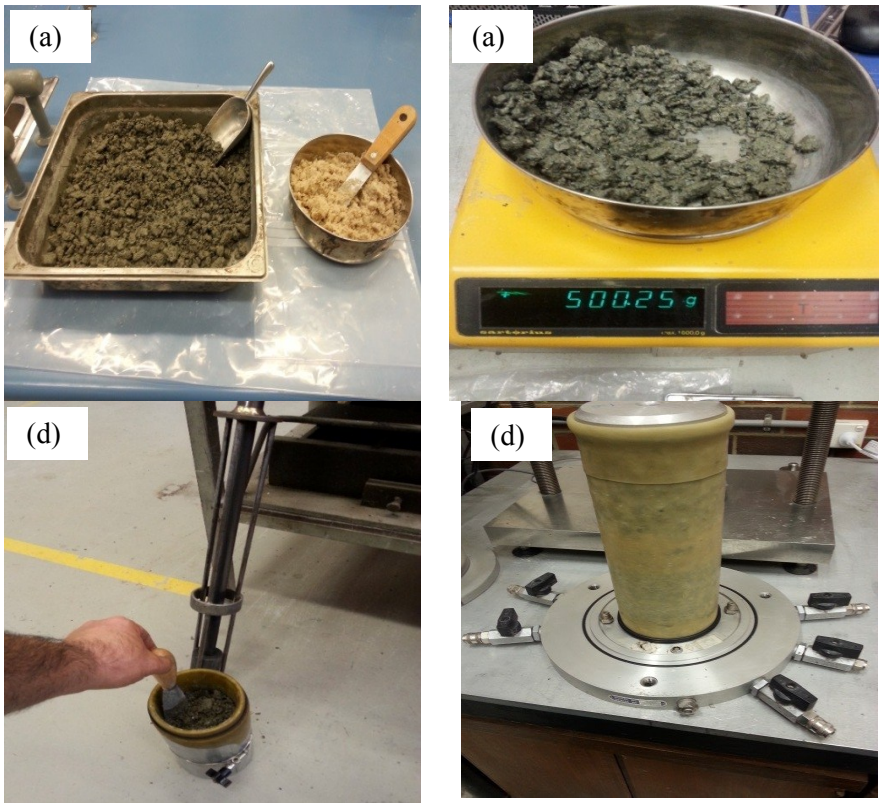

Figure 3.21 Sample preparation: a) trays of rock and sand, b) weighing each layer, c) compaction stage and d) final layout of the specimen before the RLTT

Table 3.16 Structural design of the layered samples of rock and sand

Symbol	R (100)	4R+S+3R (100)	6R+S+R (100)	R+S+6R (100)	2R+S+R+S+3R (100)	2R+S+R+S+R+S+R (100)	R+S+S+R+S+R+S+R (100)
Specimen 100 (cycles/path)	R	R R R S R R R R	R S R R R R R R	R R R R R R S R	R R R S R S R R	R S R S R S R R	R S R S R S R S
Symbol	R (100000)	4R+S+3R (100000)	6R+S+R (100000)	R+S+6R (100000)	2R+S+R+S+3R (100000)	2R+S+R+S+R+S+R (100000)	R+S+S+R+S+R+S+R(100000)
Specimen 100000 (cycles/path)	R	R R R S R R R R	R S R R R R R R	R R R R R R S R	R R R S R S R R	R S R S R S R R	R S R S R S R S

3.4.6 Layered samples of rock, bentonite, and sand

The primary objective of this section is to illustrate the effects of bentonite (BE) layers on the resilience characteristics of the rock and the rock-sand samples. Effects of the location and the number of the BE layers was also examined in this section. The procedure for forming layered samples of rock-bentonite (R-BE) and rock-bentonite-sand (R-BE-S) is detailed in Figure 3.22 (a, b, c and d). After the preparation stage, the samples were subjected to a constant stress path at a loading frequency of 2 Hz. The test tracked to the next stress path when 100 cycles had been completed. The test continued until all the stress paths were applied or the sample

failed. The stress paths used in this section is listed in Table 3.15. Structural design of the layered samples of R-BE and R-BE-S is illustrated in Table 3.17. These particular layered configurations are chosen in this study to explore best configuration by considering the RLTT. It is important to know that the full height of each sample was divided into eight layers. The location of the BE layer was also varied (i.e. top, middle and bottom).

Figure 3.22 Sample preparation: a) trays of bentonite, crushed rock and sand, b) preparation of each layer for the compaction stage, c) checking the thickness of each layer and d) fully assembled sample of rock-bentonite-sand

Table 3.17 Structural design of the layered samples of rock-bentonite and rock-bentonite-sand

Symbol	6R+BE+R (100)	R+BE+6R (100)	4R+BE+3R (100)	2R+BE+R+BE+3R (100)	2R+S+R+BE+3R (100)	2R+BE+R+S+3R (100)
Specimen	R BE R R R R R R	R R R R R R BE R	R R R BE R R R R	R R R BE R BE R R	R R R BE R S R R	R R R S R BE R R

3.5 Artificial intelligence analysis

In this section, a numerical study was performed for developing a model to predict the resilient modulus (M_r) of base and subbase materials. Artificial neural network (ANN) and genetic programming (GP) with a wide range of basic parameters were employed in this development process. In this study, these parameters were obtained from various experimental studies on different base and subbase materials. More details about the ANN, GP, and the prediction process are given below.

3.5.1 Artificial neural network

The ANN is a type of the artificial intelligence (AI) techniques used to solve linear and nonlinear complex problems. Previous studies have established that the elastic behaviour of soil is affected by some of soil properties such as the percent passing #4.75mm and #0.075mm, deviator stresses, confining stress, moisture content, and the compaction levels (Lekarp et al., 2000; Rahim & George, 2004). Thus, the ANN technique in the present study used a group of soil properties as input data for training, validation and testing the model, where most of the input data were used to train the ANN model. Fundamental properties such as moisture content (M_c%), dry density (γ_d), confining pressure (γ_c), deviator stress (σ_d), mean diameter (D_{50}), coefficient of curvature (C_c), coefficient of uniformity (C_u), and bulk stress (θ) of different base and subbase materials were used with the ANN. The MATLAB's normalisation function was used to normalised all the input values between 0 and 1 before used in the ANN. A genetic algorithm program with some hidden layers and neurons were employed in the ANN to finalise the prediction development process. The Levenberg-Marquardt back-propagation algorithm (LMA) was used in this study; it has two layers of feed-forward back-propagation and seven hidden neurons. More details on this topic can be found in Section 7.2.1 of Chapter 7. The dataset used in the ANN approach was divided randomly into three parts, 70%, 15% and 15% for training, validation and testing, respectively. As a part of the assessment process, the mean errors of the proposed model at the training, validation and testing stages were calculated. It is important to know that the proposed model is considered acceptable when the final mean squared error is the minimal and the validation set shows similar behaviour that of the test set (Demuth, Beale & Hagan, 2008).

3.5.2 Genetic programming

GP is another technique of the AI approaches which has commonly used in geotechnical applications to solve complex problems. In recent years, GP used in developing different models to predict M_r of base or subbase materials. HeuristicLab software with an extensive database was employed in the GP to completion the development process. Figure 3.23 shows a screenshot of the HeuristicLab software program. The theoretical approach of the HeuristicLab program is contributed in simplifying the complex models via a series of trial-and-error iterations. Based on the ANN results, the model which shows the best performance in the training set (the highest coefficient of determination R^2), was selected and employing in the GP technique.

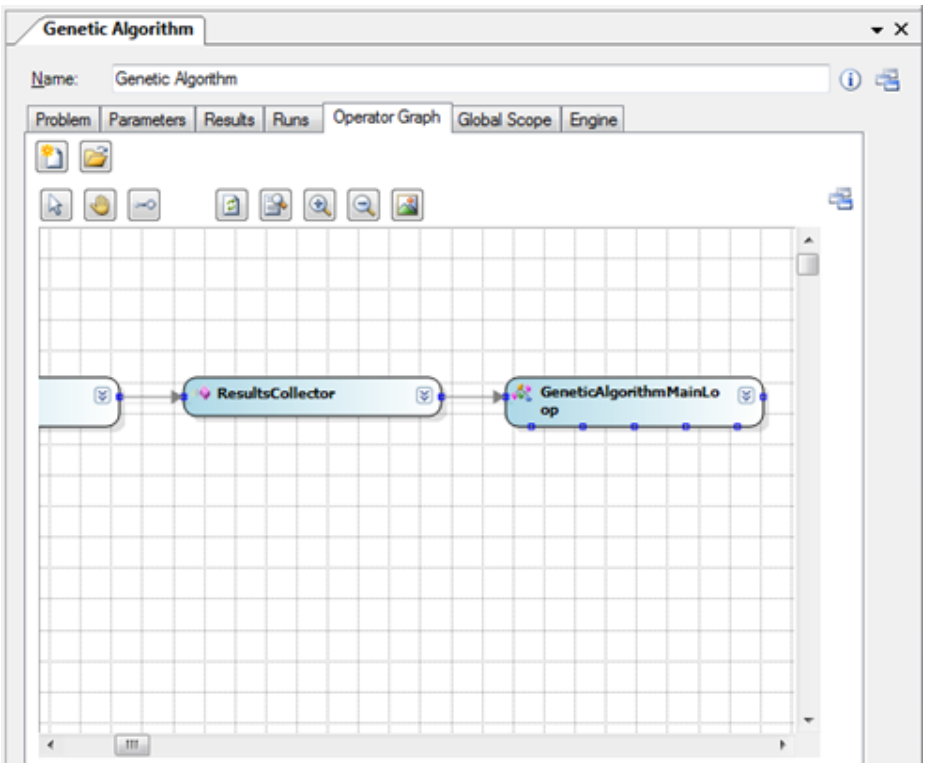

Figure 3.23 Screenshot of the HeuristicLab software program (the main window of the PC)

Before the GP was run, all symbolic regression parameters, included population size, the maximum number of generations, parent selection, replacement, crossover, mutation rate, the fitness function, and function and terminal sets, were listed. Related on the training/testing input data, any ratio can be set for the first trial (Ferreira, 2006). Generally, 80% to 90% of the input data should be employed as

training data, while 10% to 20% should be used as testing data. Therefore, training/testing ratios of 90/10, 80/20 and 70/30 were applied. The outputs were compared to evaluate the best regression models, as illustrated in Figure 3.24. The correlation between the measured values and those that predicted by the developed GP model was determined though linear regression, as detailed in Figure 3.25.

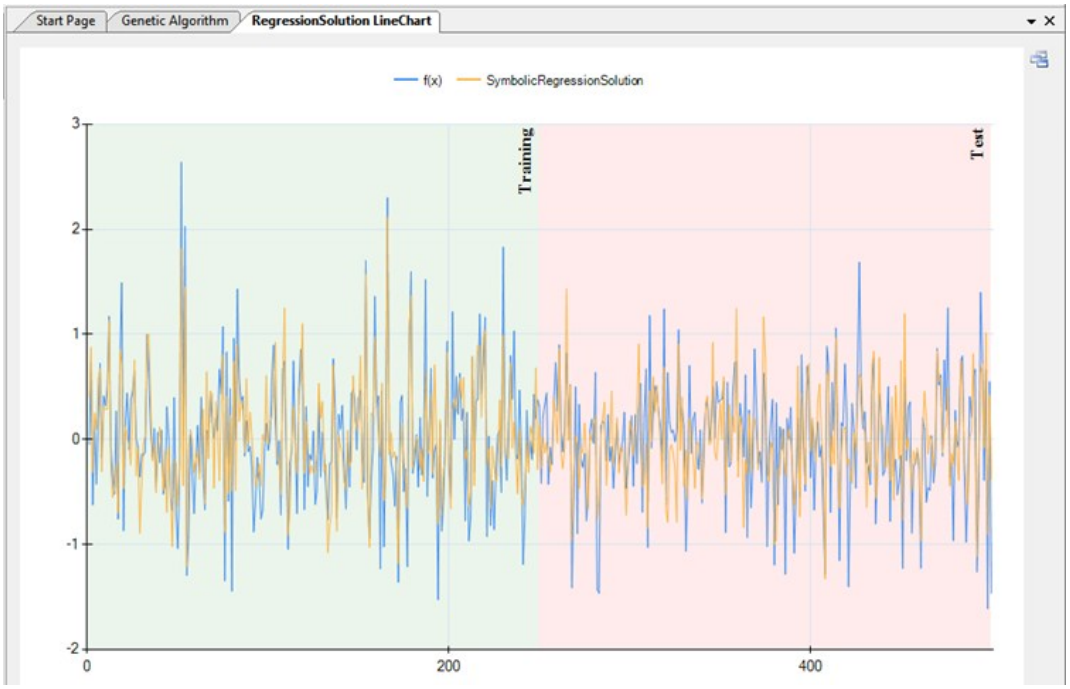

Figure 3.24 Line charts of training and test datasets (the main window of the PC)

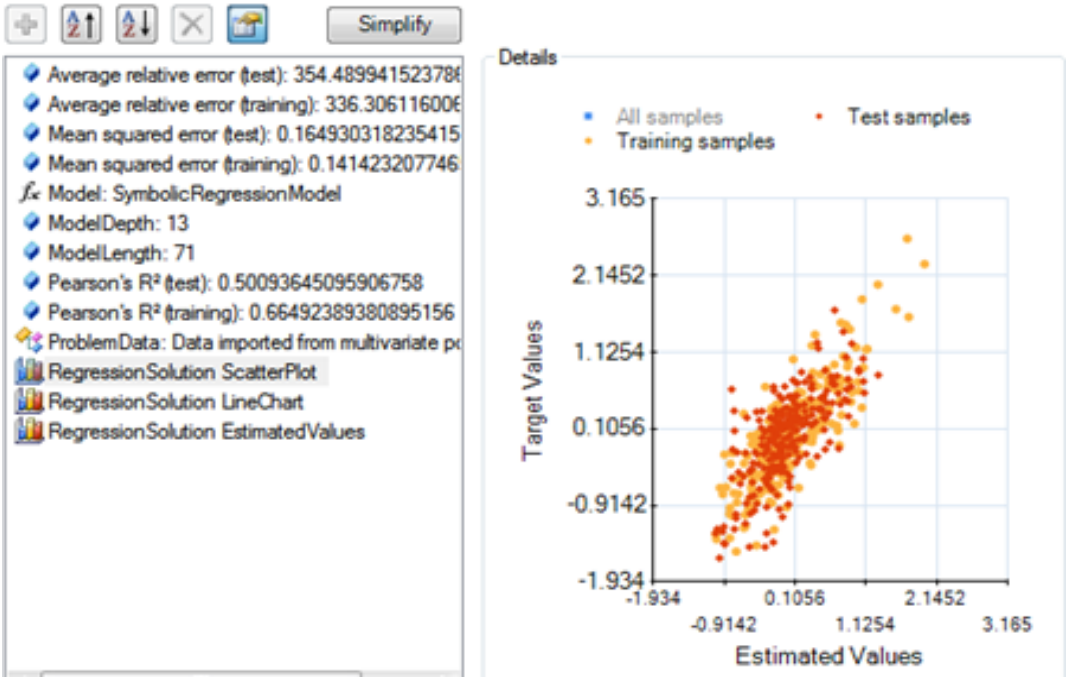

Figure 3.25 Measured vs. predicted values (the main window of the PC)

Chapter 4: Dynamic Behaviour of Homogenous samples of Glass-Rock-Rubber

4.1 Introduction

Preliminary tests were performed to evaluate the suitability of using different materials as alternative to natural rock. In this chapter, the results of preliminary and dynamic tests of glass-rock-rubber mixtures (GRT) are presented and discussed. A series of laboratory tests included modified Proctor compaction, specific gravity, water absorption, organic content, p_H and sieve analysis (before and after the compaction) was conducted on different homogenous samples of GRT mixtures to assess their engineering properties. Repeated loading triaxial tests (RLTTs) were also carried out to characterise the resilience, deformation, and shear strength behaviours of the crushed glass-crushed rock (GR), tyre rubber-crushed rock (TR) and crushed glass-crushed rock-tyre rubber (GRT) mixtures under the dynamic impacts of repeated loads. The samples were prepared by mixing crushed rock with different ratios of waste materials: 12%, 24% and 45% waste glass and 5%, 10% and 15% tyre rubber. The GRT mixtures were also prepared at 70% and 100% of the optimum moisture content (OMC) and an assessment of the effect of moisture content on the dynamic behaviour of the modified mixture was conducted to simulate typical in situ moisture conditions. The moisture content and dry density were also estimated after the RLTTs to assess the retain moisture content during the loading process. The overall structure of this chapter is founded according to the materials used in each mixture. The first set of results highlights the impact of waste glass on dynamic characteristics of rock. The second set presents the impact of rubber on dynamic characteristics of rock. The effect of the combination of glass and rubber on dynamic characteristics of rock is illustrated in the third section. The structure of this chapter is detailed in Figure 4.1. The results for pure rock, glass and tyre rubber will not be presented in this chapter because they were already presented in Chapter 3.

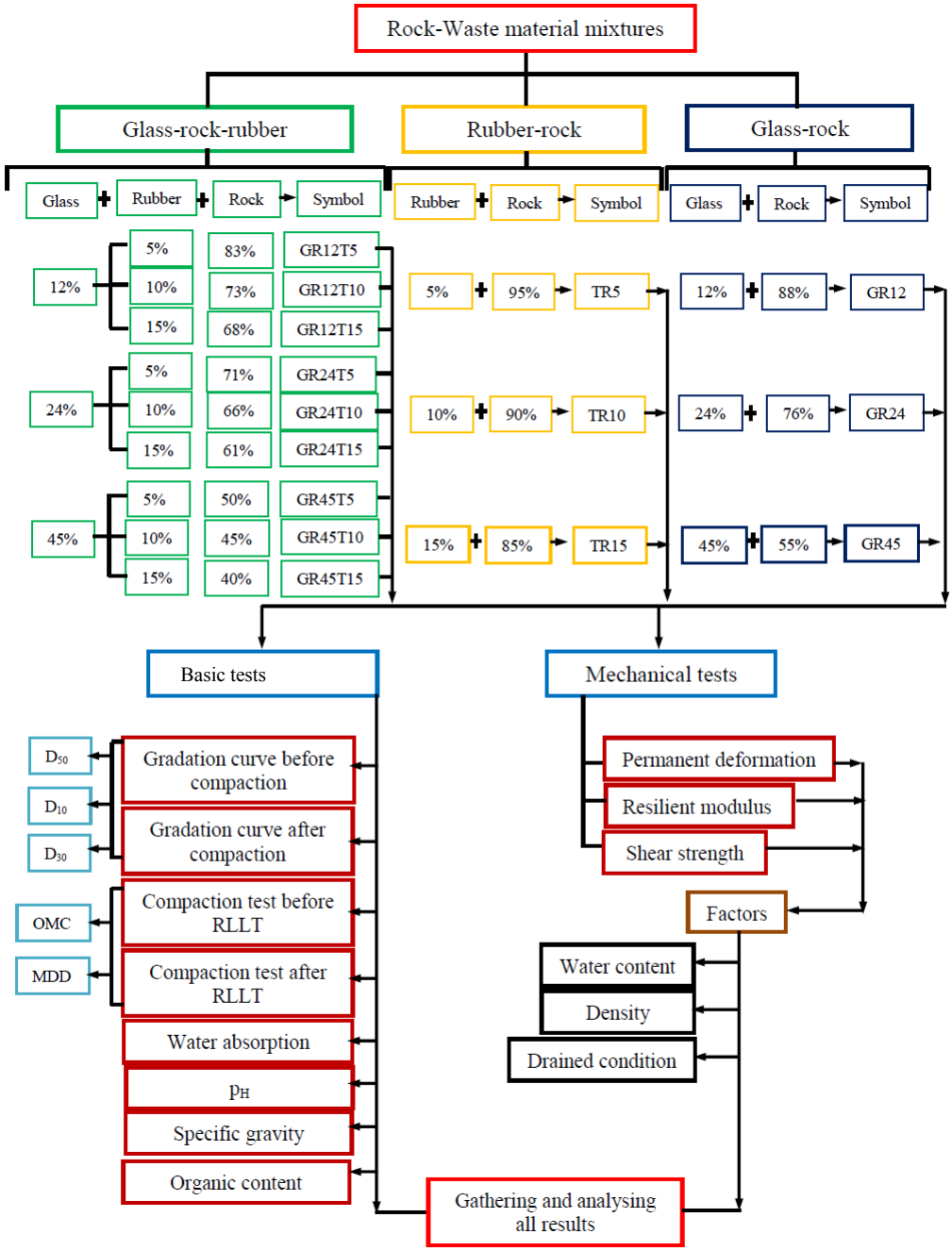

Figure 4.1 Overall plan of Chapter 4

4.2 Basic characterisation of glass-rock mixtures

The preliminary experimental works includedsieve analysis, modified Proctor compaction, specific gravity, water absorption, p_H and organic content tests were carried out at Curtin University. The results of basic characterisation of glass-rock (GR) mixtures are presented, compared and discussed in the next section.

4.2.1 Sieve analysis tests

Particle size distribution is a critical characteristic of granular materials used in different pavement layers. As detailed in Table 3.11, samples containing 12%, 24% and 45% waste glass were mixed with pure rock and labelled GR12, GR24, and GR45, respectively; then sieve analysis tests were conducted to determine their particle size distributions. Figure 4.2 illustrates the particle size distribution curves of pure rock, GR12, GR24 and GR45 before compaction impacts, and the results were compared with the upper and the lower VicRoads limits before compaction testing. The grading curves of GR12 and GR24 fall between the upper and lower limits of base course materials, whereas the GR45 specimen presented a slight divergence with the lower limits of base course materials. In general, all GR mixtures satisfied the base material requirements and are considered suitable for road applications. Figure 4.3 presents the gradation curves for pure rock, GR12, GR24 and GR45 samples after compaction testing. The figure also presents the upper and lower VicRoads limits for base materials. As expected, course and medium particles became much smaller as a result of the compaction impacts and thus, there was a significant increase in fine materials after the compaction stage. Despite the fine percentages increased after the compaction, the results reveal a satisfactory agreement between the curves of the GR12, GR24 and GR45 mixtures and the VicRoads limits.

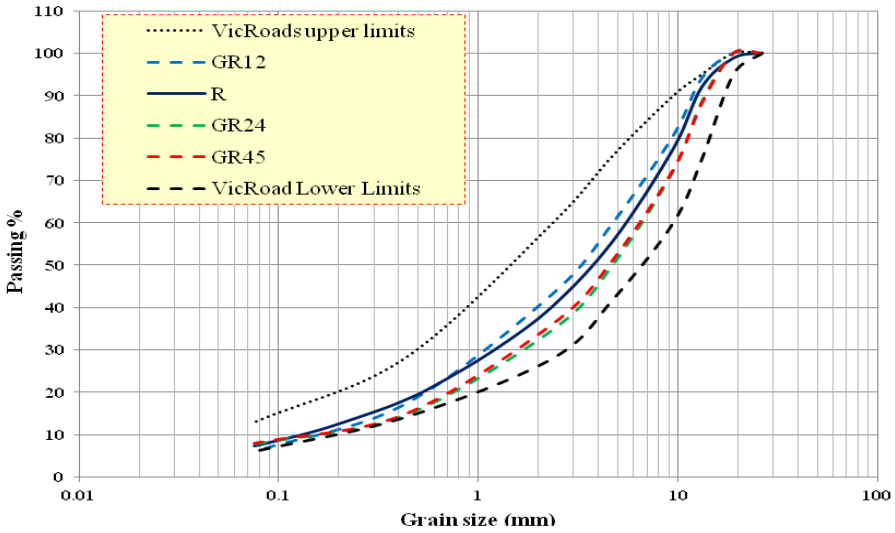

Figure 4.2 Gradation curves of pure rock, VicRoads limits and the glass-rock mixturesbefore compaction

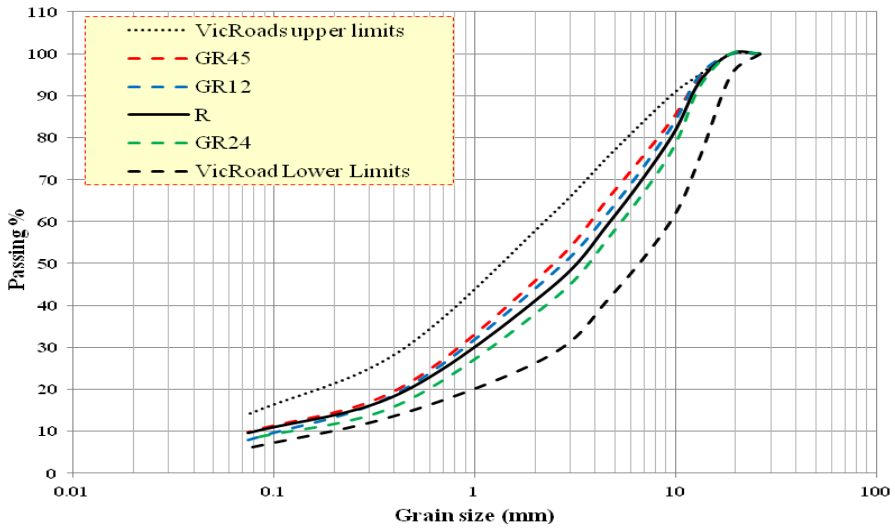

Figure 4.3 Gradation curves of pure rock, VicRoads limits andthe glass-rock mixtures after compaction

4.2.2 Modified compaction test

The compaction curves of pure crushed rock and different GR mixtures (GR12, GR24 and GR45) are presented in Figure 4.4. As expected, the maximum dry density (MDD) of pure rock decreased with an increasing of glass content. This result could be attributed to the fact that the density of glass particles is lower than that of pure rock, and this was the major cause of the steady reductions in the MDD of the GR mixtures. Figure 4.4 also shows a significant reduction in OMC of the GR12 and GR24 samples compared with the rock sample. The sensitivity of GR mixtures to the water variations gradually decreased with the glass content increase, as reported by Wartman et al. (2004) and Babiker et al. (2014). Conversely, GR45 showed an increase in OMC associated with the presence of glass. In general, the low sensitivity of glass particles to water plays a vital role in the compaction characteristics of GR mixtures and therefore, the GR curves become almost straight with increasing glass content.

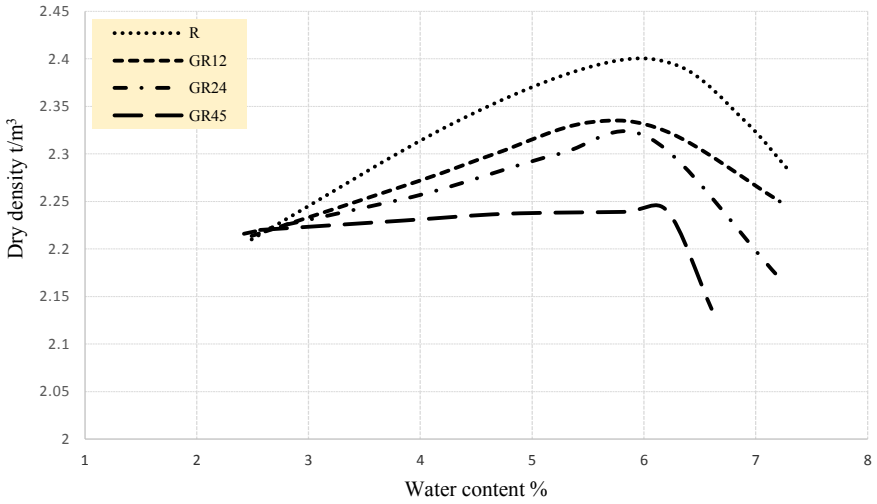

Figure 4.4 Compaction curves for rock and mixed glass-rock samples

Figure 4.5 presents the effects of glass content on the OMC and MDD of GR sample. The figure illustrates a steady reduction in the MDD value associated with the glass content increase. The value of the MDD decreased from 23.4 t/m^3 to 23.25 and to 22.48 when the glass content increased from 12% to 24% and 45%, respectively. This behaviour could be attributed to the low density of glass compared to those of crushed rock. Figure 4.5 also shows that the GR mixture reached to the lowest OMC value at 13% glass and then increased as the glass content increased. The results of the present study were consistent with the findings of Arulrajah et al. (2014), who reported that the OMC values of recycled concrete aggregate decreased steadily till 15% of fine glass, and then increased upon the addition of glass. As mentioned in the review section, the glass particles are less absorption and less sensitive to water than the natural soil and that could be explained the clear trend of the OMC reduction of the pure rock when glass content reached to 13%. After this ratio, the glass particles occupied the voids between the rock grains and increased the contact between the rock and the glass particles. Despite the smooth surfaces of glass grains, the fine grains of rock can adhere with the fine grains of glass, thereby increasing the particle surfaces which led to an increase in the water absorption area of the mixtures and consequently, increasing the OMC values.

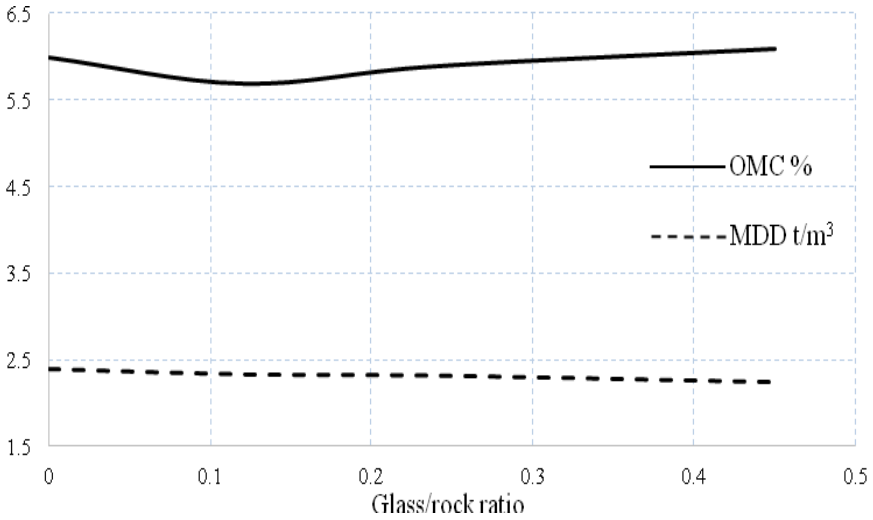

Figure 4.5 Effect of glass content on the OMC and the MDD of the glass-rock mixtures

A summary of sieve analysis, modified compaction, specific gravity, water absorption, organic content, and p_H tests of different samples of GR mixtures is detailed in Table 4.1. A considerable reduction in water absorption and organic content were associated with the glass content. The absorption and organic content values decreased from 2.6% to 2.15% and from 0.65% to 0.61% when the glass content increased from 12% to 45%, respectively. The reduction in water absorption and organic content of crushed rock when mixed with glass could be attributed to the low ability to absorb water and the smooth surface of crushed glass. These results were consistent with the findings concluded in the previous studies wherein the glass content reduced the water absorption and organic content of crushed rock (Ali et al., 2011). Whereas, a marked increase in p_H of the rock sample was associated with the glass content increase, which somewhat contradictory the findings reported in the previous sections that the presence of glass reduced the p_H of granular materials.The variation in the p_H values could be attributed to the variation of waste glass suppliers which led to varying the results of the GR mixtures (Disfani et al., 2009b).

Table 4.1 Geotechnical properties of mixed glass-rock samples

Sample	GR12 (before compaction)	GR12 (after compaction)	GR24 (before compaction)	GR24 (after compaction)	GR45 (before compaction)	GR45 (after compaction)
Glass: Rock (ratio)	12:88	12:88	24:76	24:76	45:55	45:55
D_{10}	0.17	0.09	0.18	0.13	0.185	0.08
D_{30}	1.2	0.9	1.8	1.25	1.7	0.85
D_{50}	4.75	2.8	4.5	3.9	4.3	2.5
D_{60}	4.75	4.5	6.5	5.5	6.4	3.9
C_u	27.94	50	36.11	42.3	35.13	48.75
C_c	1.78	2	2.76	2.18	2.44	2.3
Classification	SW	SW	SW	SW	SW	SW
Gravel content (%)	56.74	53	57.27	54	61.4	57.5
Sand content (%)	37.26	39	37.98	37.8	30.6	32.8
Fine content (%)	6	8	7.75	8.2	8	9.7
Specific gravity (%)	2.78	----	2.75	----	2.66	----
Water absorption (%)	2.6	----	2.4	----	2.15	----
Organic content (%)	0.65	----	0.63	----	0.61	----
p_H	8.34	----	8.7	-----	8.84	----
MDD (t/m^3)	23.4	----	23.25	----	22.48	----
OMC (%)	5.6	----	5.9	----	6.2	----

4.3 Dynamic behaviour of glass-rock mixtures

The findings of the repeated loading triaxial tests (RLTTs), included permanent deformation (P_d), resilient modulus (M_r), and dynamic shear strength results of pure rock, GR12, GR24 and GR45, are presented and discussed in the next section.

4.3.1 Resilient modulus of glass-rock mixtures

Under applied stress, granular materials are generally exhibited less P_d and more M_r under stress. Figure 4.6 reveals that a marked increase in the M_r value was noticeable with increasing sequence number. This finding provides further support for the principle of the stress hardening. It is important to note that a considerable reduction in the M_r of crushed rock was noticeable during the conditional stage of the RLTT; this result was consistent with the finding of Babiker et al. (2014).

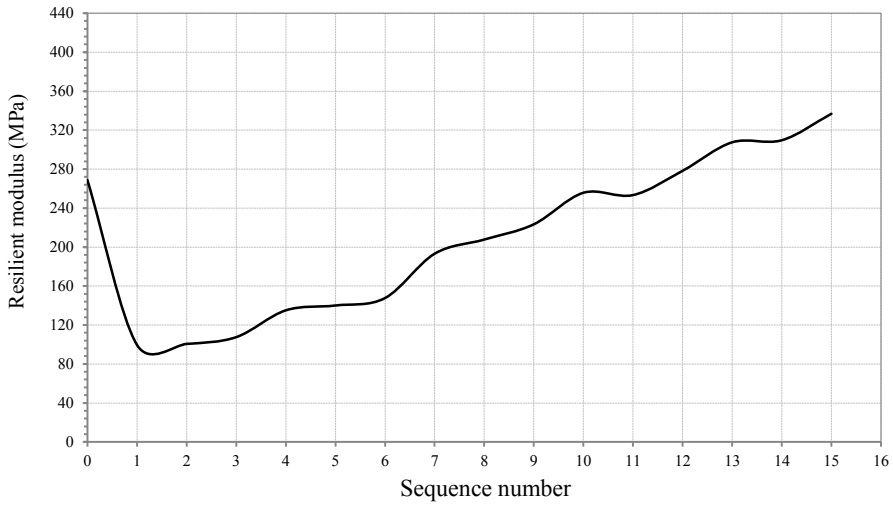

Figure 4.6 Resilience behaviour of pure rock sample

According to Ali et al. (2011), a 50% glass content does not affect the fundamental properties of pure rock in road applications. Therefore, a wide range of waste glass content was used in this investigation.The effect of the glass content (12% to 45%) on the resilience behaviour of pure rock sample is presented in Figure 4.7. It is apparent from the figure that an insignificant difference in the M_r between the R and the GR12 samples and hence, there is a clear evidence that the resilience behaviour of the GR12 mixture is similar to that of the base material. Moreover, the figure reveals a considerable increase in the M_r (from 330 to 432 MPa) as a result of increasing the glass content from 12% to 24%. In addition, the GR24 mixture showed a higher modulus than the natural rock sample. Based on this, there is a strong possibility that glass could improve the resilience behaviour of rock in the long term. In general, a 45% glass content is considered to be a high percentage of waste material in road applications. Therefore, it was an opportunity to assess the suitability of using that much of crushed glass with rock in road applications. It is apparent from this figure that the GR45 sample exhibited lower M_r than the GR24 sample during many load cycles. It is important to know that the moduli of all GR mixtures were greater than 330 MPa, which satisfies the standard range specified for base materials (AustRoads, 2004). The positive effect of the glass in improving the M_r of pure rock sample could be attributed to the stiffness of the mixtures; it improved as a result of increasing the glass content. Despite the crushed glass showed very low cohesion values, sharp edges of glass particles might be enhanced some basic properities such as the interlocking and the fabric of the GR mixtures.

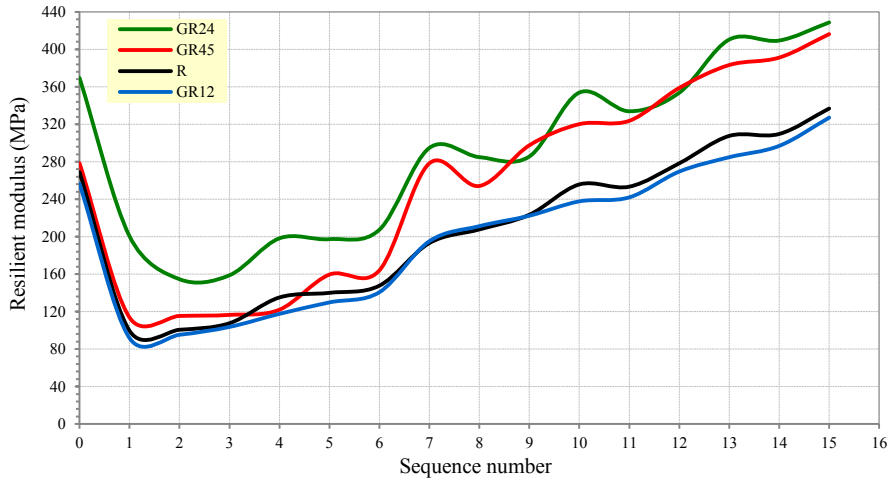

Figure 4.7 Resilience behaviour of pure rock, and GR12, GR24& GR45 mixtures

The correlation between the glass content and M_r of the GR mixtures is plotted in Figure 4.8. In this figure, there is a clear trend of decreasing the M_r of the GR mixtures from 298 MPa to 290 MPa when the glass content increased from 0% to 12%. The smooth surfaces of the glass grains which mostly smaller than 4.75mm might be distort the rock fabric, and that could be explain the slight difference in M_r. This result is consistent with the findings of Senadheera et al. (1995) and Arulrajah et al. (2014) that the M_r of the glass-soil mixtures reduced with increasing glass content. With an increase in the glass content to 24%, the glass particles filling the voids between the rock particles, causing high friction between the different particles and improve the mixture fabric, which in turn leads to improve the adhesion between glass and rock grains and therefore, improve the M_r of the mixtures, as shown in the figure. In addition, the M_r-glass curve tended towards approximately linearity with the glass content increase. It is essential to note that the glass content required achieving the optimum M_r is about 29%.

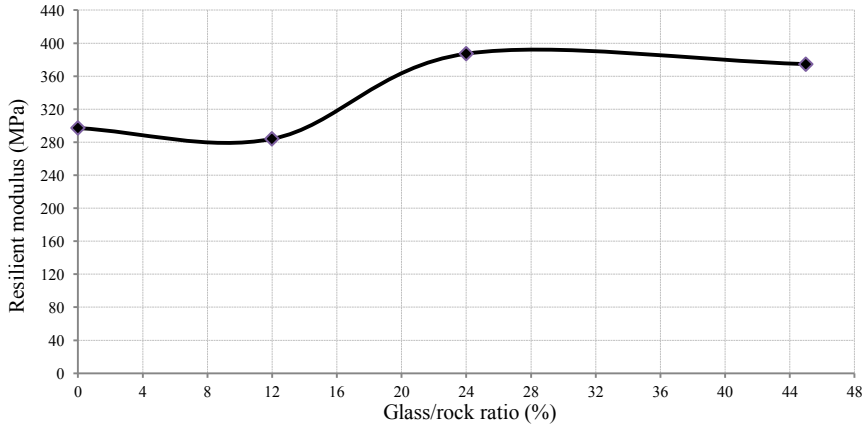

Figure 4.8 Variation in the resilience behaviour of rock with different glass content

4.3.1.1 Effect of test condition on the resilient modulus of glass-rock mixtures

Few studies have investigated the effect of undrained condition on the resilience behaviour of glass-rock mixtures as most RLTTs have been conducted under drained conditions and therefore, GR12 sample was selected as a case of study to assess the effects of undrained condition on resilience behaviour. Many previous studies have investigated different factors influenceing the resilience behavioure such as the compaction level. The volume variation significantly affected both undrained and drained tests (Ibsen, 1998) and therefore, it is a good opportunity to study the effect of the compaction level on undrained M_r. In addition, the amount of excess pore pressure, the generated deformation quantity, and the degree of saturation have a strong influence on resilience behavioure of granular materials. Figure 4.9 compares the resilience behaviour of the GR12 mixtures in drained and undrained conditions, where the drained sample exhibited a higher M_r than that of the undrained. At the last sequence of the RLTT, the value of M_r decreased from 330 MPa to 110 MPa when the test condition changed from drained to undrained condition, respectively. The positive effects of the drained condition on the resilience behaviour of the GR12 mixture might be attributed to the fact that the sample was almost water free when opening the valve, where the granular materials allow water to drain.Therefore, the soil particles will carry the addition stresses, which cause in improving the effective stress.

On the other side, preventing water from flowing out caused an increase in pore water pressure in the voids during the undrained condition and therefore, part of the applied load will transmiss to water and thus reduce the effective stress. Additionally, the pore water pressure reduced the stability of the GR12 mixture fabric as preventing the glass and rock grains from approaching each other, which negatively affect the densification and the effective stress of the mixture. It is worth mentioned that the presence of compressible gas in voids of a partially saturated sample caused a reduction in the efficiency for the pore water pressure generation. Therefore, the partially saturated samples have lower pore water pressure than that of the fully saturated samples. All the above reasons might explain the rapid reduction in M_r of the GR12 mixture under undrained condition, which was supported the previous study by Hussain et al.(2013), who concluded that the sample of granular materials in drained condition exhibited a higher M_r than that in the undrained.

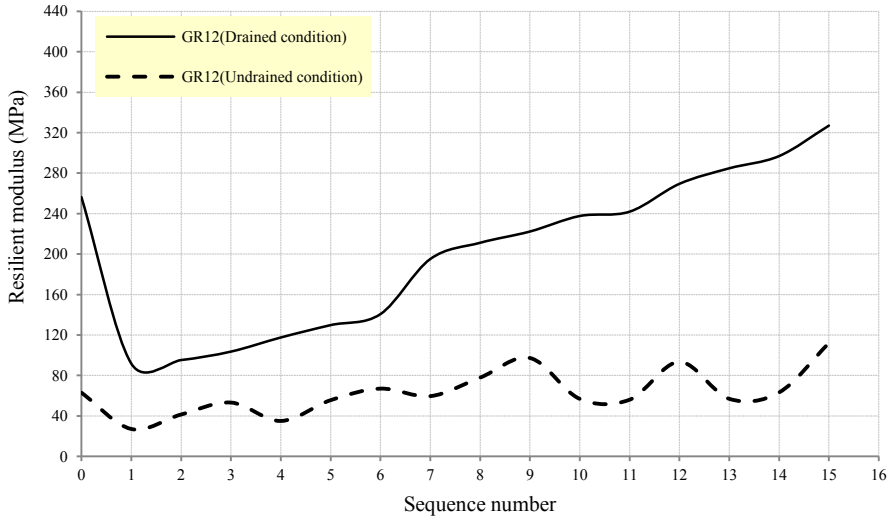

Figure 4.9 Comparison of the resilience behaviour of the GR12 mixture under drained-undrained conditions

4.3.1.2 Effect of density on the resilient modulus of glass-rock mixtures under undrained condition

Acceptable limits of base and subbase dry density in the field generally range from 90% and 95% of the MDD. With regards to this subject, GR12 sample was selected as a case of study to assess the effect of compaction level on the resilience behaviour, where the samples were compacted to 95% and 100% of the MDD. Figure 4.10 illustrates that the resilience behaviour of the GR12 mixture was positively affected by the dry density which caused a slight difference in the M_r value. The value of M_r increased from 110 MPa to 132 MPa as the compaction ratio increased from 95% to 100% of MDD, respectively.This behaviour might be attributed to the role of the density increase at the same moisture in enhancing the mixture fabric and consequently increasing the M_r. The above finding was consistent with the conclusions of Barskale and Itani (1989) and Vuong (1992), who reported a positive correlation between the density and the M_r value.

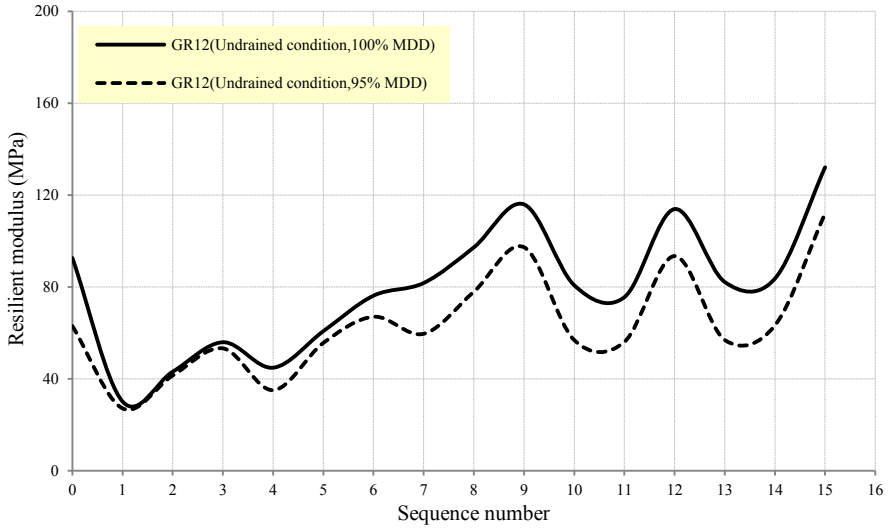

Figure 4.10 Effect of density on the resilience behaviour of the GR12 mixture under undrained condition

4.3.2 Permanent deformation of glass-rock mixtures

The deformation behaviour of the rock sample under the repeated loadings impacts is presented in Figure 4.11. It is apparent from this figure that the P_d significantly decreased during the conditioning stage (sequences 0 to 1). As soon as the conditioning stage is completed, a positive correlation was found between the P_d and the sequence number (stress path). This behaviour was consistent with the result of Babiker et al. (2014).

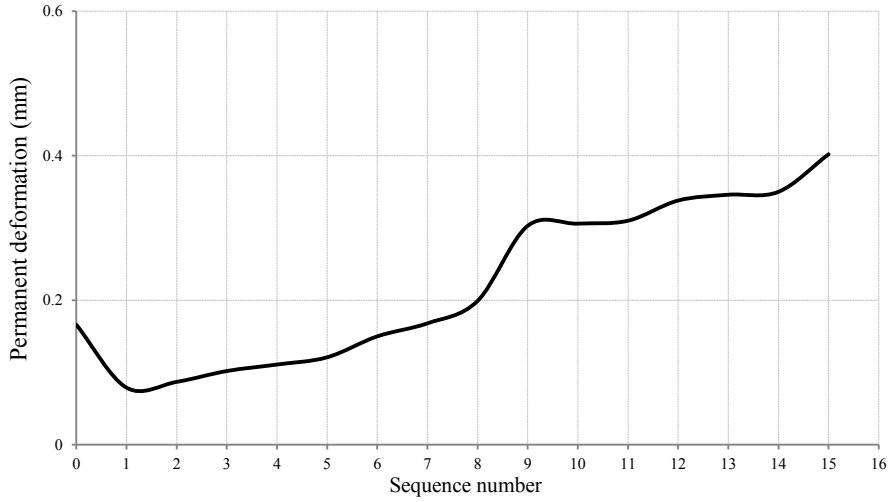

Figure 4.11 Permanent deformation of the pure rock sample

Figure 4.12 presents the P_d of the rock, GR12, GR24 and GR45 samples. It is apparent from this figure that the P_d of pure rock increased from 0.4mm to 0.87mm with increasing the glass content from 0% to 12%, respectively. In addition, the P_d

value of the R sample showed less P_d than the GR12 sample during all load sequences. The P_d value decreased from 0.87mm to 0.7mm when the glass content increased from 12% to 24%, respectively. Despite that the GR24 sample showed higher P_d than the rock, the sample illustrated higher resistance to deform than the GR12 sample. Note from Figure 4.12 that the consistency between the GR24 and GR45 samples is clear during the first five load sequences. After the fifth sequence, the GR45 sample showed high P_d than the GR24 sample. Despite that the angularity of particles positively affected the P_d of soils (Mehrjardi, Tafreshi & Dawson, 2012), the low density of the glass particles and the smoothness of their surfaces inversely affected the deformation behaviour of the glass-rock mixtures. These findings proved the previouse conclusion of (Disfani et al., 2012) concerning the using other additives to improve the mechanical properties of glass-soil blends used in pavement layers.

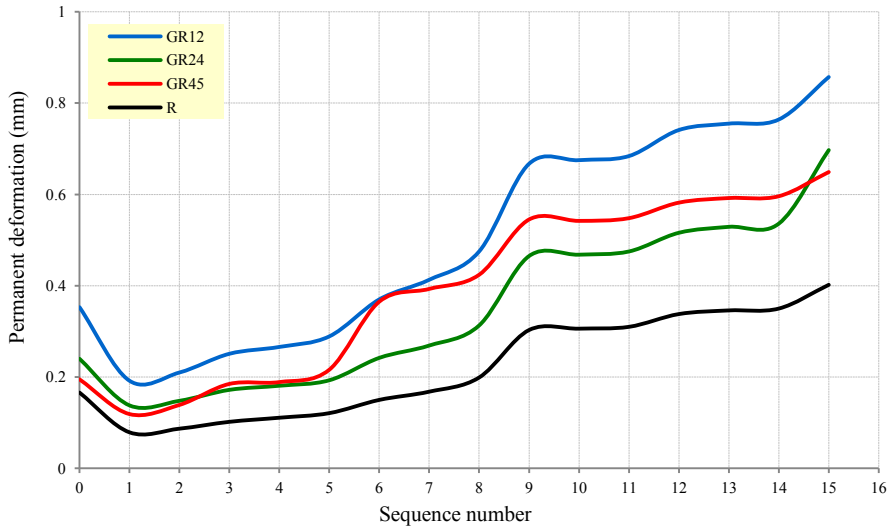

Figure 4.12 Deformation behaviour of the rock, GR12, GR24 and GR45 samples

The correlation between P_d and the glass content for various GR ratios is presented in Figure 4.13. In this figure, there is a clear trend of increasing P_d of the GR mixtures when the glass content increased from 0% to 12%. A possible explanation of the positive correlation between the glass content and the P_d might be the instability of rock fabric, which may change from stable fabric with low voids to unstable fabric with high voids when mixed with 12% of angular crushed glass and consequently, the P_d of the GR12 increased. This result was consistent with those of Arnold et al. (2008), who reported that the P_d of the GR mixtures increased as the glass content increase. With an increase in the glass content from 12% to 24%, the glass particles filled the voids between the rock particles causing an increase in the adhesion

between the glass and rock grains, which positively affected on the mixture fabric and the P_d. Note that the peak glass content of the P_d-(glass:rock) curve is about a 13% glass-rock ratio. After that ratio, the curve tended towards approximately linearity with the glass content increase. The correlation between the glass content and the P_d tends to be linear above a 24% glass-rock ratio, and the glass-rock mixture become less sensitive to the P_d with further glass content; this behaviour was consistent with those of Arulrajah et al. (2014).

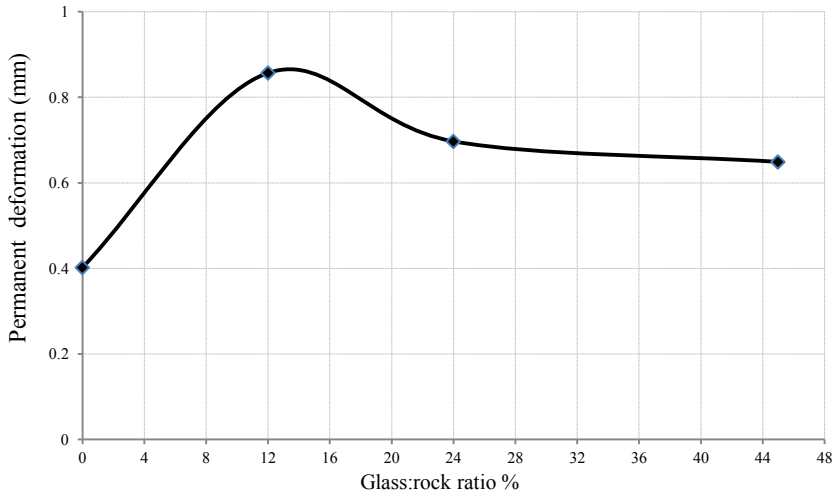

Figure 4.13 Variation in the permanent deformation of glass-rock mixtures with different glass content

4.3.2.1 Effect of test condition on the permanent deformation of glass-rock mixtures

Few studies are available on the effect of test condition on the P_d of GR blends and therefore, GR12 sample was selected as a case of study to assess the deformation behaviour of the GR mixtures under undrained condition. Figure 4.14 compares the P_d of the GR12 mixture under drained and undrained conditions. It is apparent from this figure that the drained sample reported significantly less P_d than the undrained sample, and the value of P_d of GR12 increased from 0.87mm to 5.4mm as the compaction ratio increased from 95% to 100% of MDD, respectively. Previously, Kramer (1996) reported that the increase amount of pore water pressure in a sample is usually accompanied by a clear increase in the deformation. This conclusion might explan the deformation behaviour of the GR12 mixture under undrained test. This behaviour supports the previous idea suggested by Bejarano and Harvey (2002) and Hussain et al. (2013), who concluded that materials with a maximum size of 20 mm showed the lowest P_d under drained conditions.

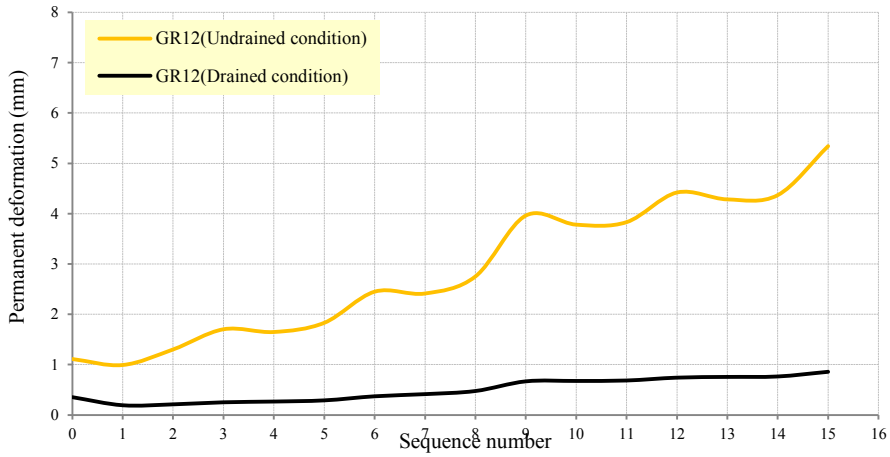

Figure 4.14 Comparison of the permanent deformation of GR12 sampleunder drained-undrained conditions

4.3.2.2 Effect of density on the permanent deformation of glass-rock samples under undrained condition

In the history of RLTTs, density has been considered a critical factor in the stiffness behaviour of granular materials (Huurman & Molenaar, 2006). In order to understand the effect of compaction level on the P_d of the GR mixture, GR12 sample was selected as a case of study and compacted to 100% and 95% of the MDD. Figure 4.15 shows that the P_d of the GR12 mixture decreased with the the density level increase, where the value of P_d of GR12 decreased from 9.5mm to 5.4mm as the compaction ratio increased from 95% to 100% of MDD, respectively.This response was attributed to the stability of the mixture fabric, as the compressibility of the mixture decreased with the density increase, which led to an improvement in the P_d of the GR12 mixture.

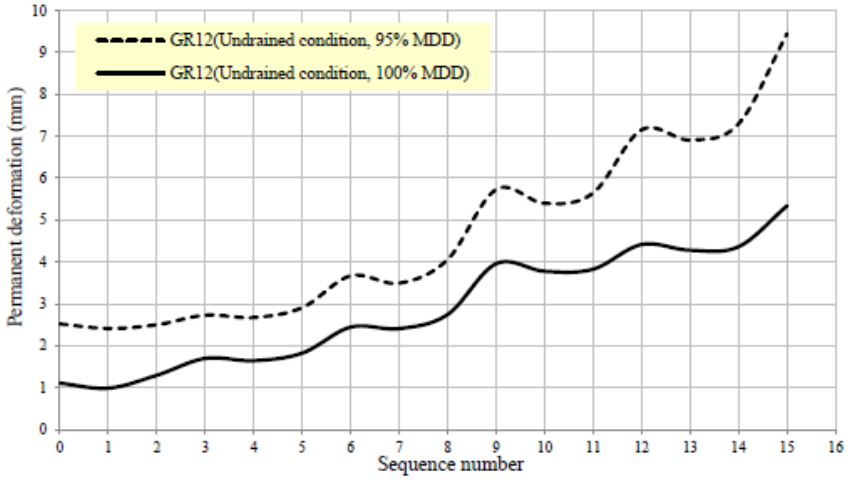

Figure 4.15 Effect of density on the permanent deformation of GR12 sample under undrained condition

4.3.3 Shear strength of glass-rock mixtures

The shear strength for the road materials has been the main criterion in road applications and flexible pavement design (Watson, 1995; Molenaar, 2005). Therefore, dynamic shear tests were conducted on different GR mixtures to evaluate the effect of glass inclusion on shear strength characteristics of the GR mixtures. It is essential to note that the tests were performed as quick shear tests using the RLTT apparatus. The result of first investigation into the shear stress-strain behaviour of pure rock is illustrated in Figure 4.16. In general, a considerable increase in the strain was associated with the stress increase until the curve approached a peak shear point, which associated with the sample failure. The elastic limit point of pure rock can also be recognised in this figure.

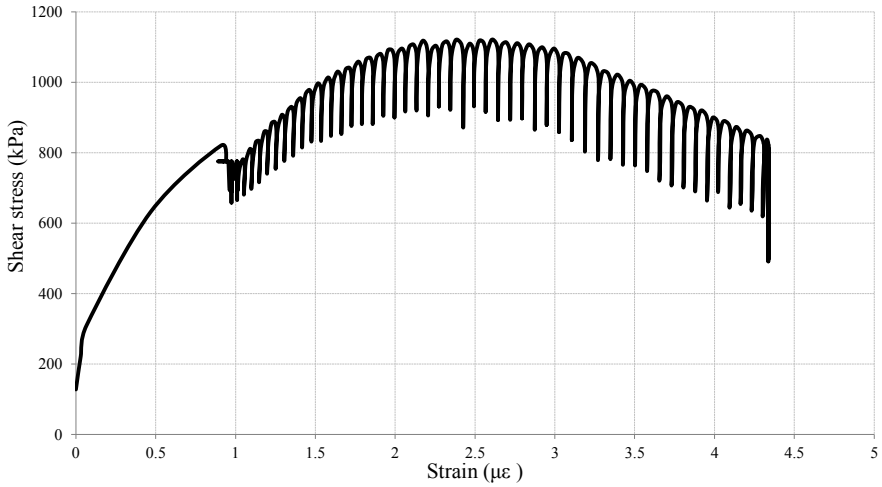

Figure 4.16 Stress-strain behaviour of the pure rock sample

A wide range of glass contents was employed to investigate the response of the GR mixtures to dynamic shear impacts. The variation in shear strength of the GR mixtures with increasing glass content is shown in Figure 4.17. It is apparent from this figure that adding 12% glass reduced the shear strength of the rock sample. Based on the elastic limit of granular materials, an apparent reduction in the elastic limit was associated with the glass presence. The peak shear strength of pure rock was reduced from 1110 kPa to 1000 kPa as the glass content increased to 12%. The effect of adding 24% glass on shear strength of the rock sample was also illustrated in Figure 4.17. There is strong evidence that the shear strength of the GR24 mixture decreased as a result of the glass increase. With increasing glass content from 24% to 45%, the result confirms the above findings and contributes additional evidence concerning the negative correlation between the shear strength and the glass content.

The peak shear values of pure rock were reduced from 1110 kPa to 940 kPa and 850 kPa when the glass content increased to 24% and 45%, respectively. In general, all stress-strain curves showed a sharp reduction in the shear stress after reaching the peak shear point. The inverse effect of the glass contents on shear strength of pure rock might be attributed to the low cohesion and internal friction angle of glass grains which produced unstable fabric of the GR mixtures under the shear forces impacts. These findings were consistent with the findings reported in the previous studies wherein the glass content reduced the shear strength of glass-soil mixtures (Viswanathan,1996 and Arulrajah et al., 2014). Note that the the stress-strain curves of the GR mixtures tend toward linearly behaviour with increasing glass content, where steady drops in the peak points were noticeable with further glass content. Also, the stress-strain curve of the GR45 sample shows less curvature than those of the other samples. In addition, the curves of the GR24 and GR45 samples flatten and approach constant values at the end of the test. The reason for the above behaviour might be related to the glass characteristics itself, where the glass grains have less cohesion and friction angle than the natural soil. With an increase in the glass content, the glass particles filled the voids between the crushed rock particles which inversely affected the stability of the mixture fabric and caused low friction forces between the mixture particles.

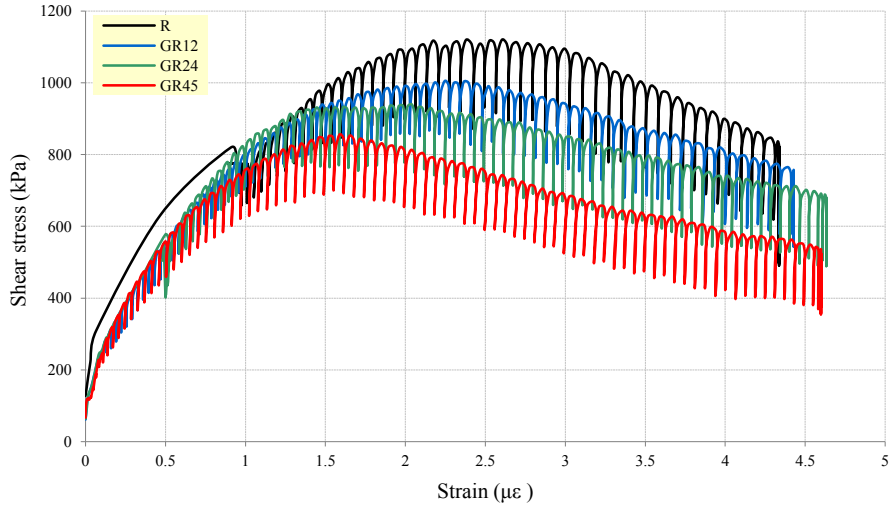

Figure 4.17 Stress-strain curves for the pure rock, GR12, GR24 and GR45 samples

4.4 Basic characterisation of rubber-rock mixtures

In this section, a series of laboratory works were carried out to investigate the effect of adding tyre rubber on the preliminary parameters of crushed rock samples. As

detailed in Table 3.12, natural crushed rock (R) was mixed with tyre rubber at three ratios: 5%, 10% and 15% by dry weight to prepare three samples labelled TR5, TR10 and TR15, respectively. A group of parameters is also presented and discussed in the following section: D_{10}, D_{30}, D_{50}, D_{60}, C_u, C_c, classification, gravel content, sand content, fine materials content, specific gravity (G_s), water absorption, organic content, p_H, dry density and compaction parameters.

4.4.1 Sieve analysis test

Figure 4.18 illustrates the particle size distribution curves for crushed rock and the TR5, TR10 and TR15 mixtures before compaction testing. The results were compared with the upper and lower VicRoads limits before compaction testing. It is apparent from this figure that the grading curves of TR5, TR10 and TR15 presented a slight divergence with the lower limits of base course materials.

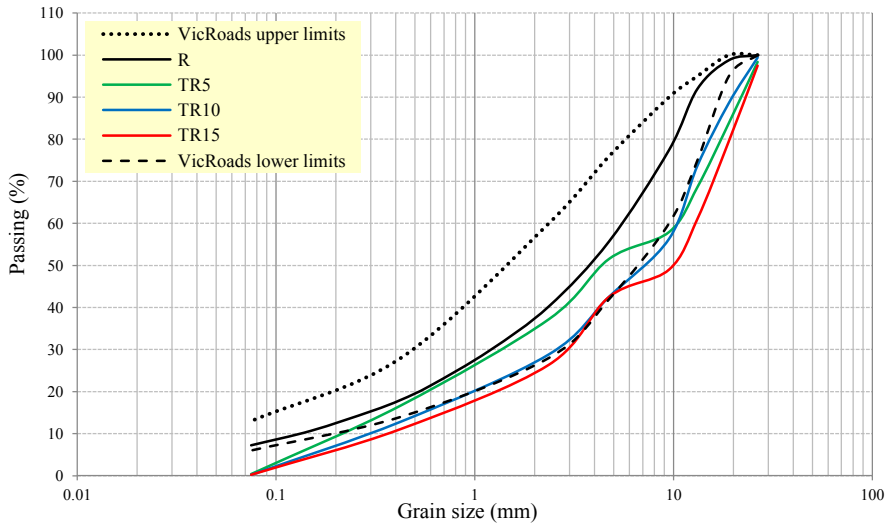

Figure 4.18 Particles size distribution curves for pure rock, VicRoad limits, TR5, TR10 and TR15 before compaction

Figure 4.19 presents the gradation curves of the TR mixtures after compaction. As expected, the course and medium particles of crushed rock become much smaller after the compaction process. Thus, the increase in fine materials is noticeable in the present results. After compaction process, the percentage of course grains in the TR mixture became more conforming to the lower limits of base course materials. The addition of course rubber (uncrushed grains) to the natural crushed rock might be related to the increase the percentage of course grains in the TR mixtures. More

details on the grain size distribution parameters of the TR5, TR10 and TR15 samples are detailed in Table 4.2.

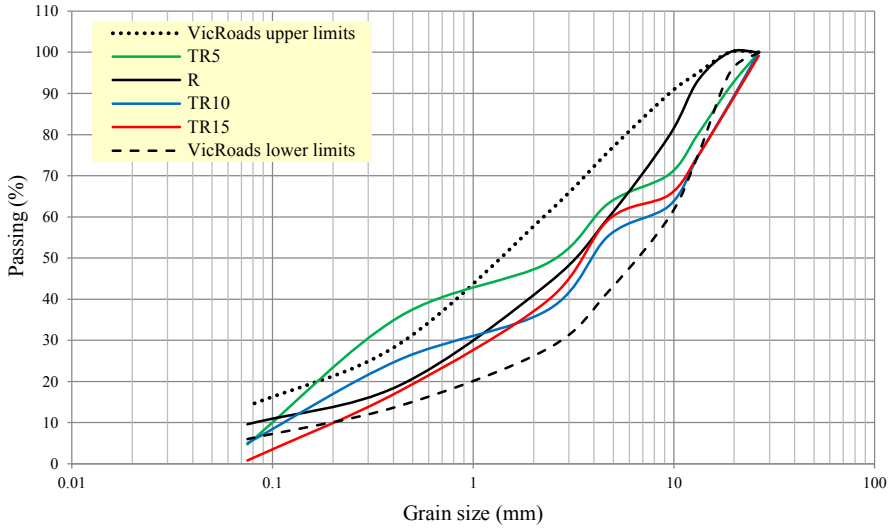

Figure 4.19 Particles size distribution curves for pure rock VicRoad limits, TR5, TR10 and TR15after compaction

4.4.2 Compaction testing

A series of modified compaction tests were conducted in this section to study the effect of rubber content on the compaction parameters of the TR mixtures. The compaction curves of pure crushed rock, as well as the TR5, TR10 and TR15 mixtures, are presented in Figure 4.20. It is important to note that the rock sample had the highest maximum dry density (MDD), while the TR15 sample had the lowest. It is also apparent from this figure that there was a clear trend of decreasing density with increasing rubber content. The low density of the rubber particles compared to that of rock particles caused to decrease the MDD of the TR mixtures. In terms of optimum moisture content (OMC), the TR5 mixture showed a significant reduction in the OMC compared with the rock specimen, whereas a steady increase in the peak of the compaction curves occurred with the further rubber contents. Note that the curvatures of the TR curves flatten and approach to constant values with the rubber content increase. This behaviour could be attributed to the low sensitivity of the rubber particles to water. These findings were consistent with those of Speir and Witczak (1996), who reported a significant rise in the OMC of the rock-aggregate mixtures as the results of the rubber increase.

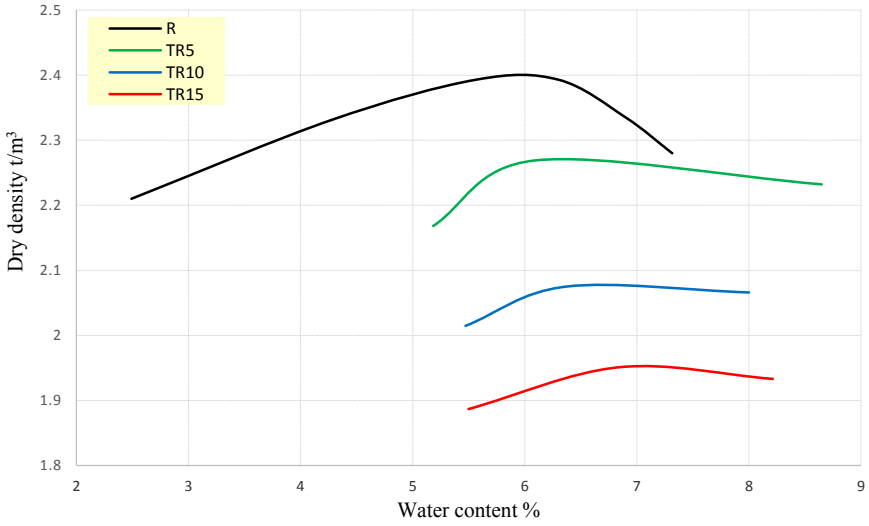

Figure 4.20 Compaction curves of pure rock and TR mixtures containing 5%, 10% and 15% rubber contents

The results of the preliminary tests of the TR mixtures are represented in Table 4.2. A significant reduction in the specific gravity, water absorption, p_H and organic content of the TR mixtures was noticeable as the rubber content increase. The basic properties of the rubber particles such as low density, insensitive to water content, rough surfaces, shape and size played a significant role in the variation of the TR mixtures characteristics. The above findings are consistent with the findings of Signes et al. (2016), who concluded that the presence of rubber reduced the specific gravity and water absorption of rubber-soil mixtures.

Table 4.2 Geotechnical properties of rubber-rock mixtures with different rubber content

	TR5 (before compaction)	TR5 (after compaction)	TR10(before compaction)	TR10 (after compaction)	TR15(before compaction)	TR15(after compaction)
Rubber: Rock ratio	5:95	5:95	10:90	10:90	15:85	15:85
D_{10}	0.22	0.11	0.3	0.11	0.35	0.2
D_{30}	1.35	0.34	2.4	0.85	2.8	1.1
D_{50}	4.5	2.6	6	4	7	3.4
D_{60}	7	4	7.1	5.9	9	5
C_u	31.8	36.36	23.66	53.6	25.7	25
C_c	1.18	0.26	2.70	1.11	2.5	1.21
Classification	GW	GW	GW	GW	GW	GW
Gravel content (%)	62.8	51.1	71.1	62.5	73.6	60.2
Sand content (%)	36.8	44	28.6	32.4	26.1	39.3
Fine Content (%)	0.4	4.72	0.22	5	0.23	0.4
Specific gravity (%)	2.37		2.34		2.26	
Water absorption (%)	0.65	----	0.55	----	0.42	----
Organic content (%)	0.43	----	0.41	----	0.4	----
p_H	8.24	----	8.15	-----	8	----
MDD (t/m^3)	2.26	----	2	----	1.95	----
OMC (%)	6.3	----	6.6	----	6.9	----

4.5 Dynamic behaviour of rubber-rock mixtures

Proportions of 5%, 10% and 15% tyre rubber were mixed with pure rock to prepare the samples. Repeated loading triaxial test (RLTT) was conducted on the samples, and the results of resilient modulus (M_r), permanent deformation (P_d) and stress-strain curves are presented in next sections.

4.5.1 Resilient modulus of rubber-rock mixtures

The resilience behaviour of the TR mixtures is presented in Figure 4.21. The M_r of pure rock and the TR5 sample after fifteen sequences are about 340 MPa and 175 MPa, respectively. In addition, a sharp decrease in the M_r was noticeable due to increase the rubber content from 5% to10% and to15%, where the M_r values of pure rock were reduced from 335MPa to 105MPa and 55MPa when the rubber content increased to 10% and 15%, respectively. In general, all TR mixtures reported lower stiffness than the natural rock sample. These findings were consistent with those of previous studies in that the M_r of unbound material decreased with an increase in the rubber content (Speir & Witczak, 1996; Papp et al., 1997 and Rao & Dutta, 2006). This behaviour could be attributed to the inversely effects of the rubber on the TR mixture fabric stability, that the addition of large sizes, low densities, and high compressibility material as rubber particles to a natural rock could changed the grain size distribution, and restructured the rock fabric from stable-high density with a low voids to unstable-low density with a high voids. Consequently, the M_r of the TR mixtures decreased as the rubber content increase.This behaviour was consistent with the findings of Rada and Witczak (1981) and Kolisoja (1997), who conclued that the M_r of unboud materials increased as the sample density increase. A comparison between the M_r of glass-rock and rubber-rock mixtures was also presented in Figure 4.21. Depending on the proportions of the additives, profound differences may be noted in the behaviour of rock sample due to the addition of glass or rubber. A considerable improvement in the M_r values was noticable with increasing the glass content. On the other hand, there was a significant reduction in the M_r as the rubber content increase. The effect of the rubber content on the resilience behaviour of the TR mixtures is presented in Figure 4.22. It is apparent from this figure that increasing rubber content caused a steady reduction in the M_r of the rock samples.

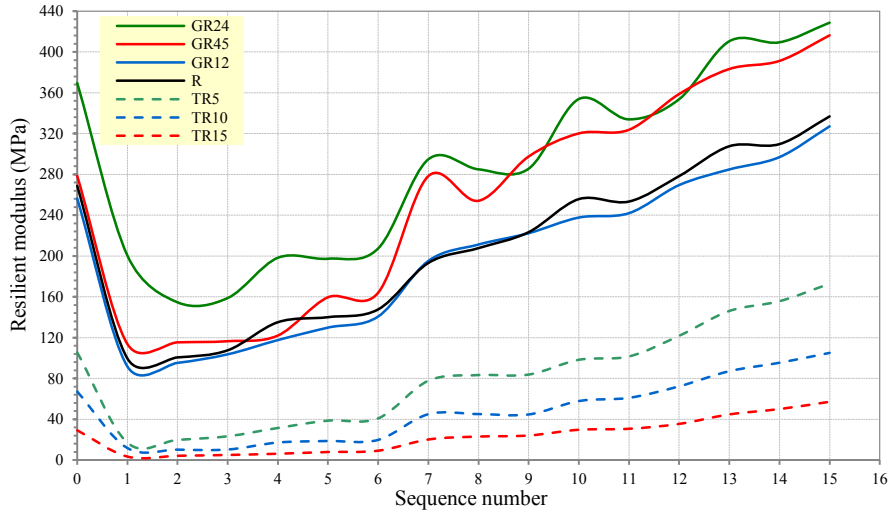

Figure 4.21 Variations in the resilient moduli of pure rock with various rubber or glass contents

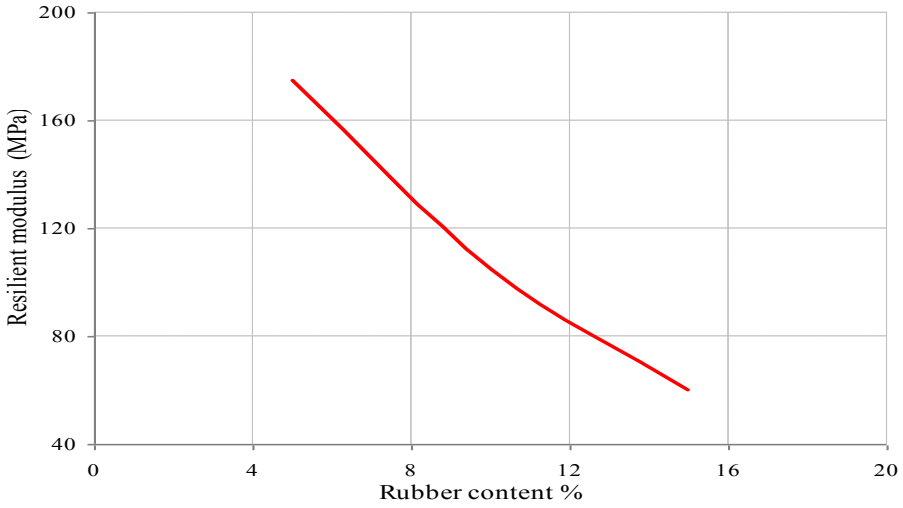

Figure 4.22 Resilient modulus-rubber content curve of TR mixtures

4.5.1.1 Effect of moisture content on resilient modulus

According to Azam and Cameron (2012), the dry back phenomena provided the most accurate description of the soil conditions in situ. Therefore, some TR mixtures were prepared at 100% and 70% of the OMC (as detailed in Table 3.12) to investigate the effect of moisture content on the M_r of the mixture. Figure 4.23 shows a variation in the M_r of the TR5, TR10 and TR15 samples at 100% and 70% of the OMC. It is apparent from this figure that insignificant differences in the M_r values between the samples at 70% and 100% OMC. In general, moisture reduction exerted inconsequential effects on the resilience behaviour of the TR mixtures. This

behaviour could be attributed to the insensitivity of the rubber particles to water content and the low water absorption of the TR mixtures.

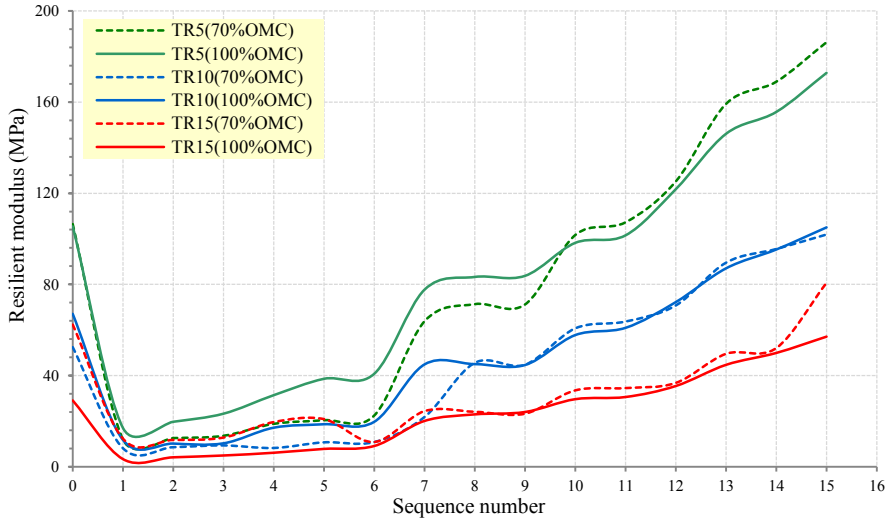

Figure 4.23 Effect of moisture content on the resilient modulus of TR5, TR10 and TR15 mixtures

4.5.2 Permanent deformation of rubber-rock mixtures

The effects of 5%, 10% and 15% of the rubber content on the P_d of pure rock are shown in Figure 4.24. A considerable increase in the P_d of the pure rock sample was associated with 5% rubber. During the last five sequences of the loading stage, it is apparent that the TR15 mixture reports higher P_d than the TR5 and the TR10 mixtures. Note that the P_d of the TR mixtures considerably increased from 0.4mm to 5.5mm, 6.8mm, and 11mm as increased the rubber content from 5%, 10%, and 15%, respectively. Figure 4.24 also plots the variation in the P_d of the GR and the TR mixtures according to their rubber and glass contents. It is not hard to distinguish that the GR samples exhibited more resistance to deform than the TR samples.

The correlation between P_d and the rubber: rock ratio is plotted in Figure 4.25. A steady increase in the P_d of pure rock sample was associated the with the rubber increase. According to the results in Table 4.2, the gravel content in the TR mixtures increased from 62.8% to 73.6% because of increasing the rubber content from 5% to 15%, while the density of pure rock decreased from 2.26 t/m^3 to 1.95 t/m^3.This change in the TR parameters could inversely affected the soil fabric and structure which resulted in unstable fabric with high voids level and thus, high P_d. It is important to know that these findings are consistent with those in the previous

studies that the P_d of granular materials increased as the rubber content increase (Signes et al., 2016 and Prasad and Raju, 2009).

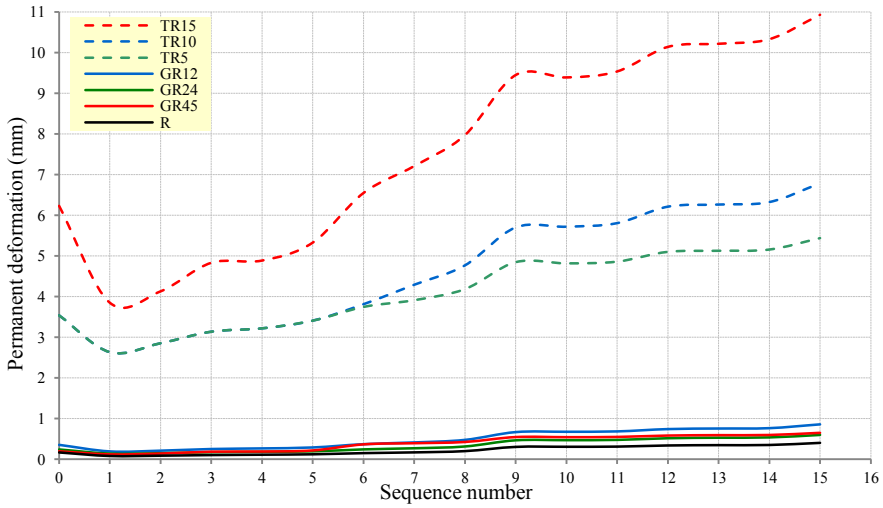

Figure 4.24 Variation in permanent deformation of the GR and the TR mixtures according to their rubber and glass contents

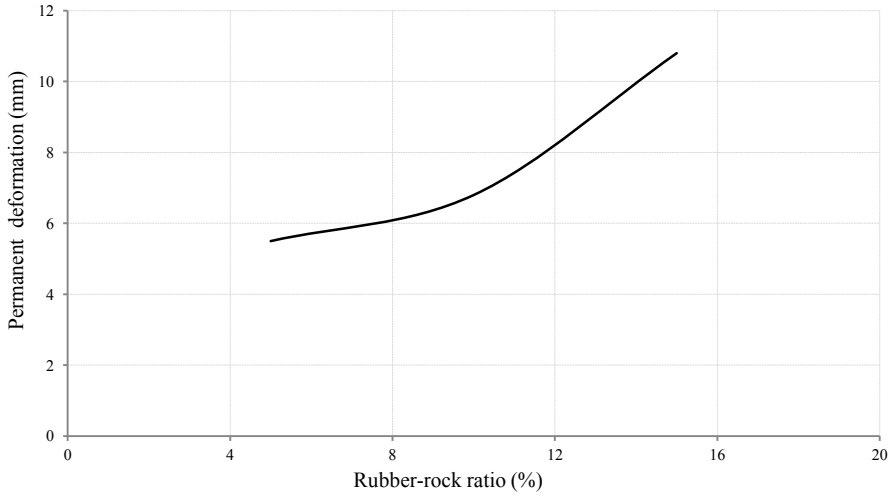

Figure 4.25 Variation in the permanent deformation of TR mixtures with different rubber content

4.5.2.1 Effect of moisture content on permanent deformation

Further RLTTs were also conducted to assess the effect of moisture content on the P_d of the TR mixtures. Figure 4.26 compares the P_d of the TR5, TR10 and TR15 samples according to their moisture contents (70% and 100% of the OMC). The values of the P_d of TR5, TR10, and TR15 at the end of the RLTTs decreased from 5.5mm, 6.8mm, and 9mm to 2.4mm, 5.7mm, and 8.6mm when the moisture content decreased from 100% to 70% OMC, respectively.This results provides additional

support for the conclusion of Kim and Santamarina (2008), who reported that the reduction in moisture content caused in reducing the P_d of the rubber-rock mixtures. This behaviour could be attributed to the role of low moisture content in enhancing the inter-particles contact which led to improve the mixture fabric stability and consequently, high resistance to deform. Note that the reduction rates in the P_d of the samples decreased with the rubber content increased, that the reduction rates in P_d of TR5 reduced from 129% to 19.3% and 3.4% with increased the rubber content from 5% to 10% and 15%, respectively. This results could be attributed to the insensitivity of the rubber particles to water content and the low water absorption of the TR mixtures. In addition, the difference between the density of the rubber and the rock particles causes somtimes to increase the particles segregation during the high pressure stage and thus, high P_d.

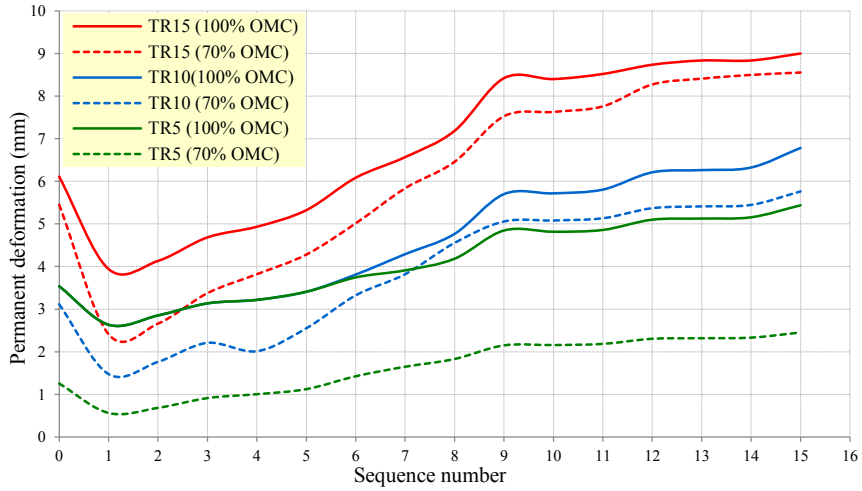

Figure 4.26 Effect of moisture content on the P_d of the TR mixtures

4.5.3 Shear strength of rubber-rock mixtures

This section presents and discusses the dynamic shear stress-strain behaviour of TR mixtures. The effects of variation in confining pressure and moisture content on the shear strength of the TR mixtures are also presented in this section.

4.5.3.1 Effect of rubber content on shear strength of the TR mixtures

The effect of varying the rubber content from 5% to 15% on the dynamic shear strength of pure rock is presented in Figure 4.27. It is apparent from this figure that a sharp decline in shear strength of the TR sample was associated with the rubber presence. Also, the shear stress-strain curve of the TR5 sample showed less curvature than that of the rock sample. Increased the rubber content from 5% to 10% and then

to 15% led to a continuous reduction in the shear strength of the TR mixtures. On the basis of the rubber grain size, fine particles of rock filled the voids between the rubber particles and therefore, shear resistance of the TR mixture was partially dependent on the rubber particles. Thus, the resistance of the TR mixture under dynamic shear impacts has become less than that of the pure rock sample. It is apparent that all curves of the TR mixture showed more softening than that of the rock sample, which is a good characteristic for base and subbase materials that the stress. The findings of the current study were consistent with those of Dawson, Mundy and Huhtala (2000), Cabalar (2011), and Ghazavi (2004), who reported a significant reduction in the shear strength of rubber-soil mixtures with the rubber content increase that the stress-strain curves of the brittle materials usually drop sharply after the peak stress point.

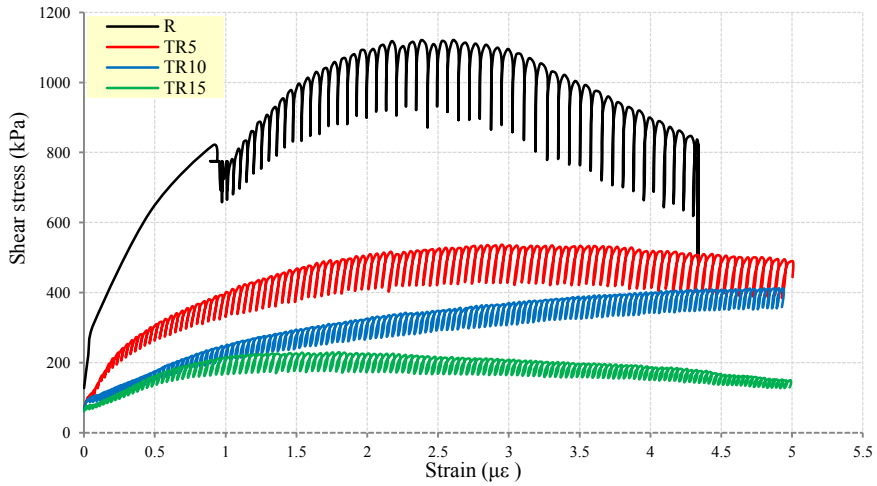

Figure 4.27 Stress-strain curves for the pure rock, TR5, TR10, and TR15 samples

4.5.3.2 Effect of moisture content on shear strength of the TR mixtures

A series of RLTT were conducted on different TR mixtures to evaluate the effect of moisture content on dynamic shear strength of the TR mixtures. It is apparent from Figure 4.28 that a clear improvement in the dynamic shear strength of the TR mixtures was noticeable when reduced the moisture content from 100% to 70% of the OMC. Rrubber particles are insensitive to water and therefore, any extra amount of water could inversely affected on the solid-water-air structure of the sample and led to reduce the stability of the TR mixture fabric which inversely influenced the dynamic shear strength of the TR sample at high moisture content.

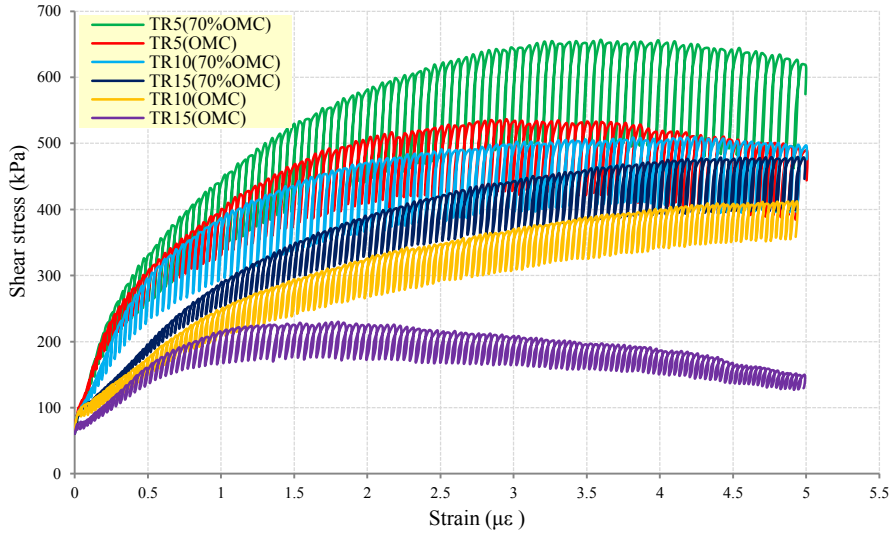

Figure 4.28 Stress-strain curves for the pure rock, TR5, TR10 and TR15 samples according to their moisture contents

4.5.3.3 Effect of confining pressure on shear strength of the TR mixtures

A series of dynamic shear tests were conducted on the TR5, TR10, and TR15 mixtures at three confining pressures (35, 70 and 150 kPa) to study the effect of confining pressure on dynamic shear strength. Figures 4.29, 4.30 and 4.31 present the stress-strain curves of the TR5, TR10 and TR15 mixtures at different confining pressure, respectively. In general, axial strain initially increased with shear stress until it reached to the peak shear. In addition, all the stress-strain curves of the TR mixtures reveal the same behaviour under different confining pressures: shear strength increased with the confining pressure increase. The ultimate shear stress value of TR5 decreased from 1150 kPa to 775 kPa and 675 kPa when confining pressure increased from 150 kPa to 70 kPa and 35 kPa, respectively. The positive effect of confining pressure on shear strength of the TR mixtures could be related to the role of confining pressure in enhancing the fabric and the uniformity of the mixtures. Consequently, the contact between the rock and rubber particles increased, which led to an improvement in the shear strength behaviour. The above results consistent with the findings of Yamamuro and Lade (1998).

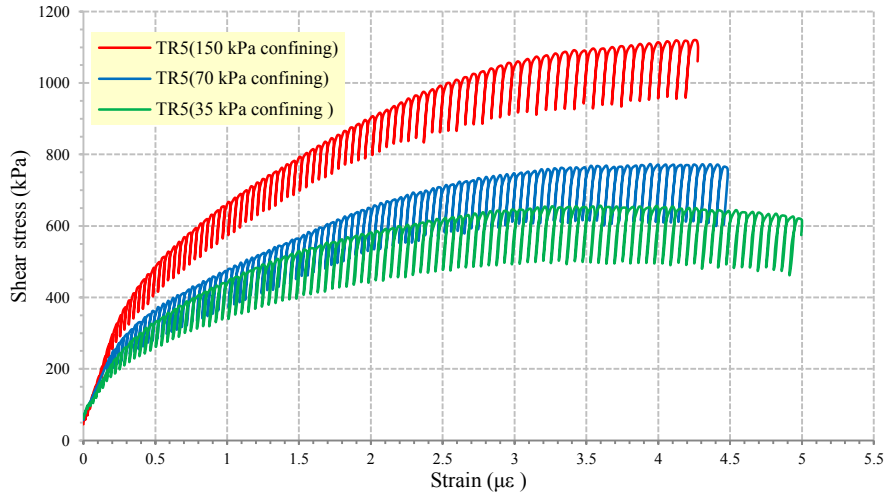

Figure 4.29 Effect of confining pressure on dynamic shear strength of the TR5 sample

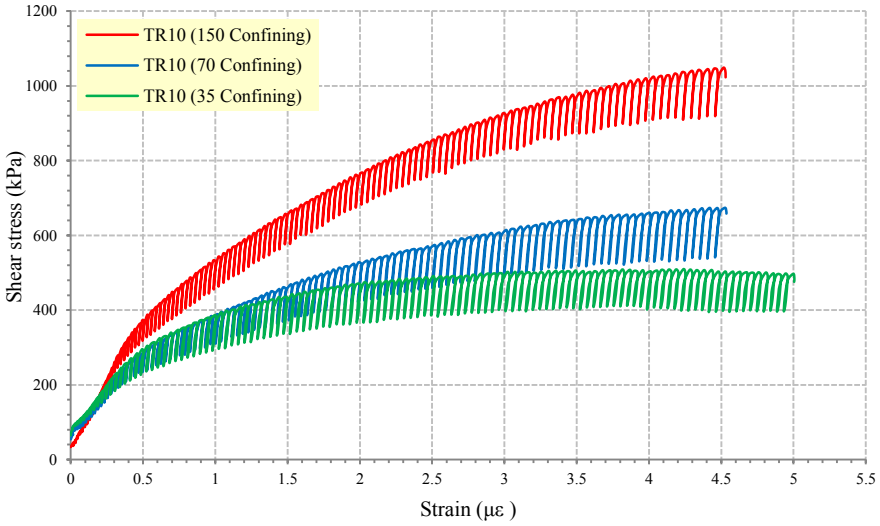

Figure 4.30 Effect of confining pressure on dynamic shear strength of the TR10 sample

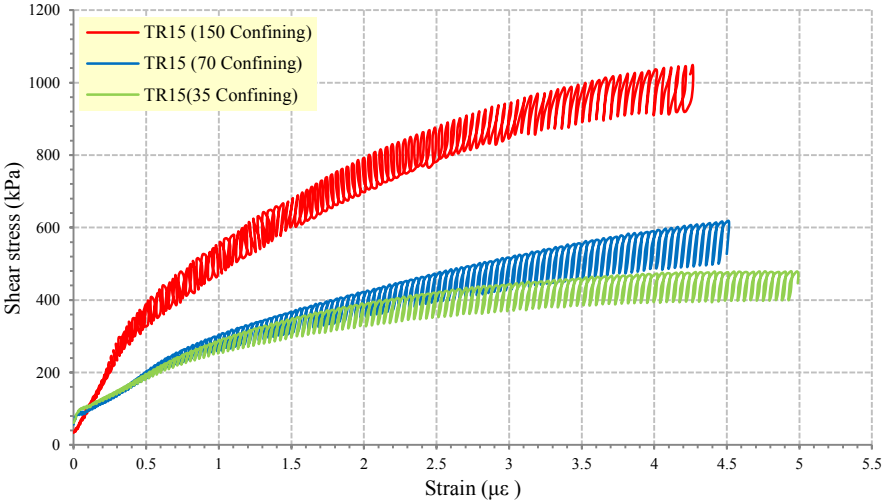

Figure 4.31 Effect of confining pressure on dynamic shear strength of TR15 sample

4.6 Basic characterisation of glass-rock-rubber

There have been little quantitative investigations of glass-rock-tyre rubber (GRT) mixtures in road applications. Therefore, a series of laboratory works was conducted to assess the fundamental properties of the GRT mixtures. As detailed in Table 3.13, samples of rubber containing 12% glass were mixed with 5%, 10% and 15% tyre rubber and labelled GR12T5, GR12T10, and GR12T15, respectively. Then, the glass content in these samples was increased to 24% and labelled GR24T5, GR24T10, and GR24T15, whereas the GRT samples are labelled GR45T5, GR45T10, and GR45T15 when increasing the glass content to 45%.The results of different tests, including sieve analyses, specific gravity, water absorption, organic content, p_H and compaction tests, are presented and discussed in the sections below.

4.6.1 Sieve analyses results for the GRT mixtures

Figures 4.32, 4.33 and 4.34 illustrate the gradient curves of pure rock and nine different samples of the GRT mixtures before the compaction tests. The results were also compared with the upper and the lower VicRoads limits for base materials. The particles size distribution curves of the GR45T5 and GR24T5 mixtures fall approximately between the upper and lower limits of the standard material, while the rest of the mixtures failed the lower limit requirements. Based on the results reported in section 4.4.1(Figures 4.18 and 4.19), Figures 4.32, 4.33 and 4.34 show positive effects of the glass presence on the distribution curves of the TR mixtures.

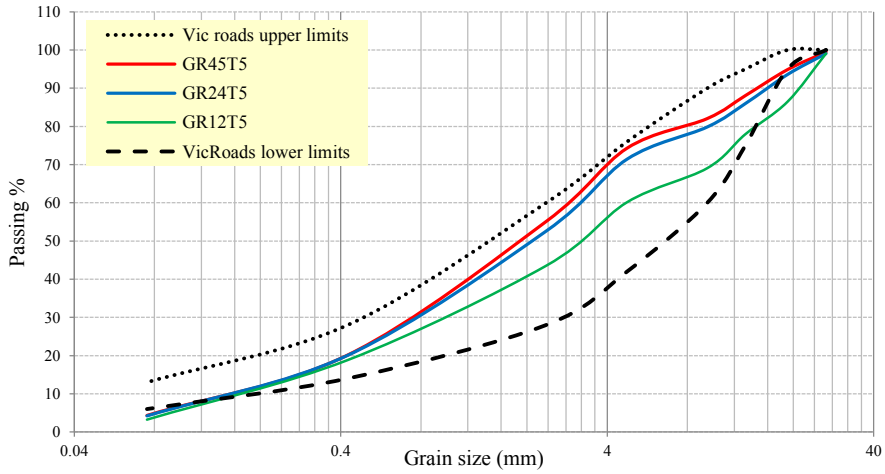

Figure 4.32 Particles size distribution curves for VicRoads limits, GR12T5, GR24T5, GR45T5 mixtures before compaction

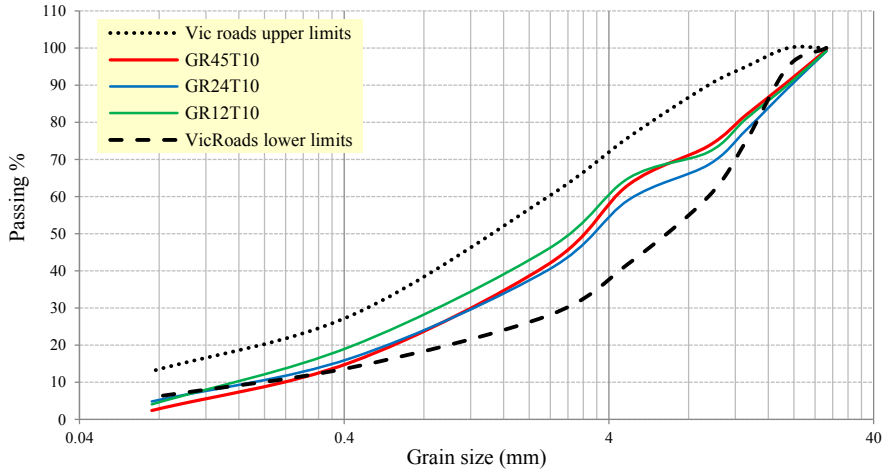

Figure 4.33 Particles size distribution curves for VicRoads limits, GR12T10, GR24T10, and GR45T10 mixtures before compaction

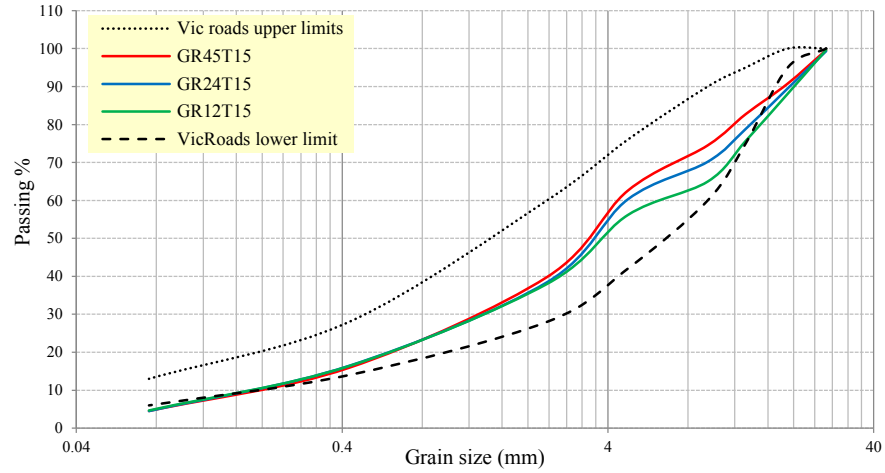

Figure 4.34 Particles size distribution curves for VicRoads limits, and GR12T15, GR24T15 and GR45T15 mixtures before compaction

Figures 4.35, 4.36 and 4.37 present the gradation curves of crushed rock and different GRT mixtures after compaction impacts. As expected, some of course and medium of rock and glass particles became much smaller after compaction and consequently, there is a significant increase in fine materials. Therefore, the gradation curves shift to the left-hand side and consequently, there is satisfactory agreement between most of the GRT curves and the VicRoads limits after the compaction impacts. Further details on the grain size distribution parameters including D_{10}, D_{30}, D_{50}, D_{60}, C_u, C_c, classification, gravel content (%), sand content (%) and fine content (%) of the GRT mixtures with different glass and rubber contents before and after compaction are reported in Tables 4.3, 4.4 and 4.5, respectively.

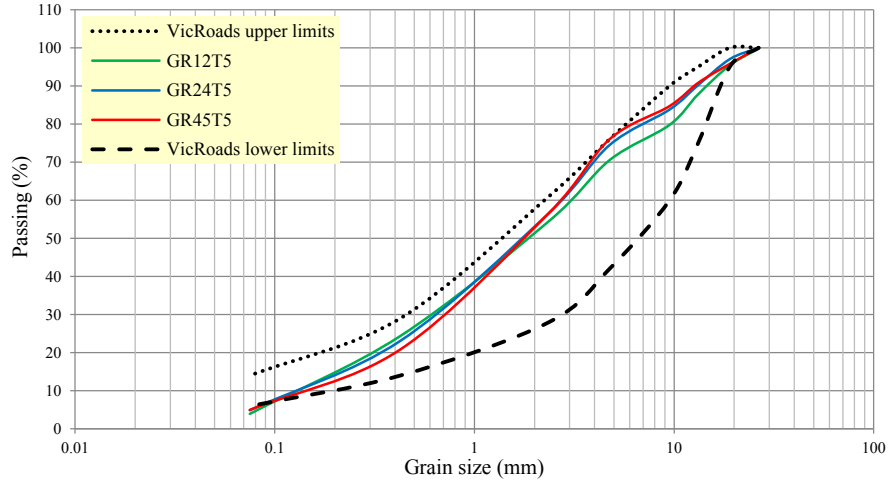

Figure 4.35 Particles size distribution curves for VicRoads limits, and the GR12T5, GR24T5 and GR45T5 mixtures after compaction

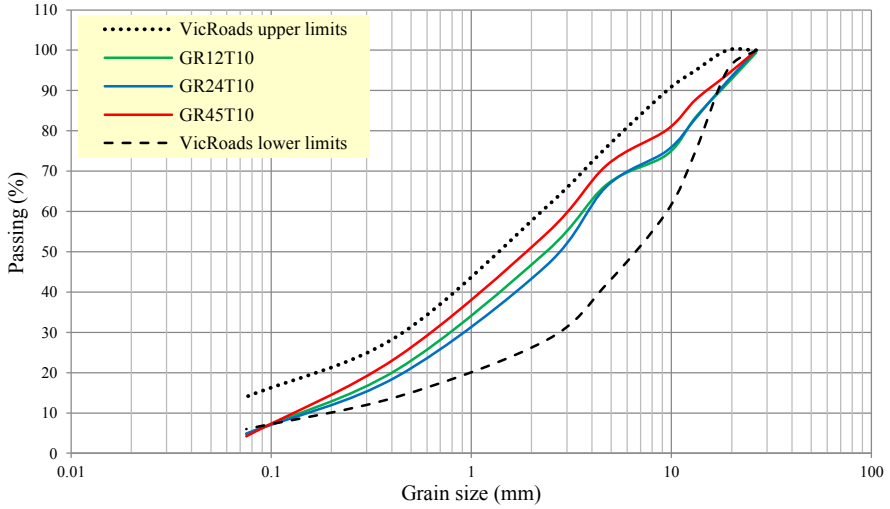

Figure 4.36 Particles size distribution curves for VicRoads limits, and GR12T10, GR24T10 and GR45T10 mixtures after compaction

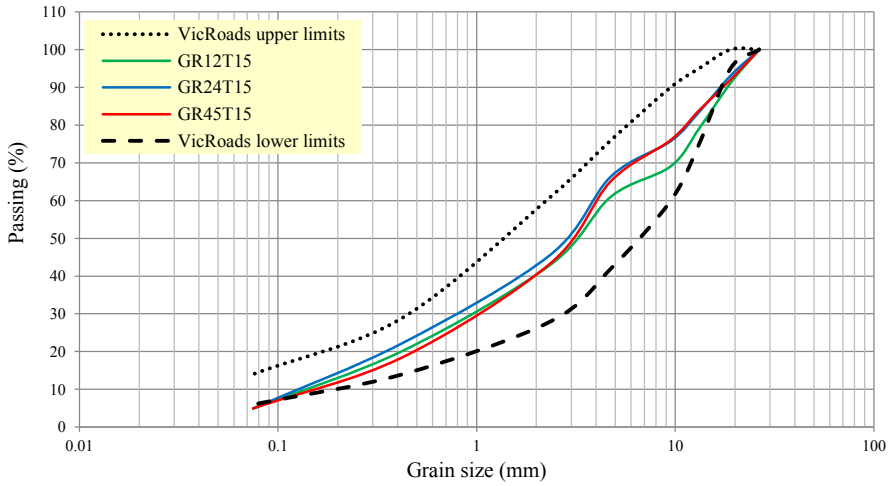

Figure 4.37 Particles size distribution curves for VicRoads limits, and GR12T15, GR24T15 and GR45T15 mixtures after compaction

4.6.2 Compaction results for the GRT mixtures

Figure 4.38 presents the effects of a combination of 12%, 24%, and 45% glass and 5%, 10%, and 15% on the compaction curves of the pure rock sample. In general, a significant reduction in the MDD of the rock was associated with the glass and rubber increase. The MDD value of GR12T5 decreased from 2.175 t/m^3 to 2.17 and 2.165 when the glass content increased from 12% to 24% and 45%, respectively. While the MDD values of GR12T15 decreased from 1.94 t/m^3 to 1.93 and 1.92 when the glass content increased from 12% to 24% and 45%, respectively. The negative effect of the glass and rubber presence on the MDD of the GRT mixtures could be related to the low density of glass and rubber particles themselves. Moreover, a positive effect was remarkable between the OMC of the GRT mixtures and the glass and rubber contents, where the OMC values of GR12T15 and GR12T15 mixtures increased from 7.3% to and 7.5% and from 8.5% to 9% when the glass content increased from 12% to 45%, respectively. The insensitivity of glass and rubber particles to water caused gradually reduction in the GRT mixtures sensitivity to water as a result of the glass and the rubber increases. Thus, the compaction curves of the GRT mixtures flatten and approach constant values as the glass and the rubber contents increase. The above findings are consistent with the results of Wartman et al. (2004) and Babiker et al. (2014), who reported that the glass content can have a vital effect on the compaction parameters of glass-soil mixtures.

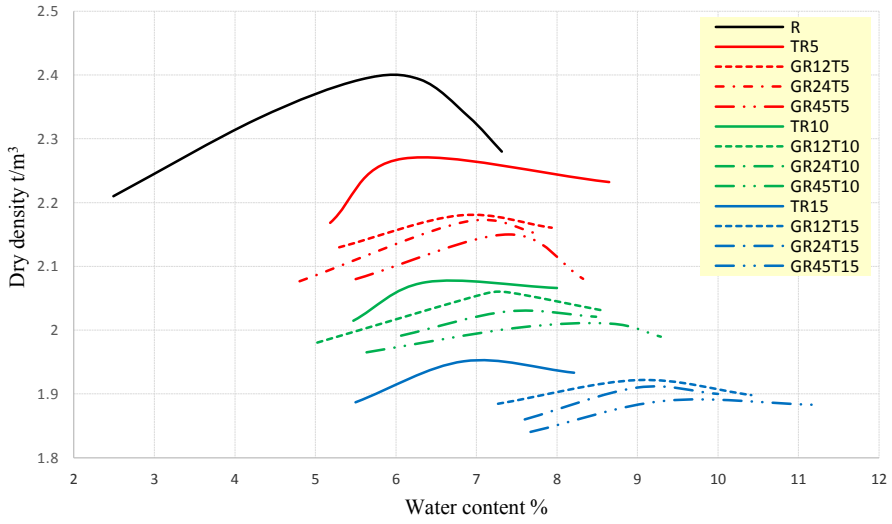

Figure 4.38 Effect of glass and rubber contents on compaction curves of pure rock

The basic properties including sieve analysis, compaction, specific gravity, water absorption, organic content, and p_H tests of GRT mixtures were presented in the present study. The output parameters of these results including D_{10}, D_{30}, D_{50}, D_{60}, C_u, C_c, classification, gravel content (%), sand content (%), fine material (%), MDD and OMC for all GRT mixtures are presented in Tables 4.3, 4.4, and 4.5. The values of the coefficients D_{10}, D_{30}, D_{50}, D_{60}, C_u and C_c were significantly reduced after the compaction tests. In addition, the values of specific gravity and water absorption were reduced directly because of the low specific gravity and the low water absorption of glass and rubber. On the other hand, the mixture with high glass and rubber contents reported the highest values of organic content and p_H value.

Table 4.3 Geotechnical properties of the GR12T5, GR24T5 and GR45T5 mixtures before and after compaction

Symbol	GR12T5 (before compaction)	GR12T5 (after compaction)	GR24T5 (before compaction)	GR24T5 (after compaction)	GR45T5 (before compaction)	GR45T5 (after compaction)
Glass: Rubber: Rock (ratio)	12:5:83	12:5:83	24:5:71	24:5:71	45:5:50	45:5:50
D_{10}	0.16	0.11	0.15	0.11	0.15	0.13
D_{30}	1	0.62	0.7	0.6	0.75	0.96
D_{50}	33	2.1	2	1.7	2	1.8
D_{60}	5	3.4	3	2.8	3.3	2.8
C_u	31.2	29	26	25.4	22	21.5
C_c	1.25	1.09	1.2	1.16	1.13	1.03
Classification	GW	SW	GW	SW	SW	SW
Gravel content (%)	56.4	45.5	51	43.4	44.6	43.4
Sand content (%)	40	50.5	44.2	51.6	50.6	51.6
Fine Content (%)	3	4	4.2	5	4.18	5
Specific gravity (%)	2.38	----	2.1	----	1.6	----
Water absorption (%)	0.75	----	0.66	----	0.56	----
Organic content (%)	0.6	----	0.6	----	0.62	----
p_H	8.45	----	8.5	-----	8.61	----
MDD (t/m^3)	2.175	----	2.17	----	2.165	----
OMC (%)	7.3	----	7.35	----	7.5	----

Table 4.4 Geotechnical properties of the GR12T10, GR24T10 and GR45T10 mixtures before and after compaction

Symbol	GR12T10 (before compaction)	GR12T10 (after compaction)	GR24T10 (before compaction)	GR24T10 (after compaction)	GR45T10 (before compaction)	GR45T10 (after compaction)
Glass: Rubber: Rock (ratio)	12:10:78	12:10:78	24:10:66	24:10:66	45:10:45	45:10:45
D_{10}	0.14	0.11	0.18	0.12	0.2	0.14
D_{30}	0.85	0.59	1.2	0.9	1.2	0.7
D_{50}	2.8	1.7	3.5	2.9	3.2	2
D_{60}	4	2.8	5	4	4.5	3
C_u	28.5	25.4	27.7	33.3	22.5	21.4
C_c	1.29	1.13	1.6	1.6	1.6	1.16
Classification	GW	GW	GW	GW	GW	SW
Gravel content (%)	54	50	59	53.5	57.7	45.6
Sand content (%)	41.8	45	35.5	41.6	39.2	50.15
Fine Content (%)	3.72	5	4.9	4.9	2.48	4.25
Specific gravity (%)	2.27		2.19		1.86	
Water absorption (%)	0.72	----	0.61	----	0.6	----
Organic content (%)	0.48	----	0.6	----	0.62	----
p_H	8.36	----	8.55	-----	8.65	----
MDD (t/m^3)	2.06	----	2	----	2	----
OMC (%)	7.4	----	7.6	----	8.4	----

Table 4.5 Geotechnical properties of the GR12T15, GR24T15 and GR45T15 mixtures before and after compaction

Symbol	GR12T15 (before compaction)	GR12T15 (after compaction)	GR24T15 (before compaction)	GR24T15 (after compaction)	GR45T15 (before compaction)	GR45T15 (after compaction)
Glass: Rubber: Rock (ratio)	12:15:75	12:15:75	24:15:61	24:15:61	45:15:40	45:15:40
D_{10}	0.15	0.13	0.17	0.12	0.17	0.15
D_{30}	1.25	0.9	1.4	0.8	1.4	0.95
D_{50}	3.7	2	3.5	2	3.2	2.9
D_{60}	5.5	4.2	4.9	3.9	4.5	4
C_u	36.6	32.3	28.8	32.5	26.4	26.6
C_c	1.89	1.4	2.35	1.36	2.56	1.5
Classification	GW	GW	GW	GW	GW	GW
Gravel content (%)	61.4	56.91	61.5	54.34	60	56.6
Sand content (%)	33.5	38.2	33.44	40.7	35.16	38.44
Fine Content (%)	4.65	4.89	4.49	4.96	4.52	4.96
Specific gravity (%)	2.2	----	2	----	1.85	----
Water absorption (%)	0.7	----	0.84	----	0.63	----
Organic content (%)	0.45	----	0.57	----	0.59	----
p_H	8.3	----	8.49	-----	8.68	----
MDD (t/m^3)	1.94	----	1.93	----	1.92	----
OMC (%)	8.5	----	8.8	----	9	----

4.6.3 Evaluation of the OMC and the MDD of the GRT mixtures after RLTTs

Further study was conducted in this section to investigate the actual moisture content and the achieved density of the samples before and after the RLTTs. The term actual moisture content used in this section refers to the moisture content of each sample estimated after the RLLTs. Figure 4.39 presents the ratio of the actual moisture content (AMC) to the intended moisture content (IMC) of each specimen at 100% and 70% of the OMC. The figure demonstrates that the GRT mixtures with a wide range of glass, rock, and rubber showed significantly higher ability to retain water than pure rock sample. Also, the high glass and rubber contents achieved the ideal moisture content ratio. The reason for this phenomenon is not entirely apparent but a probable explanation is that the variety of particle types and grains-water adhesion forces may have played a role in the retention of water during the drained tests. At the end of the RLTTs, the GR45T5, GR45T10 and GR45T15 samples reported significantly higher AMC/IMC rates than the other samples. More details on the above explanations are presented in the figure below.

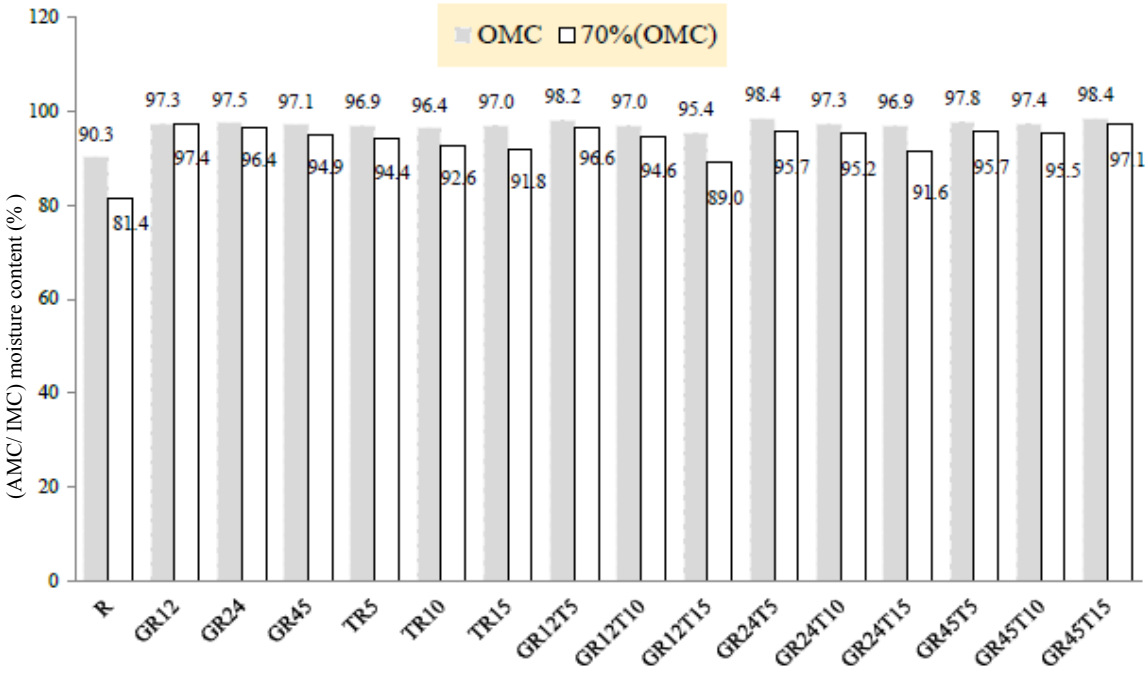

Figure 4.39 AMC/IMC ratio of pure rock, the GR, TR and GRT mixtures according to the glass and rubber contents after RLTTs

Figure 4.40 shows the ratio of achieved density (AD) to maximum dry density (MDD) of the GRT samples at 100% and 70% of the OMC. The term achieved density used in this section refers to the density of each sample estimated after the RLLTs. A marked increase in the AD/MDD ratio of the mixtures is noticeable with the glass and the rubber contents increase. Furthermore, the reduction in moisture content from 100% to 70% of the OMC caused considerable improvements in the achieved densities observed after the RLTTs.

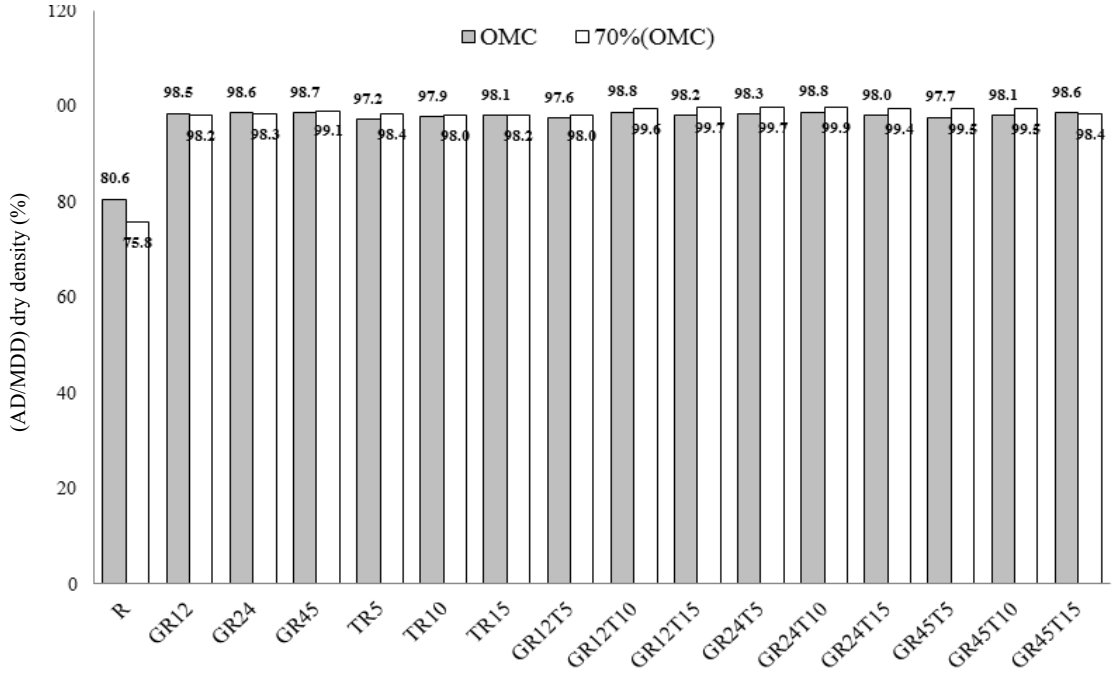

Figure 4.40 Achieved dry densities ofpure rock, and the GR, TR and GRT mixtures according to the glass and rubber contents after RLTTs

4.7 Dynamic behaviour of GRT mixtures

Most of studies in the field of using waste materials in road applications have only focused on using glass and rubber separately. With regards to this subject, the present research focuses on combining glass and tyre rubber with crushed rock. Our findings are based on the results of the RLTTs conducted on cylinder samples of crushed rock with different percentages of crushed glass and tyre rubber. The first section (4.7.1) discussed the influence of glass and rubber inclusion on the resilient modulus (M_r) of pure rock. The second part assessed the effects of glass and rubber contents on the permanent deformation (P_d) of rock samples. The last section of this study explores the dynamic shear strength of the modified mixtures.

4.7.1 Resilient modulus of the GRT mixtures

The variation in the M_r of rock material due to the presence of both glass and rubber materials is represented in this section. In Figure 4.41, a considerable reduction in the M_r of the pure rock (R) sample was associated with the presence of the rubber and the glass particles. Regarding the reverse behaviour, the sliding of the large particles of rubber into voids between the rock and the glass grains reduced the contact between the GRT mixture grains, which caused in reducing the ability of the mixture to induce the resilience behaviour. On the other side, an improvement in the M_r of the TR5 sample was noticeable with the glass presence. For example, the M_r of the TR5 sample gradually increases to 14.53%, 15.7% and 31.4% as a result of increasing the glass content to 12%, 24% and 45%, respectively. The effect of glass on the M_r of the TR5 mixture was related to its role in affecting the soil fabric, where the small particles of glass sliding into the voids between the rock and rubber grains and therefore, strong mixture fabric.

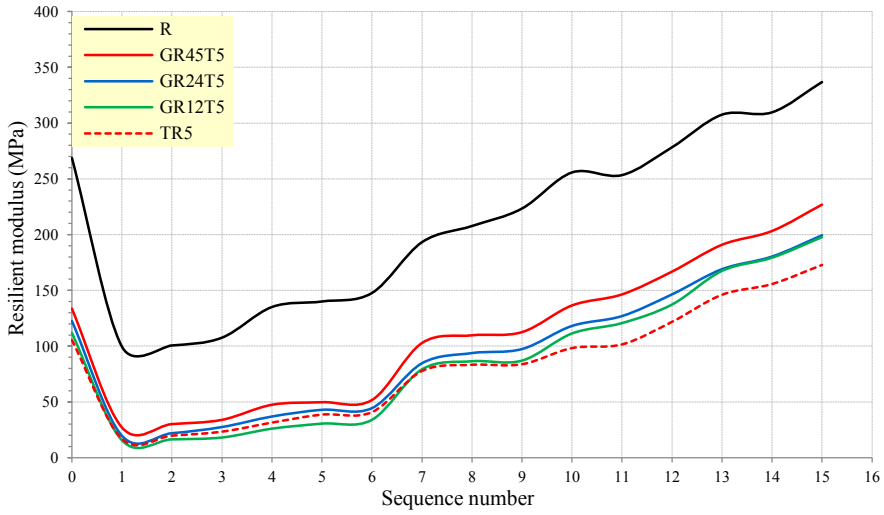

Figure 4.41 Resilience behaviour of pure rock, TR5, GR12T5, GR24T5 and GR45T5 mixtures

The findings in Figures 4.42 and 4.43 confirm the above results, which reported a significant increase in the M_r of the TR mixtures with the glass content increase. On the other hand, mixed crushed rock with high level of rubber did not improve the M_r of the GR mixtures. For example, the GR45T10, GR24T10 and GR12T10 mixtures exhibited higher M_r values than GR45T15, GR24T15 and GR12T15 mixtures. The negative effect of rubber and glass on the M_r might be attributed to the fact that the presence of rubber and glass produced unstable fabric mixtures. In addition, the

sliding of the small particles of rock and glass into the voids between the rubber grains made the large particles of rubber withstand a large portion of the applied stress and led to a decrease in the elastic resistance of the mixtures. In addition, the inverse effect of rubber and glass on the M_r might be attributed to the low densities of the rubber and glass particles compared to the pure rock density.

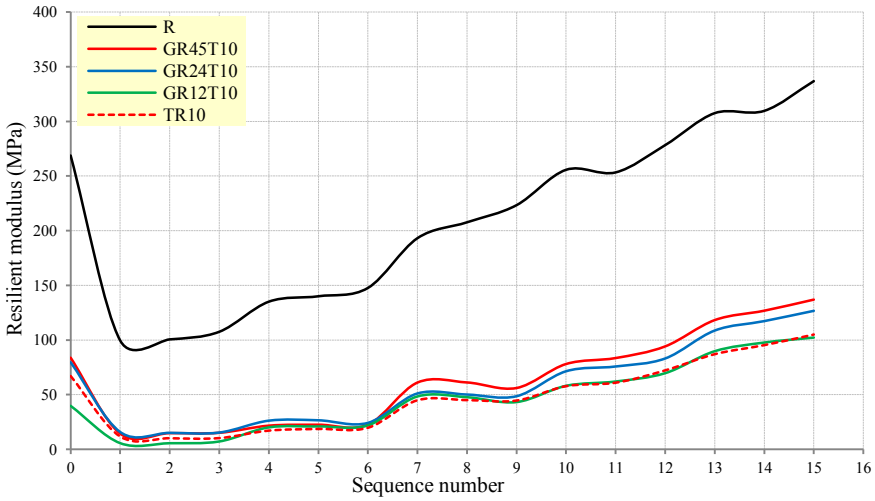

Figure 4.42 Resilience behaviour of pure rock,TR10, GR12T10, GR24T10 and GR45T10 mixtures

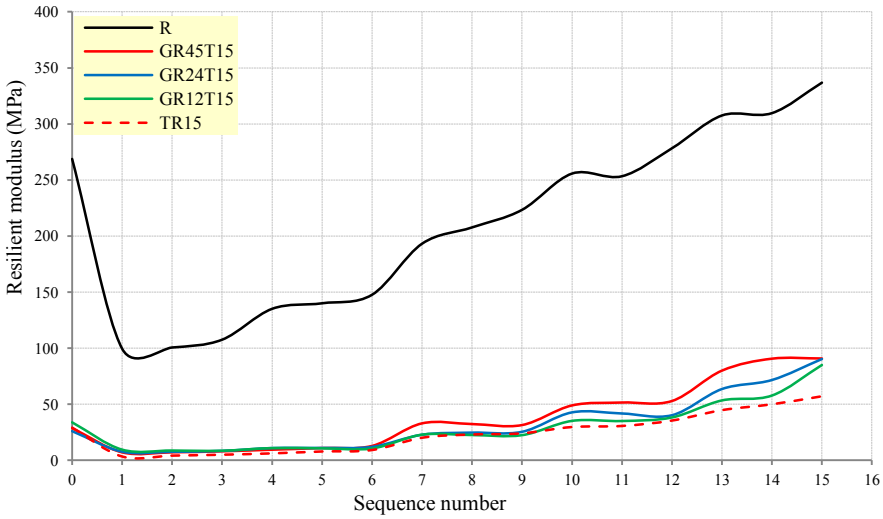

Figure 4.43 Resilience behaviour of pure rock, TR15, GR12T15, GR24T15 and GR45T15 mixtures

4.7.1.1 Effect of moisture content on the M_r of the GRT mixtures

Different samples of the GRT mixtures were prepared at different moisture contents: 100% and 70% of the OMC to assess the effect of moisture content on M_r. Figure 4.44 plots the variation in the M_r of the GR12T5, GR24T5 and GR45T5 samples

according to the moisture content. The GR45T5 and GR24T5 samples at 100% OMC showed higher M_r than the same mixtures at 70% OMC, and that one of the unanticipated findings in the present investigation, whereas it is uncertain if the moisture content influenced the M_r of the GR12T5 mixture. In Figure 4.45, there is a clear trend of increasing M_r of the GR45T10 mixtures because of the moisture decrease, whereas it is unclear if the moisture content influenced the M_r of the GR12T10 and GR24T10 samples. It is apparent from Figure 4.46 that the GR45T15 mixtureat at 70% OMC showed the highest M_r value, whereas insignificant effects of the moisture content was noticeable on the M_r of the GR12T15 and the GR24T15 mixtures. Despite an improvement in resilience behaviour of the GR45T10 and the GR45T15 mixtures as a result of decreasing moisture content, there were insignificant effects of the moisture variation on the M_r of the rest samples of the GRT mixtures. In general, moisture reduction exerted inconsequential effects on the M_r of the GRT mixtures at high levels of rubber and glass ratios, as shown in Figure 4.48, which could be attributed to the low sensitivity of rubber and glass particles to water. This behaviour is consistent with the results reported in section 4.5.1.1 that insignificant differences in the M_r values between the TR mixtures at 100% and those at 70%.

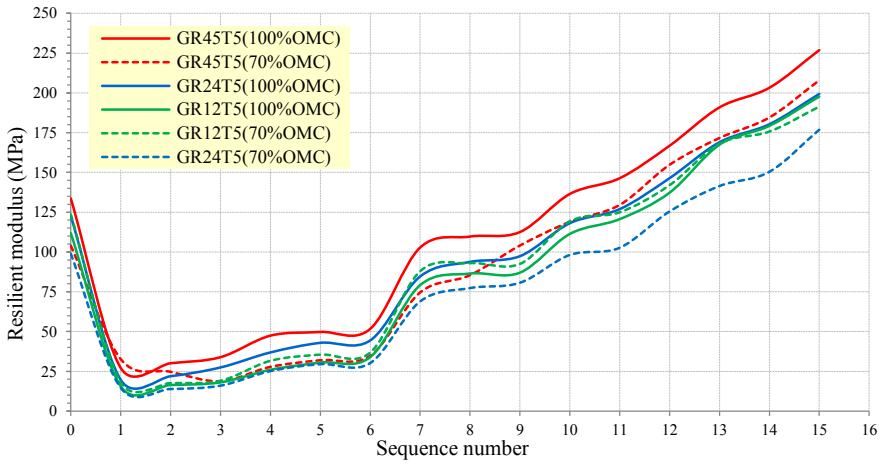

Figure 4.44 Effect of moisture content on the resilient moduli of the GR12T5, GR24T5 and GR45T5 mixtures

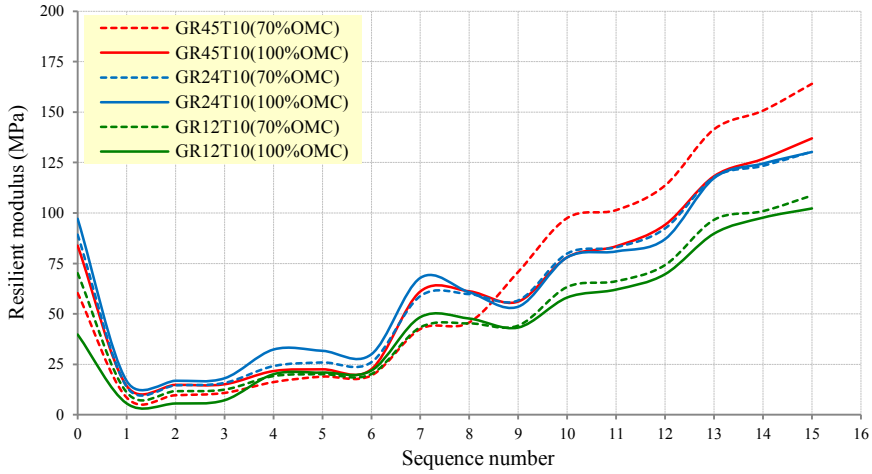

Figure 4.45 Effect of moisture content on the resilient moduli of the GR12T10, GR24T10 and GR45T10 mixtures

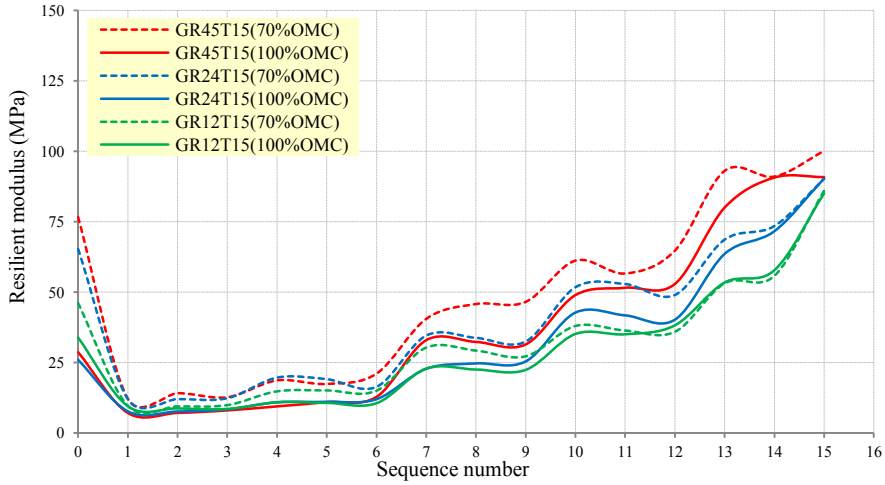

Figure 4.46 Effect of moisture content on the resilient moduli of the GR12T15, GR24T15 and GR45T15 mixtures

The effect of glass and rubber content on the M_r of pure rock is shown in Figure 4.47. It is apparent from this figure that the reduction in moisture content may have contributed in improving the M_r of some samples of the GRT mixtures which containing high glass and rubber ratios. It is important to know that the average of the last five sequences of M_r of each sample was presented in the figure. The R, GR12, GR24 and GR45, TR5, TR15, GR45T10, and GR45T15 mixtures at 70% OMC showed higher M_r than those at 100% OMC. Whereas, insignificant differences in the M_r of the GR12T15, GR24T10, and GR24T15 samples were noticeable when the moisture content decreased from 100% to 70% OMC. Otherwise, a positive correlation was noticeable between the M_r of the TR10, GR12T5, GR24T5, and GR45T5 and their moisture contents. In general, there were

inconsistent correlations between the M_r of the GRT mixtures and the moisture content. Mixing rock with different rubber and glass ratios inversely affected the soil fabric of pure rock, which reduced the contact between the mixture's particles and consequently, decreased the M_r values. In addition, the high permeability and the low sensitivity of both rubber and glass particles to water caused to increase the permeability and decrease the sensitivity of the GRT mixtures to water and thus, the M_r of the GRT mixtures was probably unaffected by the moisture variations.

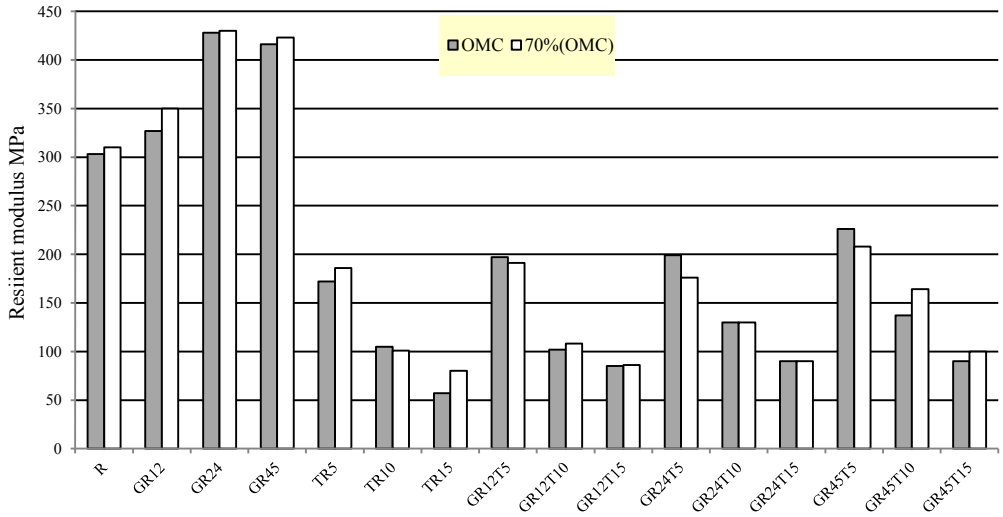

Figure 4.47 Effect of moisture content on the resilient moduli of pure rock, and the GR, TR and GRT mixtures containing different glass and rubber contents

4.7.2 Permanent deformation of the GRT mixtures

This section describes the effects of glass and rock on permanent deformation (P_d) of rock base course material. The effect of moisture content on the P_d of the GRT mixtures is also presented in this section. Figures 4.48, 5.49, and 4.50 present the variation in the Pd of the R sample with different glass and rubber content. It is apparent from Figure 4.48 that the GR12T5 sample showed higher P_d than the TR5 sample and thus, there was an uncertain advantage of mixing a 12% glass with a 5% rubber in enhancing the deformation resistence of the GRT mixtures. Whereas the P_d of the GRT mixtures which contaning 5% rubber decreased with an increase in the glass content. In Figure 4.49, the behaviour of GR12T10 sample was consistent with that of the GR12T5 sample (showed in Figure 4.48), where a considerable increase in the P_d of the TR10 mixture was noticeable when was mixed with 12% glass. In

addition, there was a significant reduction in P_d of the GR12T10 sample was associated with the increasing glass content from 12% to 24%, whereas a slight increase in P_d of the GR24T10 mixture was noticable when increasing the glass content from 24% to 45%. Overall, the TR10 mixture with 24% glass content (GR24T10 sample) presented less P_d than the other samples. Figure 4.50 presents the variation in the P_d of the pure rock with different glass content (12%, 24% and 45%) and 15% rubber content. It is apparent from this figure that a clear decrease in the P_d of the TR15 mixture was noticable when add 12%, 24% and 45% glass. Despite that the GRT samples showed higher P_d than the pure rock sample, the performance of the TR mixtures against the P_d was improved when mixed with the crushed glass. When mixed the rock, rubber, and glass particles together, the small and fine particles of glass occupied the voids between the course rubber and rock grains and improved the contact between the particles which increased the resistance of TR mixtures against the P_d. The above findings also proved that the P_d of GRT mixtures was considerably depended on the rubber and glass ratios. Comparing the results in Figures 4.48, 4.49, and 4.50, the high ratios of glass and rubber reduced the resistance of the GRT mixtures against the P_d. The inverse effect of the high glass and rubber contents might be attributed to the low density, specific gravity, and gravel content (%) of glass and rubber particles, where the presence of glass and rubber produced unstable fabric of GRT mixtures by reducing the density, the specific gravity, and the gravel content (%) of the mixtures. Consequentely, increased the voids and reduced the contact between the different particles and thus, high P_d of the GRT mixtures.

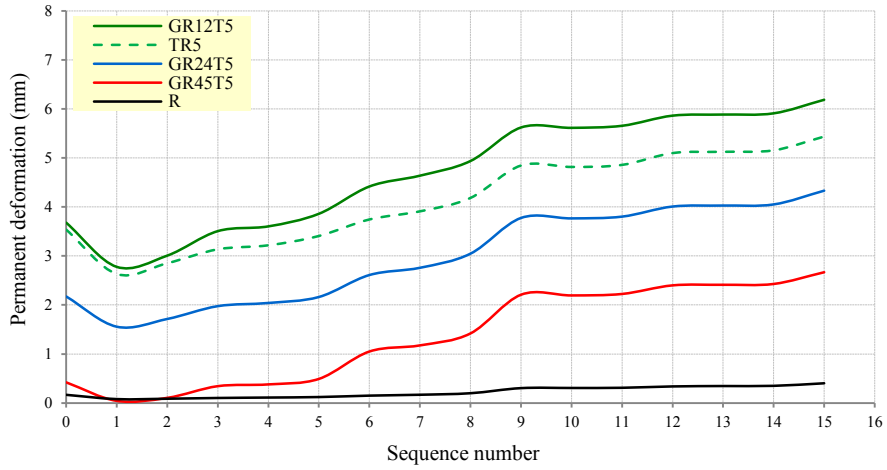

Figure 4.48 Variation in the permanent deformation of pure rock, TR5, and the GRT mixtures containnig 5% rubber with 12%, 24% and 45% glass content

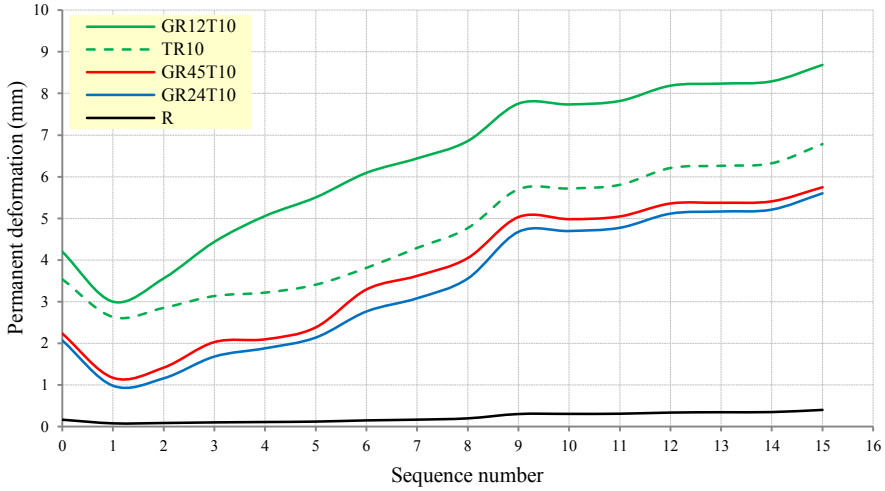

Figure 4.49 Variation in the permanent deformation of pure rock, TR10, and the GRT mixtures containing 10% rubber with 12%, 24% and 45% glass content

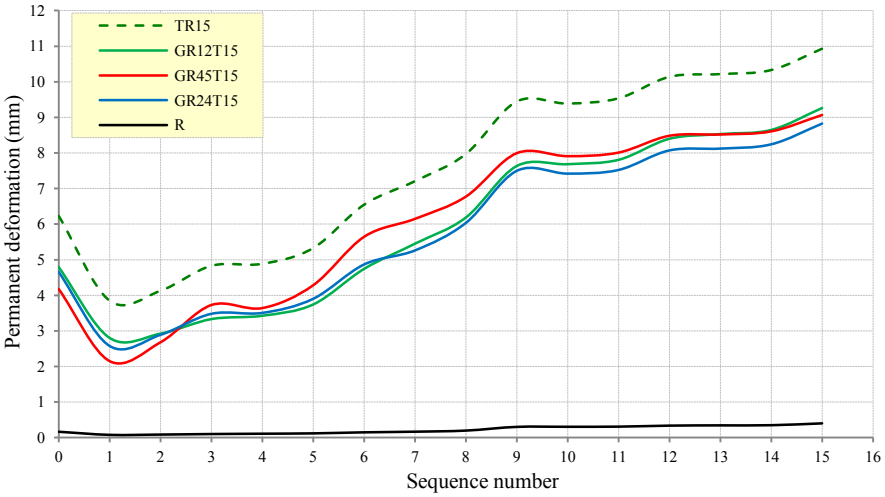

Figure 4.50 Variation in the permanent deformation of pure rock, TR15, and the GRT mixtures containing 15% rubber with 12%, 24% and 45% glass content

4.7.2.1 Effect of moisture content on the permanent deformation of the GRT mixtures

As concluded in our results, the TR mixture containing 5% rubber (TR5) provides additional support for the ideas of Cosentino et al. (2014), who reported a considerable correlation between the moisture content and the P_d of TR mixtures. The variation in the P_d of the GRT mixtures according to their moisture content is presented in Figures 4.51, 4.52 and 4.53. It is apparent from Figure 4.51 that a substantial reduction in the P_d of the GR12T5, GR24T5 and GR45T5 mixtures with the moisture content decrease. It can be observed that the P_d of the GR12T5 sample was higher sensitive to moisture content than the other samples. In Figure 4.52, a significant reduction in the P_d of the GR12T10 sample was associated with the

moisture reduction. The GR12T10 sample also showed the best improvement rate as the moisture content decreased, whereas the response of the GR45T10 sample to moisture reduction was almost imperceptible. The variations in P_d with moisture content of GR12T15, GR24T15 and GR45T15 mixtures are shown in Figure 4.53. It is apparent from this figure that the samples at 70% OMC showed less P_d than the samples at 100% OMC. In addition, the sample with the highest glass and rubber contents (GR45T15) showed the lowest P_d when its moisture content was reduced from 100% to 70% OMC. The GR45T15 sample also showed the best improvement rate of the P_d because of decreasing the moisture content. It is important to know that the results of the present study were consistent with the findings of Vuong (1992), who reported that a sample with the lowest moisture content showed less P_d than those with the highest.

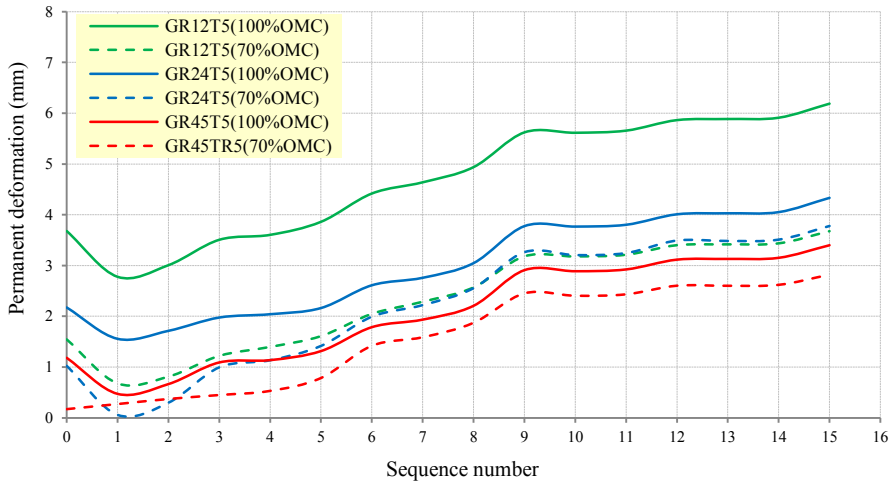

Figure 4.51 Effect of moisture content on the permanent deformation of the GR12T5, GR24T5 and GR45T5 mixtures

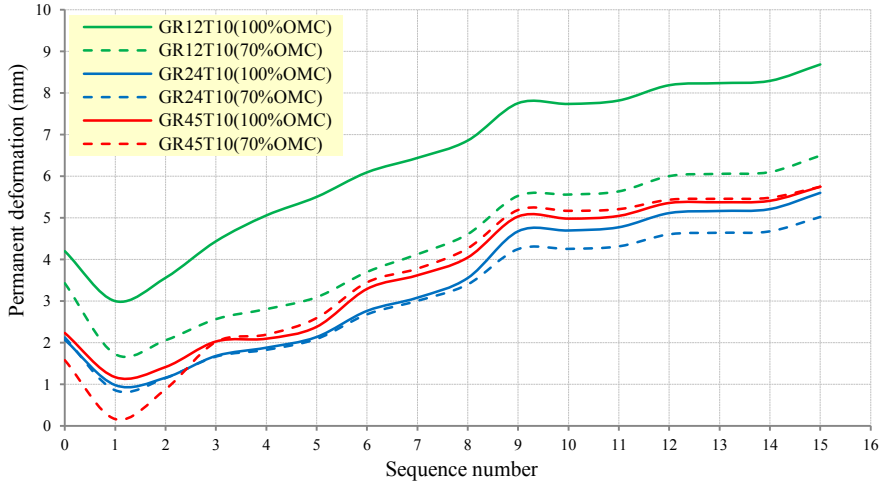

Figure 4.52 Effect of moisture content on the permanent deformation of the GR12T10, GR24T10 and GR45T10 mixtures

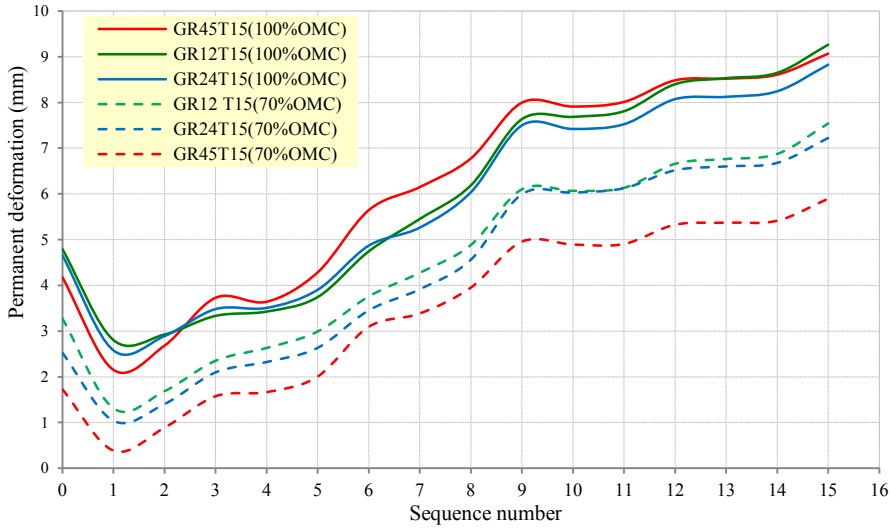

Figure 4.53 Effect of moisture content on the permanent deformation of the GR12T15, GR24T15 and GR45T15 mixtures

Figure 4.54 illustrates the correlations between the P_d and the moisture content of the GRT mixtures with various glass: rock: rubber contents. The P_d of the R, GR12, GR24, and GR45 samples showed a clear reduction as the moisture content decrease. This finding was consistent with those of previous studies by Arulrajah et al. (2014) in that the P_d of the glass-aggregate mixture decreased because of decreasing the moisture content from 81% to 74%, as shown in Figure 2.6. It is apparent from Figure 4.54 that the GR mixtures showed the lowest sensitivity to moisture compared with the TR and the GRT mixtures. This behaviour could be attributed to the fact that the effect of moisture on the P_d was hindered by the smooth surfaces-insensitivity to water of the glass particles. Figure 4.54 also shows some variations with regard to the influence of moisture content on the P_d of the TR mixtures, where the P_d of the TR5, TR10, and TR15 samples reduced because of decreasing the moisture content. Note that the sensitivity of TR mixtures to water were decreased with further rubber content and therefore, TR5 sample showed higher sensitivity to water than TR10 and TR15. Note from the figure that glass strongly influenced the P_d of the GRT mixtures prepared at 70% OMC, that the P_d of the GRT mixtures decreased with the moisture content decrease. The positive affect of glass content and the moisture reduction on P_d of the GRT mixtures could be attributed to the stability of the mixture's fabric. With the glass content increase and the moisture content decrease, the glass particles spread around the rubber grains, filling the voids between the rubber and the rock particles. Consequently, the glass particles contributed in stabilising the fabric of GRT mixtures.

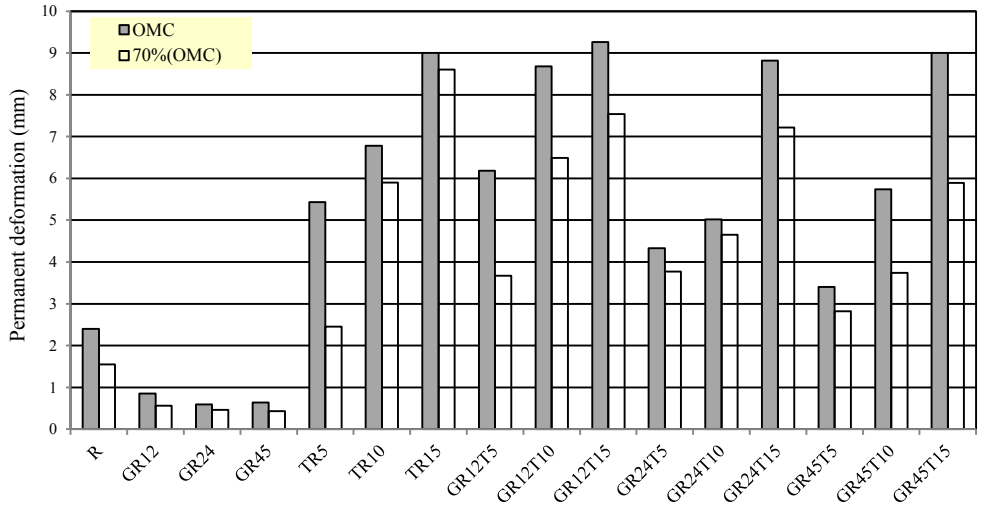

Figure 4.54 Effect of moisture content on the permanent deformation of pure rock, GR, TR and GRT mixtures containing different glass and rubber contents

4.7.3 Shear strength of GRT mixtures

The following section presents a further investigation of the stress-strain behaviours of different GRT mixtures under RLTT impacts. Based on the M_r and the P_d results of the TR mixtures, the TR5 sample showed the best dynamic behaviour. Therefore, the TR5 sample with 12%, 24%, and 45% was selected as a case of study to assess the effect of glass on shear strength. In Figure 4.55, the shear strength of pure rock decreased when mixed with 5% rubber. This behaviour was attributed to the role of rubber in increasing the voids between the rock particles, decreasing the contact between the rock particles leading to a loss of strength.The results of the present study are consistent with the findings of Cabalar (2011), who reported that both internal friction and shear strength of the course sand decreased with the rubber content increase.The effects of 12%, 24% and 45% glass on the shear strength of TR5 samples are also presented in Figure 4.55. In general, a marked improvement in shear strength of of the TR5 sample was associated with the glass presence, as evident in the GR12T5 mixture. Whereas increasing the glass content from 12% to 45% caused a serious reduction in the strength behaviour of the GRT mixture. The rubber particles at the low ratio (5%) endured some of the shear forces applied on the TR5 mixture and therefore, a significant difference between the shear strength behaviour of the TR5 mixture and the pure rock sample. It is apparent from this figure that the presence of 12%, 24%, and 45% of glass increased the internal friction of the TR mixtures. This result was consistent with the findings of Murthy et al. (2007), who reported that the presence of angular shape grains with the rounded

shape formed a good soil fabric and thus, high internal friction angle of the mixture. The glass presence plays a significant role in the positive behaviour of TR5 under dynamic shearing. The voids between the rubber and the rock particles were filled by the glass particles and thus, improved the interlocking and shear resistance of the mixture, which became dependent on the rubber, glass, and rock particles for shear resistance. Therefore, the performance of the GRT mixture under shear forces has become much better than that of the TR5.

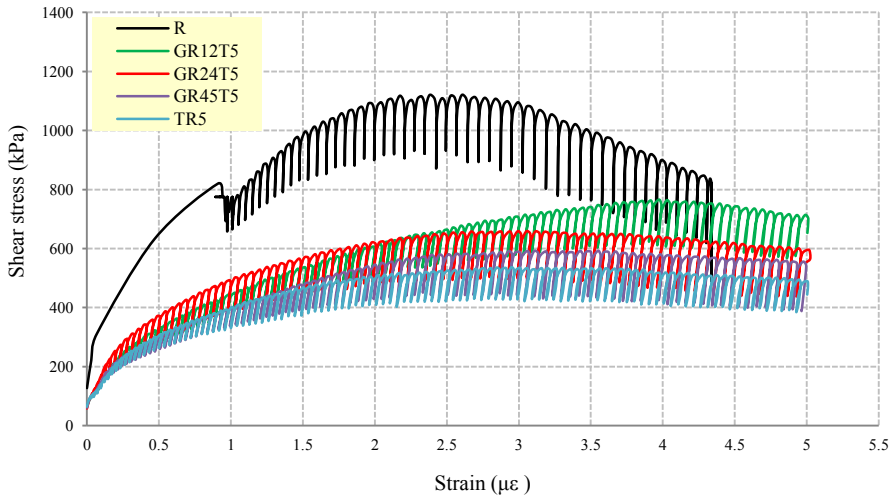

Figure 4.55 Variation in the shear behaviour of pure rock, TR5, GR12T5, GR24T5 and GR45T5 mixtures

4.7.3.1 Effect of moisture content on shear strength of the GRT mixtures

Figures 4.56, 4.57 and 4.58 illustrate the variations in shear strength of the GRT mixtures as a function of moisture content. Contrary to expectations, all GRT mixtures showed significant reductions in shear strength with decreasing the moisture content. For example, the GR12T5 mixture showed the highest shear strength at the highest moisture content, as shown in Figure 4.56. The peak shear values of GR12T5, GR24T5, and GR45T5 samples decreased from 760 kPa to 590 kPa, from 650 kPa to 510 kPa, and from 590 kPa to 480 kPa when the moisture content decreased from 100% to 70% OMC, respectively. The positive effects of the high moisture content on the stress-strain behaviour of the GRT mixtures would related to the stable fabric of the GRT mixtures, where a high moisture content makes the angular particles contributing along with the rock particles to increase the interlocking between the particles and improve the shear strength of the GRT mixtures under the dynamic shearing.

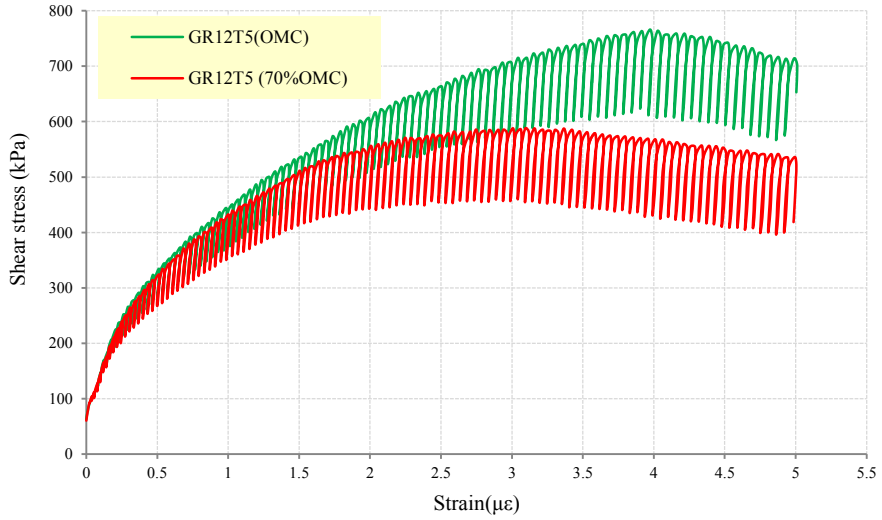

Figure 4.56 Effect of moisture content on the shear strength of the GR12T5 mixture

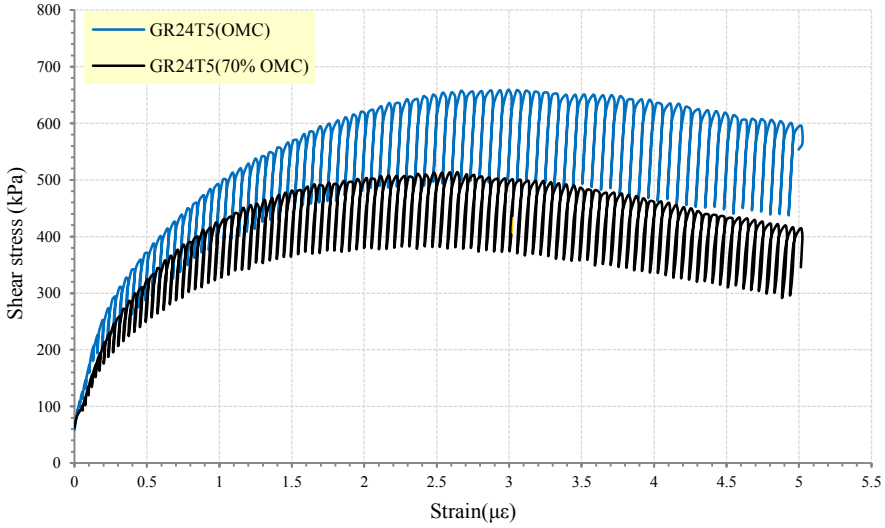

Figure 4.57 Effect of moisture content on the shear strength of the GR24T5 mixture

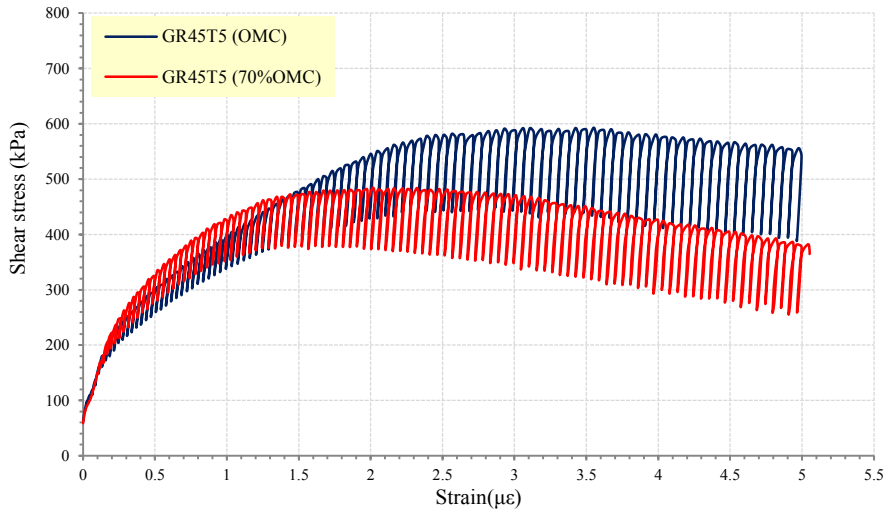

Figure 4.58 Effect of moisture content on the shear strength of the GR45T5 mixture

4.7.3.2 Effect of confining pressure on the shear strength of the GRT mixtures

A series of dynamic shear tests were conducted on the GR12T5, GR24T5 and GR45T5 mixtures at confining pressures of 35, 70 and 150 kPa to study the effect of confining pressure on shear strength. According to the variations in confining pressure, the shear strength behaviour of the GR12T5 mixture is presented in Figure 4.59. Note that the GR12T5 sample at 35 kPa confining pressure showed the lowest critical state of strain and consequently, the failure occurred at a lower stress than in other samples. Also, the findings of Figures 4.60 and 4.61 reported a significant reduction in the shear strength of the GRT mixtures as the confining pressure decrease. For example, the shear peak of GR45T5 decreased from 800 kPa to 550 kPa and 475 kPa when the confining pressure decreased from 150 kPa to 70 kPa and 35 kPa. The positive effect of the confining pressure on shear strength might be attributed to the soil fabric which could be changed from unstable fabric with a high void ratio to stable fabric with a low void ratio under high confining pressures. Consequently, improve the interlocking between the particles which led to increase the dynamic shear strength of the mixture. It is apparent from Figures 4.59, 4.60, and 4.61 that all stress-strain curves flatten and approached constant values with increasing the glass content and decreasing the confining pressure. Also, the presence of high contents of cohesionless materials such as glass in the rock-rubber mixtures decreased the shear strength of the GRT mixtures.

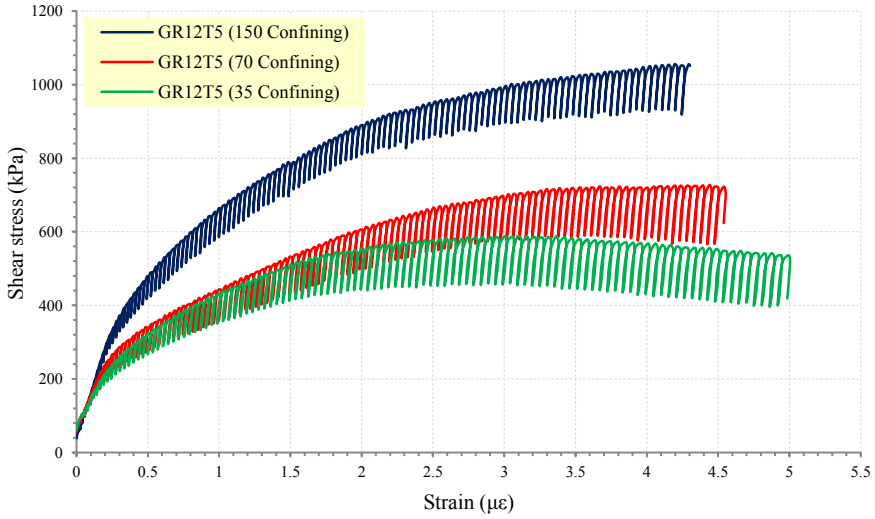

Figure 4.59 Stress-strain curves of the GR12T5 mixtures at various confining pressures

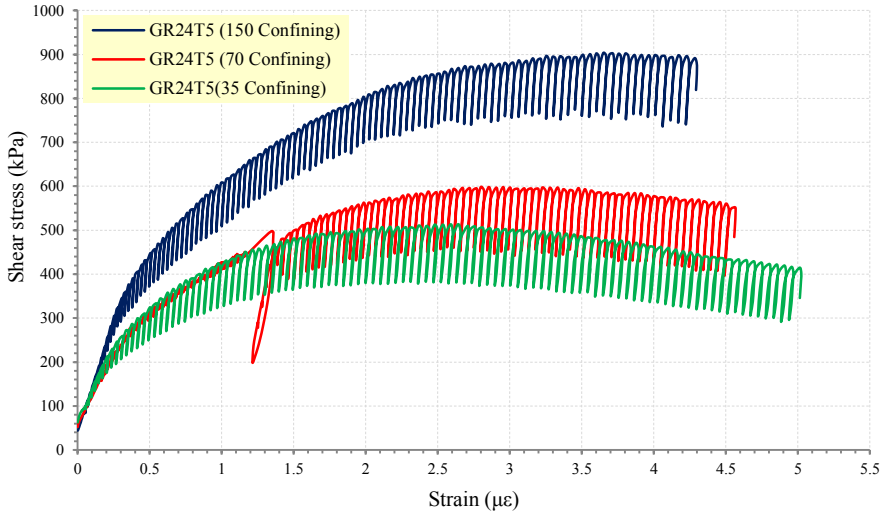

Figure 4.60 Stress-strain curves of the GR24T5 mixtures at various confining pressures

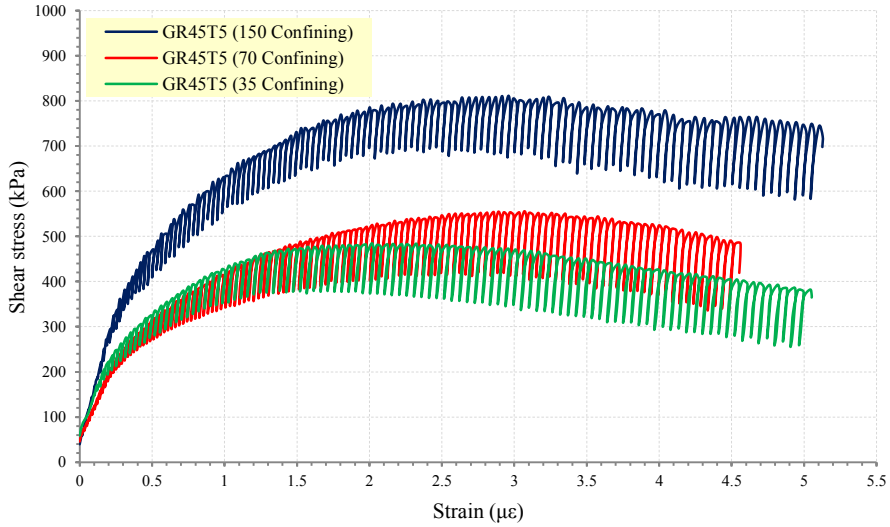

Figure 4.61 Stress-strain curves of the GR45T5 mixtures at various confining pressures

4.8 Summary

Preliminary and dynamic tests were conducted to investigate the suitability of using glass and tyre rubber in pavement applications. Samples of GR, TR, and GRT were prepared by mixing pure crushed rock with different amounts of glass (12%, 24%, 45%) and rubber (5%, 10%, 15%). Further mixtures were also prepared at different moisture contents: 100% and 70% of the OMC to assess the effect of moisture content on the dynamic behaviour of the mixtures. The effects of the density, test condition on dynamic behaviours of a specific mixture were also discussed. The effect of confining pressure on shear strength of the GRT mixtures was also

investigated in this study. Based on the sieve analysis tests results, the gradation curves of GR mixtures before and after compaction showed that all mixtures satisfied the requirements of base material. The compaction tests results showed that the glass inclusion reduced the MDD of the GR mixtures, while a considerable increase in the OMC value was associated with the glass content. The results of water absorption and organic content tests showed a significant reduction with the glass content increase, whereas an increase in p_H was associated with the glass content increase. Increasing the glass content from 12% to 45%, and reducing the moisture content of the GR mixtures from 100% to 70% OMC enhanced the M_r of the GR mixtures. In addition, the drained sample of the GR12 mixture showed higher M_r than that the undrained sample. Also, increasing the density of the GR12 sample from 95% to 100% MDD enhanced the M_r of the GR12 sample. On the other hands, the glass content, the low density, and undrained condition inversely affected the permanent deformation of the GR mixtures. Also, an inversely correlation was found between dynamic shear strength and the glass content.

Based on the rubber-rock mixture results, the gradation curves of pure rock were significantly different with 5%, 10% and 15% rubber content, and all TR mixtures do not satisfy the requirements of base materials. There were also significant reductions in the MDD, the specific gravity, the water absorption, p_H, and the organic contents of the TR mixtures with the rubber content increase, whereas the OMC of the TR mixtures increased because of increasing the rubber content. Based on the RLTTs, the results demonstrated a significant reduction in the M_r of rock specimens with increasing both rubber and moisture contents. Also, the rubber inversely affected the permanent deformation and the shear strength of the TR mixtures, while an improvement in dynamic shear strength of the mixtures was noticeable as the moisture content decrease.

The grading curves of the GR45T5 and GR24T5 mixtures before compaction were approximately between the upper and the lower limits of base materials (VicRoads), while the other mixtures did not satisfy the lower limits. The gradation curves of all mixtures after the compaction impacts were approximately within the lower and the upper limits. In addition, a significant reduction in the MDD, the specific gravity and the water absorption of pure rock was associated with increasing both the glass and rubber content. On the other side, an increase in the OMC, the organic content and p_H were noticeable with the glass and rubber content increase. Base on the RLTT tests,

the findings showed a gradual increase in the M_r of TR mixtures with increasing glass content. In addition, the GRT samples at 70% OMC showed higher M_r than those at 100% OMC. In regard to the P_d of the GRT samples, the P_d decreased steadily with increasing glass content. In general, mixing glass and rubber has a powerful effect on the P_d of the TR mixtures. In addition, reducing the moisture content from 100% to 70% of the OMC positively influenced the P_d of the GRT mixtures. The results of dynamic shear tests indicated that the shear strengths of the GRT mixtures decreased with the glass content increase. There was also a positive correlation between the shear strength of the GRT mixtures and both of the moisture content and the confining pressure.

Chapter 5: Dynamic Behaviour of Rock-Glass-Rubber Mixtures with Cement and Slag

5.1 Introduction

The primary objective of this chapter is to explore the effect of cement and slag treatments on the resilience, deformation and strength behaviour of GRT mixtures. To achieve this objective, different samples of glass-rock (GR), rubber-rock (TR), and GRT mixtures were mixed with cement and slag materials, as detailed in Table 3.14. Then, a series of repeated loading triaxial tests (RLTTs) was conducted on cylindrical samples of the modified mixtures. Factors that may influence the RLTT results were also investigated in this chapter. In the first stage of this chapter, the dynamic characteristics of treated GR mixtures were assessed. The minimum glass to rock ratio used in chapter 4 was 12% and therefore, the same ratio of glass-rock mixture was mixed with 2% Portland cement (labelled GR12C2) to investigate the effect of cement on dynamic behaviour of the cemented mixture. Slag is one of the waste materials that cheaper than another cementing agent and thus, this study trying to use slag in improving the mechanical properties of waste materials-rock mixtures. 1% of replacement of slag to cement could produce environmental and economic considerations. Based on this, a combination of 1% cement and 1% slag was mixed with the GR12 sample (labelled GR12C1S) to assess the effect of slag and cement on the dynamic behaviour of the sample. In the second stage, the dynamic characteristics of the chemical treated samples of the TR mixtures were assessed. The TR sample containing 5% tyre rubber (TR5), which is the minimum rubber to rock ratio, was mixed with 2% cement. The effect of slag and cement on dynamic behaviour of TR5 was also discussed in the second stage, where a mixture of 1% cement and 1% slag was blended with TR5 sample. In the third section, a series of RLTTs was conducted to assess the dynamic behaviours of the cement and cement-slag treated samples of the GRT mixtures containing 12% glass and 5% rubber (GR12T5). A comparison of dynamic characteristics of treated and untreated samples of the GR12, TR5 and GR12T5 mixtures is presented in the fourth stage of this chapter.

5.2 Chemical treatment of glass-rock mixtures

Chemical treatment generally of pavement materials is the addition of small amounts of cementitious binders, typically chemical binders. It is intended to improve many characteristics of materials such as the dynamic performances under repeated loads and increasing the durability of the materials. In this section, the application of chemical additives to improve the dynamic performances of treated crushed rock is to be undertaken. The process of using cement material constitutes as a chemical stabilising process. Similar to this case, the slag could be used as a chemical additive when makes contact with water and thus, slag could behave as cement and improve the soil characteristics but it takes more time than cement to attain full response Ouf (2001) and therefore, another chemical activator should mix with the slag. Also, the effects of slag on the static or dynamic performances of soils might attributed to the mechanical influences and therefore, it is a good opportunity to gather the mechanical and the chemical stabilisations of slag in enhancing the dynamic performance of pavement materials. This section presents the experimental results in terms of the dynamic behaviour of chemical treated samples of glass-rock mixture. The results comprise three main parts, focusing on the M_r, the permanent deformation (P_d) and the dynamic shear characteristics of treated samples. The GR12C2 mixtures were prepared at the optimum moisture content (OMC) and kept under controlled conditions for seven days, the sample was labelled GR12C2-7, as shown in Table 3.14. The effect of 1% cement with 1% slag on dynamic behaviour of GR12 mixture was also studied after a seven-day hydration period, labelled GR12C1S-7.

5.2.1 Resilient modulus of the treated GR12 mixture

In this part of the investigation, the resilience behaviour of the treated GR12 samples was presented and discussed. Figure 5.1 compares the variations in the M_r with of the GR12 mixture with and without 2% cement. A significant improvement in the resilience behaviour of the cement treated sample was noticeable in Figure 5.1. The M_r of the GR12 mixture increased from 320 to 500 MPa with cement presence. The present results confirm those of Komsun et al. (2009) and Siripun, Jitsangiam & Nikraz (2009), who reported a positive correlation between the M_r of crushed rock and the cement content. There was also a large difference between the resilience

behaviour of the cement treated sample and the untreated one. After the conditioning stage, a reduction in M_r was observed during the 1st, 2nd and the3rd loading sequences. Beyond that, the M_r values increased with the sequence number increase. The positive effects of the cement content on the resilience behaviour would be related to role of the chemical treatment of cement in enhancing the stability of the soil fabric. A 2% cement content contributed along with water to generate a chemical reaction which participated in improving the bonds between the rock and the glass particles with each other and then, high interaction between the rock and the glass particles. Another reason for this positive role of cement in improving the resilient modulus could be attributed to the chemical reaction of cement which might exhaust some of moisture content during the hydration period which led to a slight reduction in moisture content and so, improved the M_r of the mixture. This behaviour was consistent with the findings of Arulrajah et al. (2014), who reported that the M_r of the glass-concrete aggregate mixture increased with the moisture content decrease. The influence of replacing 1% slag instead of 1% cement on the resilience behaviourof the GR12 mixture was examined in this part of the study. It is apparent from Figure 5.1 that the GR12C2-7 sample showed a higher M_r value than the GR12C2S-7 sample. The value of M_r at the 15th sequence decreased about 25% when slag used to replace cement at 1%. Reducing the cement content from 2% to 1% could be the reason of that reduction of the M_r value. The slag presence may also obstruct the chemical treatment of cement and that could be another reason of this result. However, the cement-slag treated sample of the GR12 mixture still exhibites higher M_r than both the GR12 and the R samples.

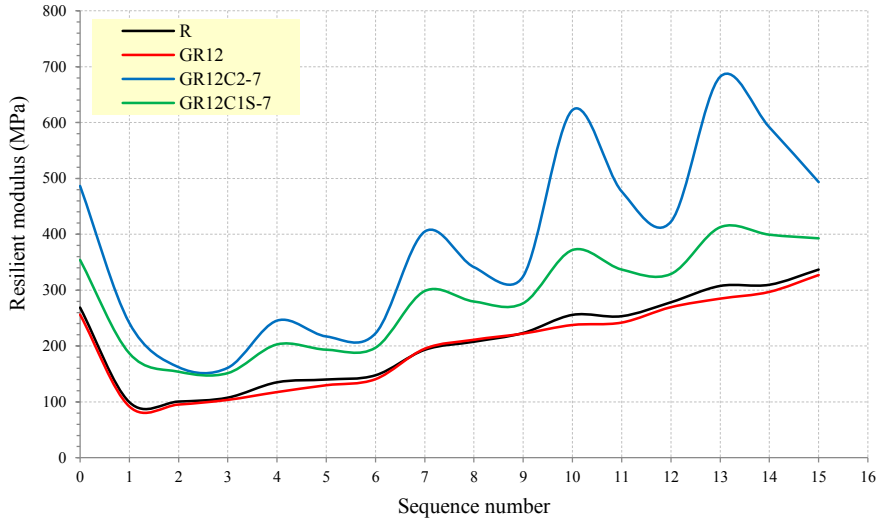

Figure 5.1 Effect of glass, glass-cement and glass-cement-slag contents on resilience behaviour of pure rock after seven days

5.2.2 Permanent deformation of treated sample of the GR12 mixture

The effect of cement treatment on the P_d of the GR12 mixtures is presented in Figure 5.2. There was an insignificant difference between the deformation behaviour of the untreated GR12 and the cement treated one after seven days (GR12C2-7). The values of P_d of GR12 and GR12C2-7 at the 15^{th} sequence are about 0.87 and 0.89 mm, respectively. The effect of mixing 1% slag and 1% cement on the P_d of the GR12 mixture is also presented in Figure 5.2. An insignificant difference between the P_d of the GR12C2-7 sample and that of the GR12C1S-7 sample during the first eight sequences; beyond that, a slight increase in the P_d of the GR12C1S-7 was observed, where the GR12C1S-7 showed higher P_d than the GR12C2-7 sample. The value of P_d at the 15^{th} sequence increased from 0.89 to 1mm when 1% of cement was replaced by1% of slag. Cement particles spread around the glass grains, and coated the smooth surfaces for glass and resulted in improving the stability of the mixture fabric during the hydration period. In fact that slag needs more time than cement to accomplish its chemical reaction and thus, the possible explanation for the negative effect of replacing cement by slag was the reduction in the effectiveness of the chemical reaction which led to decrease the chemical bonds between the glass and the cement grains after the 8^{Th} sequence. The secondary reason for the inverse effects of slag on P_d could be the loss of chemical bonds between the different grains. During the re-mixing process after the hydration phase and under the compaction

impacts during the preparation phase, the glass grains might lose some of the chemical bonds between each other and with the rock particles as well.

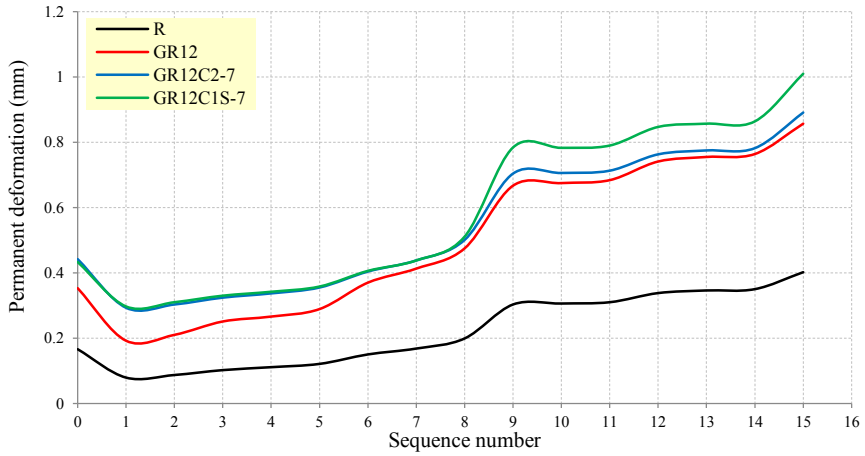

Figure 5.2 Effect of the glass, glass-cement and glass-cement-slag contents on permanent deformation of pure rock after seven days

5.2.3 Dynamic shear strength of the treated GR12 mixtures

The dynamic shear strength of the treated GR mixtures still needs more attention. Therefore, the responses of the GR12 mixtures with different proportions of cement and slag against dynamic shear is investigated via the RLTTs in this section of study. The effect of adding 2% cement on dynamic shear strength of the GR12 mixtures after seven day was investigated first. The presence of 2% cement inversely influenced the dynamic shear strength of the GR12 mixture after the hydration 7-day period, as shown in Figure 5.3. The values of peak shear decreased from 1000 kPa in the pure rock sample to 1000 kPa and 890 kPa with the presence of 12% glass and 2% cement, respectively. The reason for this negative role of cement is probably the mutate of the grains shape of rock and glass materials, where both the rock and glass grains have angular shapes, and a small amount of cement could covered the sharp edges and reduced the role of angularity factor of glass and rock grains. The new structure could inversely influence the stability of the soil structure which lead to decrease the dynamic shear strength. This behaviour was consistent with the findings of Murthy et al. (2007), who concluded that the presence of angular shape grains with the rounded ones could formed a good fabric; otherwise, the rounded or angular grains formed an instable structure. According to the stress-strain characteristics of granular materials, there is a significant reduction in the applied stress with the material deformation increase. This behaviour is known as a post peak regime which

is evident in the stress-strain curves in Figure 5.3. It is also apparent from the figure that the stress-strain curve of the cement treated mixture exhibited same behaviour as the brittle material which can be defined as the material that the stress-strain curve drops sharply after the peak stress.

The effect of cement and slag on the dynamic shear strength of the GR12 mixtures was also assessed through the dynamic shear test and the results are presented in Figure 5.3. The stress-strain curve of the cement-slag treated mixture also exhibited same behaviour as the brittle materials. Also, the peak shear of the GR12 becomes lower with the presence of cement and slag, and the strain corresponding to the peak shear also became lower. The value of peak shear decreased from 890 kPa in the GR12C2-7 sample to 860 kPa when replaced 1% cement by 1% slag. However, the stress-strain curve of the GR12C2-7 sample dropped dramatically after reaching the peak stress, whereas the GR12 sample which treated with 1% cement and 1% of non-plastic slag (GR12C1S-7) showed more strain-softening behaviour.

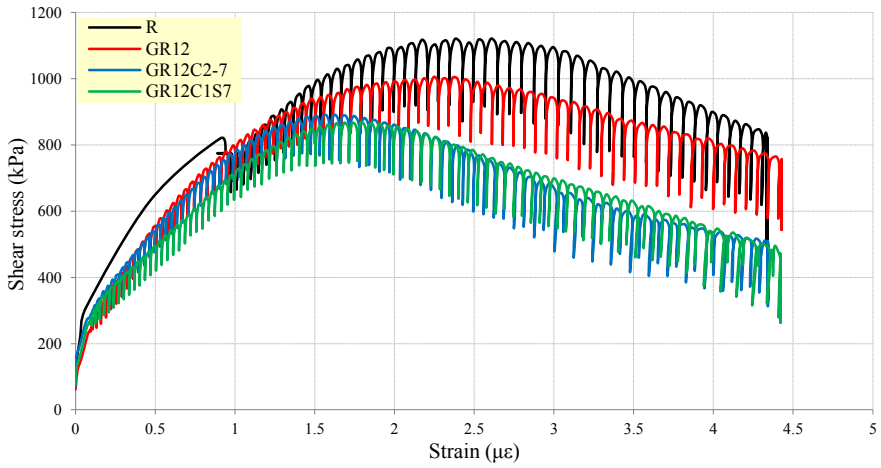

Figure 5.3 Effect of glass, glass-cement, and glass-cement-slag contentson dynamic shear strength of pure rock after seven days

The failure patterns of individual cylinders of treated and untreated GR mixtures after completing the RLLTs are presented and discussed in this section. The cement treated and cement-slag treated samples of the GR12 mixtures are shown in Figure 5.4 (a and b), and the failure of GR12 mixture is presented in Figure 5.4 (c). In general, the shear crack was observed from top to bottom through all samples. Shear failure seemed to be influenced by the presence of cementation agents. In comparing the results of the treated and the untreated samples, an apparent reduction in the general failure risk of the treated samples was noticeable because of their stiff

behaviour. Based on a simple comparison between the cement and the cement-slag treatments, the treated sample with 2% cement showed better performance against failure than that with 1% cement and 1% slag. It is apparent from Figure 5.4 (c) that the untreated sample showed a shear failure mode.

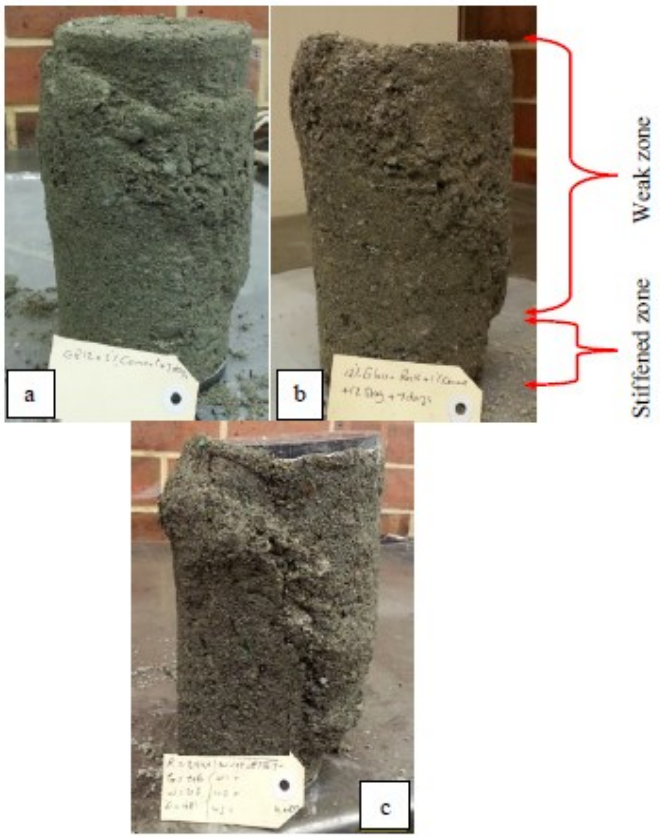

Figure 5.4 Failure patterns observed after RLTTs of GR12 mixtures: a) cement treated sample (GR12C2-7), b) cement-slag treated sample (GR12C1S-7), and c) untreated sample

5.3 Chemical treatment of rubber-rock mixtures

Although, use of tires rubber can inversely influence the dynamic performance of crushed rock material utilized in pavement layers, the presence of rubber with cement resulted in an increase in the CBR value of crushed rock subbase material (Cabalar and Karabash , 2015). Based on that, RLTTs were conducted in this section to assess the effect of cementation agents (cement and slag) on the dynamic performance of the TR5 mixture under repeated loads impacts. The dry mixtures of TR5 were mixed with 2% cement carefully and then mixed with water and kept under specific conditions for seven days. Further samples were prepared by mixing

with 1% slag and 1% cement to assess the effect of cement-slag treatment on resilience behaviour of the TR5 mixture.

5.3.1 Resilient modulus of the treated TR5 mixtures

The variations in the M_r of the TR5 mixtures as a result of the cement and slag presence are presented in this section. Based on the cement treatment, the variation in the M_r of the cement treated mixture (TR5C2-7) with loading sequence number is plotted in Figure 5.5. After seven days, a slight improvement in the M_r of the TR5 during some loading sequences as a result of presence 2% cement. In general, both TR5 and TR5C2-7 have the same value of M_r at the 15^{th} sequences, about 175 MPa. The possible reason for the unstable effect of the cement treatment was the critical chemical bonds between rubber and rock grains. The pre-mixed process and the compaction efforts after the hydration period could be the main reason for reducing the chemical bonds between the rubber and the rock grains and then, low contact between the grains which led to an unstable fabric and thus, an insignificant effect of cement on M_r of the TR5 sample.The effect of 1% slag with 1% cement on the M_r of the TR5 mixtures is also presented in Figure 5.5. The slag-cement treated sample (TR5C1S-7) showed a higher M_r than the TR5 and the TR5C2-7 samples. The value of M_r at the 15^{th} sequence increased from 175MPa in the TR5C2-7 sample to 220 MPa when replaced 1% cement by 1% slag. This positive effect of slag might be attributed to the role of both mechanical and chemical stabilisations of slag in enhancing the dynamic performance of TR5 mixture. The size and the shape of the slag grains play a significant role in the mechanical improvement of the mixture fabric stability and consequently, reducing the compressibility of the TR5 mixture. In addition, the slag grains react as a fine material additive and increase the stability of the soil fabric when it was fill the voids between rock and rubber particles and increased the stability of the TR5 mixture. Also, the angular shape of the slag grains plays a positive role in improving the mixture fabric when blended with the rubber grains. The chemical effect of slag could be attributed to its chemical stabilisation, that slag contributed (as a chemical additive) with cement to improve the resilience behaviour of the TR5 sample after seven days of hydration.

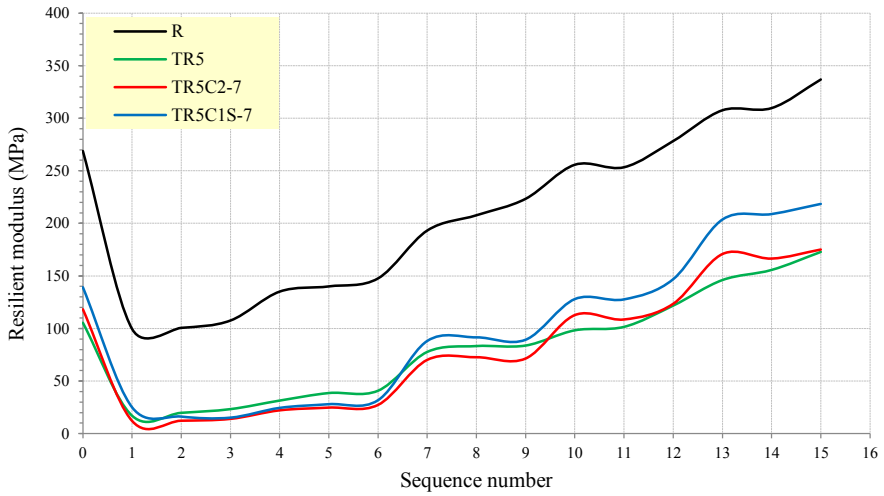

Figure 5.5 Effect of rubber, rubber-cement and rubber-cement-slag contents on the resilience behaviour of pure rock after seven days

5.3.2 Permanent deformation of the treated TR5 mixtures

In this section, a series of RLTTs was performed to investigate the effect of the cement and the cement-slag treatment on P_d of the TR5 mixture. Figure 5.6 shows the results of the P_d of rock, TR5, and the cement treated sample (TR5C2-7) plotted versus the loading sequences. After seven days of hydration, there was a significant reduction in the P_d of the TR5 sample with 2% cement. The value of P_d decreased from 5.4mm in the TR5 sample to 2.4mm kPa when mixed with 2% cement. The rate of the P_d reduction because of the cement presence with the TR5 mixture is about 125%. Depending on the conclusions of previous study in terms of the cement treatment mechanism (Cheung and Dawson, 2002), cement and the fine materials of rock spread around the rubber grains, coated the surfaces and resulted in a cementation bonding between the different grains. That could develop both of the stability of the mixture fabric and the surface friction and consequently, low P_d. This mechanism could explain the positive effect of 2% cement on the P_d of TR5 mixture. It is apparent from Figure 5.6 that the P_d value of the TR5C2-7 is consistent with that of the pure rock during the 1st sequence; beyond that, a steady increase in the P_d was noticeable till the last loading sequence. The value of P_d at the 15th sequence decreased from 0.4mm in the pure rock sample to 2.4mm with the presence of 5% glass and 2% cement. This behaviour could be attributed to the high compressibility of the rubber particles which inversely affected the chemical bonding between the rubber and the rock particles.

Figure 5.6 also shows the effect of 1% slag with 1% cement on P_d of the TR5. During the earlier stage (1st to 8th sequence), the TR5C1S-7 sample had potentially better performance than the TR5C2-7 sample. Beyond that, TR5C1S-7 sample showed higher P_d than the TR5C2-7 sample. At the end of the test, the value of P_d increased from 2.4 in the TR5C2-7 sample to 2.8mm in the TR5C1S-7 sample. This change in deformation behaviour might be related to the negative response of the TR5C1S-7 sample to high levels of confining and deviator pressure. Between the 8th and the 9th sequences, the P_d value of the TR5C1S-7 sample increased about 12.5% of the P_d value of the TR5C2-7 sample because of increasing the deviator pressure from 62 kPa to 93.1 kPa. At the 15th sequence, the increment rate of the P_d of the TR5C1S-7 sample reached to 20.8% when the confining pressure increased from 68.9 kPa to 137.9 kPa and the deviator pressure increased from 62 kPa to 248.2 kPa. This change in pressures inversely affected the chemical bonding of the cement-slag-rubber-rock sample which reduced the stability of the mixture fabric and thus, high P_d of the TR5C1S-7 sample compared to the TR5C2-7 one.

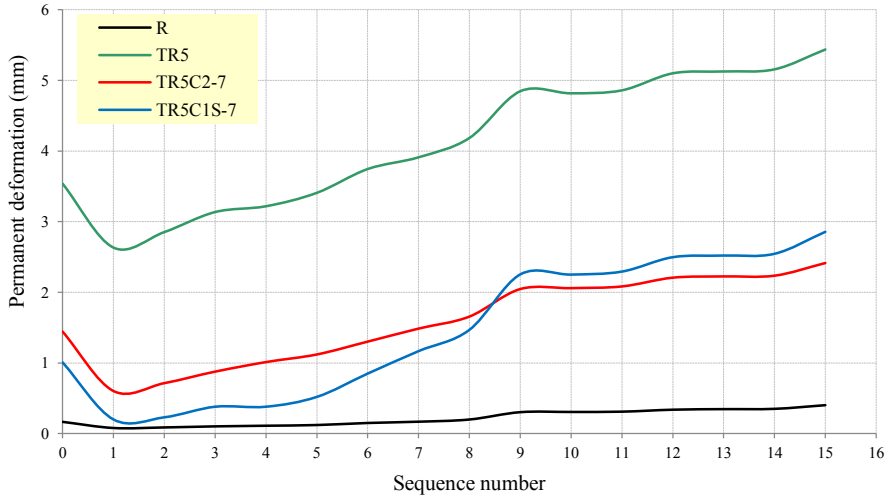

Figure 5.6 Effect of rubber, rubber-cement and rubber-cement-slag contents on permanent deformation of pure rock after seven days

5.3.3 Dynamic shear strength of the treated TR5 mixtures

It is necessary to understand the development of strength characteristics of the TR5 mixture after the chemical treatment. In this case, the effect of 2% cement on the stress-strain behaviour of the TR5 mixture over a 7 day hydration period was investigated in this section. Following this, the effect of 1% cement with 1% slag on the stress-strain behavioure of the TR5 mixture was also investigated. The shear

response of the TR5C2-7 sample are presented in Figure 5.7. It is apparent from this figure that the TR5C2-7 sample could not withstanding the increase in the shear forces and collapsed early. Interestingly, the untreated sample of the TR5 mixture showed better shear strength than the cement treated one. Despite the replacement of 1% of cement with 1% of slag was uneffected on the shear strength of the TR5C2-7 mixture, an improvement in the testability of shear strength of the TR5C2-7 mixture was noticeable because of the slag presence. Note that the TR5C1S-7 sample became sufficiently stiff to resist the excessive strain. It is apparent from this figure that the slag presence shifted the strain value corresponding to the ultimate shear strength from 2.5 με to 3.4 με. It is important to know that the chemical bonding was broken during the remixing and the compaction phases during the sample preparation. Therefore, sufficient moisture and enough hydration time are required to achieve full rehydration action for the cement and cement-slag treated sample before applying shear loadings (Siripun, Jitsangiam & Nikraz, 2009). According to that, the inverse effects of the 2% cement might be attributed to the insufficient both of the moisture and the time for the rehydration action before and between the loading phases. As mentioned above, the chemical bonding was broken during the remixing and compaction phases. After that, the dynamic shear test was conducted directly on the treated sample without additional water or enough hydration time and that could be the primary factor affected the strength behaviour of the TR5C2-7and the TR5C1S-7 samples. In addition, the shear strength ofthe TR5C1S-7 showed an improvement in the shear stability compared to the TR5C2-7 sample, and this behaviour could be considered another evidence of minimising the rehydration effects on shear strength of the TR5C2-7 when reduced the cement content from 2% to 1%.

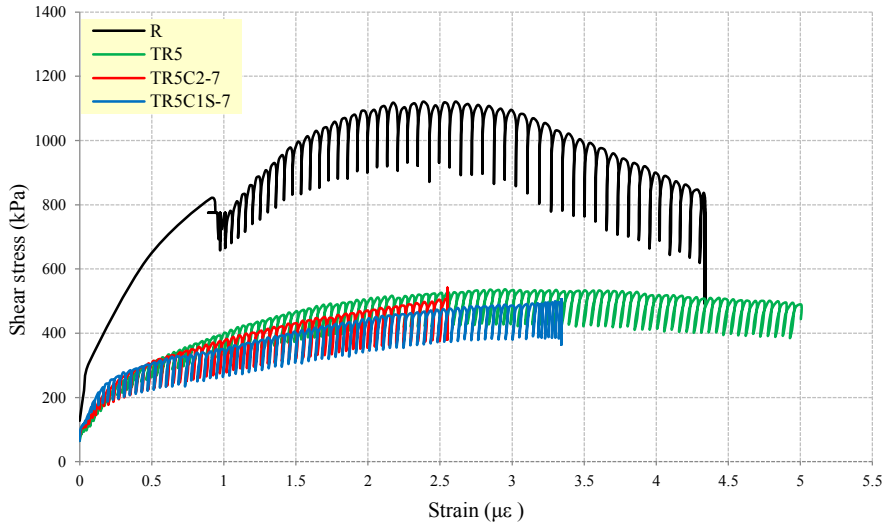

Figure 5.7 Effect of rubber, rubber-cement and rubber-cement-slag contents on the shear strength for the pure rock after seven days

It is apparent from Figures 5.8 (a and b) that the TR5C2-7 sample reached the ultimate shear strength before the TR5C1S-7 sample, and then failed. Also, longitudinal cracking was observed from the top to the centre of the TR5C2-7 sample in a direction parallel to the axial force, as shown in Figure 5.8 (a). Whereas replacing 1% of cement with 1% of slag minimised the cracking risk of the TR5C2-7 sample and delayed the failure stage, as shown in Figure 5.8 (b). Because of that, the shear strength of the TR5C2-7 sample and its resistance to fail increased when replaced 1% of cement by 1% of slag.

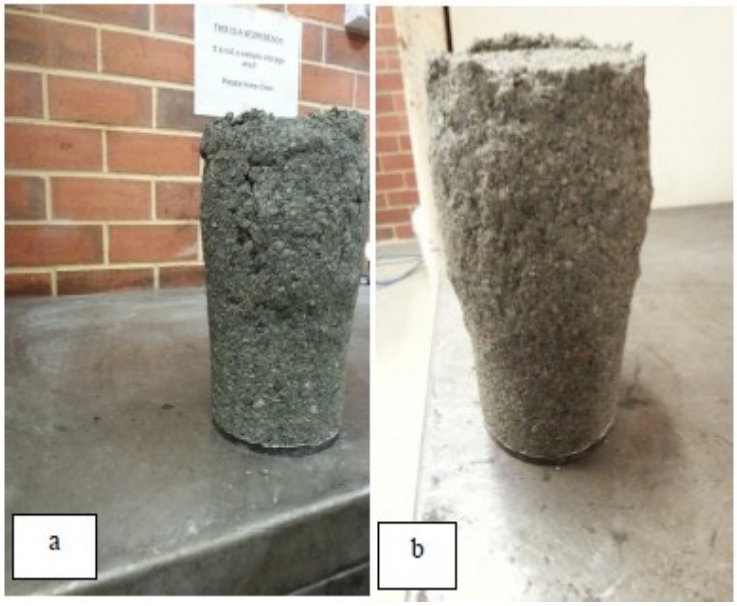

Figure 5.8 Failure patterns observed after RLTTs of TR5 samples: a) cement treated sample, b) cement-slag treated sample

5.4 Chemical treatment of glass-rock-rubber mixtures

According to the results in section 4.7, a significant improvement in both M_r and shear strength of the TR5 mixtures was noticeable with 12% of glass. However, the pure rock sample showed better dynamic performance than the sample of rock containing both rubber and glass. Therefore, the present section focuses on the chemical treatment of the glass-rock-rubber mixtures. A series of RLTTs were conducted on samples prepared by mixing the GR12T5 sample with 2% of cement to evaluate the effect of cement on the dynamic behaviour of the GR12T5 sample. The effect of replacing 1% of cement by 1% of slag on dynamic behaviour of the GR12T5 mixture was also studied in the next sections. The variations in the resilience behaviour, the permanent deformation and the dynamic shear strength of the GR12T5 mixtures because of the chemical treatment are presented in the following sections.

5.4.1 Resilient modulus of the treated GR12T5 mixtures

The effect of the cement content on the resilience behaviour of the GR12T5 mixture can be observed in Figures 5.9. Over a 7 day hydration period, an increase in the M_r of the GR12T5 sample was associated with the presence of 2% cement. The values of M_r at the 15^{th} sequence increased from 200 MPa in the GR12T5 mixture to 225 MPa with the presence of 2% of cement. The effect of replacing 1% of cement by 1% of slag on the M_r of the GR12T5 was also shown in Figure 5.9. Insignificant differences in the resilience behaviour were noticeable between the cement-slag treaded sample (GR12T5C1S-7) and the cement treated sample (GR12T5C2-7). Despite that cement and slag may react as fine materials which caused a reduction in M_r (Hicks & Monosmith, 1971), there were positive effects of the cement and cement-slag contents on the resilience behaviour of the GR12T5 mixture. The positive behaviour could be attributed to the chemical effects of the cement and slag materials when reacted as cementitious agents which enhancing the stability of the mixture fabric and led to increase the M_r of the mixture.

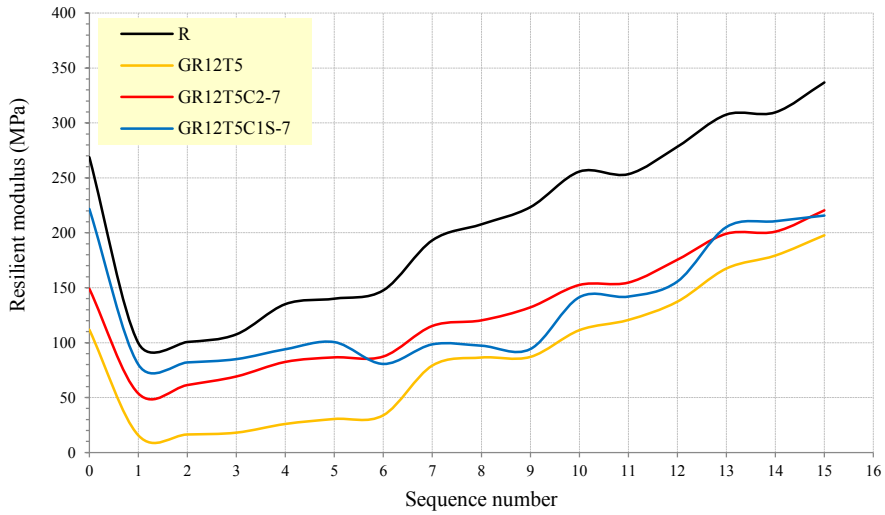

Figure 5.9 Effect of glass-rubber, glass-rubber-cement and glass-rubber-cement-slag contents on the resilience behaviour of pure rock after seven days

5.4.2 Permanent deformation of the treated GR12T5 mixtures

The results in Figure 5.10 reveal a significant reduction in the P_d of the GR12T5 mixtures as a result of adding 2% of cement. The cement treated sample showed lower P_d (about 20%) than the untreated GR12T5 sample. The effect of replacing 1% cement with 1% slag on the P_d of the GR12T5C2-7 was also presented in Figure 5.10. It is apparent from this figure that a slight increase in the P_d was associated with replacing 1% cement with 1% slag. Despite this increase in the P_d, the GR12T5C1S-7 sample remains less deformation than the untreated one (GR12T5). Despite fine materials are considered a critical factor on P_d (Magnusdottir & Erlingsson, 2002), there was positive effects of cement and slag on the P_d. This positive effect could be related to the chemical treatments of cement and slag. In addition, the mechanical stabilisation of the angular shape of slag may enhance the contact between the particles and improve the interlocking between the particles and consequently, increase the mixture resistance to deform.

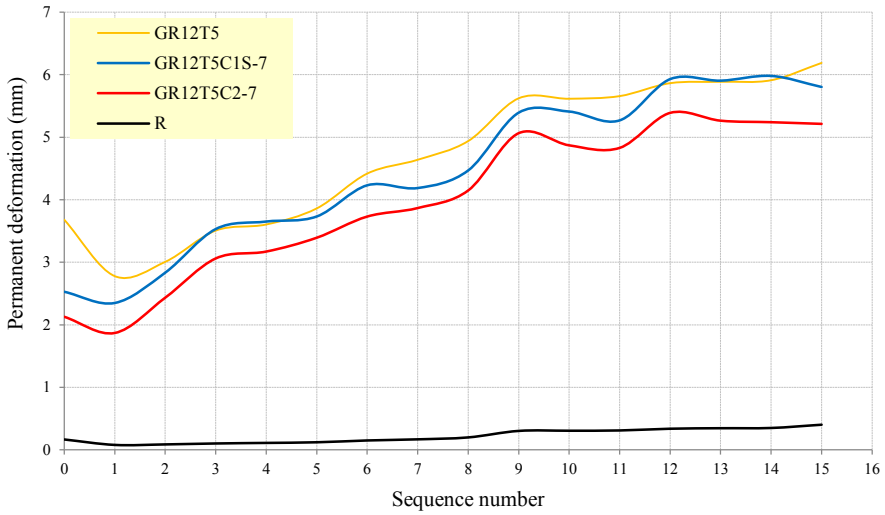

Figure 5.10 Effect of glass-rubber-cement and glass-rubber-cement-slag contents on the permanent deformation of pure rock after seven days

5.4.3 Dynamic shear strength of the treated GR12T5 mixtures

The dynamic shear strength results for the chemical treated mixtures are presented in this section. Figure 5.11 shows the effect of adding 2% cement on shear strength of the GR12T5 mixture. In general, the peak shear of the GR12T5 mixture decreased from 780 kPa to 510 kPa when mixed with 2% cement. Similarly, Figure 5.12 presents the effect of replacing 1% of cement by 1% of slag on the shear strength of the GR12T5 mixture. The shear strength of the GR12T5 mixture increased with 1% slag and 1% cement, and there is insignificant difference between the stress-strain behaviour of the GR12T5C2-7 sample and the GR12T5C1S-7 sample. According to the conclusions of the previous studies mentioned in the review chapter, shear strength of the granular materials depends on the interlocking between particles, which is in turn depends on many physical properties such as the particles shapes and the surface roughness; where the smooth rounded grains showed the lowest level of interlocking and this could be reduced the shear strength. In this case, both crushed rock and crushed glass are angular materials and that could be improved the level of interlocking between the grains of the GR12T5 mixtures, but the high compressibility of the rubber particles might inversely affected the chemical treatment of the GR12T5 sample and then, low resistance against dynamic shear. In general, these findings are considered as logical results when compared to those in Figures 5.3 and 5.7 which reported a significant reduction in shear strength of the chemical treated samples of the GR12 and the TR5 mixtures.

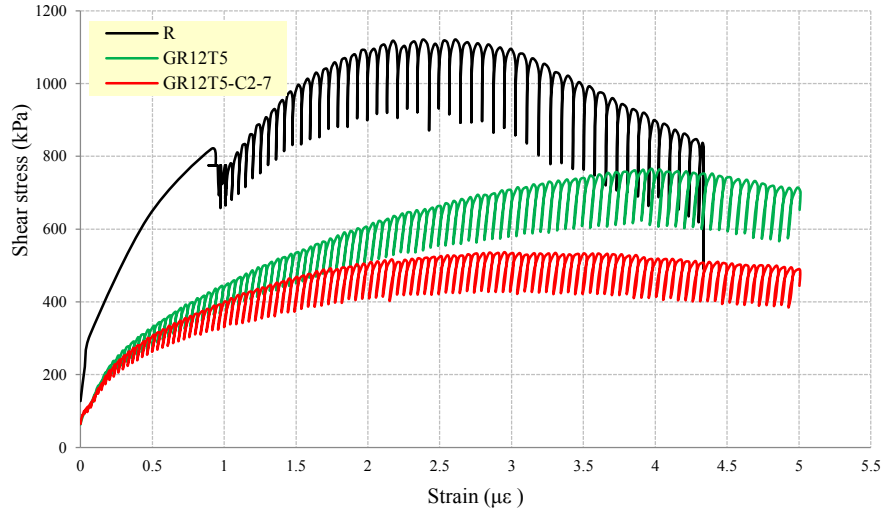

Figure 5.11 Effect of glass-rubber and glass-rubber-cement contents on the shear strength of pure rock after seven days

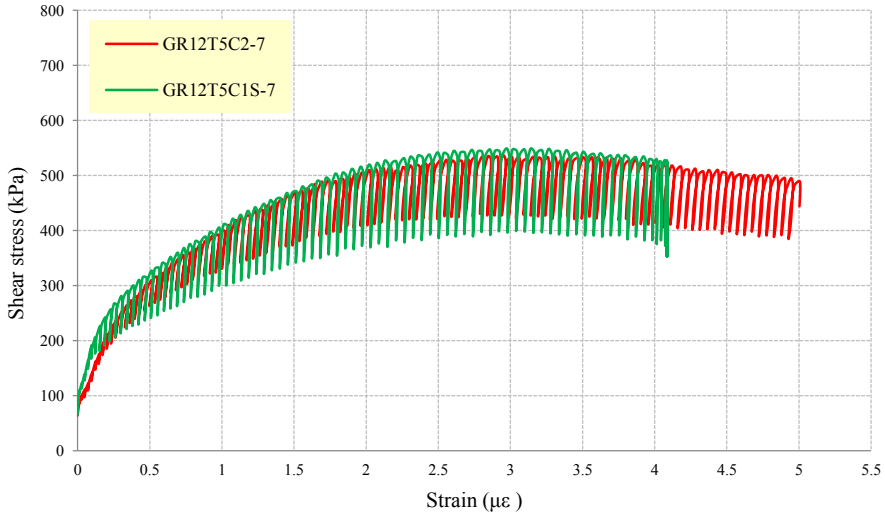

Figure 5.12 Effect of cement-slag contents on the shear strength of the GR12T5C2-7 mixture after seven days

The failure patterns of the chemical treated samples of the GR12T5C1S-7 and GR12T5C2-7 mixtures after the RLLTs are visible in Figures 5.13 (a and b), respectively. Comparing sample failures, the cement and the cement-slag treatments, the GR12T5C1S-7 sample performed better than the GR12T5C2-7 sample. It was evident that the chemical reaction of the additives contributed significantly in improving the performance of the GR12T5C2-7 sample against shear stress, but the re-mixing process during the preparation stage may prevent that contribution, whereas the sharp edges of the slag particles had a more affective in that role and that could be a possible explanation of the GR12T5C1S-7 performance under the dynamic shear loadings.

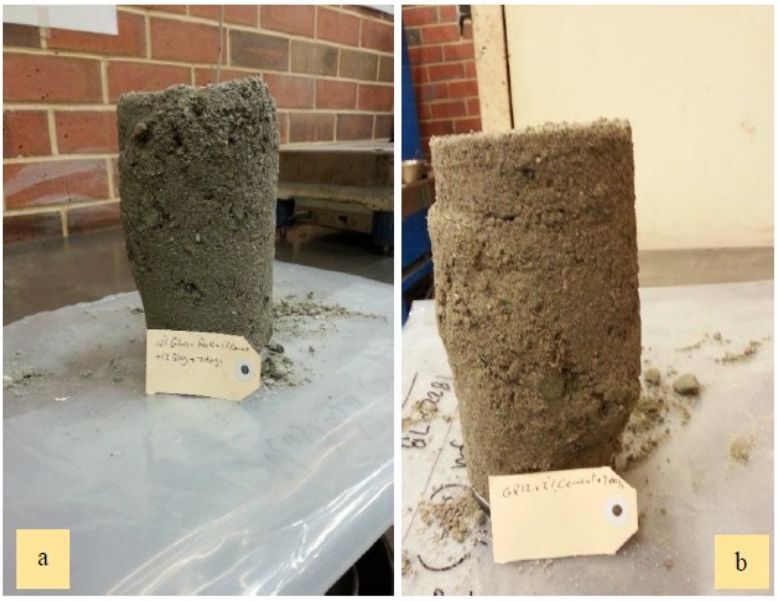

Figure 5.13 Failure patterns observed after RLTTs of the GR12T5 samples: a) cement-slag treated sample and b) cement treated sample

5.5 Comparison of the dynamic characteristics of treated and untreated GR12, TR5 and GR12T5 mixtures

A comparison of the dynamic characteristics of the treated and the untreated GR12, TR5 and GR12T5 mixtures was conducted in this section. Three sets of comparisons highlighted the impact of cementation agents (cement and slag) on M_r, P_d and dynamic shear strength of the mixtures. The M_r results of the treated and the untreated samples of the GR12, TR5 and GR12T5 mixtures are compared with pure rock base course material and presented in Figure 5.14. The treated GR12 samples showed the highest M_r, whereas the treated TR5 mixtures showed the lowest M_r. Furthermore, a positive correlation was noticeable between the M_r and the 2% cement content, where the cement treated samples of the GR12 and GR12T5 mixtures showed higher M_r than the cement-slag treated samples. Whereas the cement treated sample of the TR5 mixture showed lower M_r than the cement-slag treated sample. Note that the lowest modulus was observed in the TR5 and the GR12T5 mixtures, this result was probably because of the high compressibility of the rubber particles which hindered the chemical treatment and resulted unstable mixture fabric and consequently, inversely affected the resilience behaviour of the mixtures containing rubber particles.

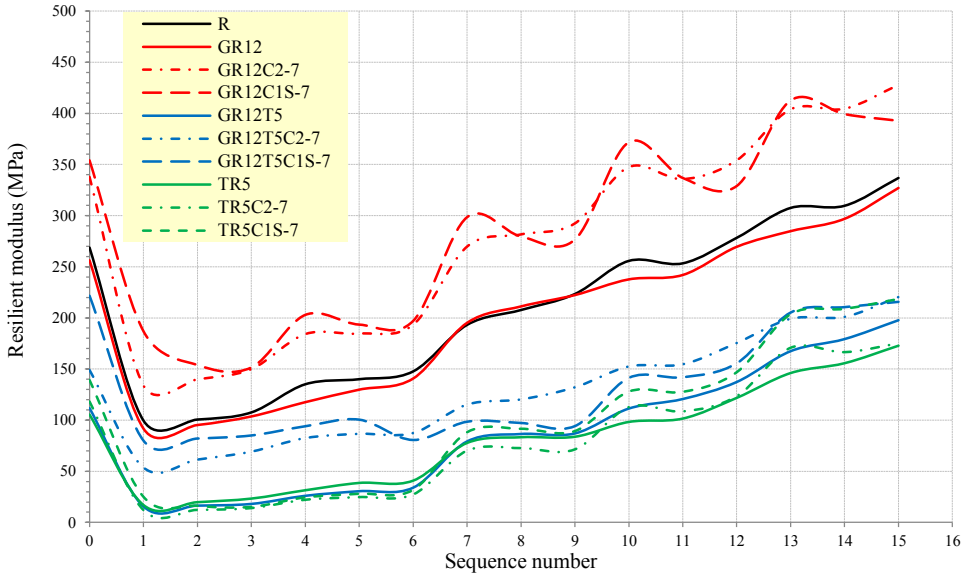

Figure 5.14 The resilient modulus of cement treated, cement-slag treated and untreated samples of the GR12, TR5 and GR12T5 mixtures

Figure 5.15 compares the P_d of the treated and the untreated samples of the GR12, TR5 and GR12T5 mixtures. The treated sample of the GR12 mixtures showed lower P_d than the treated samples of the TR5 and the GR12T5 mixtures, whereas the treated GR12T5 mixture showed the highest P_d values. It is apparent from this figure that a noticeable development in the P_d values was associated with 2% of cement, where the samples that mixed with 2% cement showed lower P_d than that with (1% cement with 1% slag). On the other hand, marked differences were found between the treated and the untreated samples of the TR5 mixture; the treated sample showed lower P_d than the untreated sample. The most exciting finding was that the cement treated sample of the TR5 mixture showed an substantial decrease in the P_d as a result of the addition of 2% cement. The positive effects of the chemical treatment on the P_d of the TR5 and the GR12T5 mixtures could be related to the role of cement and slag particles in enhancing the soil fabric, which improved the resistance of the mixtures to deform.

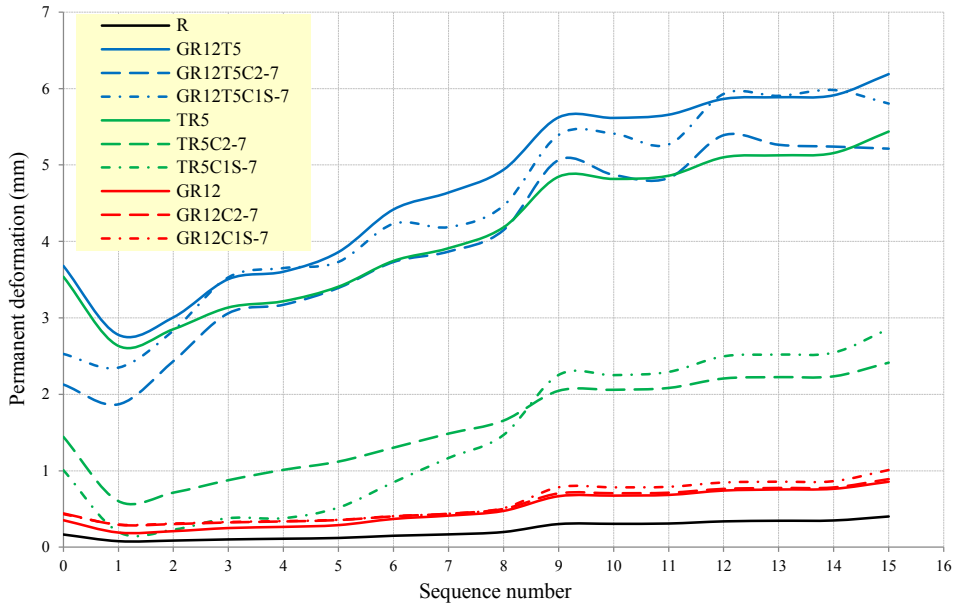

Figure 5.15 The permanent deformation of cement treated, cement-slag treated and untreated samples of the GR12, TR5 and GR12T5 mixtures

Based on the dynamic shear responses of the treated samples, a comparison of the stress-strain curves of treated and untreated GR12, TR5 and GR12T5 mixtures is presented in Figure 5.16. The treated samples of the GR12 mixture showed better dynamic shear strength than the treated samples of the TR5 and the GR12T5 mixtures, whereas the treated samples of the TR5 mixture exhibited the lowest shear strength. It is apparent from this figure that the cement treated samples presented better stress-strain behaviour than the cement-slag treated samples.The inverse effect of the rubber presence on the dynamic shear strength of the treated mixtures was due to the unability of the rubber particles to withstand the dynamic shear stress. After mixing the GRT mixture with the chemical additives, the fine materials of rock and glass were contributed with cement to form bigger particles by cementation bonds. Cement particles also covered the surfaces of course particles of rock and rubber. The nature surfaces and the high compressibility of the rubber particles hindered the stability of the chemical bonding and thus, broken up easily during the preparation and loading stages. Because of that, the course particles of rubber might endure portions of the dynamic shear force and therefore, a significant reduction was noticeable in the ability of the chemical treated mixtures which containing rubber particles to withstand the dynamic shear stresses. Furthermore, the low density and the high compressibility of the rubber particles play a significant role in generating unstable fabric, which could be the main reason for decreasing the dynamic shear

strength of the treated samples of the TR and the GRT mixtures.

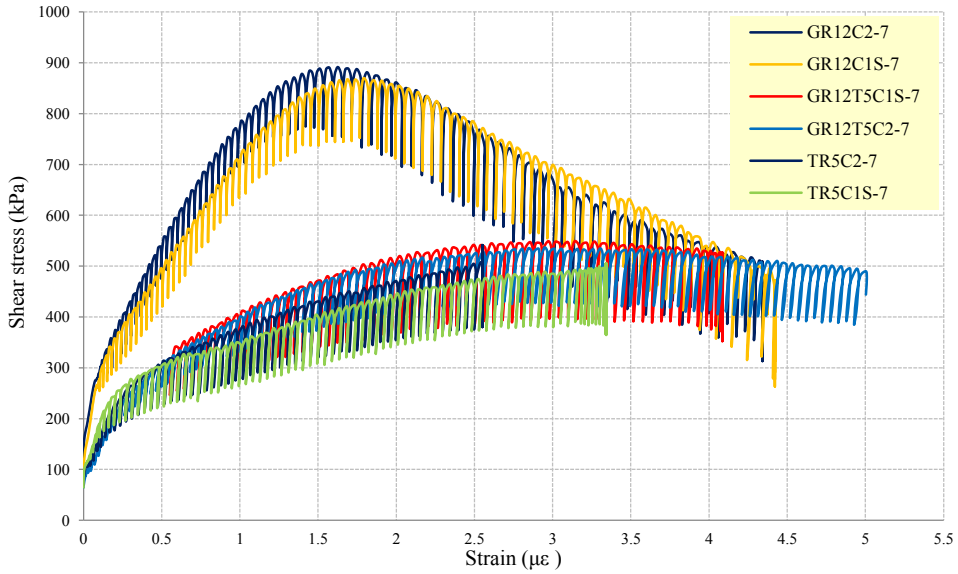

Figure 5.16 Stress-strain curves of cement treated, and cement-slag treated samples of the GR12, TR5 and GR12T5 mixtures

A series of comparisons between the M_r, P_d, and shear strength of pure rock, treated and untreated samples of the GR, TR, and GRT mixtures are presented in Figures 5.17, 5.18 and 5.19, respectively. To establish the M_r and P_d values, we used the mean of the last five M_r and P_d values of each sample, respectively. A summarised comparison between the M_r of pure rock, treated and untreated samples of the GR12, TR5 and GR12T5 mixtures is presented in Figure 5.17. The cement treated sample of GR12 mixture (GR12C2-7) showed the highest M_r value, 593.33 MPa. Whereas the untreated sample of the TR5 mixture showed the lowest M_r value, 156.67 MPa. Note that the M_r of the GR12 mixture increased from 303.34 to 593.33 MPa upon the addition of 2% of cement, and the decreased to 403.34 MPa when replaced 1% of cement by 1% of slag. In contrast, the cement treated sample of the TR5 and GR12T5 mixtures showed less M_r than that of the cement-slag treated mixtures. For example, the M_r of the TR5 mixture increased from 156.67 to 171.67 and 210.46 MPa upon the addition of 2% of cement, and the addition of 1% of cement with 1% of slag, respectively. This behaviour implied that the stabilisation of TR5 mixture was dominated more by the slag presence than the cement presence, and the mechanical stabilisation of the angular particles of slag could be affected the resilience behaviour more than the effect of the chemical treatment of cement in the mixtures containing rubber.

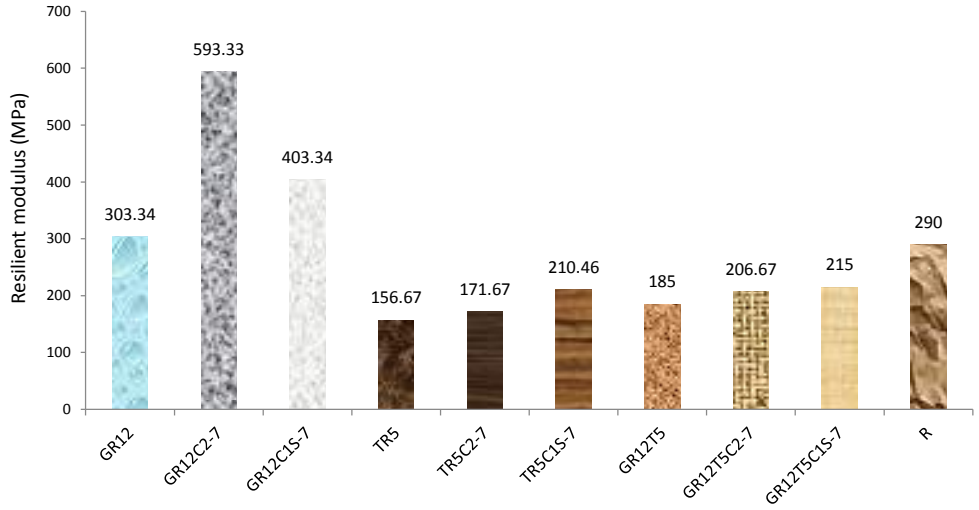

Figure 5.17 The resilient modulus of pure rock, cement treated, cement-slag treated and untreated samples of the GR12, TR5, GR12T5 mixtures

A comparison of the P_d of pure rock, treated and untreated samples of the GR12, TR5 and GR12T5 mixtures is presented in Figure 5.18. In general, the treated and the untreated samples of the GR12 mixture showed less P_d than the TR5 and GR12T5 mixtures, whereas the treated and the untreated samples of the GR12T5 mixture showed the highest rate of P_d. Moreover, Figure 5.18 shows insignificant differences between the P_d values of the GR12, GR12C2-7, and GR12C1S-7 samples, where the values of P_d of the GR12 sample increase from 0.8 to 0.83, and 0.9mm upon the addition of 2% of cement and 1% slag +1% cement , repectively. Interestingly, there was a significant reduction in the P_d of the TR5 mixture after the chemical stabilisation, where the mean P_d of the TR5 decreased from 5.18mm to 2.6mm and 2.2mm upon the addition of 2% of cement and 1% cement +1% slag, respectively. Note that the response of the TR5 mixture against the P_d seemed to be sensitive to the chemiccal treatments. In general, the cement treated sample of the all mixtures showed better resistance against the P_d than the cement-slag treated samples.

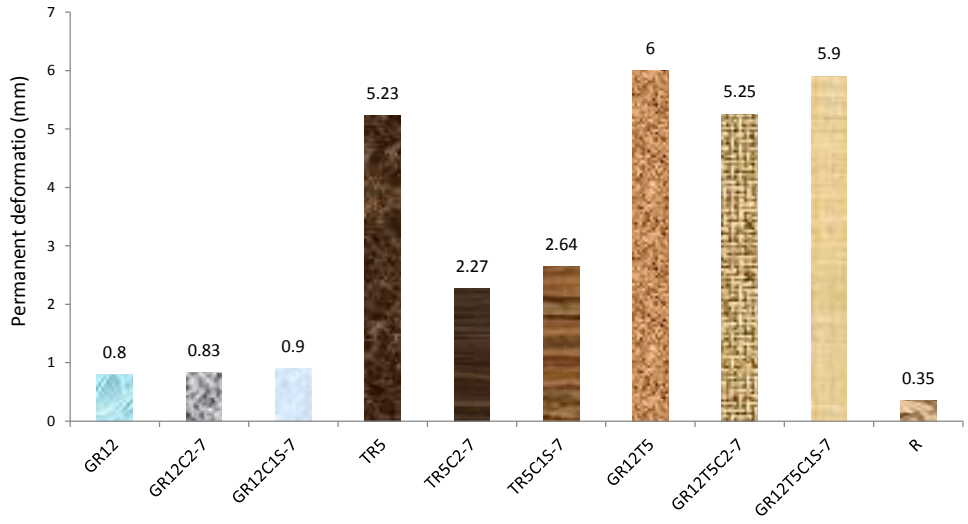

Figure 5.18 The permanent deformation of pure rock, cement treated, cement-slag treated and untreated samples of the GR12, TR5 and GR12T5 mixtures

The variations in dynamic shear strength of pure rock, treated and untreated samples of the GR12, TR5 and GR12T5 mixtures are compared in Figure 5.19. Approximately, a clear trend of decreasing dynamic shear strength of all mixture was noticable with the chemical stabilisation. It is apparent from this figure that a marked difference was found between the ultimate shear strength of the treated and the untreated samples. For example, the shear strength of untreated sample of the GR12 mixture decreased from 1000 to 900 and 830 kPa upon the addition of 2% cement and 1% cement+1% slag, respectively. In the same case, the shear strength of untreated sample of the TR5 mixture decreased from 550 to 500 and 490 kPa upon the addition of 2% cement and 1% cement+1% slag, respectively. Despite there was insignificant effect of replacing cement with slag on the ultimate strengths of the GR12T5 mixtures, the findings demonstrate that the cement-slag treated sample showed higher strength than the cement treated sample.

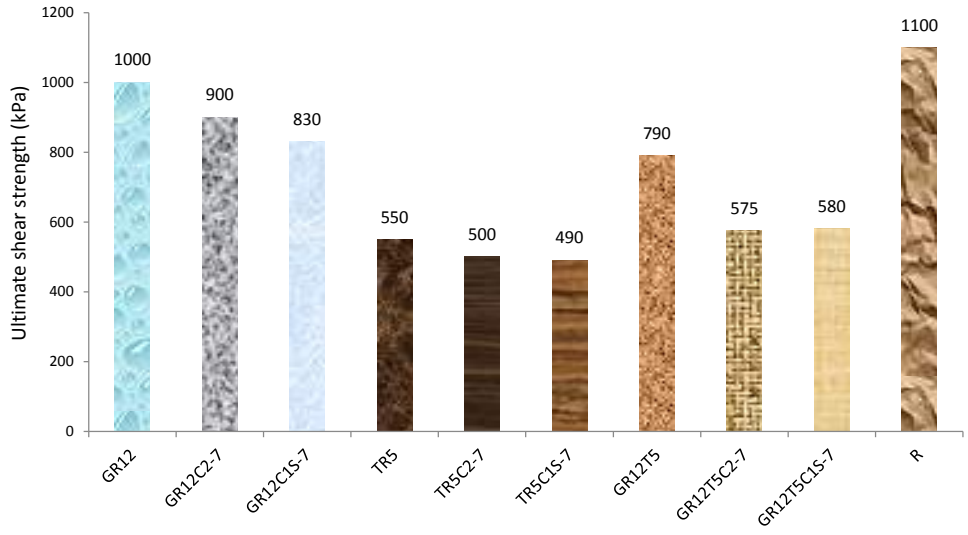

Figure 5.19 The ultimate shear strength of pure rock, cement treated, cement-slag treated and untreated samples of the GR12, TR5 and GR12T5 mixtures

5.6 Summary

A series of RLTTs was conducted to investigate the resilience, deformation and shear strength responses of glass-rock-rubber mixtures containing different cementation agents (cement and slag). The experimental program was implemented on three types of mixtures: glass-rock, rubber-rock and glass-rock-rubber (GR12, TR5 and GR12T5, respectively). These samples were treated with either 2% cement or a mixture of 1% cement and 1% slag. Comparisons between the treated and the untreated samples of all mixtures were presented. The effect of 2% cement on the M_r of the GR12 mixtures demonstrated that the cement treated sample of the GR12 mixture had the highest modulus value. In general, a significant improvement in the resilience bahaviour of the GR12, TR5, and GR12T5 mixtures were associated with cement or cement-slag treatments. Interestingly, the TR5 and the GR12T5 mixtures with 1% slag + 1% cement showed better resilience behaviour than that with 2% of cement.

In terms of the influence of chemical treatment on permanent deformation, the P_d of the GR12 mixtures was considerably lower than that of the TR5 and the GR12T5 mixtures, while the GR12T5 mixtures had the highest P_d. There was a slight difference in the P_d of the treated and the untreated samples of the GR12 mixture. Furthermore, the responses of the TR5 mixtures against the P_d decreased when 1%

cement was replaced by 1% slag. The cement treated sample of the mixture TR5 exhibited significantly lower P_d than the cement-slag treated sample. Mean while, there was an unremarked effect of cement treatment on the P_d of the GR12T5 mixture. In addition, replacing 1% cement with 1% slag increased the P_d of the cement treated sample (GR12T5C2-7). Regarding the stress-strain behaviour of the treated mixtures, the cement treated samples presented better stress-strain behaviour than the cement-slag treated samples. In generall, insignificant effect of replacing 1% cement with 1% slag on the strength characterstics of the TR and the GR12T5 mixtures. However, the chemical treatment with 1% cement and 1% of non-plastic slag showed more strain-softening behaviour.

Chapter 6: Dynamic Behaviour of Layered Samples of Rock, Glass, Sand and Bentonite:Layered Technique

6.1 Introduction

Regarding the use of waste materials in geotechnical applications, previous investigations have only focused on the use of homogenous waste-soil mixtures. Therefore, this chapter presents the results of experiments conducted to evaluate the dynamic behaviour of layered structures. A series of repeated loading triaxial tests (RLTTs) was conducted on layered samples of rock layers with different layers of waste glass, sand and bentonite, used as alternatives to crushed rock. A wide range critical factors influencing the dynamic behaviour of layered samples was considered in the present study. Based on the literature review (Chapter 2), many geotechnical characteristics of glass are similar to those of granular materials and therefore, the effects of glass content, the position, the number, and the moisture contents of the glass and the rock layers on dynamic behaviour of the glass-rock (GR) sample were also investigated. The results of the RLTTs included data on resilient modulus (M_r), permanent deformation (P_d) and dynamic shear strengthare presented in the following sections. A comparison of dynamic responses of the homogenous and layered samples was also performed in this chapter. The second section of this chapter described the dynamic behaviour of layered rock-sand (R-S) samples . As shown in Table 3.16, the effects of the sand layer location, the thickness, the cycles number and the confining pressure on M_r and P_d of the R-S samples were investigated. The third section of this chapter focused on rock-bentonite-sand samples to examine the effect of the waste bound material (bentonite) on the dynamic behaviour of rock sample. Thus, a series of RLTTs was conducted on a group of layered samples of sand-rock-bentonite materials. As detailed in Table 3.17, the effects of the bentonite presence, the location, and the number of bentonite layers on M_r and P_d of the rock-bentonite-sand sample were investigated. The effect of replacing a bentonite layer with a sand layer on the dynamic behaviour of the layered sample of rock-bentonite-sand materials was also studied in this chapter.

6.2 Resilient modulus of layered samples of rock and glass

Following the partial improvement in dynamic behaviours of the homogenous samples of glass-rock materials described in Chapter 4, further RLTTs were carried out on layered samples of glass and rock materials to assess the suitability of using layered technique with waste glass and rock in pavement applications. The (R+GR) sample consisted of a combination of rock layers (R) with layers of mixed glass-rock (GR), as detailed in Table 3.11. The results of the (R+GR) layered samples are compared with those of the GR samples. The results of the preliminary tests of the materials and the results of the homogenous samples of GR will not be discussed at any great length in this section because they were presented in Chapters 3 and 4.

6.2.1 Effect of the glass content on resilient modulus of layered samples

A series of RLTTs was conducted on R+GR samples to assess the resilience responses of modified samples. As detailed in Table 3.11, A range of glass contents was used in this research, 12%, 24% and 45%, and labelled R+GR12, R+GR24 and R+GR45, respectively. The samples were prepared with different optimum moisture contents (OMC) in each layer to evaluate their effects on M_r of the layered samples. The M_r of the pure rock, R+GR12, R+GR24 and R+GR45 samples are presented in Figure 6.1. According to the last sequence outputs, the M_r value increased from 340MPa to 390MPa because of increasing the glass content from 0% to 12%. The possible reason for this positive effect of glass was the stable fabric when combining the course sizes of crushed rock with the small sizes (smaller than 4.75mm) of crushed glass. Thus, there is a possible benefit of combining a layering technique with glass content in improving the resilience behaviour of the rock sample. Profound differences in resilience behaviour between the R+GR24 and R+GR12 specimens was shown also in Figure 6.1, where a steady reduction in the M_r of the layered sample was associated with increasing the glass content from 12% to 24%. At the last sequence, the Mr value of the R+GR24 sample became identical to that of pure rock sample. It is apparent from this figure that the value of the Mr decreased from 390MPa to 340MPa with increasing the glass content from 12% to 24%, which was similar to that of pure rock sample. If consider that the actual glass content in the R+GR24 sample is equal to that in the GR12 sample (12%), the above finding may

support and prove the findings reported in the section 4.3.1, that there was insignificant differences between the resilience behaviour of the R and the GR12 samples. The course particles of rock with this ratio of glass (12%) endured most of the loading forces and thus, no significant difference between the M_r of the GR mixture and that of the pure rock. Figure 6.1 also reports a significant increase in the M_r of the R+GR24 sample when increasing the glass content from 24% to 45%. The edges of the crushed glass particles played a significant role in the improvement of the rock fabric when mixed with 45% glass (R+GR45 sample). This result is consistent with the findings in section 4.3.1, that the M_r of rock sample increased as a result of the glass content increase. Despite that the R+GR45 sample showed a lower M_r than the R+GR12 sample, the high glass content in the R+GR45 sample performed a considerable improvement in the M_r compared to those of the R+GR24 and the rock samples.

Further investigation was needed to determine exactly how the thickness of the GR layer affects the M_r of layered rock samples. Different thicknesses of the R and GR layers were employed to prepare the layered samples, as shown in Table 3.11. Figure 6.2 (a and b) shows different fully-assembled layered samples of R with GR layers. The sample in Figure 6.2 (a) was combined from four layers of rock at the bottom and four GR layers above, these layers forming a sample labelled 4R+4GR. Note that the layered sample labelled 2R+2GR was constructed of two construction steps of compacting two R layers at the bottom and two GR layers above, as shown in Figure 6.2 (b). The effect of the GR layer thickness on the M_r of the R+GR12, R+GR24 and R+GR45 samples is also presented in Figure 6.1. The 2R+2GR12 and 2R+2GR45 samples exhibited lower M_r than the R+GR12 and the R+GR45 samples, respectively. On the other hand, a positive correlation was found between the M_r and the layer thickness during the first eleven sequences. Beyond that, the 2R+2GR24 sample showed lower M_r than the R+GR24 sample. In general, the M_r of the layered samples is considerably dependent on the thickness of the GR layer. According to a basic comparison between the R+GR and 2R+2GR samples with different glass contents (12%, 24%, 45%), the single layered samples (R+GR) exhibited higher M_r than the doubled layered samples (2R+2GR). The role of increasing the interface number between two different layers in enhancing the stable fabric around the interface layer may be responsible for increasing the M_r of the single layered samples. Around the interface layer (between the R and GR layers), fine and medium

particles of crushed rock and glass tried to fill the voids between the glass-rock mixtures, which caused in enhancing the soil fabric around the interface areas. This result was consistent with the findings of Zhang et al.(2015), who concluded that the motion of fine and course particles near the interface is more active than other parts of the layered sample, as the fine materials moved to fill the voids of the course tailing.

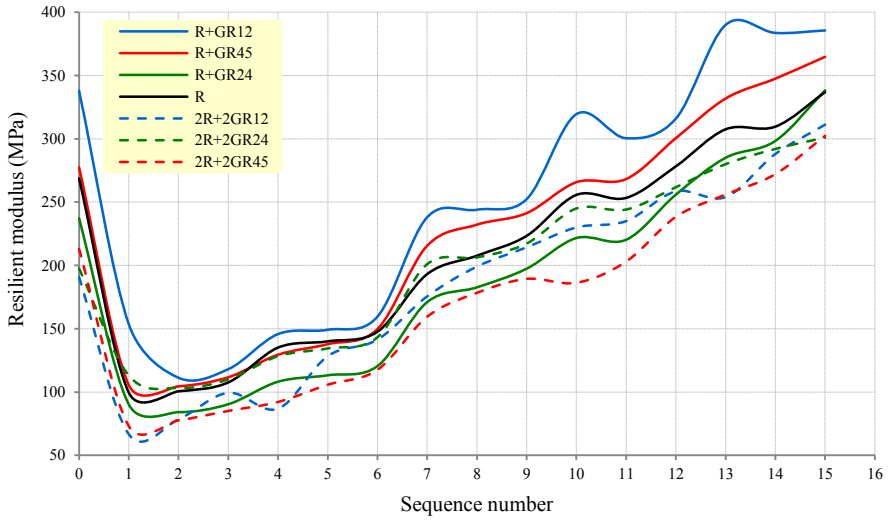

Figure 6.1 Effects of the glass content and the layer thickness on the resilient modulus of pure rock sample

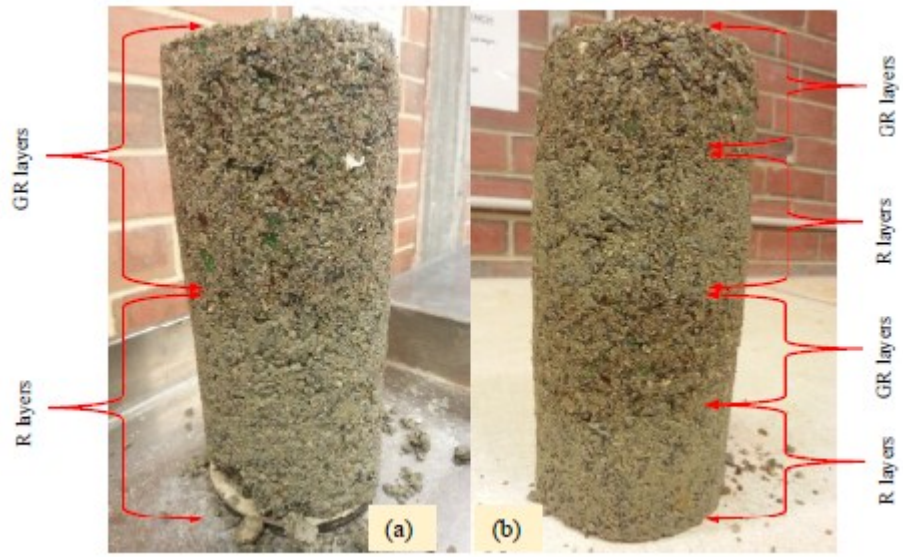

Figure 6.2 Fully-assembled of R+GR samples a) the 4R+4GR layered sample, and b) the 2R+2GR layered sample

Based on the effect of the GR24 and the GR45 thickness, the correlation between the M_r of the R+GR24 and R+GR45 samples and the layers thickness is presented in Figures 6.3 and 6.4, respectively. It is apparent from Figure 6.3 that insignificant

variations in the M_r of the R+GR24 sample was noticeable with increasing the GR24 layer thickness. However, the R+GR24 and 2R+2GR24 samples showed higher M_r than the 4R+4GR24 sample beyond the eleventh sequence. In Figure 6.4, a considerable reduction in the M_r of the R+GR45 sample was evident with increasing the layers thickness of R and GR45 to double (2R+2GR45), whereas the 2R+2GR45 sample showed better resilience performance than the 4R+4GR45 beyond the twelfth sequence.This behaviour could be related to the role of the stress level in improving the soil fabric around the interface layers, that the interlocking between the fine and the course particles did not improve at low levels of the axial and confining pressures. At high pressures levels (the last sequences), further fine materials moved inside the voids between the course particles and enhanced the interlocking between the particles which led to improve the stability of the mixture fabric around the interface layers. What is interesting in this data is that the R+GR45 sample had a significantly higher M_r than the rock specimen. In general, the resilience behaviour of layered samples at low glass content was quite sensitive to the thickness variation of the GR layer and therefore, even a small increase in the layers thickness can lead to a rather wide variation in the M_r value, as shown in Figure 6.4.

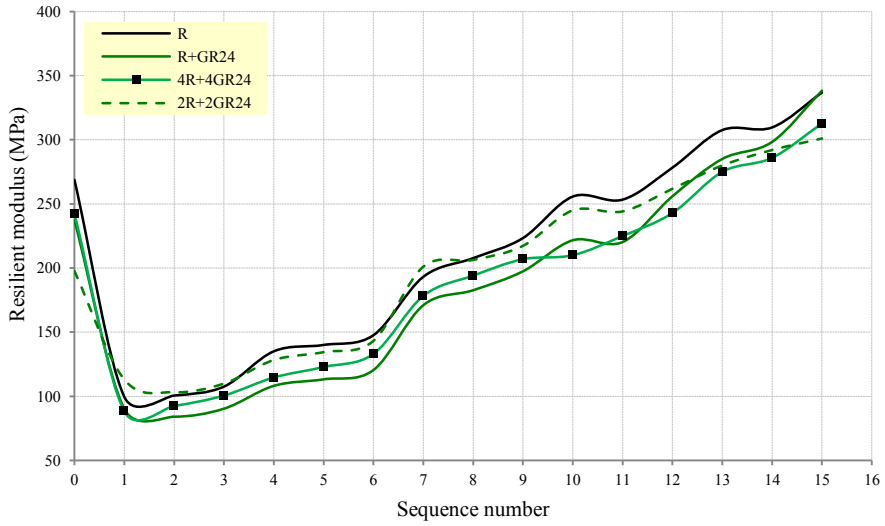

Figure 6.3 Effect of the GR24 layer thickness on the resilient modulus of the pure rock sample

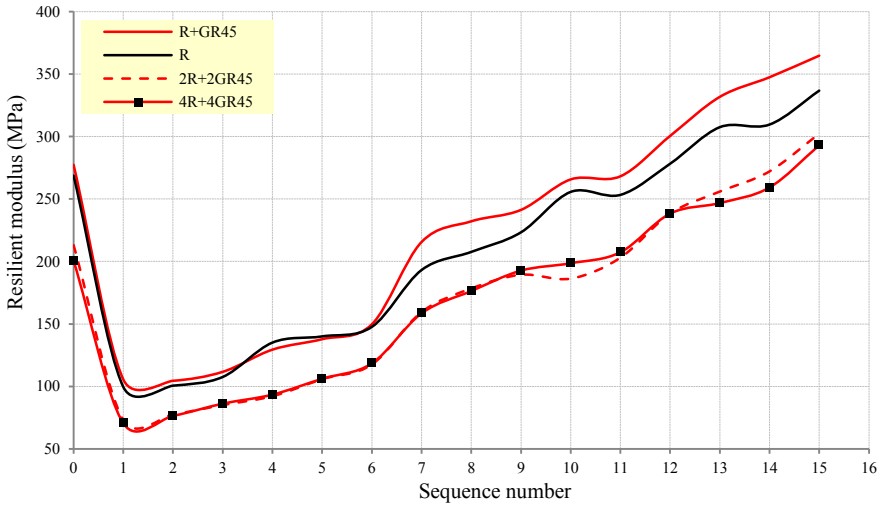

Figure 6.4 Effect of the GR45 layer thickness on the resilient modulus of the pure rock sample

6.2.3 Effect of the GR layer location on resilient modulus of layered samples

The effect of the GR layer location on the M_r of the 4R+4GR24 and 4R+4GR45 samples was investigated in this section. In both samples, four rock layers were located in the bottom half, while the GR24 and GR45 layers were located in the upper half, as shown in Table 3.11. In Figure 6.5, a reduction in the M_r of the 4GR24+4R sample was noticeable due to the rock layers located in the upper half of the sample. Hence, the role of the GR24 layer location can be considered as a significant role affecting the resilience behaviour of the 4R+4GR24 sample. It is apparent from this figure that a slight difference between the resilience behaviour of the 4R+4GR45 and the 4GR45+4R samples, where the 4R+4GR45 sample showed better resilience behaviour than that of the 4GR45+4R sample. The reason for this effect can be related to the fluctuations of axial stress transmissioned in the sample, where the stress transmission is wavily towards the lower layers of a sample (Zhang et al., 2015) and that could positively affected the interlocking between the particles of the upper layers of the sample which resulting in an early stable fabric and consequently, an improvement in resilience behaviour of the samples where the GR layers close to the top.

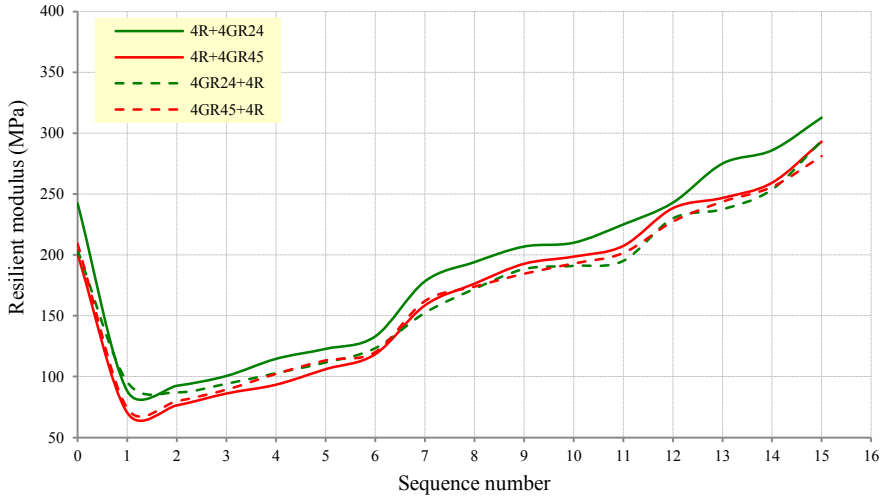

Figure 6.5 Effect of the GR24 and GR45 layer locations on the resilience behaviour of the 4R+4GR24 and the 4GR+4R45 samples

6.2.4 Effect of moisture content on resilient modulus of layered samples

This section investigates whether the M_r of the GR24 mixture was affected by its moisture content. As detailed in Table 3.11,the R+GR24 samples were prepared at different moisture contents (70% and 100% of OMC) to assess the effect of moisture content on the resilience behaviour of the layered samples. It is apparent from Figure 6.6 that a positive correlation was found between the M_r of R+GR24 sample and the moisture content, which contrasted with some existing studies (Disfani et al., 2012 and Azam & Cameron, 2012). In the absence of a micro-mechanism study of the R+GR24 samples, the positive effect of the moisture might be contributed to the lubricating effect of water around the interface layers between the R and the GR layers. Note that the permeability of the GR layer is higher than that of the R layer and thus, water gathered around the interface layers for a short time during the initial loading stage. This phenomenon could positively affect the particles movements of fine materials around the interface layers and thus, high M_r of the layered sample at 100% OMC.

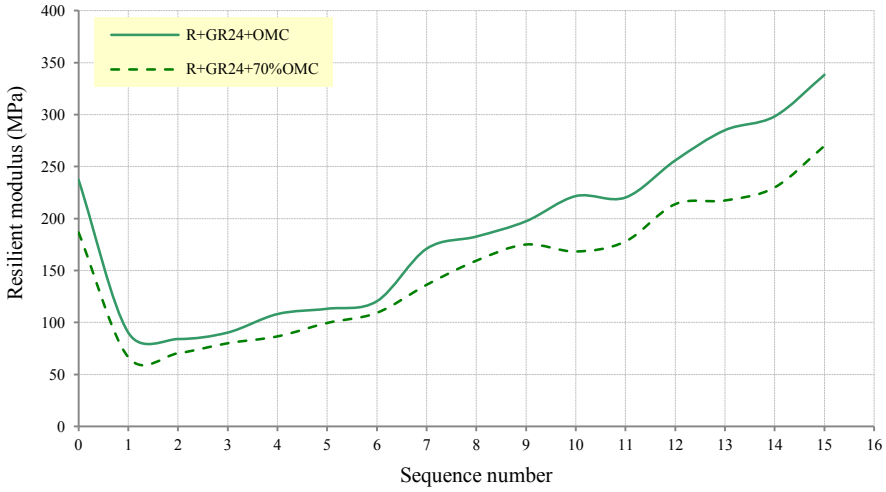

Figure 6.6 Effect of moisture content on the resilient modulus of R+GR24 sample

6.3 Permanent deformation of layered samples of rock and glass

Further investigation was performed to assess the effects of varying the number, the position and the moisture content of the GR layer on P_d of R+GR layered samples. Crushed rock with a range of glass contents (12%, 24% and 45%) was employed to prepare layered samples to characterise their deformation responses under repeated loadings.

6.3.1 Effect of glass content on permanent deformation

The effects of having different glass contents on the P_d of layered R+GR samples are presented in Figure 6.7. A comparison between the P_d of the R and R+GR12 samples illustrated a strong evidence that the P_d of the pure rock increased because of the glass presence, where the R+GR12 sample showed much higher P_d than the pure rock sample. At this ratio of glass, the smoothness of their surfaces couldinversely influenced the dynamic behaviour of the R+GR12 sample (Cheung & Dawson, 2002). It is apparent from Figure 6.7 that an increase in the P_d of the R+GR group was associated with increasing the glass content from 12% to 24%. This finding wss consistent with the findings of Ali et al. (2011) who concluded that the presence of glass caused an increas in the P_d of GR mixtures. Whereas a considarable reduction in the P_d of the layered samples when the glass content increaed from 24% to 45%. With an increase in the glass content to 45%, the fine and medium particles of glass

and rock filling the voids between the course rock particles causing a high interlocking between the particles which improved the mixture fabric and changed it from unstable fabric to stable fabric at a low void ratio and consequently, reduced the P_d of the R+GR45 sample. If considered that the actual glass content in the R+GR24 and the R+GR45 samples are equal to 12% and 22.5%, this behaviour could be consistent with the deformation behaviour of the GR24 and the GR45 samples in section 4.3.2, where the P_d of the GR24 sample showed less P_d than the GR12 sample. It is also apparent from Figure 6.7 that a sharp reduction in the P_d of the double-layered samples (2R+2GR) was associated with the glass content increase. For example, the double-layered samples with 12% glass content (2R+2GR12) exhibited higher P_d than the 2R+2GR45 sample. Also, the 2R+2GR12 sample exhibited higher P_d than the the single-layered sample at same glass content (R+GR12), whereas an insignificant effect on the P_d of the R+GR24 and R+GR45 samples by increasing the GR24 and the GR45 layers thickness, respectivelly.

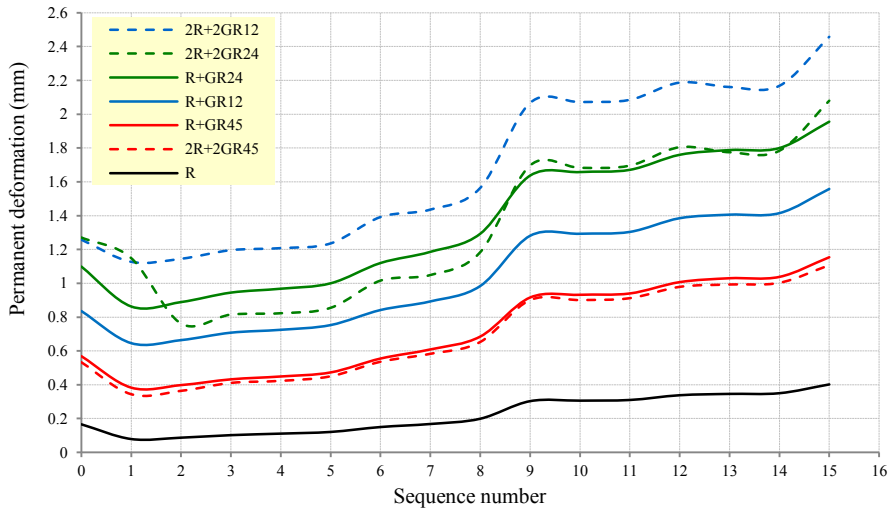

Figure 6.7 Effects of glass content and the layer thickness on the permanent deformation of pure rock sample

Further investigation on the R+GR24 and R+GR45 samples is necessary to check whether the GR layer thickness affects the P_d of the layered samples. The variation in P_d of single, double, and four-layered samples at 24% and 45% glass content is presented in Figures 6.8 and 6.9, respectively. It is apparent from Figures 6.8 that when four layers of GR24 mixture were compacted sequentially, the P_d of the 4R+4GR24 sample decreased about 42.85% compared to that of the 2R+2GR24 specimen. Figure 6.8 also shows insignificant differences in the P_d between the R+GR24 sample and the 2R+2GR24 sample. Similar to this results, the 4R+4GR45

sample presented higher resistance to P_d than the R+GR45 and 2R+2GR45 during the early stages of loading, as shown in Figure 6.9. After that, the resistance of the 4R+4GR45 sample to P_d tended to decrease continuously with increasing the load sequence. Despite this reduction in resistance, the 4R+4GR45 showed less P_d than those of the R+GR45 and 2R+2GR45 samples. The positive role of the thickness increase might be related to the locations of the GR and the R layers themselves. According to the result in the previous section, stresses are transmitted as waves towards the lower layers of the soil sample and thus, an improvement in the interlocking between the particles of the upper layers (GR24 or GR45) was occurred and consequently, low P_d of the samples that the GR layers close to the top decreased.

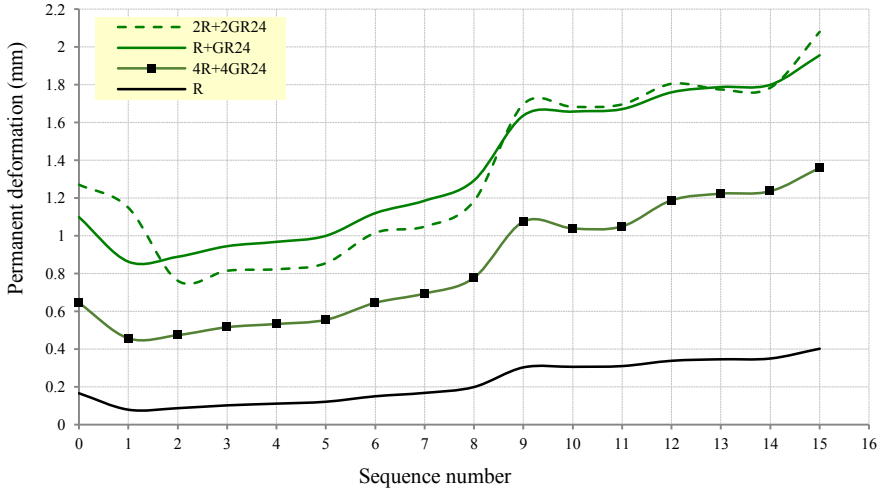

Figure 6.8 Effect of the GR24 layer thickness on the permanent deformation of pure rock specimen

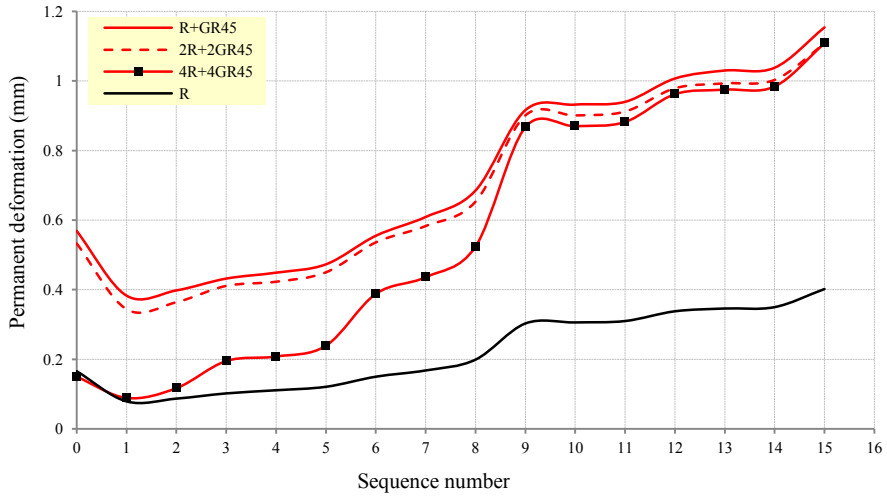

Figure 6.9 Effect of the GR45 layer thickness on the permanent deformation of pure rock specimen

6.3.2 Effect of the GR layer location on permanent deformation of layered samples

Further investigation on layered samples which consisted of four sequential layers of GR layers with others of R was conducted in this section to determine whether layer position influences the P_d of the layered samples. It is apparent from Figure 6.10 that the 4R+4GR sample showed less P_d than the 4GR+4R sample. The advantage of placing the R layers at the bottom and the GR layers at top of the sample is noticeable in the figure. The P_d of the 4R+4GR45 sample was also influenced by the high glass content, which caused to increase the resistance of the sample to deform. The improvement in the P_d of the 4R+4GR45 and 4R+4GR24 samples was related to the role of the stresses in improving the upper layers fabric of the GR conjection with the glass content increase, as discussed in the previous section.

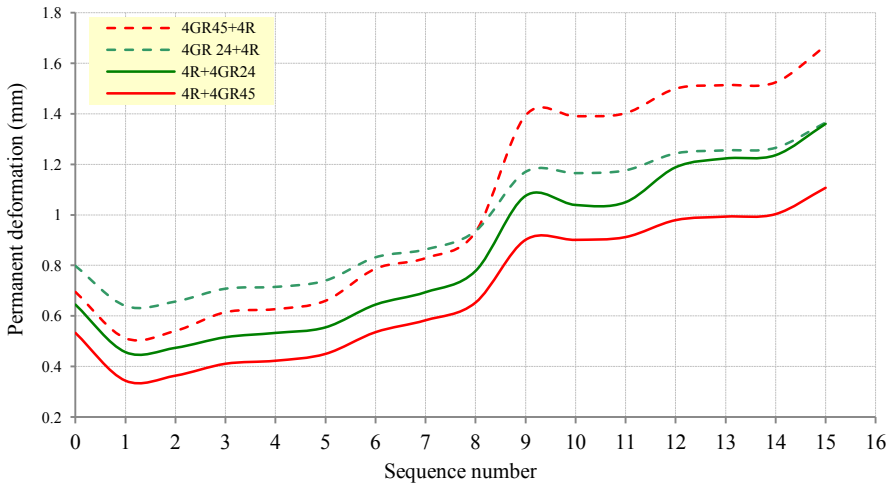

Figure 6.10 Effect of the GR24 and GR45 location on permanent deformation of the 4R+4GR24 and 4R+4GR45 samples

6.3.4 Effect of moisture content on the permanent deformation of R+GR samples

Considering the dry-back process in the field, GR24 and R layers was prepared at 100% and 70% of the OMC to assess the effect of moisture content on the P_d of R+GR24 samples. Figure 6.11 reveals that the R+GR24+70% OMC showed less P_d than that at 100% OMC. The slight improvement in P_d was attributed to the mixture fabric stability, as the voids are filled with fine materials instead of the drained water which led to the development of density and consequently, low P_d of the sample.

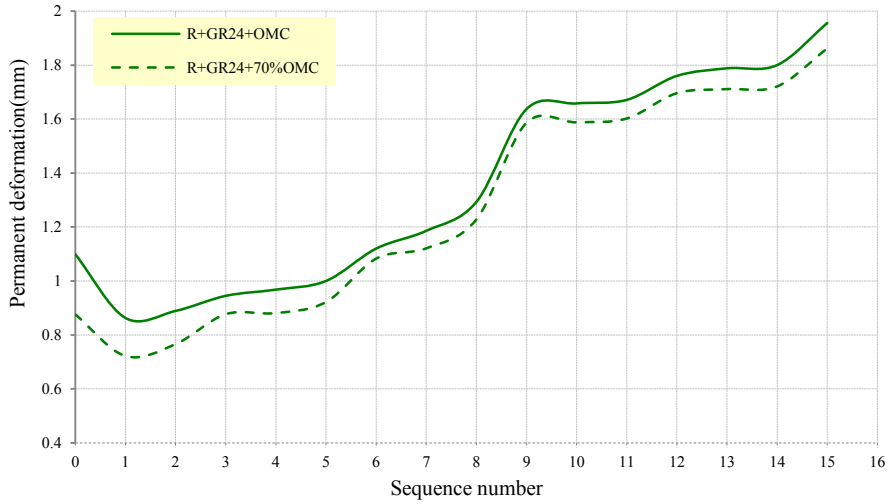

Figure 6.11 Effect of moisture content on the permanent deformation of R+GR24 specimen

The glass-P_d curves of the layered specimens are shown in Figure 6.12. The different structures of layered samples showed different responses to P_d. A steady increase in the P_d of the R+GR group was associated with the glass content increase, where the peak of the R+GR group curve was occurred at a 23% glass content. After that ratio, the R+GR specimen tended to improve its resistance to P_d. Based on the behaviour of the 2R+2GR group, a sharp increase in the P_d was associated with the glass content increase. The peak P_d of the 2R+2GR curve was occurred at a 15% glass content; behind that point, the P_d of the group decreased with the glass content increase. Similar to the R+GR and 2R+2GR group, the 4R+4GR group showed the same glass-P_d correlation but it showed less P_d than the R+GR and 2R+2GR group. Also, there is a clear reduction in the peak glass ratio from 23% in the R+GR group to 17% in the 4R+4GR group, and this is a good indication of the resistance improvement of the layered samples against P_d. Note that the homogenous sample (GR) showed the lowest P_d compared to the layered samples (R+GR).

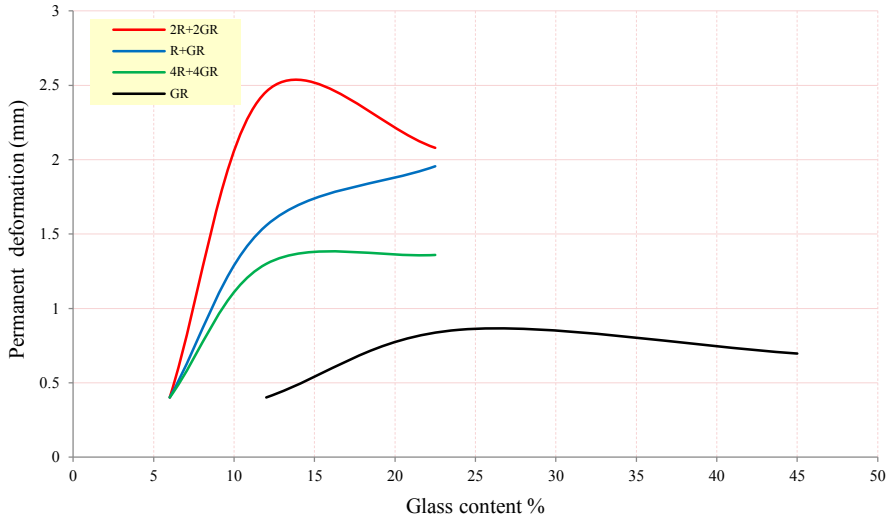

Figure 6.12 Effect of glass content on permanent deformation of the GR, R+GR, 2R+2GR and 4R+4GR groups

6.4 Shear strength of layered samples of rock and glass

A series of dynamic shear tests was conducted to assess the strength features of layered samples under dynamic shear impacts. Multilayered samples of rock and glass-rock mixtures (R+GR) with different glass contents were prepared, and a range of factors such as the layer thickness and moisture content considered during the investigation of stress-strain behaviour of the layered samples. In addition, a comparison between the layered and homogenous samples is made in this section.

6.4.1 Effect of glass content on shear strength of R+GR samples

Figure 6.13 exhibits a series of stress-strain curves of R, R+GR12, R+GR24 and R+GR45 samples resulting from the dynamic shear tests. In general, the strain initially increased with shear stress until reaching a peak shear point. Beyond that point, shear stress decreased with increasing shear strain. At low glass content (12%), the layered sample (R+GR12) showed the highest shear strength. By comparing this result with the result in Figure 4.17 which reported that the GR12 sample showed lower shear strength than that of the R and therefore, the low glass content with the layered technique may play a significant role in improving the shear strength of pure rock. A possible explanation for the positive effect of layered technique could be the high interlocking between the glass and rock particles around the interface layers. In fact that the ability of fine materials for rotating under the influence of shear forces

reduces their susceptibility to breaking or crushing compared to the course particles (Zhang et al., 2015). Therefore, the level of interlocking and the soil fabric around the interface layers could be improved when some fine particles move to settle into the voids between the course grains under the effect of shear forces and consequently, increasing the resistance of R+GR12 sample against the dynamic shear forces. Figure 6.13 also showed that the shear strength of the layered sample reduced when the glass content increased from 12% to 24%, while insignificant effects of shear strength was noticeable when the glass content increased from 24% to 45%. It is important to know that the course particles of waste glass are easily crushed under the influence of dynamic loads (Disfani et al.,2009), and this could be the reason of increase the fine particles in the layered samples, which caused a reduction in shear strength of the sample at high glass content. Further, course particles showed more resistance against shear strength than fine particles (Wei et al., 2009), and that could be another reason of reducing the dynamic shear strength of layered sample at high glass content, where the particles size may change from course-medium particles with a high shear strength to fine particles with a low shear strength. In general, these findings were consistent with those of Arulrajah et al. (2014) in that the shear strength of the glass-aggregate mixtures decreased with an increase in the glass content. It would be interesting to note that the R+GR12 specimen showed higher shear resistance than the pure rock sample itself.

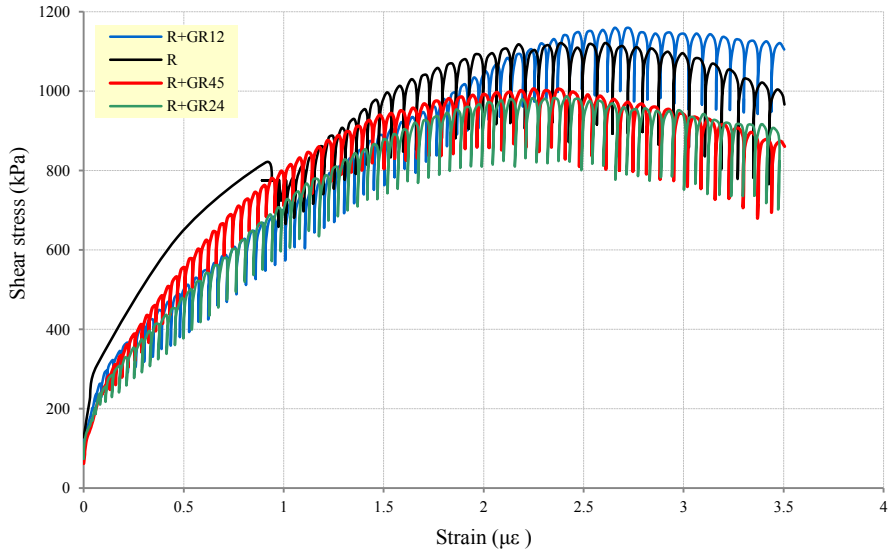

Figure 6.13 Stress-strain curves of the R, R+GR12, R+GR24, and R+GR45 samples

6.4.2 Effect of the GR layer thickness on shear strength of layered samples

Further investigations were carried out to assess the effects of thickness and moisture content of the GR layer on the strength behaviour of layered samples. Figure 6.14 shows that there was a steady reduction in the shear strength of the R+GR group with increasing the thickness and glass content. Also, the response of the 2R+2GR group to dynamic shear seems to follow the behaviour of the R+GR group in Figure 6.13. In addition, the 2R+2GR12 sample exhibited higher strength than the other layered samples, which is the same performance as the R+GR12 sample in Figure 6.14. The effect of layer thickness on shear strength need to be investigated further and thus, the RLTT was conducted on single layered (R+GR24), double layered (2R+2GR24), and four-layered sample (4R+4GR24), as detailed in Table 3.11. Increasing the GR24 layer thickness caused in decrease the shear strength, as shown in Figure 6.15. In generally, a negative correlation was found between the GR24 layer thickness and the shear strength. The negative role of increasing the GR layer thickness might be related to the number of the interface layers between the GR and the R layers. Depending on the findings in section 6.4.1, there was a positive role of the interface layers in improving the interlocking between particles which produced stable fabric around the interface layers. Therefore, the number of interface layer between the R and GR24 layers had a positive effect on the shear behaviour of R+GR24 sample. Hence, it can be concluded that when the thickness of GR24 layers is low, the specimen tends better perform against dynamic shear stress.

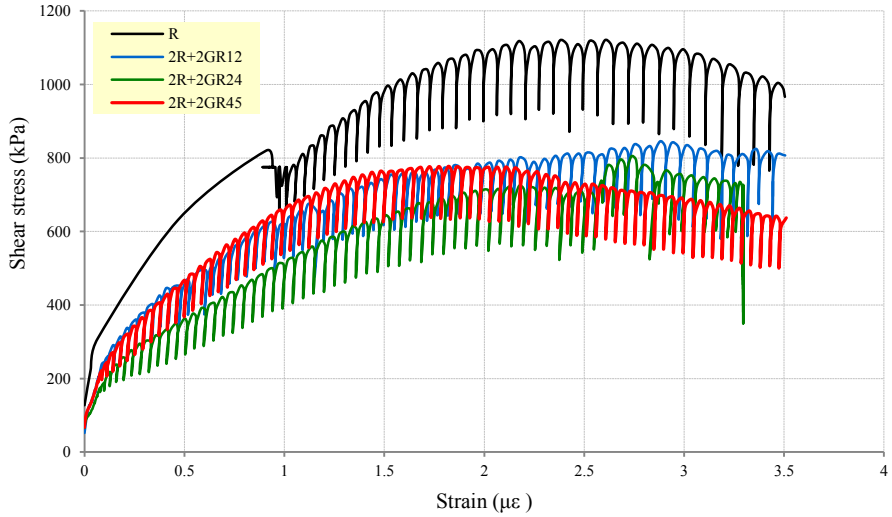

Figure 6.14 Stress-strain curves for the R, 2R+2GR12, 2R+2GR24 and 2R+2GR45 samples

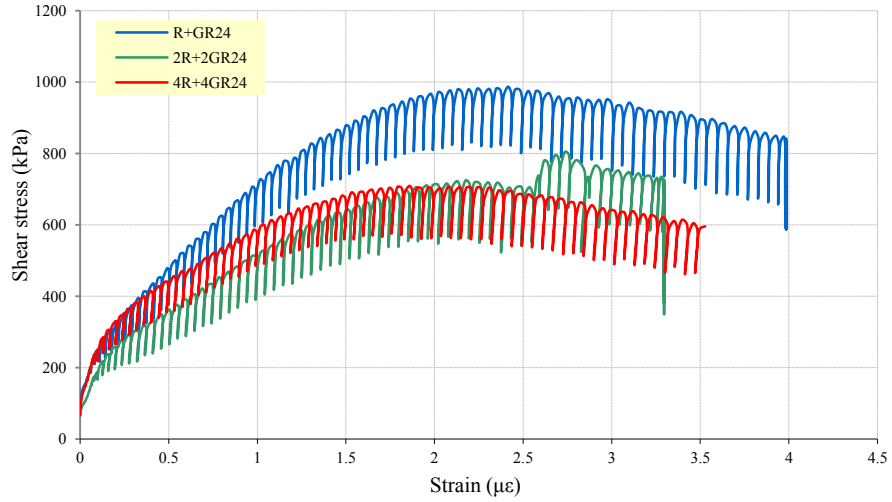

Figure 6.15 Effect of the GR24 layer thickness on shear strength of R+GR24 sample

6.4.3 Effect of moisture content on shear strength of layered samples

Rock and GR24 layers were prepared at 100% and 70% of the optimum moisture content to evaluate its effect on the shear strength of the R+GR24 sample. Contrary to expectations, shear strength increased with the moisture content increase, as shown in Figure 6.16. This unexpected finding was consistent with the another unexpected finding concluded in section 6.2.4, wherein the reduction in moisture content reduced the M_r of the layered samples. As explained in section 6.2.4, this unexpected behaviour might be attributed to the effect the water lubricating around the interface layers at100% OMC which caused in enhancing the soil fabric around

the interface areas, which positively affected on shear behaviour of the R+GR24 sample.

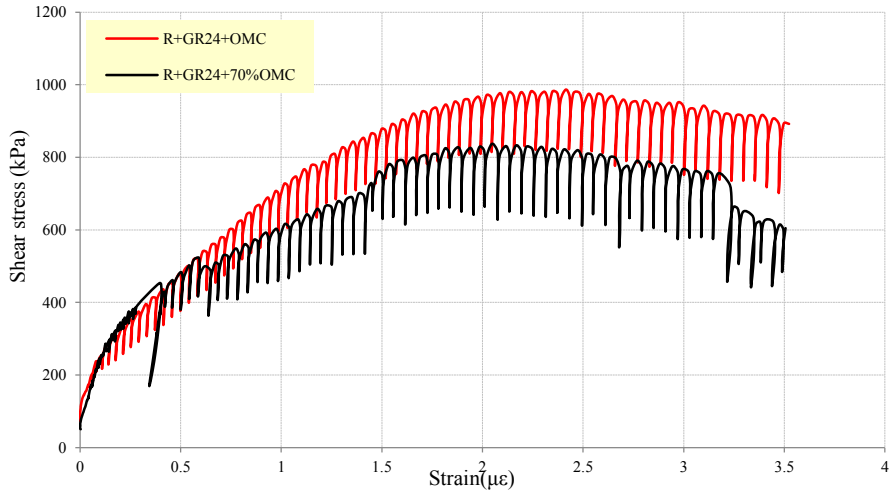

Figure 6.16 Effect of moisture content on shear strength of the R+GR24 sample

6.4.4 Comparison of layered and homogenous structures

Wide variations in dynamic behaviour were noticeable when comparing the two techniques: layered and homogenous. The first comparison was of the M_r of GR mixtures which used in homogenous and layered structures, as illustrated in Figure 6.17. At high glass proportions (24% and 45%); it is evident that the homogenous samples showed higher M_r than the layered samples. It is important to note that the layered sample with 12% glass (R+GR12) showed higher M_r than the rock and GR12 sample. In general, the GR24, GR45, R+GR12 and R+GR45 samples showed better resilience behaviour than the rock sample due to the glass contents and the layered technique. The P_d of homogenous and layered samples is compared in Figure 6.18. The homogeneous samples with 12%, 24% and 45% glass exhibited lower P_d than the layered samples. In general, the homogenous samples group showed significantly less P_d than the layered samples group. As explained before, the effect of the layered technique on the resilience and deformation behaviour of pure rock sample could be related to many roles such as the glass presence, the interface layers, and the improvement of the GR mixture fabric when the fine materials occupied the voids between the course particles.

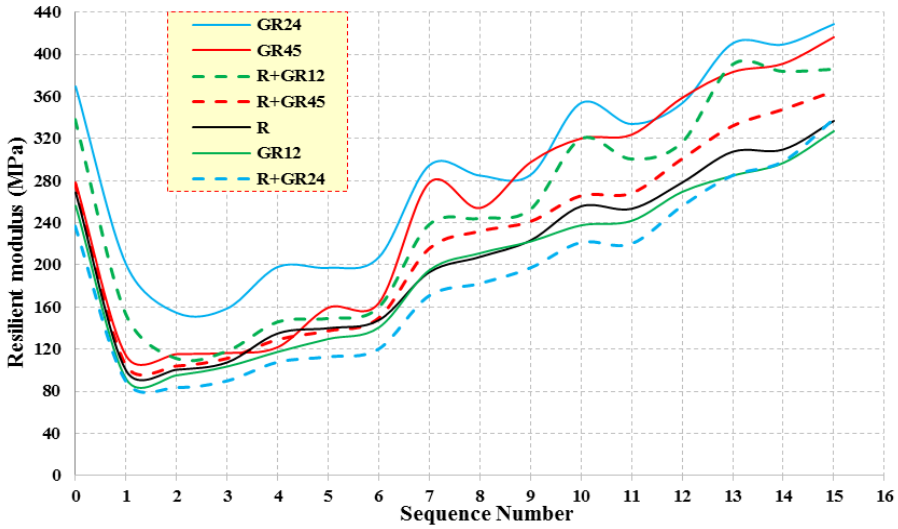

Figure 6.17 Resilient modulus of the homogenous and the layered GR samples containing 12%, 24% and 45% glass contents

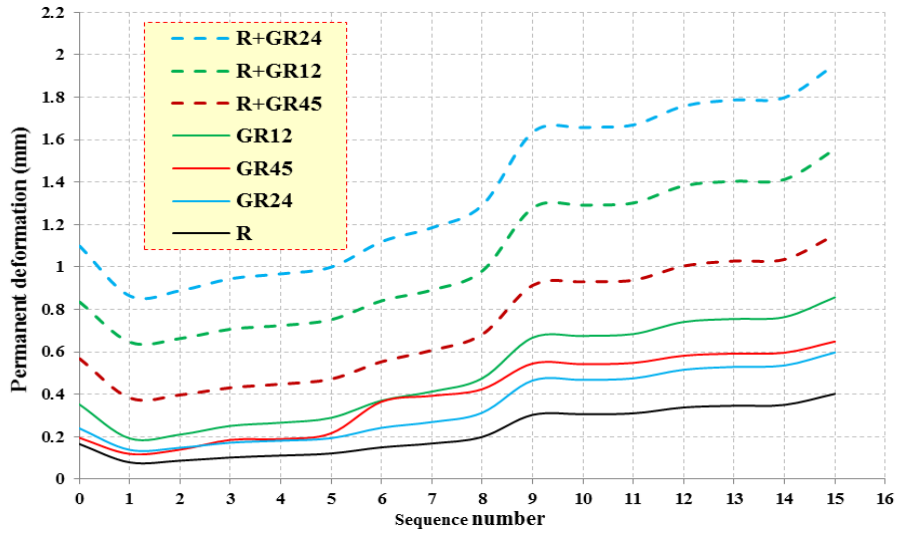

Figure 6.18 Permanent deformation of the homogenous and the layered GR samples containing 12%, 24% and 45% glass contents

Figures 6.19 (a, b and c) compares the shear stress-strain behaviour of homogenous and layered samples at different glass content. In general, all layered samples showed higher strength than the homogenous samples. In addition, the peak shear of the layered and the homogenous samples decreased by the glass content increase. Note that the R+GR curves showed more softening than that of the GR samples which is a good characteristic for base and subbase materials, as the stress-strain curves of brittle materials usually drop sharply after the peak shear. In addition, the GR12,GR24 andGR45 samples showed lower peak shear as compared to the R+GR12, R+GR24 and R+GR45, respectivily. This reduction in the peak shear

values of the GR samples was associated with the strain decrease. These results proved that the interface layers between the GR and R layers played an important role in the development of stress-strain behaviours of the layered samples.

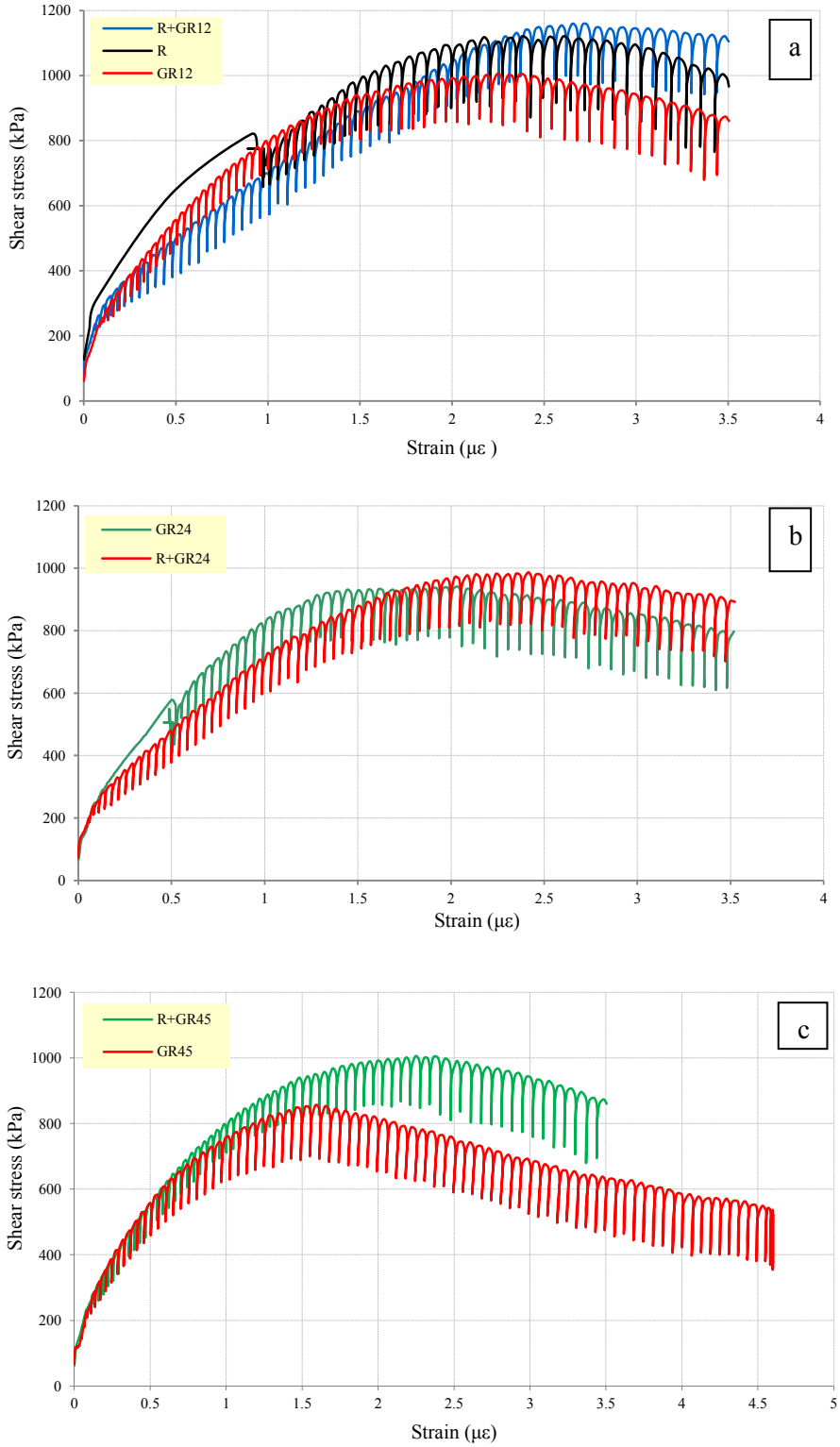

Figure 6.19 Stress-strain curves of the layered and the homogenous GR samples containing: (a) 12% glass content, (b) 24% glass content, and (c) 45% glass content

The failure pattern of an individual cylindrical layered 4R+4GR45 sample is shown in Figure 6.20. A longitudinal crack was observed from top to middle of the sample through the 4GR45 layer parallel to the axial force. It is apparent from this figure that the rock layer located at the bottom of the cylindrical sample was probably hindered the effect of the crack. It is important to note that the failure mode of the 4GR45 layers is considered a partial failure mode.

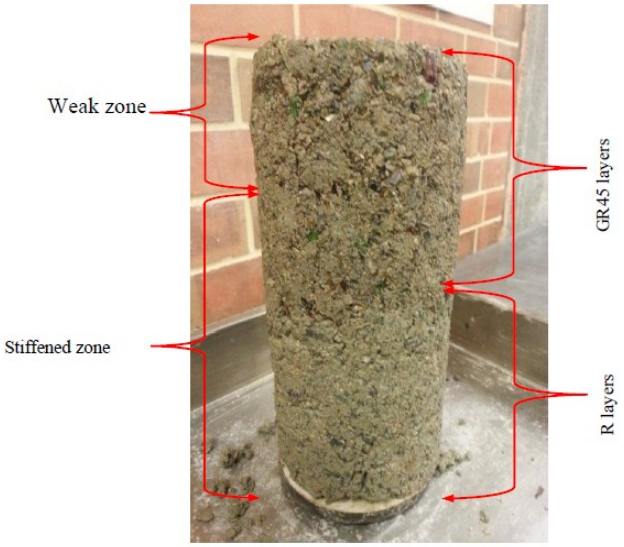

Figure 6.20 Failure patterns observed after RLTT of a 4R+4GR45 sample

6.5 Resilient modulus of layered rock-sand samples

The influence of waste glass on resilience behaviour of natural rocky samples was investigated in the previous section. The factors affecting the resilient modulus (M_r) of modified samples were also investigated. Based on the similarity between the geotechnical characteristics of glass and sand, and the lack of information about sand-rock (R-S) layered structures, further investigation needed to be performed on layered samples of R-S to assess their resilient modulus. Samples of layered R-S were subjected to an initial conditioning stage to minimise the effects of cap and base, as detailed in Table 3.15. After this stage and at the 1st stress path, the sample was subjected to 20 kPa confining pressure with 20, 35, 50 and 70 kPa deviator stresses, then the sample was ready for running the next stages of the stress path. This investigation has listed many factors influencing the M_r including the number of load cycles in each path, and the number and the location of sand layers. Scanning

electron microscopy (SEM) and optical microscopy were also conducted to support this investigation. It is important to note that the results of the SEM and optical microscopy are not presented in this section as they were already presented in Chapter 3. To study the effect of the sand layers location on dynamic bahaviour of the R-S sample, sand layers were located at top, bottom and middle of the R-S samples, as presented in Table 3.16. In addition, each test was run for two cycles number in each stress path (i.e. 100 and 10,000). Thus, the numbers 100 and 10,000 in front of each sample refer to the number of load cycles in each stress path.

6.5.1 Effect of the sand layer location on the M_r of layered R-S samples for 100 loading cycles per path

The effect of the sand layer location on the M_r of R-S samples tested for 100 cycles per path is investigated and presented in Figure 6.21. It is understandable that rock samples showed the highest M_r as compared to the R-S layered samples. There are two primary reasons to explain the reverse R-S sample behaviour; the first reason is laying layers of rounded particles of sand between the crushed rock layers. This results is consistent with Allen (1973), Barskale and Itani (1989), and Arnold (2004) who concluded that the M_r of angular particles is higher than the rounded ones.The low M_r of sand as compared to that of rock is the second reason of the significant reduction in the M_r of the rock sample which may support the findings of Rada and Witczak (1981), who concluded that the course particles have a greater effect on resilience behaviour than the fine materials. In Figure 6.21, the 4R+S+3R(100) sample showed higher M_r than the R+S+6R(100) and 6R+S+R(100) samples during the first three hundred cycles. After that, the R+S+6R(100) sample showed higher M_r than the 4R+S+3R(100) and the 6R+S+R(100) samples. Note that the M_r of pure rock decreased to 57.2%, 60%, and 71.4% when the sand layer was located in the bottom, middle, and top of the sample, respectively. This results may support the role of the sand layer location on the M_r of the rock sample, that the sample which the sand layer was closed to the top showed the lowest M_r. The varies behaviour of the R-S samples could be related to the fluctuations of axial stress transmission in the layered sample, as explained insection 6.2.3.

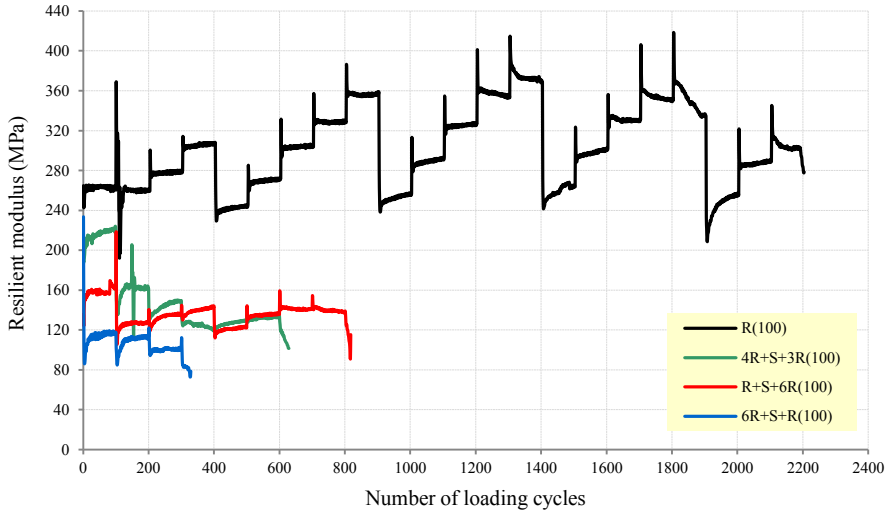

Figure 6.21 Effect of the sand layer location on the resilient modulus of rock-sand samples for 100 loading cycles /path

6.5.2 Effect of the number of sand layers on resilient modulus of the rock-sand sample for 100 loading cycles per path

The effect of the number of sand layers on M_r of the R-S samples tested for 100 cycles/path is shown in Figure 6.22. The highest value of M_r was observed for the 4R+S+3R(100) sample, whereas the lowest value was related to the R+S+R+S+R+S+R+S(100) sample. Note that the number of loading cycles corresponding to the failure point of 4R+S+3R(100) sample decreased from 630 cycles to 360, 175, and 100 cycles when the sand layers increased to two, three, and four layers, respectively. The main reason for the inversely effect of increasing the sand layers was the inability of the sand layers to withstand the dynamic loads alone. Therefore, the M_r of R-S samples decreased with an increase in the number of sand layers. In addition, the resilience behaviour of the R-S samples was considerably affected by increasing the interface layers between rock and sand layers resulted in unstable fabric, causing an increasing in P_r around the interface layers and then decreased the M_r of R-S samples. This finding was consistent with those of the micro-deformation study of Zhang et al. (2015), who concluded that the layered sample containing interface layers between fine and course materials showed the highest deformation compared with those without interface layers.

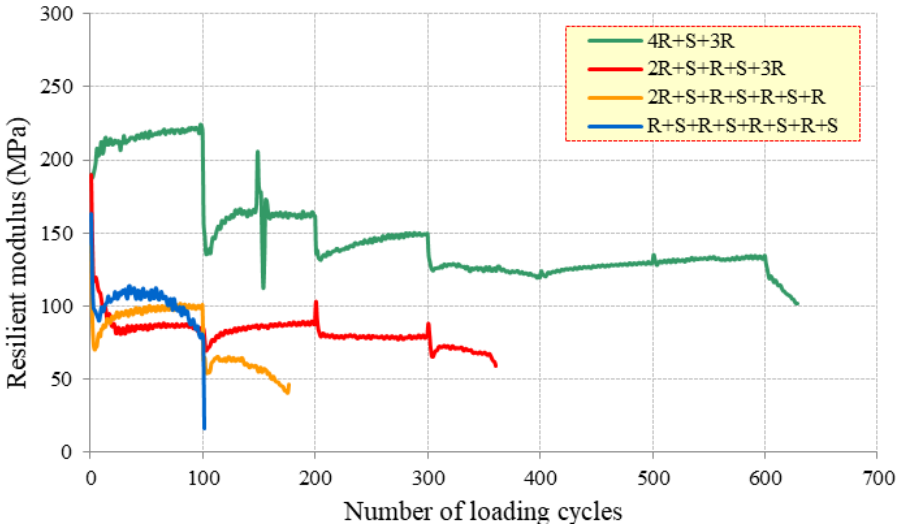

Figure 6.22 Effect of the number of sand layers on the resilient modulus of the rock-sand sample for 100 loading cycles /path

6.5.3 Effect of the sand layer location on the resilient modulus of rock-sand samples for 10,000 loading cycles per path

Since the intent of this test is to ascertain the onset of the layered samples damage, the test was allowed to be running for 10,000 cycles per path. Figure 6.23 shows the resilience behavior of the R-S samples tested for 10,000 cycles/path. Note that the pure rock sample showed the highest M_r value, while the sample that the sand layer located close to the surface showed the lowest M_r. Also, the M_r of pure rock decreased to 57%, 62%, and 65% when the sand layer was located in the bottom, middle, and top of the sample, respectively. This result was consistent with the finding reported in section 6.5.1. Furtheremore, the resilience behaviour trend of the layered samples under 10000 cycles/path showed the same behaviour of those under 100 cycles.

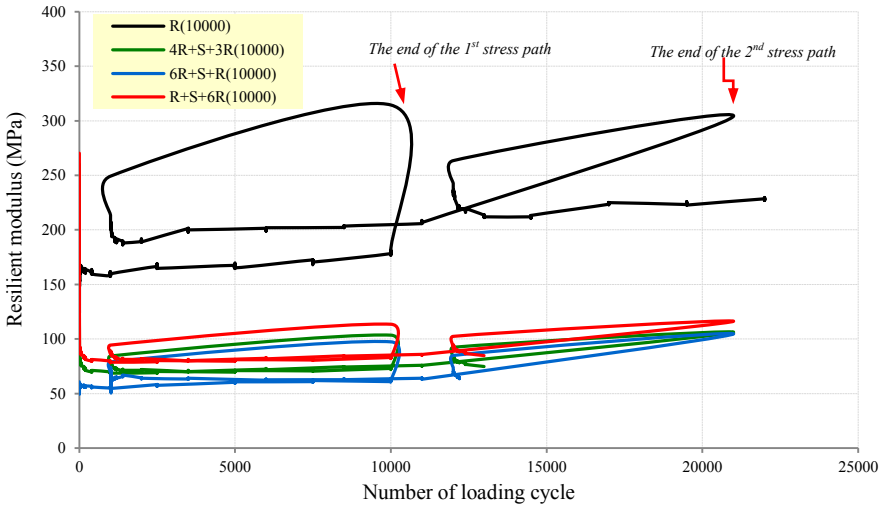

Figure 6.23 Effect of the sand layer location on the resilient modulus of the rock-sand samples for 10000 loading cycles /path

6.5.4 Effect of the number of sand layers on the resilient modulus of rock-sand samples for 10,000 loading cycles per path

The variation in the M_r of R-S samples as a function of the number of sand layers is shown in Figure 6.24. In general, a clear reduction in the M_r was associated with increasing the sand layer number. Based on the number of cycles corresponding to the failure point, the failure stage of the rock and 4R+S+3R(10000) samples occurred entirely beyond two stages of stress paths (20,000 cycles), whereas the failure of the 3R+S+R+S+2R(10000) sample occurred after one stage of stress paths (10,000 cycles). It is important to state that the 2R+S+R+S+R+S+R(10000) specimen could not complete one stage of stress paths and the failure stage of the sample occurred earlier (after 7500 cycles). This set of analyses confirms the results in section 6.5.2, which concluded that the M_r of the rock-sand samples decreases with increasing sand layers.

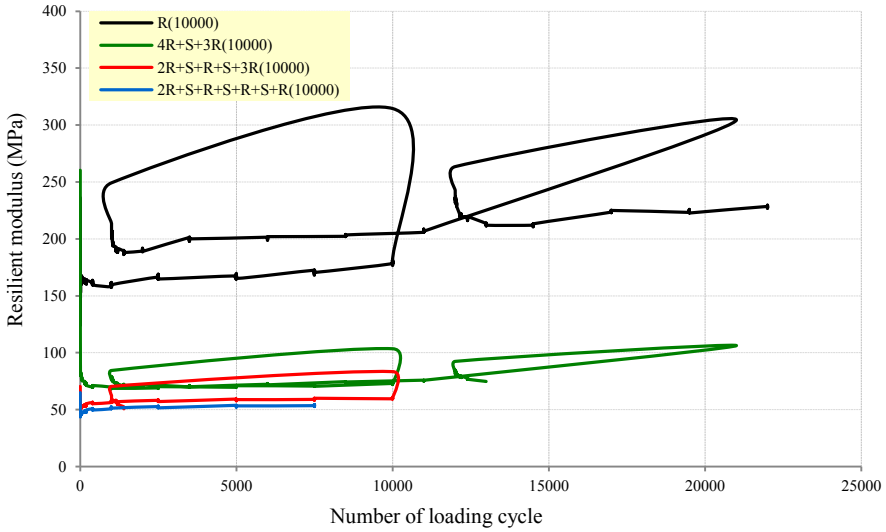

Figure 6.24 Effect of the sand layer number on the M_r of the rock-sand samples for 10000 loading cycles /path

6.6 Permanent deformation of layered rock-sand

A series of RLTTs was conducted on rock samples for 100 loading cycles per stress path to assess the influence of deviator stress on permanent deformation (P_d) behaviour. Based on the variation of confining pressure, a correlation between the P_d of rock samples and the maximum deviatoric stress is detailed in Figure 6.25. The results indicate that the rock sample under 100 kPa confining pressure failed precisely at the 23rd stress path. This result was consistent with the findings of Werkmeister et al.(2003b), who pointed toward the stress levels of repeated loading having an adverse effect on the M_r of granular materials underneath the asphalt layer. It was also consistent with the results of Zakaria and Lees (1996); Lekarp et al. (2000); and Van Niekerk et al. (2002), who reported that the rate of P_d directly increases with stress level. The same sample of rock was subjected to different numbers of load cycles in each loading path to investigate the onset of damage stage. Cycle numbers were increased from 100 to 10,000 cycles per path. Figure 6.26 shows the maximum deviator stress recorded versus the permanent deformation. It is important to note that the onset of damage depended more on the stress level than the number of cycles. Thus, the rock sample tested at 10,000 cycles/path showed higher stress-P_d capacity than the rock sample tested at 100 cycles/path. The effect of the number of cycles on the P_d of the R(100) and R(10000) samples is illustrated in Figure 6.27. The results in the figure are consistent with those in Figure 6.26: the number of cycles may improve the P_d resistance of the sample.

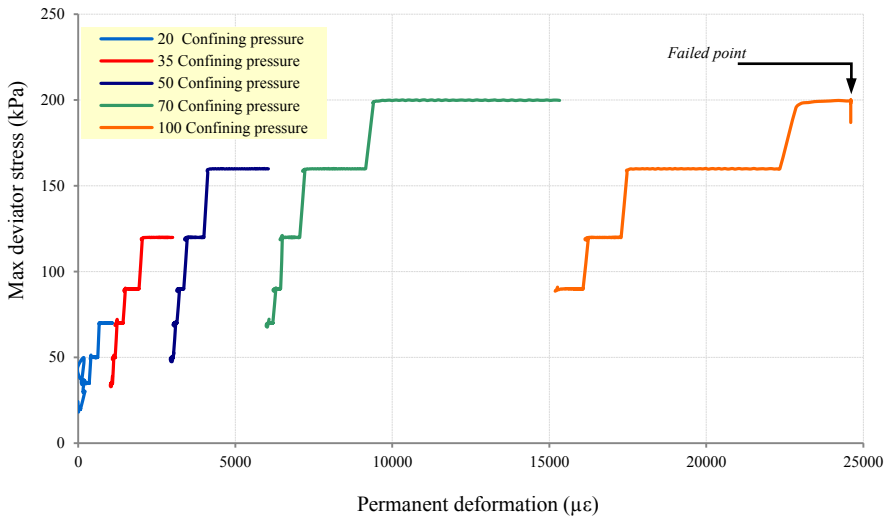

Figure 6.25 Maximum deviatoric stress *vs*. permanent deformation for pure rock sample

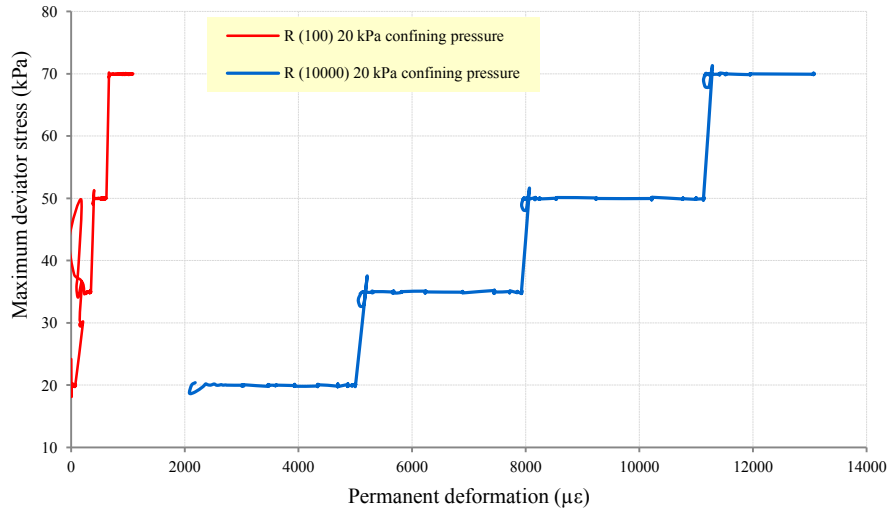

Figure 6.26 Maximum deviatoric stress *vs*. permanent deformation for rock sample for 100 and 10000 loading cycles during the first stage of the RLTT (20 kPa confining pressure)

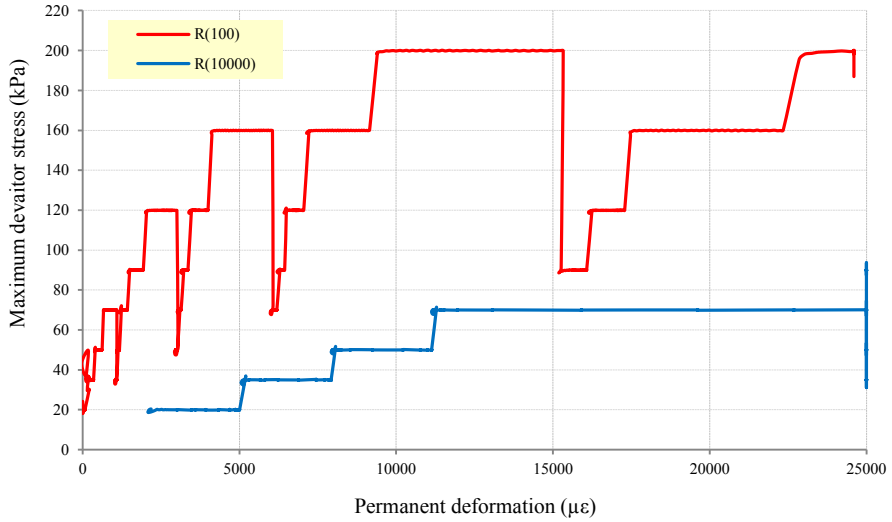

Figure 6.27 Maximum deviatoric stress *vs*. permanent deformation for rock sample for 100 and 10000 loading cycles during the all stages of the RLTT (20, 35, 50, 70 and 100 kPa confining pressure)

To reflect the correlation between P_d and the number of load cycles, Figure 6.28 illustrates the P_d-cycle number correlation of rock specimens tested for 100 and 10,000 cycles/path. In general, it appears that the failure of the rock sample was significantly affected by the stress level more than the number of loading cycles.

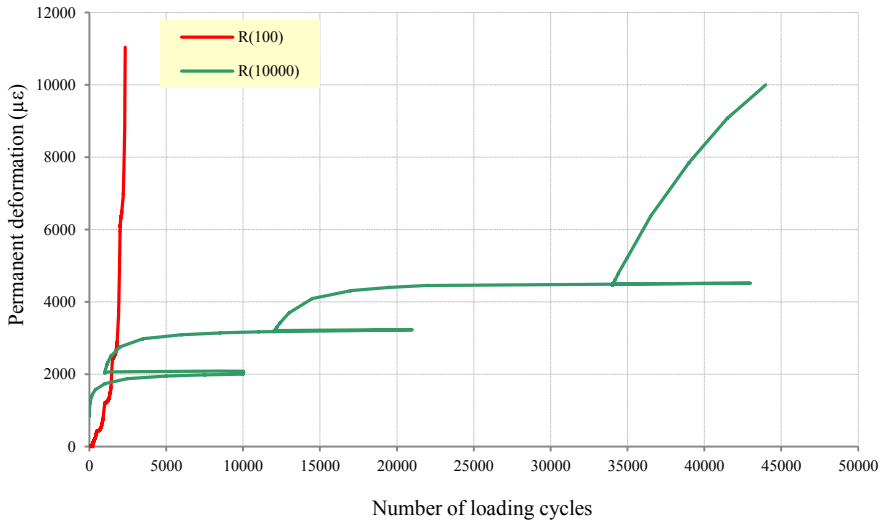

Figure 6.28 Number of loading cycles *vs*. permanent deformation for rock samples tested for 100 and 10,000 loading cycles/path

6.6.1 Effect of the sand layer location on the permanent deformation of rock-sand samples for 100 loading cycles per path

It is apparent from Figure 6.29 that the effect of the sand layer location on the P_d of R-S samples. In general, the P_d of the pure rock sample was adversely affected by the sand layer inclusion. In comparison, the R (100) specimen showed lower P_d than other layered samples, which was consistent with the findings of the micro-deformation study of Zhang et al. (2015), that the deformation of the layered sample containing interface layers between course and fine materials was greater than that of the sample without an interface. The deformation values of the R-S samples were dependent on the location of the sand layer (top, middle or bottom). It is important to note that the R-S sample which containing a sand layer located close to the base (R+S+6R(100)) showed less P_d than the other samples. Also, the sample which containing a sand layer located in the middle (4R+S+3R(100)) showed less P_d than 6R+S+R(100) sample. Figure 6.30 presents the effect of the sand layer location on the P_d of the R-S samples for 100 cycles per path. In general, the pure rock sample showed lower P_d than the R-S samples. The figure also confirms the above results: that the R-S sample which containing a sand layer close to the bottom showed the lowest P_d. For example, the P_d of the R, R+S+6R(100) and 4R+S+3R(100) samples corresponding to the 500^{th} cycle were approximately about 1000 με, 9000 με and 13,000 με, respectively, while the 6R+S+R(100) sample had failed when reaching that number of the cycles. According to the findings of Zhang et al., (2015), the kinetic activities of the particles are higher around the interface layer during the loading stage, and since the applied stresses are transmitted from the source through the soil as waves, the upper layers of the sample are directly affected by those waves; this could be explained the instability of soil fabric and thus, high permanent deformation susceptibility of the soil. Therefore, the deformation of R-S samples was higher in the sample where the sand layer is close to the surface of the sample.

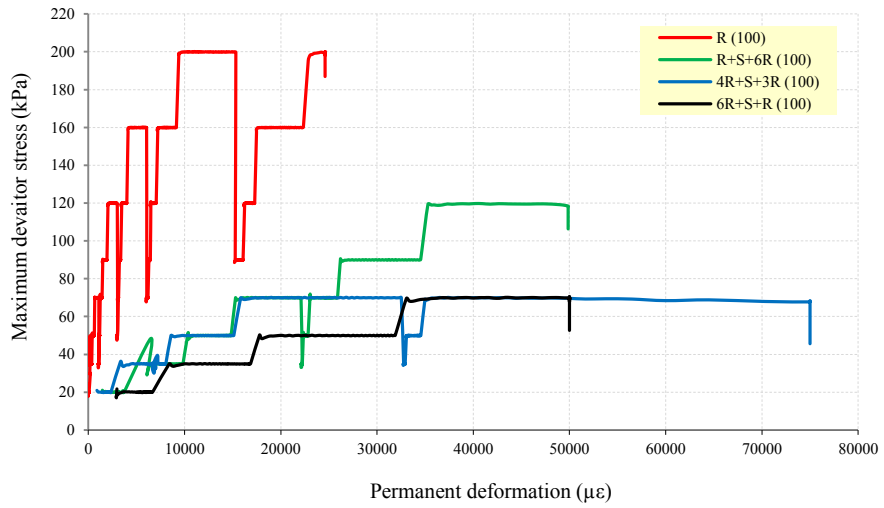

Figure 6.29 Maximum deviator stress *vs*. permanentdeformation for rock-sand samples with sand layers in different locations tested for 100 cycles/pathduring the all stages of the RLTT (20, 35, 50, 70 and 100 kPa confining pressure)

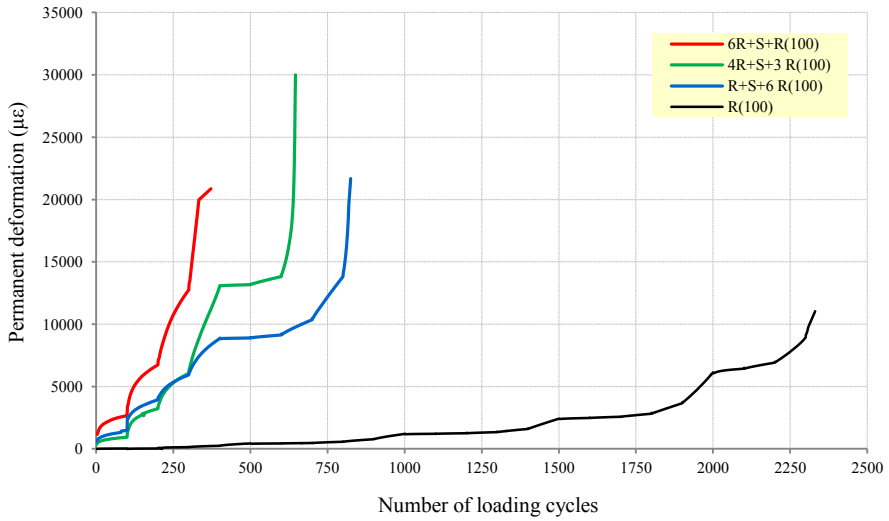

Figure 6.30 Effect of the sand layer location on the permanent deformation of rock-sand specimens tested for 100 cycles/path

There is limited understanding regarding the failure behaviour of R-S samples and therefore, this subsection provides further discussion of the failure mechanism of R-S samples according to their sand layer location. A comparison of the failure patterns of the 6R+S+R(100), 4R+S+3R(100) and R+S+6R(100) samples is illustrated in Figures 6.31 (a, b and c, respectively). It was identified that the failure in the rock layers of the 6R+S+R(100) sample was associated with the sensitivity of the interface layer between the sand and rock layers, as shown in Figure 6.31 (a). The negative effect of the sand layer on the P_d of the rock sample could be attributed to the initial failure around the interface layer between the rock and sand layers where

the highest shear stress was concentrated. Figure 6.31 (b) illustrates the failure pattern of the 4R+S+3R(100) sample, which had a sand layer near the middle of the cylindrical sample. It can be seen that the sand layer reached its ultimate strength earlier and, consequently, the failure occurred in the rock layers, which were supported by the sand layer below. In Figure 6.31(c), the failure of the R+S+6R(100) sample started at the sand layer, which was located close to the bottom. Longitudinal cracking was observed from the top to the bottom of the rock layers, which were above the sand layer, in a direction parallel to the axial force. The above findings proved the negative effect of the sand layere on permanent deformation of the rock-sand samples.

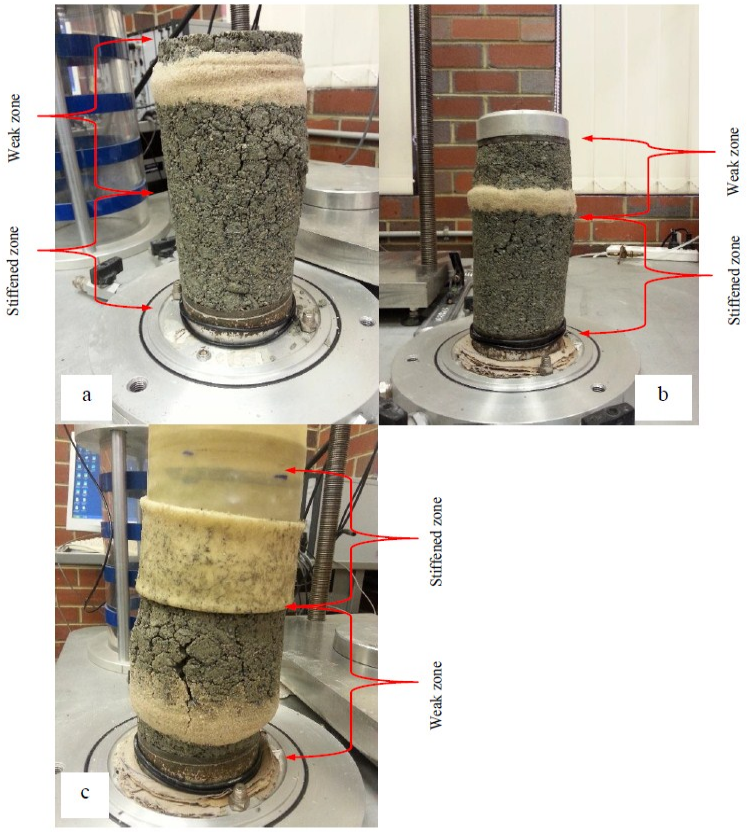

Figure 6.31 Effect of the sand layer location on the failure patterns of rock-sand samples after RLTTs: a) 6R+S+R(100), b) 4R+S+3R(100) and c) R+S+6R(100) samples

6.6.2 Effect of the sand layer location on the permanent deformation of rock-sand samples tested for 10,000 loading cycles per path

In certain instances, the test was allowed for running for more than 100 to 10000 loading cycles per path to ascertain the onset of the layered specimen's failure. Figure

6.32 plots the maximum deviator stress versus P_d of the R(10000), 4R+S+R(10000), R+S+6R(10000) and 6R+S+R(10000) samples. Generally, the rock sample showed the lowest P_d, and the effect of the sand layer location became more visible during the second stress path. Thus, the R+S+6R (10000) sample showed lower P_d than the other R-S samples. For example, the P_d of R(10000) and R+S+6R(10000) corresponding to 60 kPa confining pressure were approximately 11,250 με and 16,250 με, respectively. While the 4R+S+3R(10000) and the 6R+S+R(10000) specimen had failed before reaching 60 kPa confining pressure.

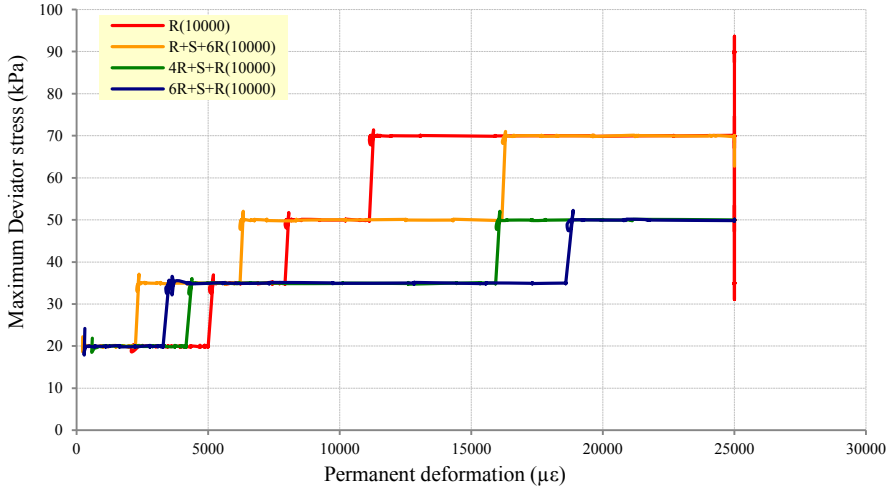

Figure 6.32 Effect of the sand layer location on the permanent deformation of sand-rock specimens tested for 10000 cycles/path during the all stages of the RLTT (20, 35, 50, 70 and 100 kPa confining pressure)

According to the sand location, the variation in the P_d of R-S samples tested for 10000 cycles per path is presented in Figure 6.33. At early stages of of the RLTT, R(10,000) showed the highest P_d rate compared to the other samples. At the final stages, a clear improvement in the P_d of R(10,000) samples was associated with the number of cycles. It is important to note that the R+S+6R(10,000) sample showed higher resistance against P_d than the other layered R-S samples during the loading stages. In general, a positive correlation was noticeable between the P_d of the R-S sample and the distance between the sand layer and the sample base. This result is consistent with the above results concerning the effect of the sand layer location on P_d.

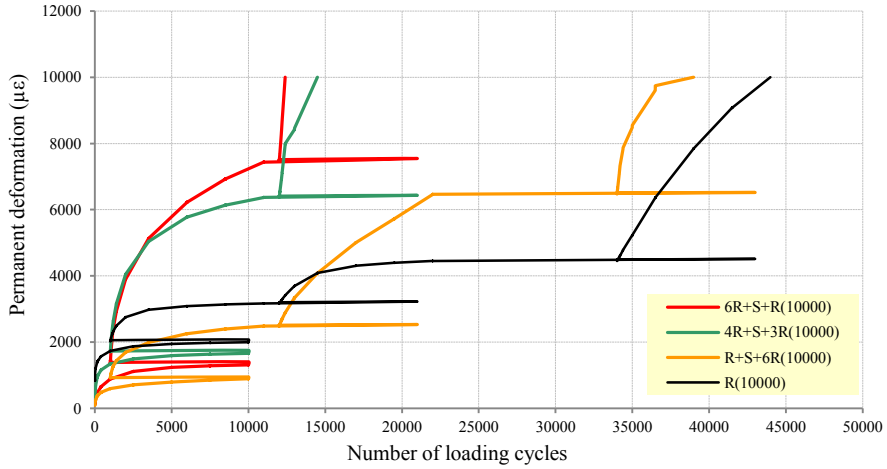

Figure 6.33 Effect of the sand layer location on the permanent deformation of sand-rock samples tested for 10,000 cycles/path

According to the variation in the cycles number (100 and 10000), a comparison between P_d s of the 6R+S+R, 4R+S+3R and R+S+6R samples is presented in Figure 6.34, which shows the effect of the sand layer location on the P_d of the R-S samples. It is essential to note that the R-S sample produced the best performance against P_d when the sand layer was located close to the sample base. Similar to the results in the previous section, the 6R+S+R sample showed the highest value of P_d. In addition, the sand layer location played a significant role in the P_d evaluation under repeated loadings. It is apparent that the layered samples tested under 100 cycles/path showed higher P_d than that of the others for 10000 cycles/path and thus, the deformation susceptibility of the R-S samples depended on the stress path rather than on the cycles number.

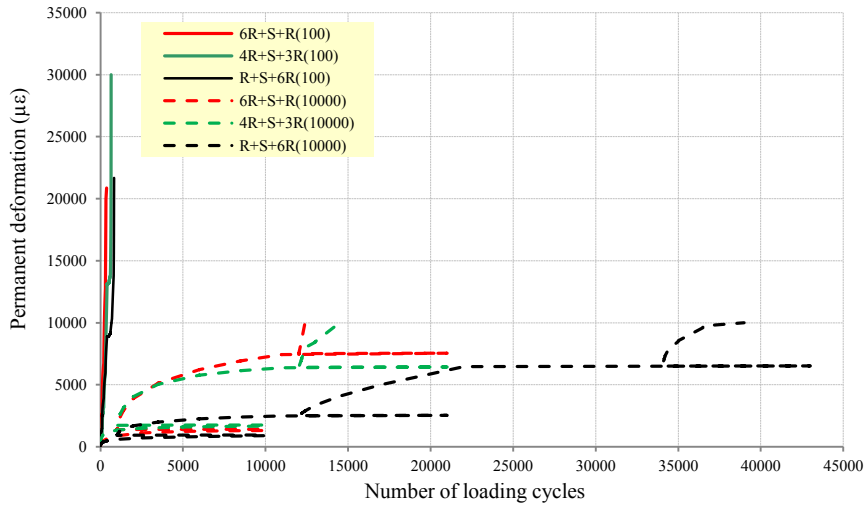

Figure 6.34 Permanent deformation of the sand-rock samples tested under 100 and 10000 cycles/path

6.6.3 Effect of the number of sand layer on the permanent deformation of rock-sand sample tested for 100 loading cycles per path

Further study was performed to assess the effect of the number of sand layers on the P_d of R-S samples tested for 100 loading cycles per path. As presented in Figure 6.35, R(100) showed the lowest P_d, whereas the S+R+S+R+S+R+S+R(100) sample showed the highest. It is apparent from this figure that the deformation behaviour of the R-S samples depended considerably on the number of sand layers in the sample. This behaviour could be attributed to the role of the sand layers in producing low stablility sample and consequently, decreasing the number of cycles that the R-S samples can withstand before collapsed. For instance, by increasing the number of sand layers from two to three layers, the number of cycles decreased from 350 cycles to 200 cycles (i.e., 75%) before collapsed.

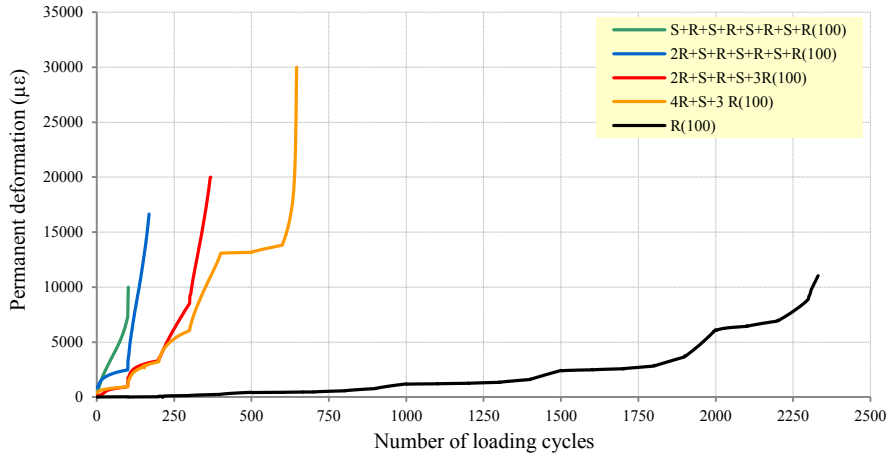

Figure 6.35 Effect of the number of sand layers on permanent deformation of the rock-sand specimens tested for 100 cycles/path

6.6.4 Effect of the number of sand layers on permanent deformation of rock-sand samples tested for 10000 cycles/path

In the section above, a direct dependency was observed between the number of sand layers and the P_d resistance of rock samples tested for 100 loading cycles per path. Thus, further investigation was necessary to assess the effect of the number of sand layers on the P_d of R-S samples tested for 10000 cycles per path. The correlation between P_d of the R-S samples and the number of sand layers is shown in Figure 6.36. The result was consistent with the findings in section 6.3.3 that a reduction in

P_d was noticeable as the number of the sand layers decreased. It is apparent from this figure that the 4R+S+3R(10000) sample showed less P_d than the 2R+S+R+S+3R(10000) and 2R+S+R+S+R+S+R (10000) samples. Note that after two stress paths of the loading stages, the R(10000) and 4R+S+3R(10000) samples remained stable under repeated loading impacts, while the 3R+S+R+S+2R(10000) sample collapsed before that stage, whereas the 2R+S+R+S+R+S+R(10000) specimen collapsed after several cycles and could not complete a single stress path. This set of analyses concludes that the resistance of rock specimens to P_d decreasing as the number of sand layers increased.

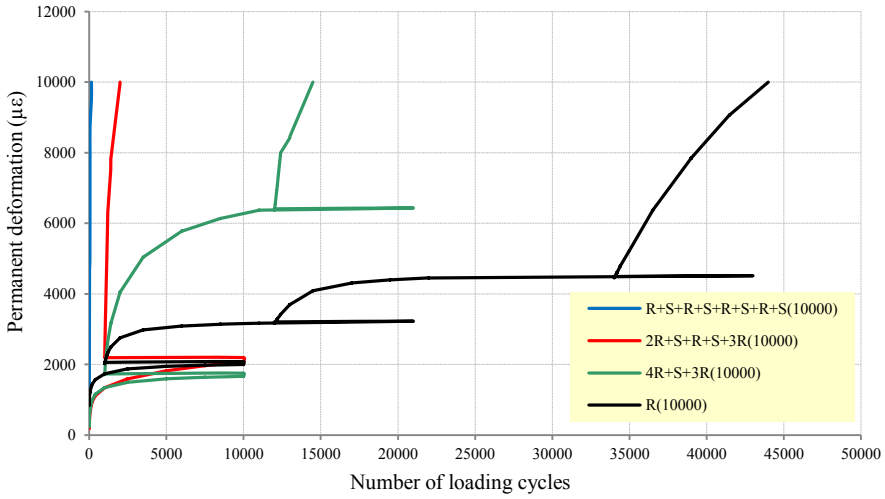

Figure 6.36 Effect of the number of sand layers on the permanent deformation of rock-sand samples tested for 10000 cycles/path

The failure pattern of the cylindrical 2R+S+R+S+R+S+R(100) sample after completion the RLTT is visible in Figure 6.37. A remarkable reduction in the sample stiffness was noticeabled around the interface layers between the rock and sand layers and thus, the collapse stage has started from the sand layers. This finding was attributed to the high sensitivity of the sand layer to dynamic stresses compared to the pure rock one.

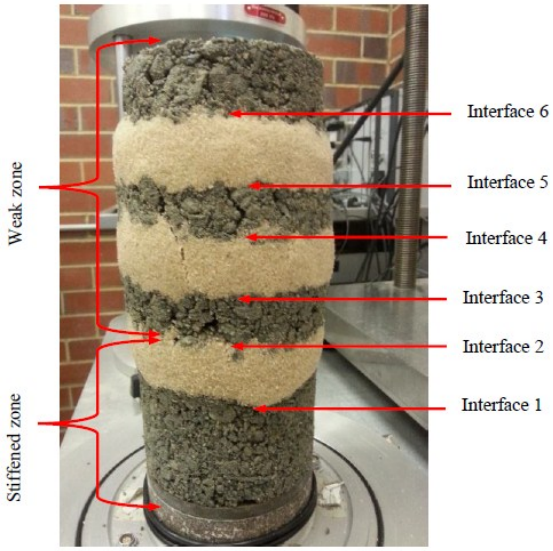

Figure 6.37 Failure pattern of 2R+S+R+S+R+S+R(100) sample after completion the RLTT

6.7 Resilient modulus of layered samples of rock-bentonite and rock-bentonite-sand materials tested for 100 cycles per path

The previous sections showed a considerable influence of crushed glass (G), tyre rubber (T) and sand on dynamic behaviour of rock (R) samples. Hence, the influence of fine bound materials (materials passing a sieve no. 200) on the dynamic behaviour of layered rocky samples needs to be investigated further. More recent studies, however, have reported that fine materials play a significant role in the dynamic performance of unbound-bound mixtures in pavement applications (Perlea, 2000; Perlea, Koester & Prakash, 1999). Bentonite (BE) is one of the waste fine bound materials commonly used in geotechnical applications and therefore, this section examined the effect of the BE presence, the number, and the location of BE layers on dynamic characteristics of rock samples. The development in dynamic behaviour of R samples as a result of the presence of the BE and the sand layers is also investigated in this section. According to Table 3.17, layered samples of rock-bentonite (R-BE) and rock-bentonite-sand (R-BE-S) were prepared. A series of RLTT was conducted on the layered samples to assess their resilience and deformation behaviour under 100 cycles per each path, as detailed in Table 3.15.

6.7.1 Effect of the location of bentonite layer on resilient modulus of the rock-bentonite samples

The fundamental objective of this research was to evaluate the resilience behaviour of layered samples of R-BE materials. As shown in Table 3.17, layers of rock were removed from the rock samples and replaced by layers of BE in different locations, and the samples were labelled 6R+BE+R(100), 4R+BE+3R(100) and R+BE+6R(100) according to whether the layers were at the top, middle or bottom of the sample, respectively. It is apparent from Figure 6.38 that a significant differences were noticeable in the M_r values between the R(100) and R-BE(100) samples. The R(100) sample showed the highest M_r value, whereas the R+BE+6R(100) sample showed the lowest value. Based on the results of Rada and Witczak (1981), course materials showed higher M_r than fine materials. Therefore, this results can be considered logical if the previouse results of the resilience behaviour of the bound fine materials compared to the unbound course materials are adopted. This result is consistent with the findings of Hicks and Monosmith (1971) who reported a reduction in M_r of crushed aggregate as a result of the fine materials presence. One of the most significant findings of such research is that the 6R+BE+R(100) sample, where the BE layer was located near the top, showed a higher M_r than the 4R+BE+3R(100) and R+BE+6R(100) samples. Based on the development in resilience behaviour of the R-S samples in section 6.5.1, a comparison between the resilience behaviour of the R-S and the R-BE samples tested for 100 (cycles/path) is presented in Figure 6.39. It is apparent from this figure that the R-BE sample showed a sharper reduction in the M_r compared to that of the R-S samples. For instance, the range of M_r decreased from (80-120) to (40-80) because of replacing BE layer instead of sand. However, the R-BE samples showed higher failure resistance than that of the R-S samples, which collapsed before the R-BE samples. In contrast to the R-S samples, the M_r of R-BE samples increased directly with the distance reduce between the BE layer and the surface. This performance could be related to the gradual increases the interlocking between the course particles of R and the fine materials of BE around the interface layer, which was more effective under high pressure at the top of the sample.

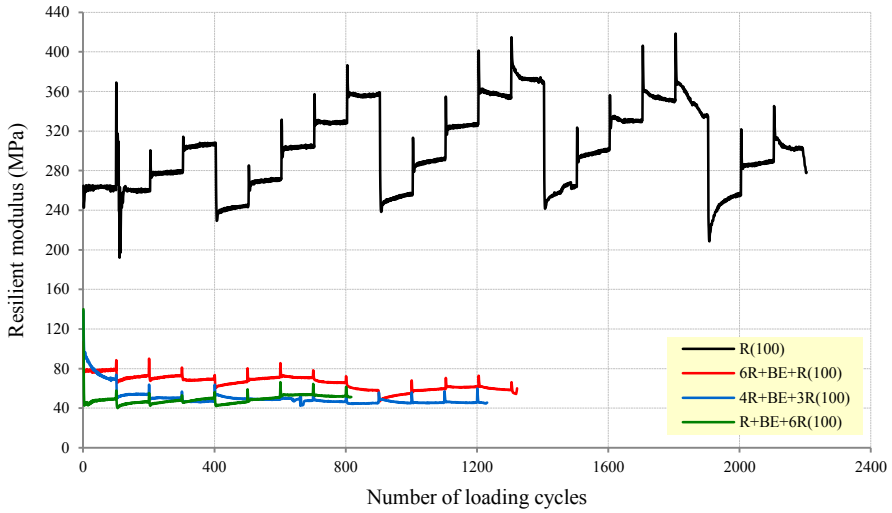

Figure 6.38 Effect of the bentonite layer location on the resilient modulus of R-BE samples tested for 100 cycles/path

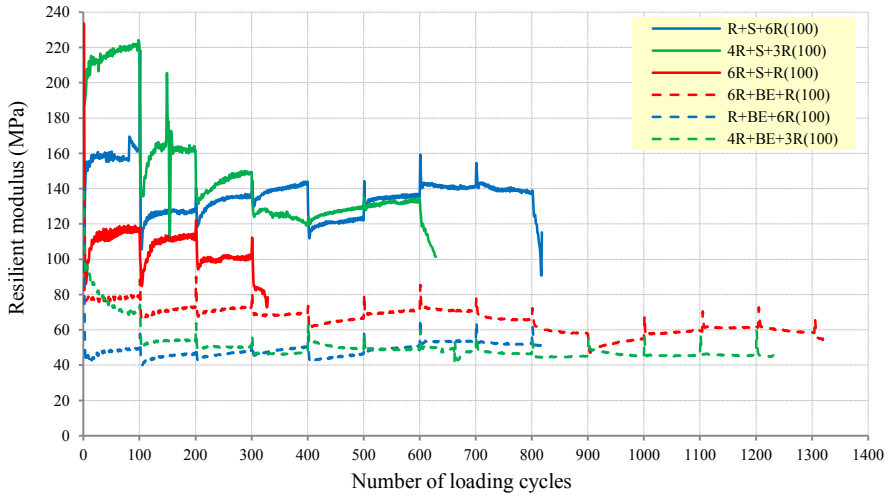

Figure 6.39 Effect of the sand and bentonite layers locations on the resilient modulus of rock samples tested for 100 (cycles/path)

6.7.2 Effect of the number of bentonite layer on the resilient modulus of rock-bentonite samples

Figure 6.40 details the effect of the number of bentonite layers on the M_r of R-BE samples teste for 100 cycles/path. It is apparent from this figure that there was a significant reduction in the Mr of the 4R+BA+3R(100) with increasing the number of BE layers, which indicated that adding more layers of BE caused in decline the ability of the layered sample to withstand this type of stiffness behaviour. This behaviour is consistent with the result reported in section 6.6.4, that the R-S sample with a sand layer showed a higher M_r than that with two layers.

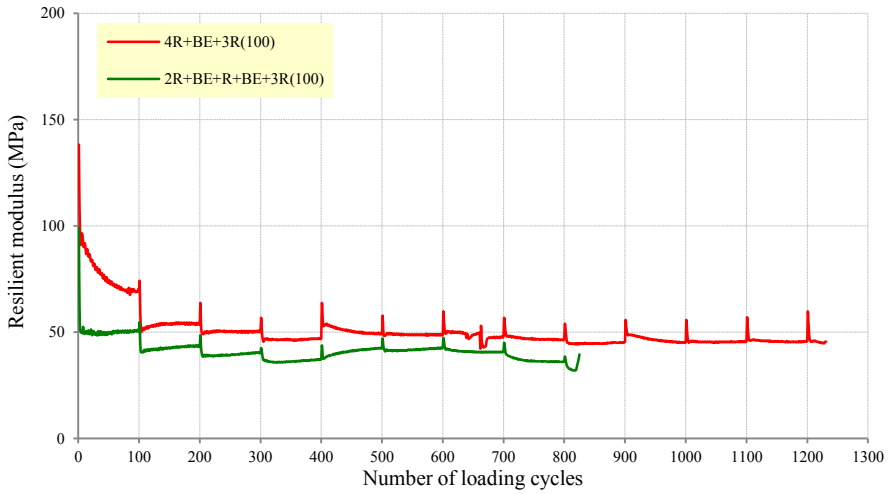

Figure 6.40 Effect of the number of bentonite layerson the resilient modulus of the rock-bentonite sample tested for 100 cycles/path

6.7.3 Effect of replacing sand and bentonite layers with rock layers on the resilient modulus of rock-bentonite and rock-sand samples

To explore the effect of unbound materials of sand rather than fine materials of bentonite on the resilience behaviour of the 2R+BE+R+BE+3R(100) sample, two layers of bentonite were replaced by sand layers and labelled the 2R+S+R+S+3R sample. As shown in Figure 6.41, the 2R+S+R+S+3R(100) sample reported a high improvement in resilience behaviour because of replacing sand layers that the M_r of 2R+BA+R+BA+3R(100) increased about 50% because of replacing the bentonit layers with sand layers. On the other hand, there was a significant reduction in the onset of the structural collapse in the 2R+BA+R+BA+3R(100) sample as a result of swapping sand layers instead of BE, the failure stage of 2R+BA+R+BA+3R(100) occurred beyond 800 cycles, whereas the failure of 2R+S+R+S+3R(100) occurred after 200 cycles.

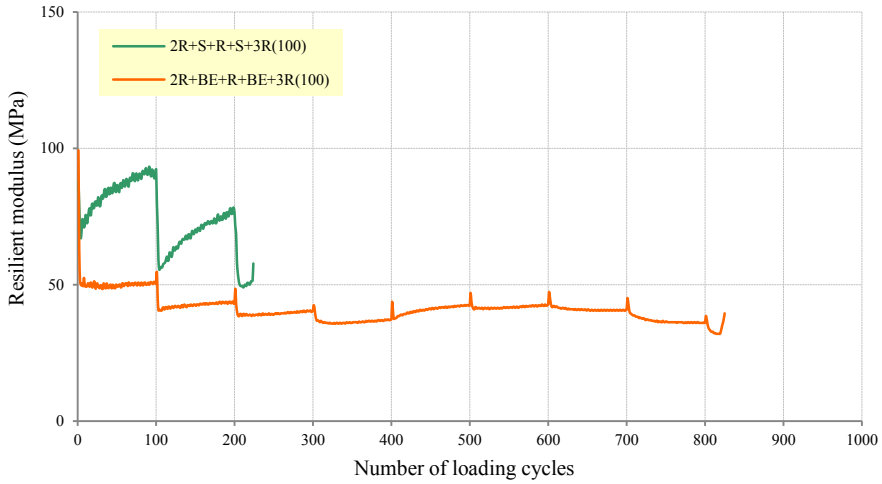

Figure 6.41 Resilience behaviour of rock-sand and rock-bentonite layered samples tested for 100 loading cycles/path

6.7.4 Effect of sand and bentonite layers on the resilient modulus of rock-sand-bentonite samples

Sand, rock and bentonite layers were employed in the present sudy to assess the effect of the sand and the bentonite layer locations on the resilince behaviour of the 2R+BE+R+S+3R(100) sample. According to the results in Figure 6.42, the 2R+S+R+BE+3R(100) sample showed a higher M_r than the 2R+BE+R+S+3R(100) sample. This result was consistent with a summary of the above results which suggested that the sample with a sand layer close to the bottom and a bentonite layer close to the top of a sample was stiffer than the other samples.

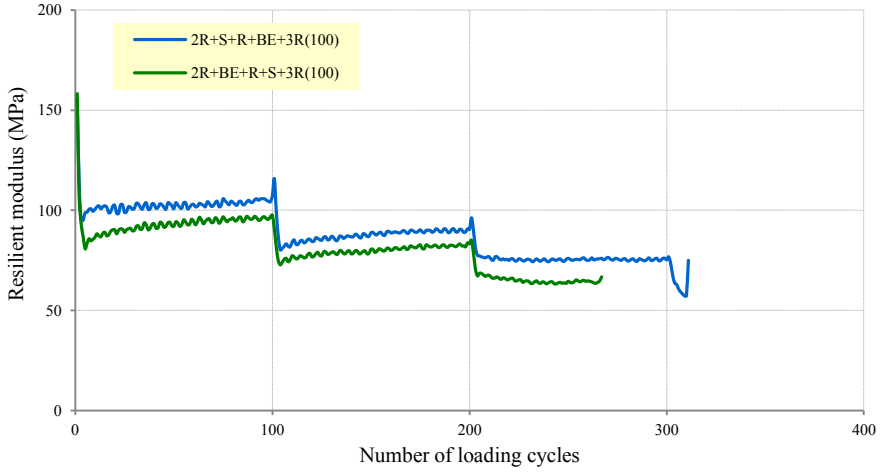

Figure 6.42 Effect of the sand and the bentonite layer locations on the resilince behaviour of the 2R+BE+R+S+3R sample tested for 100 loading cycles/path

6.8 Permanent deformation of layered samples of rock-bentonite and rock-bentonite-sand materials tested for 100 cycles per path

In this section, a series of RLTTs was conducted to assess the P_d of the R-BE samples under different test conditions. The results will be used in the initial assessments of deformation behaviour of rock-fine materials samples under repeated loading impacts.

6.8.1 Effect of the location of bentonite layer on the permanent deformation of rock-bentonite samples

The effect of the location of BE layer on the P_d of R-BE samples tested for 100 cycles per path is illustrated in Figure 6.43. In contrast to the results for the R-S samples presented in the previous section, the R-BE sample with a bentonite layer close to the bottom showed more P_d than the 4R+BE+3R(100) and 6R+BE+R(100) samples. According to the distance of the BE layer from the base, a negative correlation was found between the P_d and the BE layer distance. A comparison of the P_d of the R-S group and R-BE group is illustrated in Figure 6.44. It is visible that the P_d of the R-BE samples shifted to the right-hand side more than the R-S lines, which is mean that the R-BE group generally presented less deformation than the R-S group. For example, the P_d of the 6R+BE+R(100) sample corresponding to the 500^{th} cycle was approximately about 5000 με, while the 6R+S+R(100) had failed when reaching that number of cycles. The BE layer location may also play a significant role in the deformation behaviour, where the P_d of the R-S samples increased when the distance between the sand layer and the sample base increased; whereas a clear reduction in the P_d of the R-BE group was associated with increasing the distance between the BE layer and the base, as clear in the 6R+BE+R (100) sample. As mentioned in section 6.7.1, the contradictory findings in the P_d might be considerably dependent on the role of the fine materials in enhancing the soil fabric and the interlocking between particles around the interface layer, which is more active under high repeated pressures at the top of the sample.

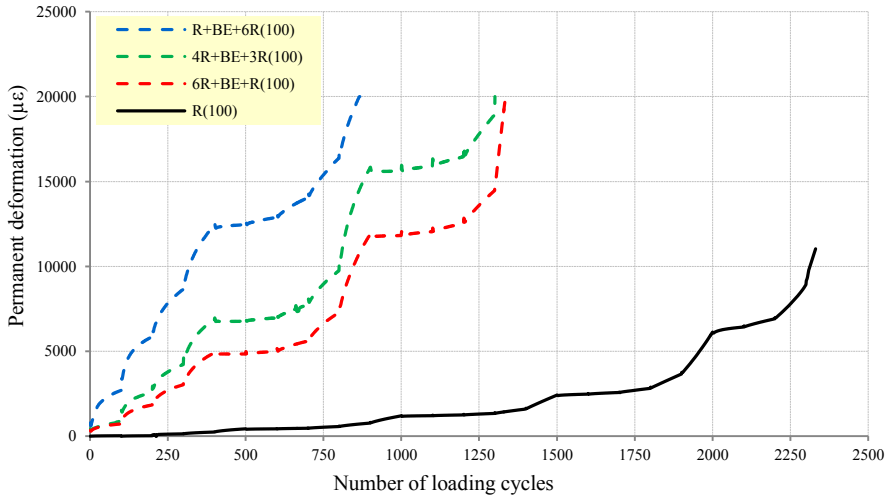

Figure 6.43 Effect of the location bentonite layer on the permanent deformation of rock-bentonite samples tested for 100 loading cycles/path

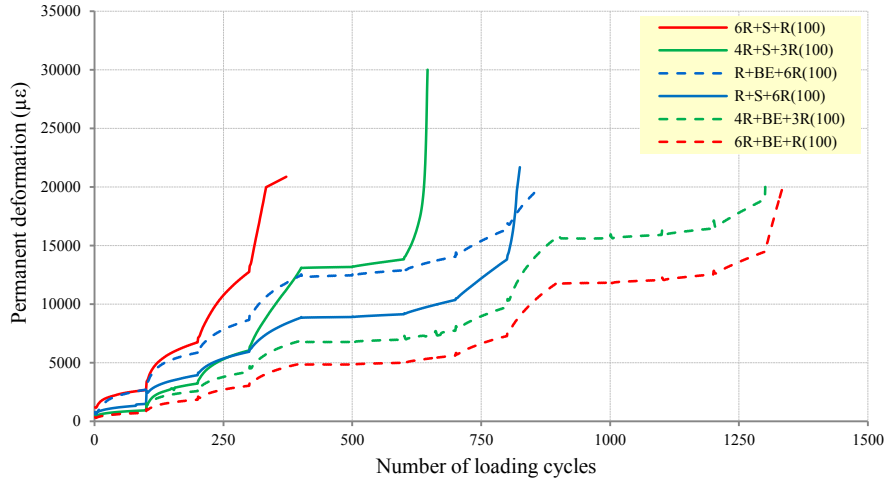

Figure 6.44 Permanent deformation of rock-sand and rock-bentonite samples tested for 100 loading cycles/path

6.8.2 Effect of the number of bentonite layers on the deformation of rock-bentonite samples

Figure 6.45 presents the variation in the Pd of the R-BE samples because of the variety in the number of the BE layers. It is apparent from this figure that the 4R+BE+3R(100) sample showed lower Pd than the 2R+BE+R+BE+3R(100) sample. Generally, a positive correlation was found between the P_d of the R-BE samples and the number of BE layer. This result can be an indication of the validity of previous results of Magnusdottir and Erlingsson (2002) concerning the determination of the

fine materials ratios that can be used to improve the performance of granular materials against P_d.

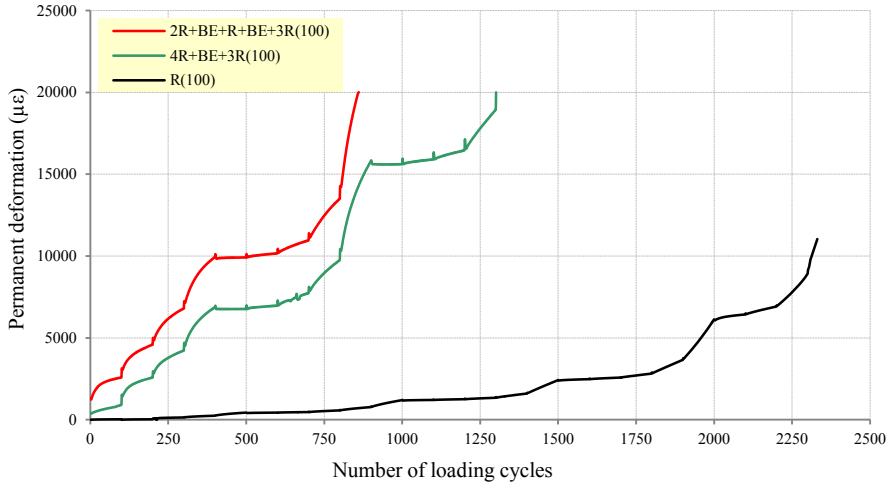

Figure 6.45 Effect of the number of bentonite layers on the permanent deformation of rock-bentonite samples tested for 100 loading cycles/path

The failure pattern of the cylindrical 2R+BE+R+BE+3R(100) sample after completion of the RLTT is presented in Figure 6.46. The failure in the rock layers at the top of the sample was associated with the sensitivity of the BE layer to dynamic loads. The BE layer close to the surface reached the ultimate strength before the another bentonite layer. With further applied stress, the upper layer of bentonite collapsed and consequently, the failure in the rock layer located above the bentonite layer occurred. In addition, it is not difficult to notice the high level of interlocking between the bentonite and rock particles around the interface layers.

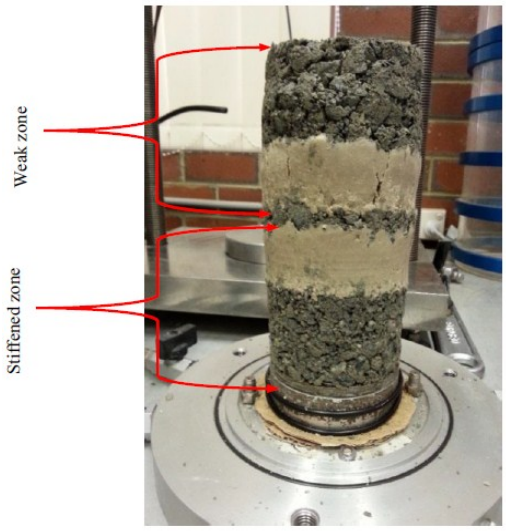

Figure 6.46 Locations of failure zones and failure patterns of 2R+BE+R+BE+3R (100) sample after RLTT

6.8.3 Effect of replacing sand with bentonite layer on the permanent deformation of rock-bentonite-sand samples

The effect of replacing sand with bentonite on the P_d of the rock-sand-bentonite (R-B-S) group is presented in this section. A sand layer was replaced by bentonite to prepare the 2R+S+R+BE+3R(100) sample which was used to assess the effect of sand and bentonite layers on P_d of the R-BE-S samples. It is apparent from Figure 6.47 that the 2R+S+R+BE+3R(100) sample showed less P_d than the 2R+BE+R+BE+3R(100) sample before 300 cycles. For example, the P_d of the 2R+BE+R+BE+3R(100) sample corresponding to the 250th cycle was approximately about 6000 με, while the P_d of the 2R+S+R+BE+3R(100) sample was about 5000με. Beyond that, the elastic characteristic of BE were probably the primary cause of the recoverable behaviour of the 2R+BE+R+BE+3R(100) sample, where an increase in the P_d of the R-B-S group was noticeable upon the replacing sand layer with bentonite one. However, a reduction in the P_d of the R-BE sample was associated with sand layer presence during the low cycles.

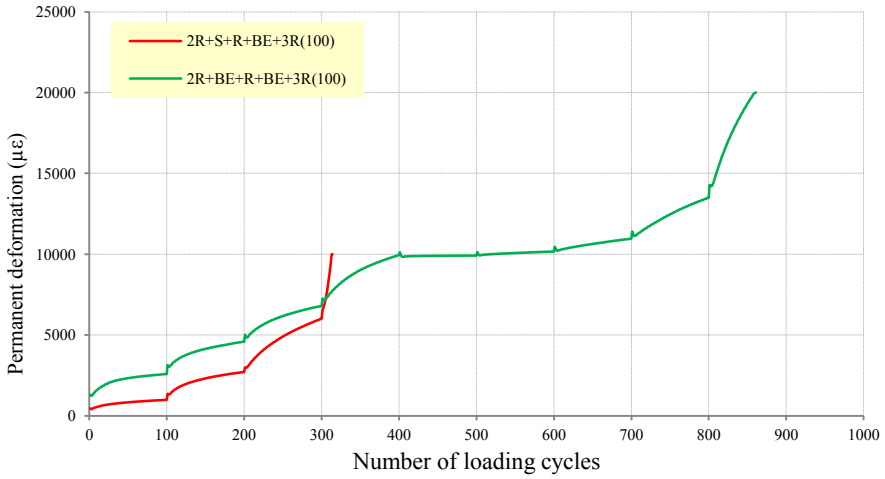

Figure 6.47 Effect of replacing sand with bentonite layer on the permanent deformation of rock-bentonite-sand samples tested for 100 loading cycles/path

6.8.4 Effect of the sand and bentonite layers locationon the permanent deformation of the rock-bentonite-sand samples

A series of the RLTTs was conducted on the 2R+S+R+BE+3R(100) and 2R+BE+R+S+3R(100) samples to investigate the effect of the sand and bentonite layers location on the P_d of the R-BE-S group. It is apparent from Figure 6.48 that

the 2R+S+R+BE+3R(100) sample showed lower P_d than the 2R+BE+R+S+3R(100) sample. The P_d of the the 2R+S+R+BE+3R(100) sample corresponding to the 250th cycle was approximately about 4800 με, while the P_d of the 2R+BE+R+S+3R(100) sample was 8000με. It is apparent from this figure that asimilarity was noticeable between the results in Figure 6.48 and the results in sections 6.8.1 and 6.6.1, which suggested that the rock sample with the sand layer close to the bottom and the bentonite layer close to the top showed less deformation than the other samples of R-BE-S group. Figure 6.49 illustrates the full image of the 2R+S+R+BE+3R(100) sample. It is clear that the crack was observed at the lowest sample where the sand layers there. It is therefore likely that the advantage of locating the bentonite layer between the rock layers hindered the cracks. In addition, it is almost certain that the failure mode of the sample was a general failure mode. It is apparent from this figure that the interlocking between the bentonite and rock particles around the interface layers was higher than that between the sand and rock paricles.

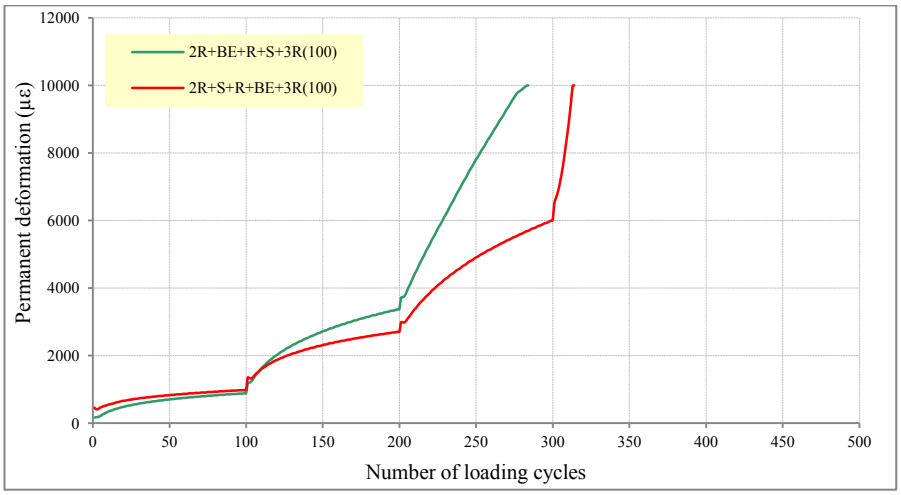

Figure 6.48 Effect of the sand and bentonite layer locations on the permanent deformation of the 2R+BE+R+S+3R sample tested for 100 loading cycles/path

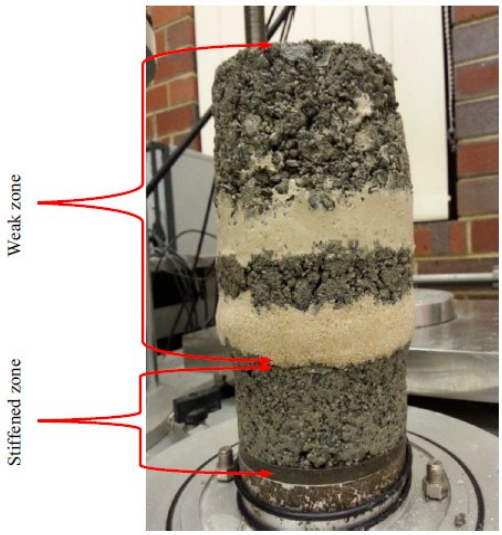

Figure 6.49 Locations of failure zones and failure pattern of 2R+S+R+BE+3R(100) sample after RLTT

6.9 Summary

A layering technique and the RLTT were employed to assess the dynamic behaviour of crushed rock samples containing layers of different materials. A range of glass proportions (12%, 24%, 45%) was used in preparing layered samples of the rock and the glass-rock mixtures (R+GR). The effects of the location and the number of the GR layerson resilient modulus (M_r) of the R+GR samples were also investigated. In addition, the GR and Rlayeres were prepared at different moisture contents to investigate the effect of moisture content on resilience behaviour. The results of R+GR samples showed that the M_r increased as the glass content increased. What is interesting in this data is that the R+GR12 and the R+GR45 samples showed a higher M_r than the rock sample. In addition, a significant reduction in the M_r of the R+GR group was associated with increasing the number of the GR layers. Also, the single-layered group (R+GR) showed higher M_r than the doubled-layered group (2R+2GR). Moreover, it is clear from the results that the samples with the GR layer located close to the sample surface showed lower M_r than that with the GR layer near to the bottom. Concerning the effect of moisture content on M_r of R+GR samples, a positive correlation was found between the M_r and the moisture contents. The correlation between the permanent deformation (P_d) of the R+GR samples and the glass content showed a significant increase in the P_d of the samples asthe glass

content increase. Regarding the thickness (the number) of the GR layer, an improvement in the P_d of the R+GR12 sample was associated with the layer thickness decrease. On the other hand, the P_d of the R+GR group at 24% (R+GR24) and 45% (R+GR45) were approximately constant with increasing the thicknesses of the GR24 and GR45 layers. It is also important to note that a high percentage of glass led to increase the P_d during the last seven loading sequences. Furthermore, the P_d of the GR sample decreased with decreasing the moisture content. However, moisture content played a significant role in the dynamic responses of the layered samples. Based on dynamic shear tests, the 12% glass content in the R+GR12 layered sample was considered as the best ratio of glassused in improving the shear resistance of the R+GR group. Moreover, when the number of the GR layers was lesser, the R+GR groups tended to show the best shear strength. Contrary to expectations, there was an improvement in shear strength of the R+GR group with increasing moisture content. Also, the M_r of the rock-sand samples decreased because of increasing the number of sand layers. Note that the rock-sand samples with a sand layerat the bottom showed lower P_d than the other samples, while the P_d of the rock-sand samples increased as the number of sand layers increased.

The dynamic behaviour of rock-bentonite samples was also considerably dependent on the position and the number of bentonite layers. Note that the M_r of the rock-bentonite samples decreased when the number of bentonite layers increase. It is apparent that the M_r value was the highest when the bentonite layer is close to the surface. The results of the rock-sand-bentonite samples indicated that the sample which the sand layer was located close to the bottom and the bentonite layer was located close to the top, showed the highest M_r value. The dynamic study results of the rock-bentonite sample concluded that the P_d of the samples increased because of increasing the number of bentonite layers, and the P_d of the samples increased when the bentonite layer was located near tothe bottom. However, two layers of bentonite enhanced the recoverable deformation of the rock-sand samples during the late stages of the tests. Moreover, the rock-sand-bentonite sample (R+S+R+BE+3R (100)) which the sand layer was located close to the base and the bentonite layer was located near to the top, showed less P_d than the R+BE+R+S+3R (100) sample.

Chapter 7: Modelling Resilience Susceptibility Using Artificial Intelligence

7.1 Introduction

In recent years, an increasing number of research works have focused on the use of artificial intelligence (AI) in engineering applications. The wide range of the sources and the soil fabric variations of granular materials led to large differences in the physical and chemical compositions and therefore, establishing a comprehensive model to predict the resilient modulus (M_r) depending on basic specifications of the base and subbase materials is a complex approach and contains many contradictions. A prediction model for M_r of base and subbase materials based on the IA with the basic characteristics of the materials still need further development. In the present study, two AI methods were used to achieve this development, artificial neural network (ANN) and genetic program (GP) models. It is important to mention that all of the datasets that have been used in this study were collected from test results of the previouse published works. Simply, the ANN and GP are defined as mathematical programs used to solve many complex problems at the same time. According to the previous studies, these programs can offer keys for high-level problems and submit approximate solutions for many problems concernthe geotechnical engineering applications and recently, they have widely used in developing models for the prediction of M_r of different soilsbased on their basic properties.

7.2 Artificial neural networks

ANNs have been effectively used to develop models for many geotechnical applications, such as 'determination of the swell potential of Kansas Soils' (Najjar et al., 2000), predicting settlement problems (Shahin et al., 2004), and predicting the M_r of subgrade and subbase soils (Park et al., 2009). The ANNs are multilayered network systems consisting of a group of layers: an input layer, an output layer and one or more hidden layers. A trial and error is a method of problem solving which employed in this study to obtain the optimum model of the ANN. Matlab's Neural Network Toolbox was also used in the ANN to analyse and normalise the input datasets. It is important to note that the input datasets used in this study were

collected from the results of the experimental studies of Gudishala (2004), Kim et al. (2007) and Siripun et al. (2009). These studies conducted a series of repeated loading triaxial tests (RLTTs) on different base materials, namely, crushed rock, crushed aggregate (Minnesota/USA) and crushed limestone (1&2), Table 7.1 illustrates the critical characteristics of these laboratory tests which employed with the AI to predict a M_r. It is important to mention that different RLTT protocols were conducted to prepare the samples used in previous studies, the first protocol for RLTT was the NCHRP 1-28A protocol, which involved thirty stress stages. In each stage the sample was subjected to a 100 loading cycles of a 207 kPa of deviator stress and a 103.5 kPa of confining pressure. Another RLTT protocol was Aust-Roads (APRG) protocol which involves of sixty-five stress paths. Each path is repeated two hundred cycles and each cycle consists of 0.1 seconds of loading followed by a 0.2 second rest period. The third protocol was AASHTO T-294 protocol, which involves of sixteen loading sequences including one conditioning sequence. In the conditioning stage, the loading cell applied 103 kPa of deviator pressure and 103 kPa of confining pressure during 1000 cycles. After the conditioning stage, each sample was subjected to 100 cycles; each cycle consisted of a 0.1-second loading period followed by a 0.9-second rest period.

In the present study the main parameters affecting the M_r of base and subbase materials were collected and used as input data. After collection stage, normalisation the datasets was implemented in this study to reduce the data redundancy and improve the data integrity. Table 7.2 shows the statistical distribution of each parameter. The input layer of the ANN involved of eight nodes, one node for each parameter. The input data included moisture content (M_c), dry density (γ_d), confining pressure (σ_c), deviator stress (σ_d), mean diameter (D_{50}), coefficient of curvature (C_c), coefficient of uniformity (C_u) and bulk stress (θ), as shown in Figure 7.1. It is apparent from this figure that the output layer consists of one node, which represents the M_r parameter. Based on the input and the output datasets, the ANN manages a complicated algorithm to estimate data values. According to Zaman et al. (2010), the feedforward network method is the best type of ANN for predicting M_r of granular materials. The information in feedforward networks travels only forward through the input nodes, hidden nodes and finally, the output nodes. The ANN in this study employed Levenberg-Marquardt back-propagation algorithm (LMA) method, which comprises of two layers of feedforward back-propagation and seven hidden neurons

to solve non-linear least squares problems and achieve a good curve fitting. To achieve a typical performance of the ANN, a trial and error approach was employed in the ANN to estimate the optimal number of nodes in the hidden layer and consequently, achieve the least root mean square error (RMSE). Based on the trial-and-error process and the efficiency of the outcomes, the coefficient of determination (R^2) value should be around 90%. The R^2 can be defined as the ratio between predicted M_r and that observed during experimental tests. As mentioned above, the independent variables used in this study were collected from previous laboratory studies concerning the calculation of the M_r value. Many previous studies have concluded that the moisture content, dry density and coefficient of uniformity of granular materials directly affect their M_r. Yang et al. (2005), Bilodeau and Doré (2012) and Rahman et al. (2016) reported a considerable effect of moisture content on the M_r values. There was also strong evidence that the M_r value depends on the particles shape, fine materials content and the particle size distribution of granular materials (Allen, 1973; Barksdale & Itani, 1989; Arnold, 2004). Whereas, Uzan (1985), Sweere (1990), Zakaria and Lees (1996), Maher et al. (2000), Dawson et al. (2000), and Van Niekerk et al. (2002) reported that the resilience behaviour of granular materials is very sensitive to the confining and deviator stresses levels. Rodgers (2006) used the ANN for developing a model to predict M_r values of two road base materials. Different parameters were employed in the development process including particles shape, plasticity index, liquid limits, moisture content, confining and deviator stresses. It is important to mention that the input datasets were divided into different groups and then used in the ANN. For example, the input datasets of Ohio soil were selected randomly from the input parameters and placed into training, validation and testing sets, while the input data of Mississippi soil were selected and split into training and testing sets. In conclusion section, Rodgers (2006) reported that the prediction results of Ohio soil showed higher accuracy compared to prediction results of Mississippi soil.

Based on the information above and according to the previous studies mentioned in section 2.10, the procedures followed in the present study for developing a model to predict the M_r value for base and subbase materials involved many steps:

1. Collection stage: collect input parameters from previous experimental studies, as presented in Table 7.1. Many independent variables were collected, including M_c%, γ_d, γ_c, σ_d, D_{50}, C_c, C_u and θ.

2. Normalisation stage: it is necessary in ANN normalising the input datasets before use it and so, all parameters values were normalised to values between 0 and 1.
3. Statistical distribution stage: statistical distribution program was used in this analytical study, and a summary of the statistical distribution of each parameter is presented in Table 7.2.

Table 7.1 Properties of base course materials

	RLTT method	M_C (%)	γ_d (kg/m^3)	D_{10}	D_{30}	D_{50}	D_{60}	Σc (MPa)	M_r (MPa)	Reference
crushed limestone (1&2)	AASHTO T-294	3.2-5.9	19.8-21.1	0.11-0.2	1- 1.2	4.2-4.7	7-7.1	21-41	190-246	Gudishala, (2004)
Minnesota, crushed aggregate	NCHRR 1-28A	4.7- 8.8	19.64-20.32	0.13-0.35	0.42-2.3	1.5-3.5	2.6-4.3	20-140	100-700	Kim et al., (2007)
Gosnolse quary, crushed rock	AUSTROADS (APRG)	4.96-6.2	23.2	0.212	1.18	3.1	5.2	20-150	95-330	Siripun et al., (2009)

Table 7.2 Statistical distribution of each parameter in the normalisation database

Parameters	M_C (%)	γ_d (kg/m^3)	σ_c (MPa)	σ_d (MPa)	D_{50}	C_c	C_u	θ	M_r (MPa)
Mean	0.07	20.20	0.07	0.11	3.54	2.23	29.7	0.3	0.30
Standard Error	0.00	0.06	0.00	0.00	0.10	0.12	2.10	0.01	0.01
Median	0.07	20.32	0.06	0.06	3.6	1.82	20	0.3	0.3
Mode	0.05	20.32	0.05	0.01	1.5	0.53	20	0.35	0.35
Standard Deviation	0.02	0.86	0.04	0.12	1.31	1.59	26.7	0.14	0.14
Sample Variance	0.00	0.75	0.00	0.01	1.72	2.53	15.7	0.02	0.02
Kurtosis	-0.64	1.89	-1.21	1.50	-0.93	-0.83	0.76	-0.64	-0.64
Skewness	0.51	-1.12	0.32	1.61	-0.34	0.63	1.47	0.08	0.08
Range	0.06	3.71	0.12	0.4	4.2	4.89	86.3	0.63	0.63
Minimum	0.04	18	0.02	0.01	1.5	0.46	7	0.07	0.07
Maximum	0.11	21.71	0.14	0.45	5.7	5.35	93.3	0.7	0.7

The present study tried to select the best strategy and network architecture to achieve the best performance of a model to predict the M_r. According to the previous studies, the dataset was randomly divided into three groups in proportions of 70%, 15% and 15% for the training, testing and validation datasets, respectively. It is important to note that the training dataset was used to estimate the weights of the datasets. A schematic representation of ANNs including the input, hidden and output layers is shown in Figure 7.1. It is apparent that the model consists of eight input parameters in the input layer, two hidden layers and one output layer. Three main factors can affect the ranking of the ANN model: the number of hidden neurons, and the performances of the training, testing and validation sets. Based on the trial-and-error stage, the number of ANN parameters was varied to achieve the best performance and according to that, five models were tried in this study. Note that the training set played a significant role in the prediction process, and the best performance of the ANN models was nominated when the R^2 value around 90% and the RMSE is the minimal (Das & Basudhar, 2008; Muduli & Das, 2014a).

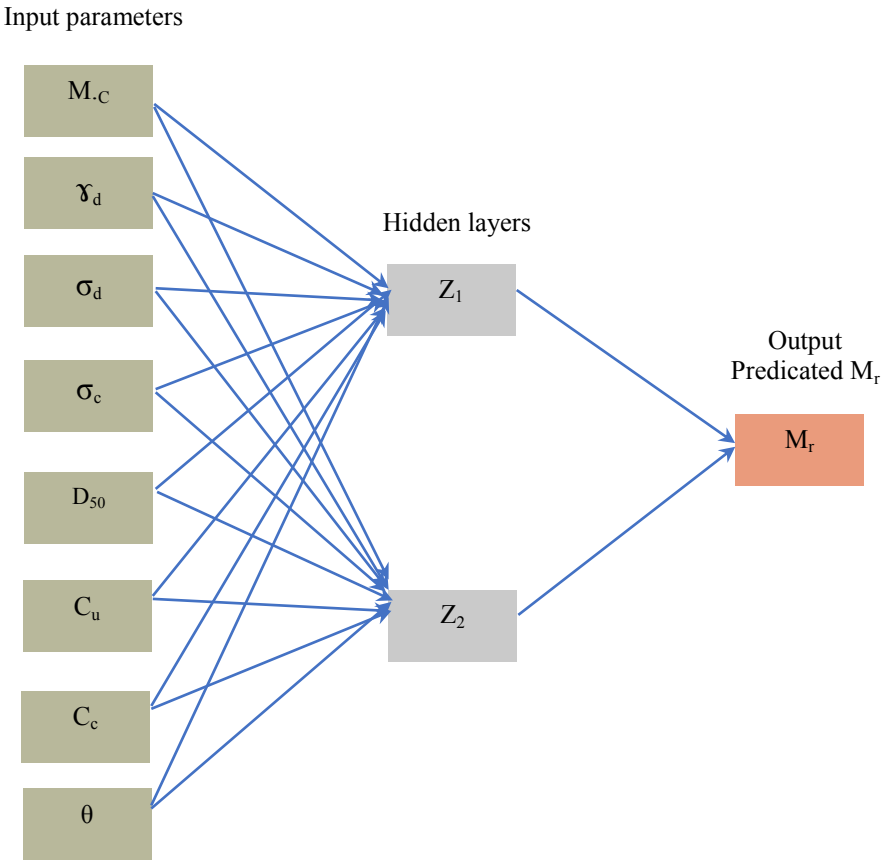

Figure 7.1 Schematic representation of artificial neural networks

Based on the input datasets of model 1, all parameters including M_c, γ_d, σ_c, σ_d, D_{50}, C_c, C_u and θ were used in the ANN program, and the results of R^2 for mode l are presented in Table 7.3. The values of R^2 were 0.985, 0.986, 0.989 and 0.981 for the overall, training, testing and validation datasets, respectively. It is apparent from the table that the RMSE of the overall dataset was 0.0442, which was the lowest overall value among the models. It is clear from the results that the R^2-value of model 1 was > 0.9 and therefore, the performance of model 1 could be the best. A comparison of the measured and the predicted M_r for model 1 is presented in Figure 7.2. It is important to note that model 1 showed the highest R^2 for both the overall and testing sets compared to the other models. Figure 7.3 illustrates the accuracy assessment of training, validation, testing, and overall sets of model 1.

Table 7.3 Details of the performance of model 1

Model no.	Input parameters	Number of hidden layers	Datasets	Performance	
				R^2	RMSE
1	M_c, γ_d, σ_c, σ_d, D_{50}, C_c, C_u, θ	2	Overall	0.985	0.0442
			Training	0.986	0.0355
			Testing	0.989	0.0880
			Validation	0.981	0.1095

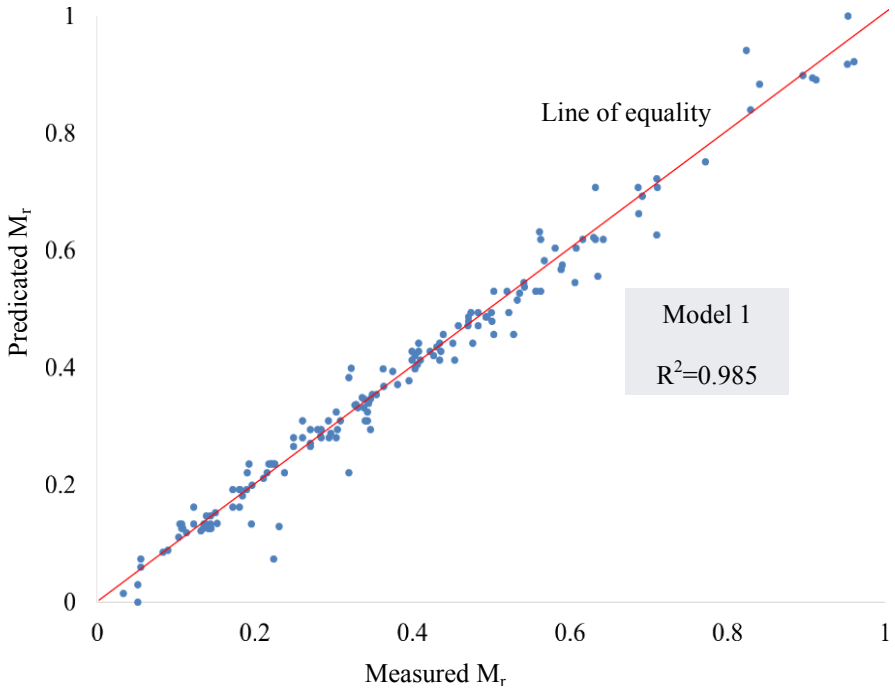

Figure 7.2 Measured *vs.* Prediction resilient modulus for ANN model 1

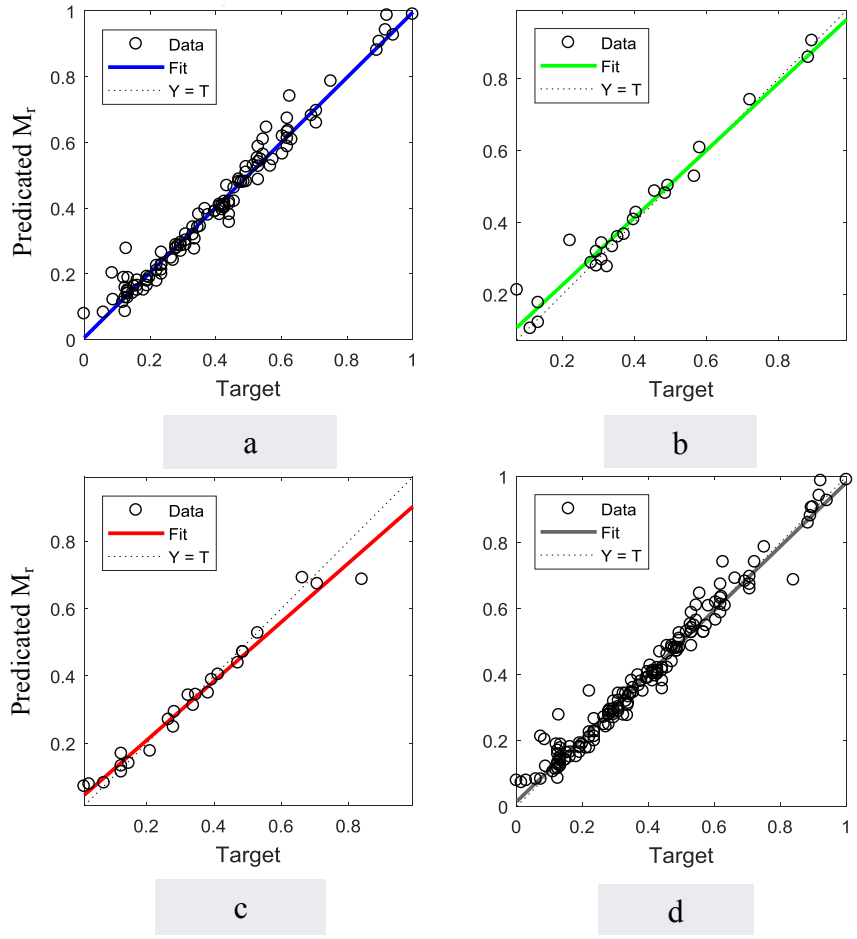

Figure 7.3 Accuracy assessment of model 1: a) training, b) validation, c) testing, and d) overall sets

It is apparent from Table 7.4 that the R^2 values for model 2 are 0.92, 0.989, 0.81 and 0.960 for the overall, training, testing and validation datasets, respectively. Note that the overall RMSE value was 0.0744. There was a reduction in the adjusted R^2 of the testing set of model 2 from 0.989 to 0.81 and an increase in the RMSE from 0.0880 to 0.1424 as a result of the C_c exclusion from the input data of the ANN. A comparison of the measured and the predicted M_r for model 2 is presented in Figure 7.4. The reduction in the R^2 values for the overall was related to the role of the C_c on the M_r prediction. Figure 7.5 illustrates additional evidence that the predictive accuracy of the model was affected by the C_c exclusion from the ANN dataset.

Table 7.4 Details of the performance of model 2

Model no.	Input parameters	Number of hidden layers	Datasets	Performance	
				R^2	RMSE
2	M_c, γ_d, σ_c, σ_d, D_{50}, C_u, θ	2	Overall	0.955	0.0744
			Training	0.989	0.0155
			Testing	0.81	0.1424
			Validation	0.960	0.1780

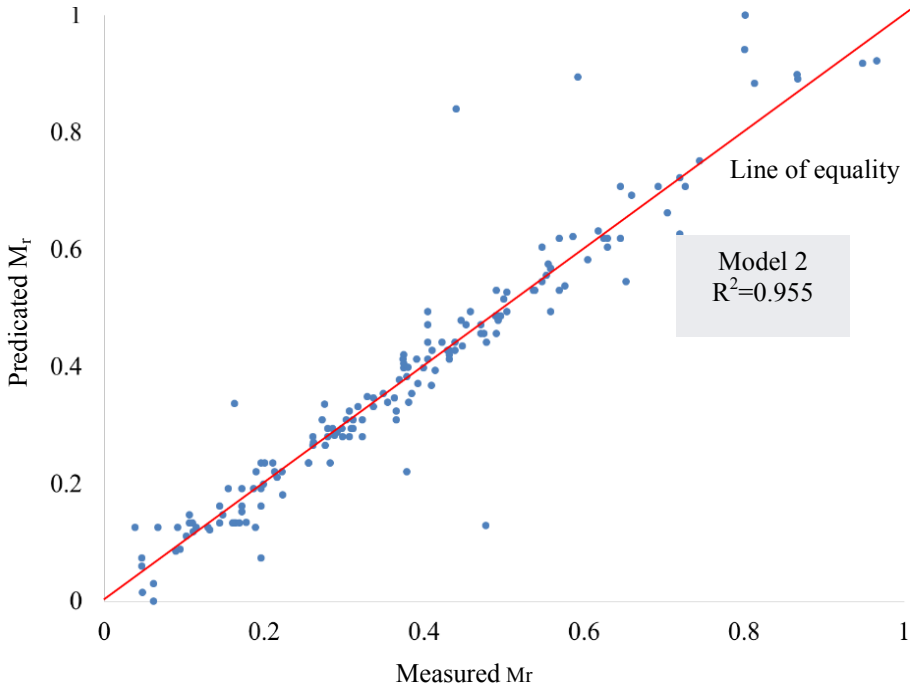

Figure 7.4 Measured *vs*. predicted resilient moduli for ANN model 2

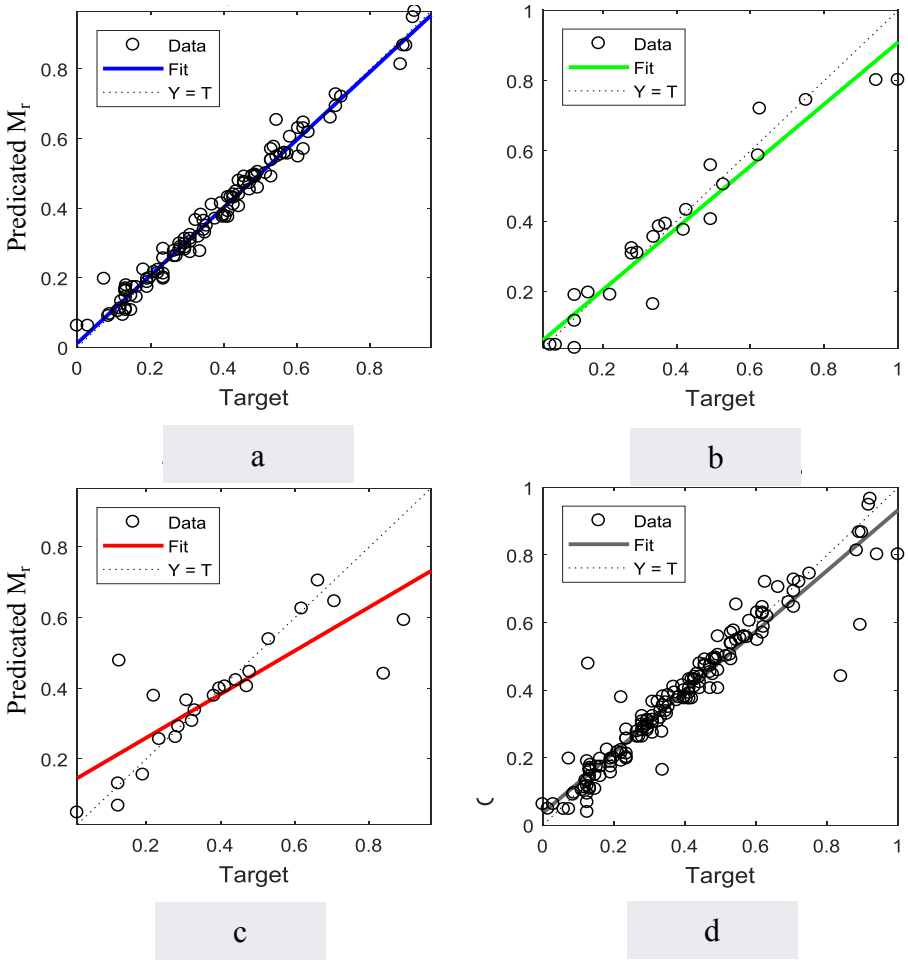

Figure 7.5 Accuracy assessment of model 2: a) training, b) validation, c) testing, and d) overall sets

As shown in Table 7.5, the R^2 values of model 3 for the overall, training, testing and validation datasets were 0.970, 0.997, 0.847 and 0.982, respectively. It is apparent from the table the RMSE of the overall dataset was 0.0469. It is also clear from Figure 7.6 that there was a significant reduction in R^2 of the testing set from 0.989 to 0.847 and an increase in RMSE from 0.0880 to 0.1816 as a result of the exclusion Cu from the ANN input data. Also, a marked drop in the accuracy of training, validation, and testing datasets for model 3 was noticeable because of the Cu exclusion from the input data, as shown in Figure 7.7.

Table 7.5 Details of the performance of model 3

Model no.	Input parameters	Number of hidden layers	Datasets	Performance	
				R^2	RMSE
3	M_c, γ_d, σ_c, σ_d, D_{50}, C_c, θ	2	Overall	0.970	0.0469
			Training	0.997	0.0151
			Testing	0.847	0.1816
			Validation	0.982	0.0693

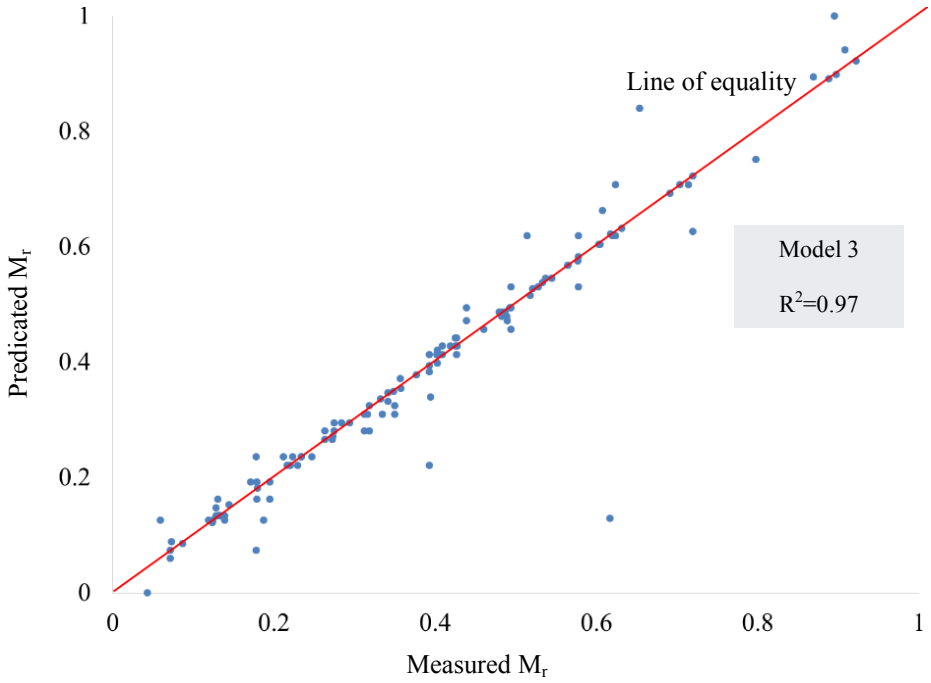

Figure 7.6 Measured *vs.* Prediction resilient moduli for ANN model 3

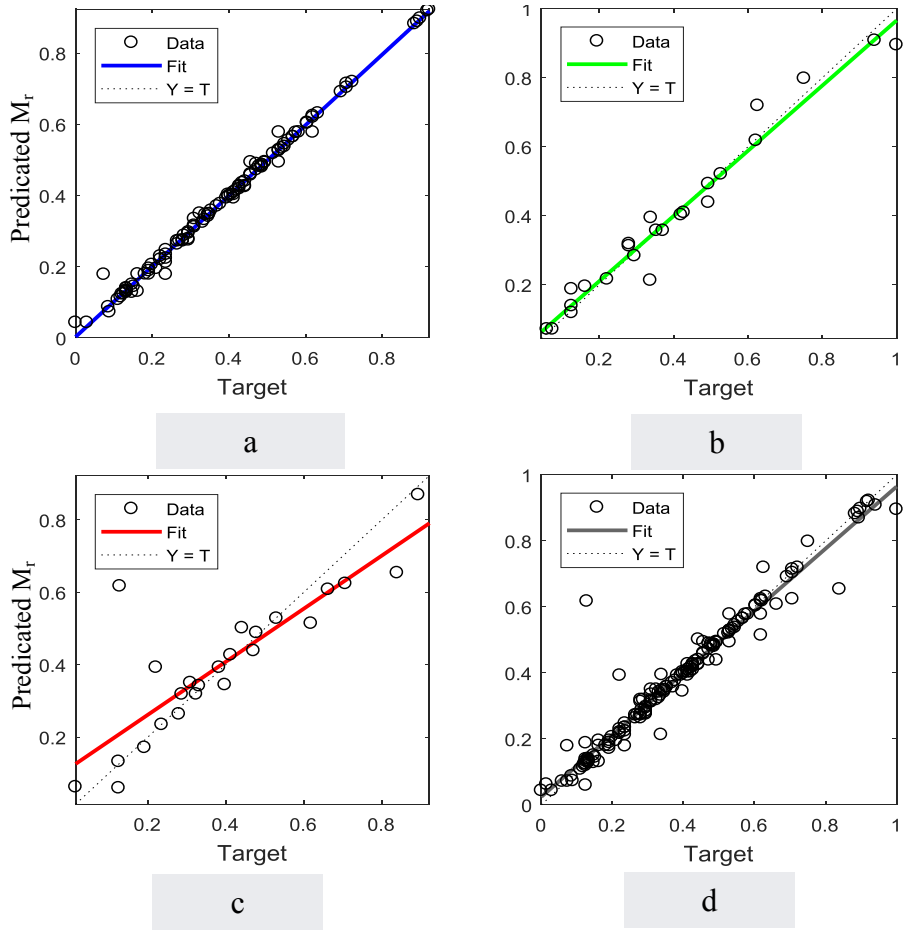

Figure 7.7 Accuracy assessment of model 3: a) training, b) validation, c) testing, and d) overall sets

As detailed in Table 7.6, an increase in the RMSE of the testing set of model 4 from 0.0880 to 0.1533 was associated with the D_{50} exclusion. As can be seen from Figure 7.8, the R^2 value was unaffected by the D_{50} exclusion from the ANN dataset. Figure 7.9 provides further evidence of the result above, that the model of M_r was unaffected by the D_{50} exclusion.

Table 7.6 Details of the performance of model 4

Model no.	Input parameters	Number of hidden layers	Datasets	Performance	
				R^2	RMSE
4	M_c, γ_d, σ_c, σ_d, C_c, C_u, θ	2	Overall	0.982	0.060
			Training	0.993	0.020
			Testing	0.950	0.1533
			Validation	0.944	0.1278

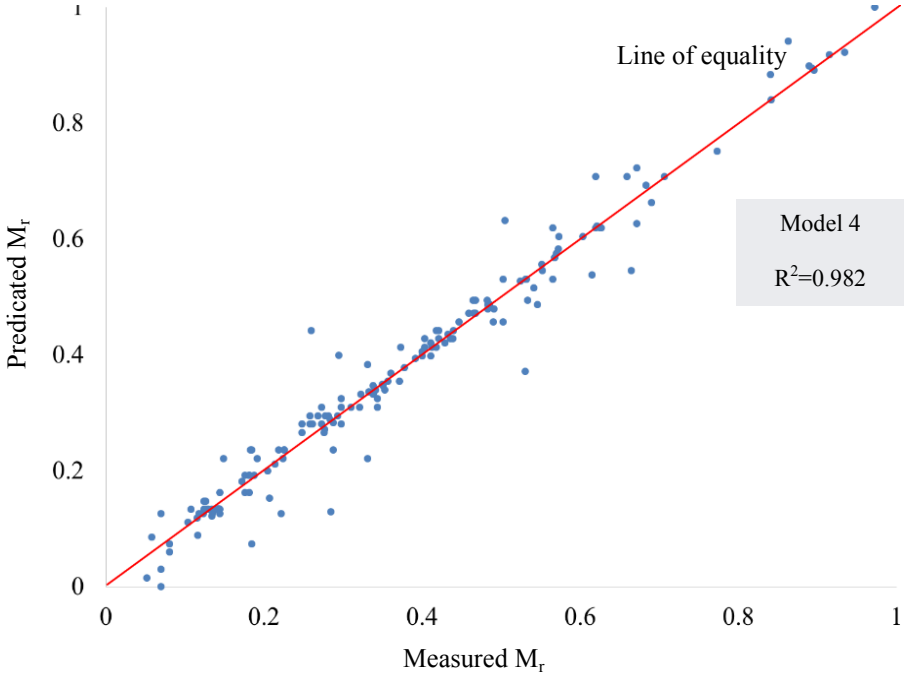

Figure 7.8 Measured *vs.* Prediction resilient moduli for ANN model 4

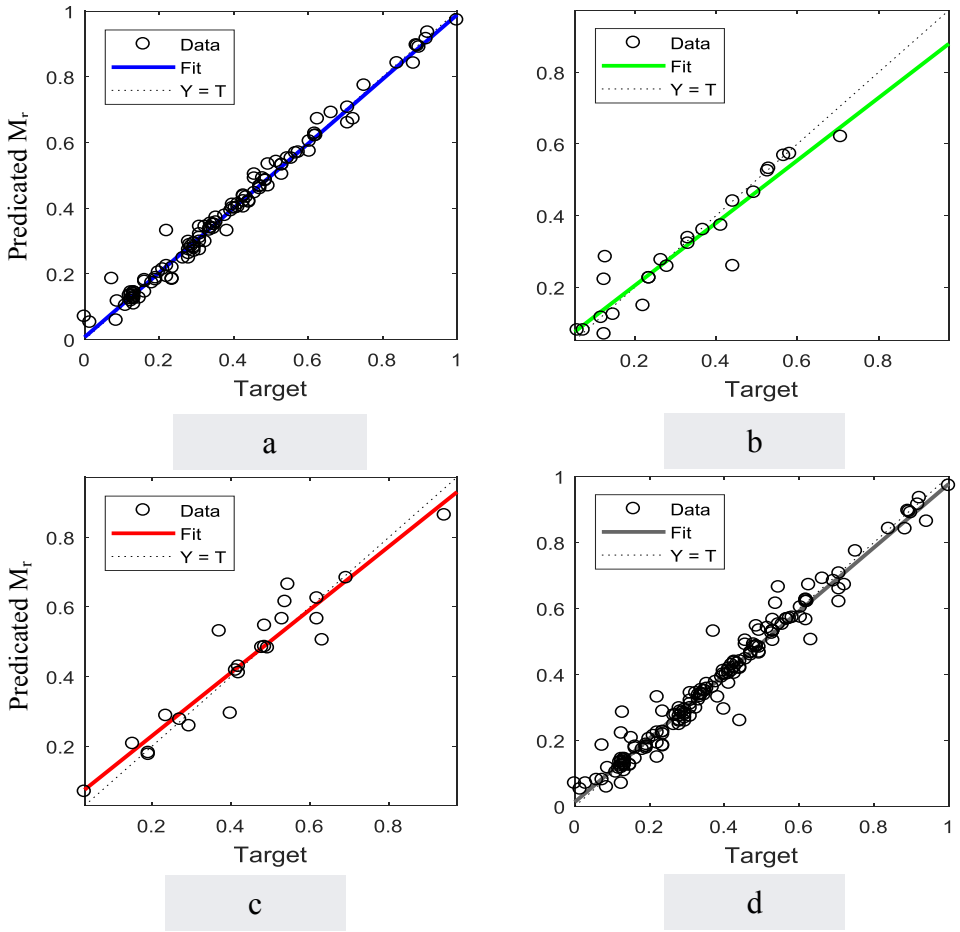

Figure 7.9 Accuracy assessment of model 4: a) training, b) validation, c) testing, and d) overall sets

The M_c was excluded from the input data of the ANN to create model 5. According to Table 7.7 and Figure 7.10, model 5 reported the lowest R^2 and highest RMSE values. The R^2 values of the overall and testing sets were 0.81 and 0.707, respectively; the overall RMSE value was 0.2549. Based on these results, M_c was considered a significant influence on the M_r prediction. Figure 7.11 presents the prediction ranking of model 5, which demonstrated the accuracy-values for the training, validation and testing datasets.

Table 7.7 Details of the performance of model 5

Model no.	Input parameters	Number of hidden layers	Datasets	Performance	
				R^2	RMSE
5	γ_d, σ_c, σ_d, D_{50}, C_c, C_u, θ	2	Overall	0.810	0.2549
			Training	0.830	0.0824
			Testing	0.707	0.2756
			Validation	0.860	0.2073

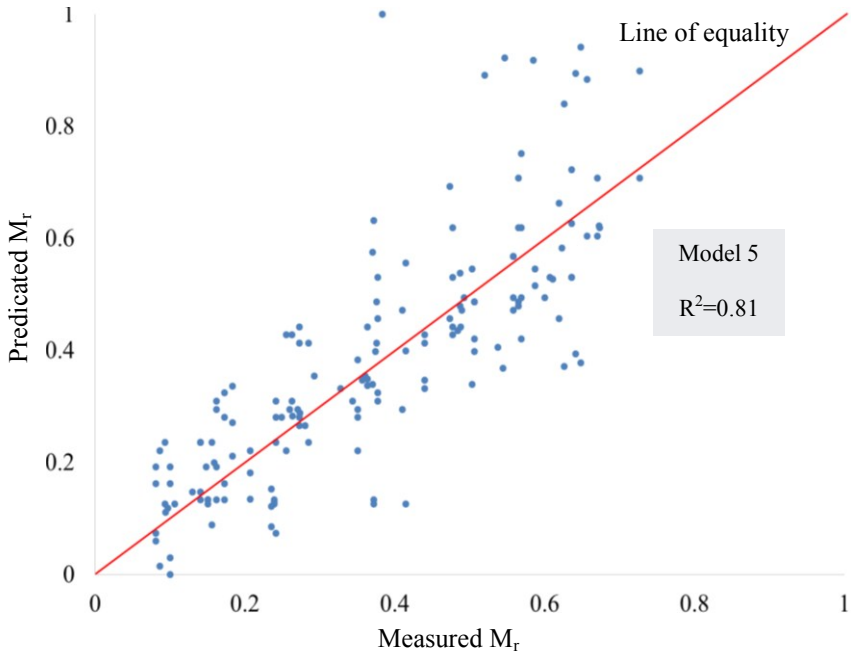

Figure 7.10 Measured *vs.* Prediction resilient moduli for ANN model 5

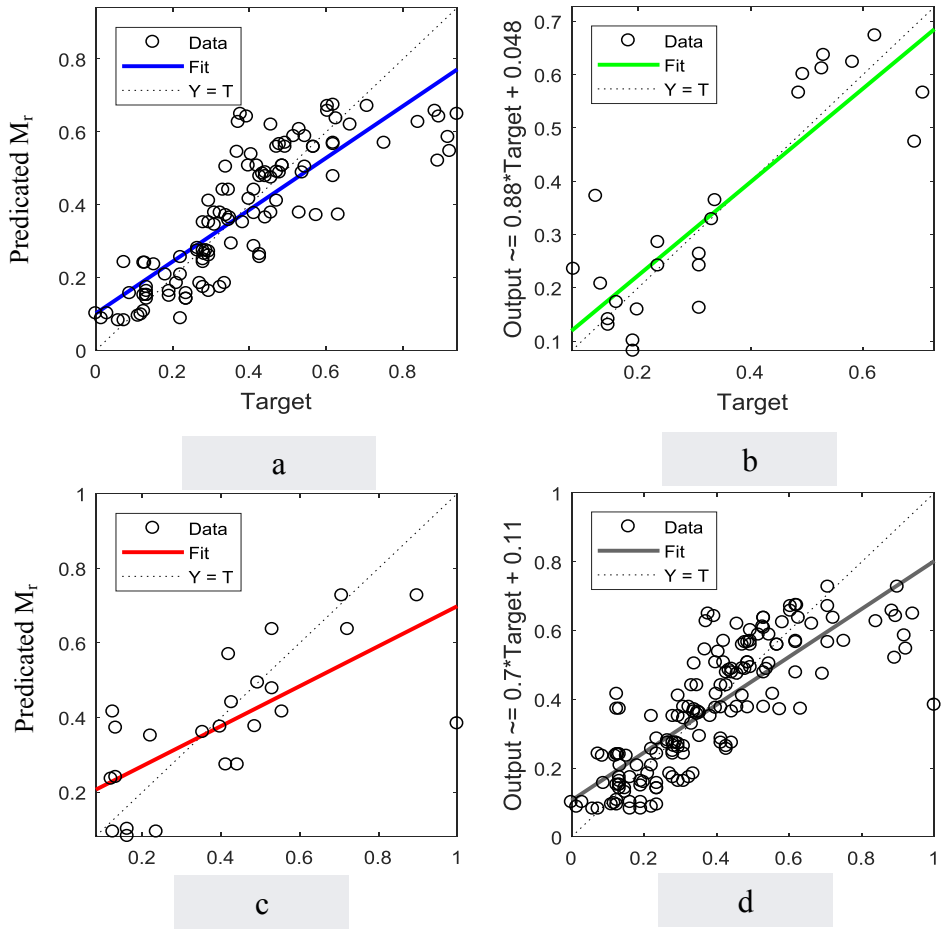

Figure 7.11 Accuracy assessment of model 5: a) training, b) validation, c) testing, and d) overall sets

Figure 7.12 illustrates the correlation between the M_r predicted by the ANN models (1, 2, 3, 4 and 5) and the measured M_r. Except for model 5, the developed models showed high ability to predict M_r with a high efficiency. The figure also shows that all predicted points are around the bisector line, which is a good indication of the models performances.

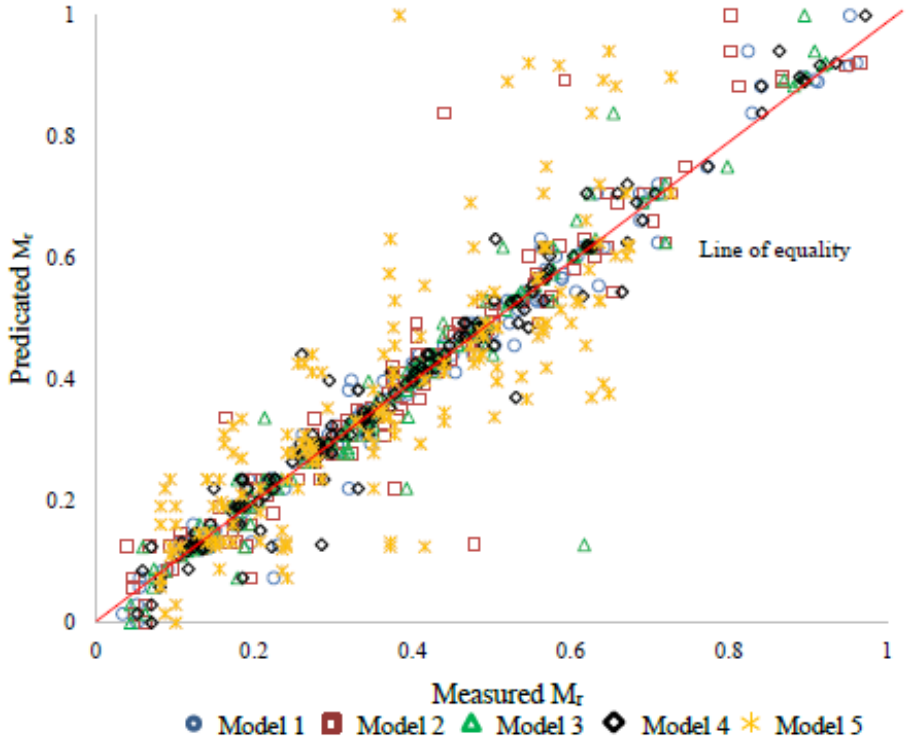

Figure 7.12 Measured *vs.* Prediction resilient moduli for all ANN models

7.3 Genetic programming

In the present study, genetic programming (GP) was used to construct a model of M_r of base and subbase materials. Based on Heuristic Lab software, an extensive database was employed with the ANN model to develop a modelfor the M_r prediction. In the ANN section above, model 1 exhibited the highest value of R^2 for the training set and displayed the best performance concerning the M_r prediction. As mentioned before, eight independent variables were employed as input datasets in the GP model: M_c, γ_d, σ_c, σ_d, D_{50}, C_c, C_u and θ, whereas the output was the M_r value. The symbolic regression parameters of the GP are detailed in Table 7.8. Based on the training/testing ratio, the weight of the input data varied between (90/10), (80/20) and (70/30). The high performance of the GP happened when 80% of the input data was used as a training set and 20% as a testing set. It is apparent from Table 7.8 that the maximum number of generations that applied by the software program for achieving a high R^2 for training and testing and consequently the best model is 100 cycles. Equation 7.1 expresses the mathematical correlation between the input and the output data. The coefficients of the constant values such as c_1 and c_2 are represented in Table 7.9.

Table 7.8 Symbolic regression parameters

Parameters	Value
Population size	1000
Maximum number of generations	100
Parent selection	Tournament (group size 7)
Replacement	1-Elitism
Crossover	Sub-tree-swapping
Mutation rate	15%
Fitness function	R^2 and RMSE
Function set	+, −, *, Log
Terminal set	Constant, variable

$$M_r=(((c_1\times M_c)-(s(0.8701\times\sigma_c-(1.2624\times C_u+c_2)+c_3)\times(((0.69774\times M_c+0.73812)-c_4)+0.42171\times(0.43505-\mathrm{Log}(0.27338C_u))))+((c_5+0.62938\times\gamma_d)\times(0.8701\times\sigma_c-\mathrm{Log}((0.69774\times M_c+1.2042\times\gamma_d)))\times c_5+(c_1\times\gamma_d)-c_6))+(0.8701\times\sigma_c+4.5981)))\times(-0.0099981)+c_7) \quad (7.1)$$

Table 7.9 Coefficients of Equation (7.2)

c_1	c_2	c_3	c_4	c_5	c_6	c_7
12.353	0.73812	0.75301	1.5	-5.009	3.1141	0.36381

According to Equation 7.1, M_c, σ_c, C_u and γ_d are considered the most relevant state variables to characterise the resilience behaviour of base and subbase materials. M_c is an important parameter in relation to the dynamic response of base and subbase materials.This result was consistent with the conclusions by many previous studies (Yoder et al., 1975; Yang et al., 2005; Bilodeau & Doré, 2012; Rahman & Erlingsson, 2016). In addition, the shape of the σ_c plays a significant role in determining the M_r value of granular materials, and this finding was also consistent with the previouse results of laboratory studies (Morgan, 1966; Uzan, 1985; Sweere

,1990; Zakaria and Lees, 1996; Maher et al., 2000; Dawson et al., 2000; Van Niekerket al., 2002). The present result was also consistent with the previous results concerning the effect of Cu variable on the M_r value, which referred to the importance role of Cu when studying the resilience behaviour of roadbase and subbase materials (Papin, 1979;and Thom & Brown, 1988). It is also apparent that the resilence behaviour of base and subbase materials is affected by the γ_d factor. This result of the present study was consistent with the findings of Barksdale and Itani (1989), and Vuong (1992), who reported thatthe M_r values of granular materials was influenced by density. As mentioned before, the R^2 and RMSE were employed in the present study to assess the performance of the developed models. Table 7.10 shows the performance of the developed GP model for the training and testing datasets.

Table 7.10 Performance of the resilient modulus model for the training and testing datasets

Dataset	Performance	
	R^2	RMSE
Training	0.83	0.09
Testing	0.81	0.09

Figure 7.13 shows the typical genetic programming tree for the GP model. A series of central and binary nodes were connected to build the tree, as shown in the figure. In the tree, the nodes are including but not limited to constants, variables, functions.

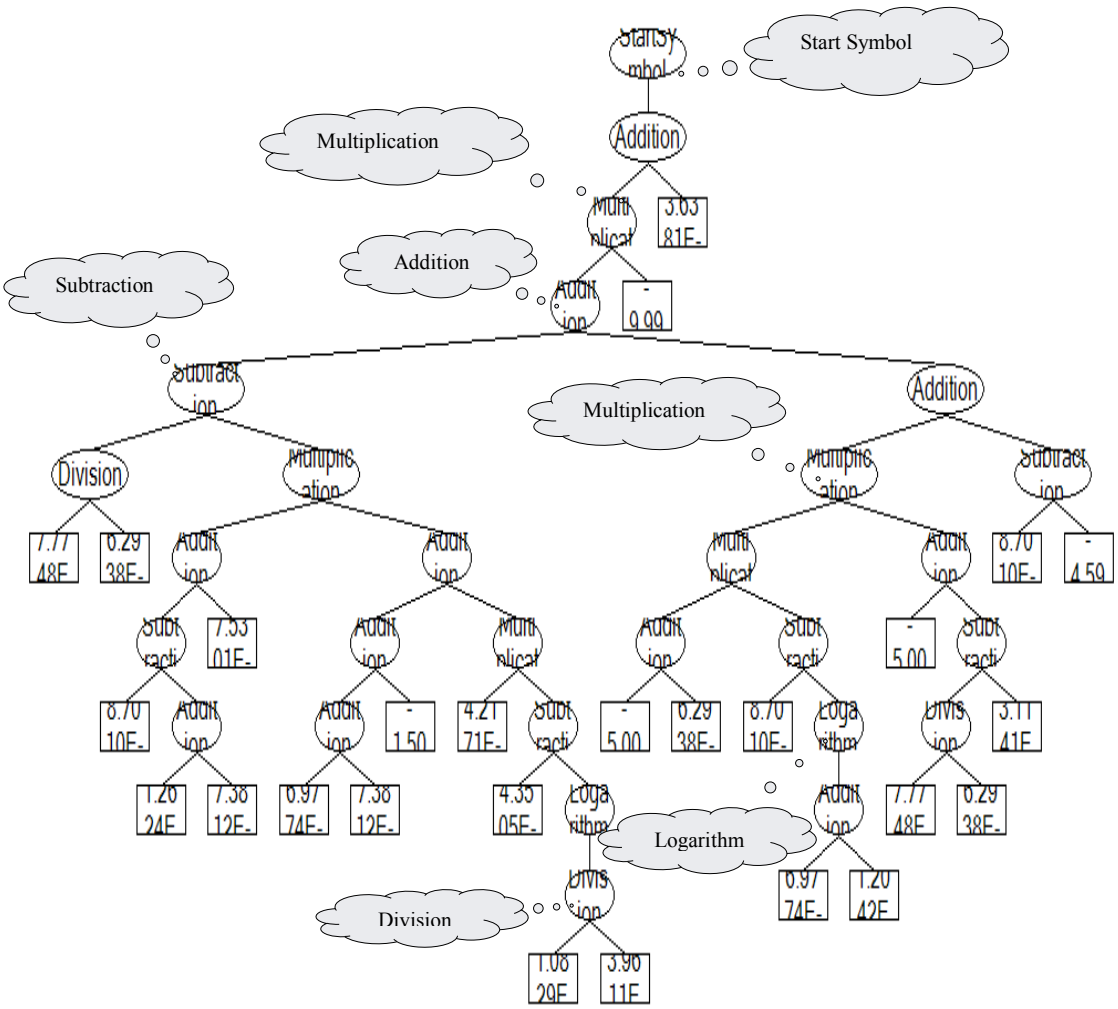

Figure 7.13 Tree of the GP model

Based on Equation 7.1, Figure 7.14 illustrates the measured values of the M_r against those the predicted by the GP model. It is apparent from this figure that the almost M_r values are distributed around the line of equality, which indicated a good agreement between the measured and the predicted M_r values. Therefore, the modified model is considered reasonably well and has great ability to predict the M_r value with a high accuracy. Figure 7.15 shows a comparison between the M_r of the training and testing sets of the GP model with the target M_r (the estimated). It is apparent from this figure that a significant similarity was noticeable between the training-testing outcomes and the estimated ones.

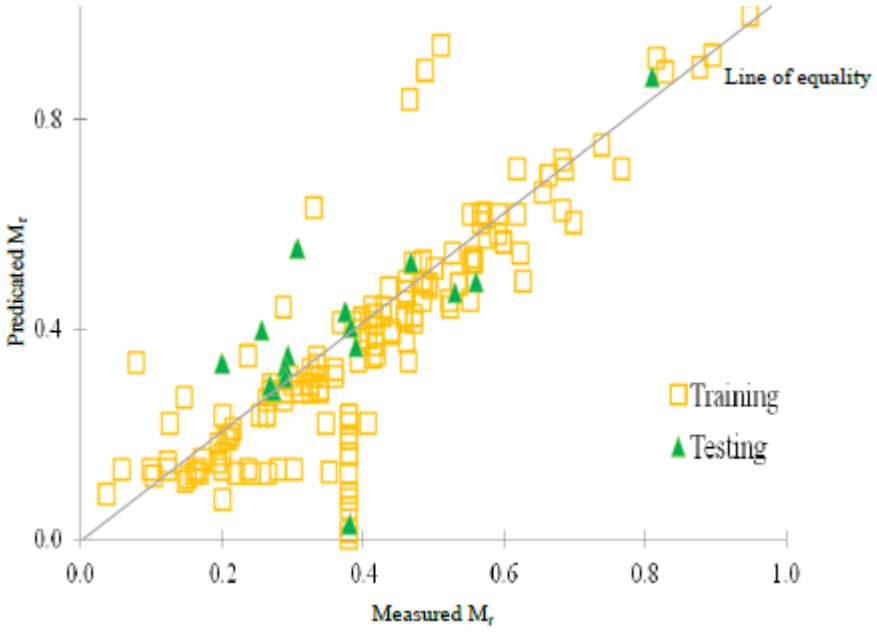

Figure 7.14 Measured values of resilient modulus *vs.* those predicted by the GP model

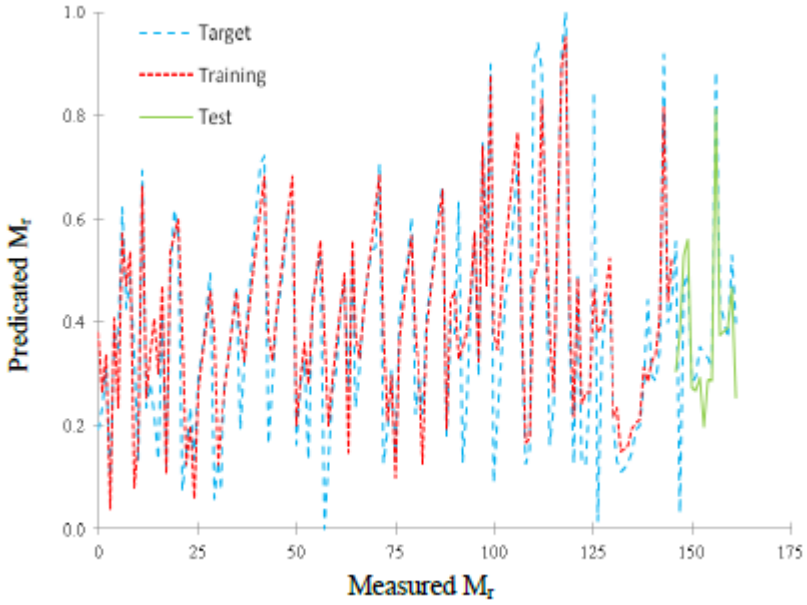

Figure 7.15 Line charts of training and test datasets of the GP model (a comparison between the resilient modulus of the training-testing sets and the estimated resilient modulus)

7.4 Summary

Many basic parameters, which considered as influencing factors on the resilient modulus (M_r) value of granular materials, were employed in this chapter with artificial neural network (ANN) and genetic algorithm (GP) to develop a model for

predicting the M_r value of base and subbase materials. The basic parameters, including M_c, γ_d, σ_c, σ_d, D_{50}, C_c, C_u and θ, were collected from the published experimental studies, and then used as an input dataset in the ANN to develop a model. In general, the results of the ANN model and the GP model illustrated high accuracy with respect to the prediction of the M_r value of base and subbase materials, where the values of R^2 of the testing set were 0.985 and 0.81 for the ANN and GP models, respectively. Based on the results of the ANN models, model 1, which all eight parameters were used with the ANN, showed the highest R^2 value at the testing set and the lowest RMSE value. This behaviour is a strong indication that model 1 is the best model for predicting the M_r of base and subbase materials. Depending on the results of model 2, the drop in the prediction accuracy of the ANN model was associated with the C_c exclusion from the input dataset. In addition, model 3 revealed a marked drop in the R^2 value in the training, validation and testing sets because of the C_u exclusion. In model 4, it is uncertain that the D_{50} exclusion affected on the ANN results. In model 5, the moisture content showed the highest influence on the prediction accuracy of the ANN. According to the GP results, the mathematical formula for estimating the M_r value was influenced by many basic parameters of base and subbase materials: M_c, σ_c, C_u and γ_d. Additionally, the findings stated an agreement between the ANN and the GP models concerning the prediction of the M_r. Even though that the AI models were successful in developing high accuracy models to predict the resilient modulus of base ans subbase materials, the predicted models still need more attention.

Chapter 8: Conclusions and Recommendations

8.1 Introduction

The influence of waste materials on the dynamic behaviour of foundation materials in road applications has been widely addressed in previous studies. With regards to this subject, preliminary and dynamic investigations were conducted on different samples of rock material containing a range of glass and tyre rubber materials to assess the dynamic performance of the developed mixtures. Based on a layering technique, the effect of inclusion of different layers of glass, sand and bentonite on dynamic behaviour of rock samples was also investigated. A comparison between layered and homogenous structures was also presented to identify the advantages and disadvantages of each type. Further studies were performed to assess the effect of cement and slag inclusion on the resilience performance of rock-glass-rubber mixtures under repeated loading. An analytical study was also performed to develop models for predicting resilient modulus (M_r) of base and subbase materials. The study used genetic algorithm and artificial neural network approaches to produce models based on basic preliminary parameters of base and subbase material. These efforts help to develop the current state of knowledge regarding the effect of waste materials and preparation techniques on the dynamic behaviour of crushed rock base materials, and also help in developing a high accuracy model for predicting M_r of base and subbase materials.

8.2 Conclusions

The present research provides significant conclusion results concerning the suitability of using different waste materials in road layers; the following overall conclusions are drawn.

8.2.1 Characterisations of glass-rock mixtures

1. The results of the particle size distributions showed that all the samples of glass-rock mixtures containing 12%, 24%, and 45% glass were satisfied the base material requirements of VicRoads before and after compaction stage. Concerning the results of the modified compaction tests, the maximum dry

densities (MDDs) are 2.4 tons/m^3 and 1.77 ton/m^3 for crushed rock and crushed glass, respectively, whereas the optimum moisture contents (OMCs) are 6% and 1.8% for crushed rock and crushed glass, respectively. In addition, a steady reduction in the MDD of glass-rock mixtures occurred with the addition of glass, where the MDD of glass-rock mixtures were 2.34, 2.325 and 2.248 tons/m^3 for the GR12, GR24 and GR45 samples, respectively. The OMC of the GR12, GR24 and GR45 mixtures were 5.6, 5.9 and 6.2, respectively. It is important to note that the (glass/rock)-OMC curve reached to the peak point at 13% of the glass content, after this ratio the OMC increased with the glass increase. According to the results of specific gravity and water absorption tests, the specific gravities of crushed rock and crushed glass were 2.96 and 2.28, respectively. A reduction in the specific gravity of glass-rock mixtures was noticeable with increasing glass content. This result was attributed to that the crushed rock contains high densities course particles more than the crushed glass. The specific gravities of the GR12, GR24 and GR45 mixtures were 2.78, 2.75 and 3.66, respectively. Furthermore, significant reductions in water absorption and organic content were associated with the glass content increase. On the other hand, an increase in the p_H of glass-rock mixtures was observed with increasing the glass content.

2. Regarding the results of repeated loading triaxial test (RLTT), increasing the glass content from 12% to 45% caused in improving the M_r of rock from 6.6% to 50%. Regarding the influence of moisture on the M_r of glass-rock mixtures, reducing the moisture content from 100% to 70% of the OMC played a vital role in improving the M_r. Further investigation of drained-undrained conditions of the RLTT was also performed. The results indicated that the M_r value of drained mixture showed higher M_r than the undrained one.
3. The permanent deformation (P_d) of pure rock at 100% OMC changed significantly with glass content. The glass presence inversely affected on the rock fabric and consequently, increased the P_d. Also, a positive correlation was found between the P_d of glass-rock mixtures and the glass content increase.
4. A clear reduction in shear strength of the rock-glass mixtures was associated with the glass content increase. The stress-strain curve of the GR12 sample showed significantly more curvature than the curve of the rock sample. In addition, a dramatic drop in the peak shear was associated with increasing the glass content.

8.2.2 Characterisations of tyres rubber-rock mixtures

1. The gradation curves of the rubber-rock mixtures were significantly influenced by rubber contents (5%, 10%, and 15%). According to the upper and the lower VicRoads limits, all rock-rubber mixtures were unsatisfied the requirements of base materials before and after compaction. The results of modified compaction tests indicated that a significant reduction in the MDD of rock-rubber samples was associated with the rubber content increase. Also, there was an apparent reduction in the OMC of pure rock sample when blended with 5% rubber. It is important to know that the peak points of the compaction curves steadily increased with increasing rubber content, which is mean a steady increase in the OMC of the rubber-rock mixtures was associated with the rubber content increase. In addition, the compaction curves flattened and approached constant values with increasing rubber content. The results of preliminary tests indicated that significant reductions in the specific gravity, water absorption, p_H and organic content of pure rock were occurred with increasing rubber content.
2. Based on the RLTT results, there was a significant reduction in the M_r of rock specimens with increasing rubber content. It is important to note that the sample prepared at 70% OMC showed a higher M_r than that at 100% OMC. In general, rubber exerted a significant effect on the M_r values when prepared at 70% OMC. The rubber-rock mixture at 15% rubber content (TR15) showed much higher P_d than the samples with 5% and 10% rubber contents. Additionally, there was a positive correlation between the moisture content and the P_d of rubber-rock mixtures with 5% rubber content (TR5). On the other hand, the TR10 and TR15 specimens at 70% OMC showed more P_d than that at 100% OMC during the final stages of the RLTT.
3. Regarding the shear responses of the rubber-rock mixtures, a sharp reduction in shear strength was noticeable with increasing rubber contents. It is interesting to note that the stress-strain curves of the rubber-rock mixture showed more softened than the curve of pure rock. In addition, the mixture at 100% OMC appeared to have lower shear strength than that at 70% OMC. In terms of the confining pressure variation, the peak of the stress-strain curves became higher at higher confining pressures.

8.2.3 Characterisations of glass-rock-rubber mixtures

1. According to results of sieve analyses tests, the grading curves for the GR45T5 and GR24T5 mixtures before compaction fell approximately between the upper and the lower VicRoads limits. After the compaction stage, the particle size distribution curves for all specimens were approximately within the VicRoads limits. Based on modified compaction tests, a significant reduction in the MDD was associated with the glass and rubber presence, while a positive correlation was noticeable between the OMC of glass-rock-rubber mixtures and the glass and rubber content increase. The results of the glass-rock-rubber mixtures indicated that the values of specific gravity and water absorption were reduced directly by increasing the glass and rubber content. At high glass and rubber contents, the glass-rock-rubber mixture showed the highest organic content and p_H values.
2. The results from the RLTT indicated that the M_r values of the GR12T5, GR24T5 and GR45T5 samples increased by the addition of glass content from 12% to 45%. Whereas a steady reduction in M_r of the glass-rock-rubber mixtures was noticeable as the rubber content increased from 5% to 15%. One unanticipated finding was noticeable in the glass-rock-rubber mixtures at 5% rubber, where a clear trend of decreasing M_r as the moisture content decreased. Whereas the mixtures with 10% and 15% rubber contents showed the highest M_r at lowest moisture content.
3. Based on the P_d results for the glass-rock-rubber mixtures, the P_d decreased with glass content, while a dramatic increase in P_d was associated with the rubber increase. In general, mixing glass and rubber with rock exerted a powerful effect upon the P_d of rubber-rock mixtures during the RLTTs. In addition, the results demonstrated a positive correlation between the moisture content and the P_d for all mixtures. It is important to note that glass content exerted a strong influence on the P_d of rubber-rock mixtures at 70% OMC.
4. Based on the results of dynamic shear tests, the shear strength of glass-rock-rubber mixtures decreased with the glass content increase. The results also indicate that the mixture at 100% OMC showed higher shear strength than the mixture at 70% OMC. The stress-strain curves of the glass-rock-rubber mixtures were significantly affected by the confining pressures (35, 70 and 150 kPa). This

finding indicates that all mixtures exhibited a significant increase in shear strength as a result of increasing the confining pressure.

8.2.4 Characterisations of glass-rock-cement and the glass-rock-cement-slag mixtures

1. The M_r of cement-treated samples showed a wide range of variation depending on the mixture type. The glass-rock-cement mixture with 12% glass and 2% cement showed higher M_r than the pure rock sample after seven days of hydration. The M_r increased from 300 to 500 MPa as a result of mixing 2% cement with the GR12 mixture. It is clear from the RLTTs that cement-slag addition influenced the M_r of glass-rock mixtures. It is essential to note that an improvement in the M_r of the GR12 sample was associated with 1% cement and 1% slag. The M_r of the GR12 sample increased from 300 to 400 MPa as a result of adding cement and slag. On the other hand, the cement treated sample of the GR12 mixture (GR12C2-7) showed a higher M_r than the cement-slag treated sample (GR12C1S-7).
2. The influence of cement on the P_d of the GR12 mixture was also considered. The results indicated that a slight difference in the P_d was found between the treated and the untreated GR12 mixtures.
3. A negative correlation was found between the shear strength of the GR12 mixture and the cement presence. However, the cement treated sample of the GR12 mixture after seven days exhibited lower shear strength than the untreated sample. The presence of 1% slag and 1% cement could not improve the shear strength of the GR12 mixture. However, the GR12C2-7 mixture exhibited higher shear strength than the GR12C1S-7 mixture.

8.2.5 Characterisations of rubber-rock-cement mixtures (TR5C2-7) and rubber-rock-cement-slag mixtures (TR5C1S-7)

1. According to the results of RLTTs, 2% cement addition slightly improved the M_r of the TR5 mixture after seven days. One of the significant findings was that the M_r of untreated TR5 mixtures was influenced by the mixture of 1% cement and 1% slag more than that by 2% cement and consequently, the TR5C1S-7 mixture showed a higher M_r than the TR5C2-7 mixture.

2. The tyre-rock mixture with 5% rock and 2% cement (TR5C2-7) showed lower P_d than (up to 60% after seven days) the untreated sample (TR5). It is essential to know that the rubber-rock-cement-slag mixture (TR5C1S-7) showed less P_d than the TR5C2-7 sample. Therefore, using slag can play a significant role in improving the resistance of rubber-rock-cement mixtures against P_d.
3. According to the results of dynamic shear tests, the presence of 2% cement inversely influenced the ultimate shear strength of rubber-rock-cement mixtures. The cement treated TR5C2-7sample showed less shear strength than the untreated sample. A considerable improvement in the stress-strain curve of the TR5C2-7 mixture was found after replacing 1% cement with 1% slag (TR5C1S-7 sample). In addition, slag inclusion shifted the strain point corresponding to the peak shear of TR5C2-7 mixture from 2.5 με to 3.4 με.

8.2.6 Characterisations of different samples of the GR12T5C2-7 and the GR12T5C1S-7 mixtures

1. The glass-rock-rubber mixture treated with 2% cement after seven days (GR12T5C2-7) showed high M_r than the untreated sample GR12T5. Whereas the M_r of the GR12T5C2-7 sample was uninfluenced by replacing 1% cement with 1% slag. Thus, the GR12T5C2-7 samples showed approximately the same resilience behaviour as GR12T5C1S-7 sample.
2. There was a considerable improvement in the P_d of the GR12T5 following the addition of 2% cement, whereas a slight increase in the P_d of GR12T5C2-7 sample when replaced 1% cement with 1% slag. It is unclear whether the cement-slag treatment affected the P_d of GR12T5 mixtures.
3. According to the results of dynamic shear tests, the peak stress of the GR12T5 sample shifted from 780 kPa to 510 kPa following the addition of 2% cement. Thus, the cement treated sample showed less shear strength than the untreated sample, where the GR12T5C2-7 sample showed lower shear strength than the untreated one. Based on cement-slag treatment, there was an insignificant difference between the maximum shear strengths of the GR12T5C2-7 and GR12T5C1S-7 samples.
4. Through a simple comparision between the dynamic responses of the GR12, TR5, and GR12T5 samples to the chemical treatement, it was clear that the treated GR12 mixtures showed higher M_r than TR5, GR12T5, and the pure rock

samples as well. On the other hand, the treated TR5 mixture showed the lowest response to the chemical treatment. What is interesting that the cement-slag treatment played a significant role in the resilience behaviour of all mixtures. Furthermore, the chemical treatment response of the GR12 sample against deformation was the highest comparing to the rest samples of TR5 and GR12T5, whereas the response of the treated GR12T5 sample was the lowest. Further results indicated that slag content played a significant role in the deformation behaviour of all mixtures. What is interesting is that the resistance of the GR12T5C2-7 sample against P_d was improved by cement-slag treatment, and the GR12C2-7 sample showed the same P_d when replacing 1% cement with 1% slag. Based on the comparison between the shear strengths of the treated mixtures, the GR12 mixture showed a better response to the chemical treatment than the GR12T5 and TR5 mixtures. On the other hand, it is unclear whether slag inclusion affected the shear strength of the mixtures; however, the TR5 mixture with 2% cement appeared to have better shear strength than that with the cement-slag.

8.2.7 Dynamic evaluation of layered glass-rock samples

1. Regarding the results of the RLTTs, the glass content played a significant role in dynamic behaviour of layered samples of the rock+ (glass-rock) (R+GR) group under repeated loading. The layered sample with 12% glass (R+GR12) showed the highest M_r. In addition, a considerable reduction in the M_r values of the R+GR group was noticeable when the glass content increased from 12% to 24%. What is interesting is that the R+GR12 and R+GR45 samples showed higher M_r than the R+GR24 and rock samples. Note that the number of the glass-rock (GR) layers played a significant role in the stiffness responses of all R+GR samples. Hence, a negative correlation was found between the M_r of the layered samples and the number of GR12 layers. Whereas, a positive correlation was found between moisture content and the M_r of the R+GR12 sample. In addition, an insignificant effect of the GR layer location was noticeable on M_r of the R+GR12 sample.
2. According to the results of P_d, high glass content (45%) improved the resistance of the R+GR45 sample to P_d, the P_d decreased when the glass content increased from 12% to 45%. The effect of the number of GR layer on the M_r of layered

samples was also explored in this section, the double-layered sample with 12% glass content (2R+2GR12) showed a lower M_r than the singled-layered sample (R+GR12), whereas an insignificant difference was found in the P_d values between the R+GR45, 2R+2GR45, and 4R+4GR45. The advantage of using a rock layer close to the bottom of the layered sample on its P_d was noticeable, where the 4R+4GR group showed significantly lower P_d than the 4GR+4R one. In addition, the layered sample at 70% OMC tended to have better resistance against P_d than the specimen at 100% OMC.

3. In terms of shear strength, the R+GR12 sample showed the highest shear strength. Also, a positive correlation was found between the glass content and the shear strength of the layered samples. What is interesting in this result is that the layered sample with 12% glass content showed higher shear strength than the pure rock sample. On the other hand, there was a negative correlation between the shear strength and the number of GR layers. Unexpectedly, the layered sample with a high moisture content (100% OMC) showed higher shear strength than the sample at 70% OMC. Based on the comparison between the homogenous and the layered techniques in terms of dynamic behaviour, the homogenous samples showed lower P_d than the layered ones. While the layered samples with different glass contents (12, 24, 45%) showed higher shear strength than the homogenous samples.

8.2.8 Dynamic evaluation of layered rock-sand samples

1. Based on the resilient modulus results, the presence of a sand layer between rock layers inversely affected the M_r. It is important to note that the presence of a sand layer close to the bottom of the sample clearly improved the M_r. Consequently, the M_r of rock-sand samples decreased as a result of increasing the distance between the sand layer and the base. The adverse effects of the number of sand layers on M_r of the rock samples could be attributed to the role of the interface layers between the rock and sand layers.
2. In terms of shear strength, a significant effect of the location and the number of sand layers was found on P_d of the rock-sand samples. A positive correlation was also found between P_d and the number of sand layers. The rock-sand sample with a sand layer close to the base showed less P_d than the other samples.

Consequently, there was a positive correlation between P_d of the rock-sand sample and the distance between the sand layer and the base.

8.2.9 Dynamic evaluation of layered rock-bentonite-sand samples

1. Concerning the resilience behaviour, the Mr of rock-bentonite (R-BE) samples tested for 100 cycles/path significantly decreased when the location of the BE layer was close to the base. Based on the comparison between the Mr of the rock-sand and the R-BE samples, the R-S sample showed a higher Mr than the R-BE sample. In terms of the failure response, the R-BE sample presented significantly better behaviour than the R-S sample against collapse, whereas the R-BE sample showed more resistance against collapse than the R-S sample. The results also highlighted that the M_r of R-BE sample decreased as the number of BE layers increase. The results also showed that a significant improvement in the resilient behaviour was associated with the replacement of two of the BE layers by two of the sand layers.
2. In terms of permanent deformation, the R-BE sample which the BE layer was close to the bottom showed higher P_d than the other samples, and this behaviour was inconsistent with the behaviour of the R-S sample. Interestingly, the P_d of R-BE sample was significantly lower than that of the R-S sample. Like the behaviour of R-S samples, the P_d of the R-BE sample increased with the increasing the number of BE layers. In addition, the (R+S+R+BE+3R (100)) which the sand layer was near to the base and the BE layer was near to the top showed less P_d than the R+BE+R+S+3R (100) sample.

8.2.10 Artificial intelligence approaches: modelling of resilient modulus

The results of the artificial intelligence approaches highlighted that the artificial neural networks (ANN) and the genetic algorithms (GP) can develop effective models to predict M_r for base and subbase materials. It is apparent that the ANN and the GP models showed high accuracy regarding the M_r prediction. The values of R^2 for the testing set were 0.98 and 0.81 for the ANN and GP models, respectively. Concerning the variables that could affect the predicted model, moisture content was the most important, while D_{50} showed an insignificant effect on the predicted model. In addition, a significant drop in R^2 of the training,

validation and testing datasets as a result of excluding the C_u variable from the ANN dataset.

8.3 Recommendations

A wide range of experimental and empirical investigations were conducted in this thesis to assess the dynamic behaviour of crushed rock base course material mixed with different percentages of glass, rubber, cement and slag. A layering technique was also used to prepare samples of rock-glass, rock-sand and rock-sand-bentonite to assess the suitability of such samples as foundation materials in pavement applications. Two types of artificial intelligence approaches with basic parameters of different granular materials were used to develop a model for predicting resilient modulus of base and subbase materials. Even though this combination of studies provides some supports for the idea of using alternative materials in road applications, future study in this field is recommended as follows:

1. In future investigations, it might be possible to investigate the suitability of using specific sizes of glass and rubber with crushed rock.
2. It is recommended that more research be undertaken in coating techniques, which are used in a wide range of concrete applications to cover glass and rubber materials before using them with rock material.
3. Further experimental study with more focus on the effects of extra cement and slag addition is suggested, and more work required establishing the effect of the curing period.
4. Future studies on the effect of using layering techniques to assess the dynamic behaviours of waste rock-cement and waste rock-cement-slag mixtures are also recommended.
5. In this thesis, the lowest proportions of waste materials were mixed with rock to prepare cement-treated and cement-slag-treated samples (12% glass and 5% rubber). Therefore, several questions remain unanswered regarding the dynamic behaviour of cement and cement-slag treated mixtures of rock containing high proportions of glass (24% and 45%) and rubber (10% and 15%).
6. Repeated load triaxial tests in drying and wetting phases were not investigated in this thesis, especially in samples that contained bentonite. Therefore, additional investigations on that topic are required in future.

7. A cost analysis would help designers determine the most economical solutions for certain conditions.

8. Further ANN and GP approachesare required to delope models for predicting M_r of rock-waste materials or rock-waste materials-cement mixtures could be conducted. Moreover, other software programs with extra data are required to capture the dynamic behaviour of base and subbase materials.

References

1. AASHTO, T. (2003). 307, Determining the Resilient Modulus of Soils and Aggregate Materials, Standard Specifications for Transportation Materials and Methods of Sampling and Testing, Washington, D.

2. Adams, R. (1972). McC., 1981, Heartland of Cities. *Surveys of Ancient Settlement and Land Use on the Central*.

3. Ali, M. Y., Newman, G., Arulrajah, A., & Disfani, M. M. (2011). Application of recycled glass-crushed rock blends in road pavements. *Aust. Geomech. J*, *46*(1), 113-121.

4. Allen, J. J. (1973). *The effects of non-constant lateral pressures on the resilient properties of granular materials* (Doctoral dissertation, University of Illinois at Urbana-Champaign).

5. American Foundrymen's Society (2004). Foundry Sand Facts for Civil Engineers.Report No.: FHWA-IF-04-004 Prepared by *American Foundrymen's Society Inc. for Federal Highway Administration Environmental Protection Agency Washington*, DC, USA, p. 80.

6. Arnold, G. K. (2004). *Rutting of granular pavements* (Doctoral dissertation, University of Nottingham).

7. Arnold, G., Alabaster, D., Ellis, J., & Lowe, J. (2008, June). The performance of New Zealand basecourse aggregates and glass aggregate mixtures found from repeated load triaxial testing. In *Recycling and Stabilisation Conference, 2008, Auckland, New Zealand*.

8. Arora, S., & Aydilek, A. H. (2005). Class F fly-ash-amended soils as highway base materials. *Journal of Materials in Civil Engineering*, *17*(6), 640-649.

9. Arulrajah, A., Ali, M. M. Y., Disfani, M. M., & Horpibulsuk, S. (2014). Recycled-glass blends in pavement base/subbase applications: laboratory and field evaluation. *Journal of Materials in Civil Engineering*, *26*(7), 04014025.

10. Arulrajah, A., Piratheepan, J., Disfani, M. M., & Bo, M. W. (2012). Geotechnical and geoenvironmental properties of recycled construction and

demolition materials in pavement subbase applications. *Journal of Materials in Civil Engineering*, *25*(8), 1077-1088.

11. ASTM, D. (2007). Standard test methods for moisture, ash, and organic matter of peat and other organic soils. *D2974-07*.

12. Attom, M. F. (2006). The use of shredded waste tires to improve the geotechnical engineering properties of sands. *Environmental Geology*, *49*(4), 497-503.

13. Australian Bureau of Statistics, Australian Government (2016). Viewed 13 December 2018, fromhttp://www.abs.gov.au/.

14. Australian Government response to the Climate Change Authority's Review of the National Greenhouse and Energy Reporting Legislation 2016, viewed 13 January 2018, from https://www.environment.gov.au/protection/nationalwaste-policy/tyres.

15. Austroads. (2008). The development and evaluation of protocols for the laboratory characterisation of cemented materials, *AP-T101-08, Austroads, Melbourne, Australia.*

16. Azam, A. M., & Cameron, D. A. (2012). Geotechnical properties of blends of recycled clay masonry and recycled concrete aggregates in unbound pavement construction. *Journal of Materials in Civil Engineering*, *25*(6), 788-798.

17. Babiker, A. F. A., Smith, C. C., Gilbert, M., & Ashby, J. P. (2014). Nonassociative limit analysis of the toppling-sliding failure of rock slopes. *International Journal of Rock Mechanics and Mining Sciences*, *71*, 1-11.

18. Barskale, R. D., & Itani, S. Y. (1989). Influence of aggregate shape on base behavior. *Transportation research record*, (1227).

19. Bejarano, M. O., & Harvey, J. T. (2002). Accelerated pavement testing of drained and undrained pavements under wet base conditions. *Transportation Research Record*, *1816*(1), 137-147.

20. Bejarano, M. O., Heath, A. C., & Harvey, J. T. (2003). A low-cost high-performance alternative for controlling a servo-hydraulic system for triaxial

resilient modulus apparatus. In *Resilient modulus testing for pavement components*. ASTM International.

21. Bilodeau, J. P., & Doré, G. (2012). Water sensitivity of resilient modulus of compacted unbound granular materials used as pavement base. *International Journal of Pavement Engineering*, *13*(5), 459-471.

22. Briaud, J. L., & Shields, D. H. (1970). Use of a pressuremeter test to predict the modulus and strength of pavement layers.'. *Transportation Research Board, Washington, USA.(To be published) Mr J. SHREWSBURY*.

23. Cabalar, A. F. (2011). Direct shear tests on waste tires-sand mixtures. *Geotechnical and Geological Engineering*, *29*(4), 411-418.

24. Cabalar, A. F., & Karabash, Z. (2015). California bearing ratio of a sub-base material modified with tire buffings and cement addition. *Journal of Testing and Evaluation*, *43*(6), 1279-1287.

25. Carmichael III, R. F., & Stuart, E. (1985). Predicting resilient modulus: A study to determine the mechanical properties of subgrade soils (abridgment). *Transportation Research Record*, (1043),145-148.

26. Center, C. W. (1993). Using recycled glass as a construction aggregate, a summary of the glass feedstock evaluation project. *Clean Washington Center, a Division of the Department of Trade and Economic Development, undated*.

27. Center, C. W. (1998). A tool kit for the use of post-consumer glass as a construction aggregate. *Prepared by Soil & Environmental Engineers, Inc and Resourcing Associates, Inc*.

28. Chegenizadeh, A., Keramatikerman, M., & Nikraz, H. (2016). Flexible pavement modelling using kenlayer. *EJGE*, *21*, 2467-2479.

29. Cheung, L. W., & Dawson, A. R. (2002). Effects of particle and mix characteristics on performance of some granular materials. *Transportation Research Record*, *1787*(1), 90-98.

30. Chou, Y. T. (1976). *Evaluation of nonlinear resilient moduli of unbound granular materials from accelerated traffic test data* (No. WES-TR-S-76-12). Army Engineer Waterways Experiment Station Vicksburg, Miss.

31. Circular, T. R. B. (1999). Use of artificial neural networks in geomechanical and pavement systems. *Transportation Research Board, National Research Council, Washington, DC Report No. E-C012*.

32. Coleri, E., Guler, M., Gungor, A. G., & Harvey, J. T. (2010). Prediction of subgrade resilient modulus using genetic algorithm and curve-shifting methodology: Alternative to nonlinear constitutive models. *Transportation Research Record*, *2170*(1), 64-73.

33. Collins, H. J., & Hart, C. A. (1936). *Principles of road engineering* (Vol. 6). E. Arnold.

34. Cosentino, P. J., Bleakley, A. M., Armstrong, A. T., Misilo, T. J., & Sajjadi, A. M. (2014). *Ground tire rubber as a stabilizer for subgrade soils* (No. BDK81 977-03). Florida Dept. of Transportation Research Center.

35. Das, B. M. (2007). *Principles of foundation engineering (6^{th} ed)*. PWS: Pacific Grove, California.

36. Das, S. K. (2013). 10 Artificial Neural Networks in Geotechnical Engineering: Modeling and Application Issues. *Metaheuristics in Water Geotech Transp Eng*, *45*, 231-267.

37. Das, S. K., & Basudhar, P. K. (2008). Prediction of residual friction angle of clays using artificial neural network. *Engineering Geology*, *100*(3-4), 142-145.

38. Dawson, A. R., Mundy, M. J., & Huhtala, M. (2000). European research into granular material for pavement bases and subbases. *Transportation Research Record*, *1721*(1), 91-99.

39. De Vos, K. (2006). Universal Testing System (UTS009) Unbound Materials Resilient Modulus & Shear Test Software Reference.*IPC Global Limited.*

40. Demuth, H., Beale, M., & Hagan, M. (2008). Neural network toolbox™ 6. *User's guide*, 37-55.

41. Disfani, M. M., Arulrajah, A., Bo, M. W., & Hankour, R. (2011). Recycled crushed glass in road work applications. *Waste Management*, *31*(11), 2341-2351.

42. Disfani, M. M., Arulrajah, A., Bo, M. W., & Sivakugan, N. (2012). Environmental risks of using recycled crushed glass in road applications. *Journal of Cleaner Production*, *20*(1), 170-179.

43. Disfani, M. M., Arulrajah, A., Suthagaran, V., & Bo, M. W. (2009, October). Geotechnical characteristics of recycled glass-biosolid mixtures. In *Proceedings of the 17th International Conference on Soil Mechanics and Geotechnical Engineering, Alexandria, Egypt* (pp. 5-9).

44. Disfani, M., Arulrajah, A., Suthagaran, V., & Bo, M. (2009, September). Shear strength behavior of recycled glass-biosolids mixtures. In *62nd Canadian Geotechnical Conference and 10th Joint CGS/IAH-CNC Groundwater Conference*. International Association of Hydrogeologists/Canadian Geotechnical Society Halifax, Canada.

45. Drumm, E. C., Boateng-Poku, Y., & Johnson Pierce, T. (1990). Estimation of subgrade resilient modulus from standard tests. *Journal of Geotechnical Engineering*, *116*(5), 774-789.

46. Drumm, E. C., Reeves, J. S., Madgett, M. R., & Trolinger, W. D. (1997). Subgrade resilient modulus correction for saturation effects. *Journal of Geotechnical and Geoenvironmental Engineering*, *123*(7), 663-670.

47. Du, Y. J., Wei, M. L., Jin, F., & Liu, Z. B. (2013). Stress-strain relation and strength characteristics of cement-treated zinc-contaminated clay. *Engineering Geology*, *167*, 20-26.

48. Du, Y., Li, S., & Hayashi, S. (1999). Swelling-shrinkage properties and soil improvement of compacted expansive soil, Ning-Liang Highway, China. *Engineering Geology*, *53*(3-4), 351-358.

49. Edeskär, T. (2006). *Use of tyre shreds in civil engineering applications: technical and environmental properties* (Doctoral dissertation, Luleå Tekniska Universitet).

50. Edil, T. B., & Bosscher, P. J. (1994). Engineering properties of tire chips and soil mixtures. *Geotechnical Testing Journal*, *17*(4), 453-464.

51. Edinçliler, A., Baykal, G., & Dengili, K. (2004). Determination of static and dynamic behavior of recycled materials for highways. *Resources, Conservation and Recycling*, *42*(3), 223-237.

52. EN, B. (2004). 13286-7 (2004) Unbound and hydraulically bound mixtures

53. Estevez, M. (2009). Use of coupling agents to stabilize asphalt-rubber-gravel composite to improve its mechanical properties. *Journal of Cleaner Production*, *17*(15), 1359-1362.

54. Farrar, M. J., & Turner, J. P. (1991). *Resilient modulus of Wyoming subgrade soils* (No. MPC Report No. 91-1).

55. Farrokhzad, F., Choobbasti, A., & Barari, A. (2010). Artificial neural network model for prediction of liquefaction potential in soil deposits.

56. Fausett, L. V. (1994). *Fundamentals of neural networks: Architectures, algorithms, and applications* (Vol. 3). Englewood Cliffs: Prentice-Hall.

57. Feng, Z. Y., & Sutter, K. G. (2000). Dynamic properties of granulated rubber/sand mixtures. *Geotechnical Testing Journal*, *23*(3), 338-344.

58. Ferreira, C. (2006). *Gene expression programming: Mathematical modeling by an artificial intelligence* (Vol. 21). Springer.

59. Figueroa, J. L., & Thompson, M. R. (1980). Simplified structural analyses of flexible pavements for secondary roads based on ILLI-PAVE. *Transportation Research Record*, (766).

60. Fleming, P. R., Rogers, C. D. F., Frost, M. W., & Dawson, A. R. (1998). Subgrade equilibrium water content and resilient modulus for UK clays.

61. Foose, G. J., Benson, C. H., & Bosscher, P. J. (1996). Sand reinforced with shredded waste tires. *Journal of Geotechnical Engineering*, *122*(9), 760-767.

62. George, K. P. (2004). *Prediction of resilient modulus from soil index properties* (No. FHWA/MS-DOT-RD-04-172). University of Mississippi.

63. Ghazavi, M. (2004). Shear strength characteristics of sand-mixed with granular rubber. *Geotechnical & Geological Engineering*, *22*(3), 401-416.

64. Gidel, G., Hornych, P., Breysse, D., & Denis, A. (2001). A new approach for investigating the permanent deformation behaviour of unbound granular

material using the repeated loading triaxial apparatus. *Bulletin des Laboratoires des Ponts et Chaussées*, (233).

65. Gischig, V. S., Eberhardt, E., Moore, J. R., & Hungr, O. (2015). On the seismic response of deep-seated rock slope instabilities: Insights from numerical modeling. *Engineering Geology*, *193*, 1-18.

66. Goh, A. T. (1996). Neural-network modeling of CPT seismic liquefaction data. *Journal of Geotechnical engineering*, *122*(1), 70-73.

67. Gravanis, E., Pantelidis, L., & Griffiths, D. V. (2014). An analytical solution in probabilistic rock slope stability assessment based on random fields. *International Journal of Rock Mechanics and Mining Sciences*, *71*, 19-24.

68. Grubb, D. G., Gallagher, P. M., Wartman, J., Liu, Y., & Carnivale III, M. (2006). Laboratory evaluation of crushed glass-dredged material blends. *Journal of Geotechnical and Geoenvironmental Engineering*, *132*(5), 562-576.

69. Gudishala, R. (2004). Development of resilient modulus prediction models for base and subgrade pavement layers from in situ devices test results.

70. Hagan, M. T., Demuth, H. B., & Beale, M. H. (2002). *Neural network design*. Singapore: Thomson Learning.

71. Hall, T. (1991). Reuse of shredded tire material for leachate collection systems. In *Proceedings of the 14th Annual Conference* (pp. 367-376). University of Wisconsin.

72. Hataf, N., & Rahimi, M. M. (2006). Experimental investigation of bearing capacity of sand reinforced with randomly distributed tire shreds. *Construction and Building Materials*, *20*(10), 910-916.

73. Hazarika, H., Yasuhara, K., Karmokar, A., & Mitarai, Y. (2007, November). Shaking table test on liquefaction prevention using tire chips and sand mixture. In *Proceedings of the International Workshop on Scrap Tire Derived Geomaterials—Opportunities and Challenges, Yokosuka, Japan* (pp. 215-222).

74. Hicks, R. G., & Monismith, C. L. (1971). Factors influencing the resilient response of granular materials. *Highway Research Record*, *345*, 15-31.

75. Hidalgo Signes, C., Martínez Fernández, P., Garrido de la Torre, M. E., & Insa Franco, R. (2015, December). An experimental study of a new soil-rubber mix for railway embankment. In *13th Arab Structural Engineering Conference ASEC, University of Blida, Algeria* (pp. 13-15).

76. Hill, T., Lewicki, P., & Lewicki, P. (2006). *Statistics: methods and applications: a comprehensive reference for science, industry, and data mining*. StatSoft, Inc..

77. Humphrey, D. N., & Manion, W. P. (1992). Properties of tire chips for lightweight fill. In *Grouting, soil improvement and geosynthetics* (pp. 1344-1355). ASCE.

78. Humphrey, D. N., & Sandford, T. C. (1993, October). Tire chips as lightweight subgrade fill and retaining wall backfill. In *Proceedings of the symposium on recovery and effective reuse of discarded materials and by-products for construction of highway facilities* (pp. 5-87). US Department of Transportation, Federal Highway Administration.

79. Humphrey, D. N., Sandford, T. C., Cribbs, M. M., & Manion, W. P. (1993). Shear strength and compressibility of tire chips for use as retaining wall backfill. *Transportation Research Record*, (1422).

80. Hussain, J., Wilson, D. J., Henning, T. F., & Alabaster, D. (2013). Comparing results between the repeated load triaxial test and accelerated pavement test on unbound aggregate. *Journal of Materials in Civil Engineering*, *26*(3), 476-483.

81. Huurman, R., & Molenaar, A. A. (2006). Permanent deformation in flexible pavements with unbound base courses. *Transportation Research Record*, *1952*(1), 31-38.

82. Ibrahim, S.F., Kadhim, D.A., & Othman, H. (2017). Prediction of resilient modulus using artificial neural network and extreme learning machine from index properties for Iraqi subgrade soil.*Imperial Journal of Interdisciplinary Research*, *3*(2), No. 169.

83. Ibsen, L. B. (2018). The mechanism controlling static liquefaction and cyclic strength of sand. In *Physics and mechanics of soil liquefaction* (pp. 29-39). Routledge.

84. Jameson, G., Voung, B., Moffatt, M., Martin, A., & Lourensz, S. (2010). *Assessment of rut resistance of granular bases using the repeated load triaxial test*. Austroads Ltd, Sydney.

85. Jitsangiam, P., & Nikraz, H. (2009). Mechanical behaviours of hydrated cement treated crushed rock base as a road base material in Western Australia.

86. Johnson, T. C. (1974). *IS GRADED AGGREGATE BASE THE SOLUTION IN FROST AREAS?* (No. Conf Paper).

87. Kalcheff, I. V. (1974). Characteristics of Graded Aggregates as Related to Their Behavior Under Varying Loads and Environments. *Publication of: National Crushed Stone Association*.

88. Kalcheff, I. V., & Hicks, R. G. (1973). A test procedure for determining the resilient properties of granular materials. *Journal of Testing and Evaluation*, *1*(6), 472-479.

89. Khabiri, M. M. (2010). The effect of stabilized subbase containing waste construction materials on reduction of pavement rutting depth. *Electronic Journal of Geotechnical Engineering*, *15*, 1211-1219.

90. Khogali, W. E., & Mohamed, E. H. H. (2004). Novel approach for characterization of unbound materials. *Transportation Research Record*, *1874*(1), 38-46.

91. Kim, H. K., & Santamarina, J. C. (2008). Sand-rubber mixtures (large rubber chips). *Canadian Geotechnical Journal*, *45*(10), 1457-1466.

92. Kim, I. T., & Tutumluer, E. (2006). Field validation of airport pavement granular layer rutting predictions. *Transportation Research Record*, *1952*(1), 48-57.

93. Kim, W., Labuz, J. F., & Dai, S. (2007). Resilient modulus of base course containing recycled asphalt pavement. *Transportation Research Record*, *2005*(1), 27-35.

94. Kolisoja, P. (1997). *Resilient deformation characteristics of granular materials* (pp. 188-201). Finland, Publications: Tampere University of Technology.

95. Kramer, S. L. (1996). *Geotechnical earthquake engineering*. Pearson Education India.

96. Lee, J. H., Salgado, R., Bernal, A., & Lovell, C. W. (1999). Shredded tires and rubber-sand as lightweight backfill. *Journal of Geotechnical and Geoenvironmental Engineering*, *125*(2), 132-141.

97. Lekarp, F. & Dawson, A.R. (1998). Some influences on the permanent deformation behavior of unbound granular materials. *US Transportation Research Board*.

98. Lekarp, F. (1999). *Resilient and permanent deformation behavior of unbound aggregates under repeated loading.* (Doctoral dissertation, Institutionen för Infrastruktur och Samhällsplanering).

99. Lekarp, F., Isacsson, U., & Dawson, A. (2000). State of the art. I: Resilient response of unbound aggregates. *Journal of Transportation Engineering*, *126*(1), 66-75.

100. Lekarp, F., Richardson, I. R., & Dawson, A. (1996). Influences on permanent deformation behavior of unbound granular materials. *Transportation Research Record*, *1547*(1), 68-75.

101. Levey, J. R., & Barenberg, E. J. (1970). A PROCEDURE FOR EVALUATING PAVEMENTS WITH NONUNIFORM PAVINGS MATERIALS. *Highway Research Record*, (337).

102. Li, D., & Selig, E. T. (1994). Resilient modulus for fine-grained subgrade soils. *Journal of Geotechnical Engineering*, *120*(6), 939-957.

103. Lin, P. L., Hsu, K. C., Lin, C. W., & Hwung, H. H. (2015). Modeling compaction of multi-layer-aquifer system due to groundwater withdrawal. *Engineering Geology*, *187*, 143-155.

104. Ma, L. J., Liu, X. Y., Wang, M. Y., Xu, H. F., Hua, R. P., Fan, P. X., ... & Yi, Q. K. (2013). Experimental investigation of the mechanical properties of rock

salt under triaxial cyclic loading. *International Journal of Rock Mechanics and Mining Sciences*, (62), 34-41.

105. Magnusdottir, B., & Erlingsson, S. (2002). Repeated load triaxial testing for quality assessment of unbound granular base course material. In *Proceedings, 9th Nordic Aggregate Research Conference, Reykjavik, Iceland* (p. 5).

106. Maher, A., Bennert, T., Gucunski, N., & Papp Jr, W. J. (2000). *Resilient modulus properties of New Jersey subgrade soils* (No. FHWA NJ 2000-01).

107. Main Roads Western Australia (2006). Crushed rock base basecourse. *Retrieved December 2018 from www.mainroads.wa.gov.au.*

108. Main Roads Western Australia (2007). Test method WA 133.1 dry density/moisture content relationship: Modified compaction fine and medium grained soils. *Perth, WA*.

109. MAIN ROADS Western Australia. (2006). "Test Method (Aggregate)."*Retrieved February 2020 fromhttp://www.mainroads.wa.gov.au/NR/mrwa/frames/standards/standards.asp?G={1532D87F-C1AC-4386-9968-5E5F4FD002E5}*.

110. Mehrjardi, G. T., Tafreshi, S. M., & Dawson, A. R. (2012). Combined use of geocell reinforcement and rubber-soil mixtures to improve performance of buried pipes. *Geotextiles and Geomembranes*, *34*, 116-130.

111. Moayedi, H., Kazemian, S., Prasad, A., & Huat, B. B. (2009). Effect of geogrid reinforcement location in paved road improvement. *Electronic Journal of Geotechnical Engineering*, *14*, 1-11.

112. Mohammad (1994). Effect of strain measurements on resilient modulus of sands. In *Dynamic Geotechnical Testing II*. ASTM International.

113. Mohammadinia, A., Arulrajah, A., Sanjayan, J., Disfani, M. M., Win Bo, M., & Darmawan, S. (2016). Stabilization of demolition materials for pavement base/subbase applications using fly ash and slag geopolymers. *Journal of Materials in Civil Engineering*, *28*(7), 04016033.

114. Molenaar, K. R. (2005). Programmatic cost risk analysis for highway megaprojects. *Journal of Construction Engineering and Management*, *131*(3), 343-353.

115. Momeni, A., Karakus, M., Khanlari, G. R., & Heidari, M. (2015). Effects of cyclic loading on the mechanical properties of a granite. *International Journal of Rock Mechanics and Mining Sciences*, *100*(77), 89-96.

116. Monismith, C. L., Hicks, R. G., & Salam, Y. M. (1971). *Basic properties of pavement components* (No. FHWA-RD-72-19 Final Rpt.).

117. Monismith, C. L., Seed, H. B., Mitry, F. G., & Chan, C. (1967). Predictions of pavement deflections from laboratory tests. In *Second International Conference on the Structural Design of Asphalt Pavements, University of Michigan, Ann Arbor*.

118. Montoya Rodriguez, C. G. (2015). *Predicting pavement performance under traffic loading using genetic algorithms and artificial neural networks to obtain resilient modulus values* (Doctoral dissertation, The Ohio State University).

119. Morgan, J. R. (1966). The response of granular materials to repeated loading. *Australian Road Research Board Proc*.

120. Mosa, A. M. (2017). Neural network for flexible pavement maintenance and rehabilitation. *Applied Research Journal*, *3*(4), 114-129.

121. Muduli, P. K., & Das, S. K. (2014). CPT-based seismic liquefaction potential evaluation using multi-gene genetic programming approach. *Indian Geotechnical Journal*, *44*(1), 86-93.

122. Murthy, T. G., Loukidis, D., Carraro, J. A. H., Prezzi, M., & Salgado, R. (2007). Undrained monotonic response of clean and silty sands. *Géotechnique*, *57*(3), 273-288.

123. Nagase, H., & Ishihara, K. (1987). Effects of load irregularity on the cyclic behaviour of sand. *Soil Dynamics and Earthquake Engineering*, *6*(4), 239-249.

124. Najjar, Y. M., Basheer, I. A., Ali, H. E., & McReynolds, R. L. (2000). Swelling potential of Kansas soils: Modeling and validation using artificial neural network reliability approach. *Transportation research record*, *1736*(1), 141-147.

125. Nakhaei, A., Marandi, S. M., Kermani, S. S., & Bagheripour, M. H. (2012). Dynamic properties of granular soils mixed with granulated rubber. *Soil Dynamics and Earthquake Engineering*, *43*, 124-132.

126. Nazzal, M. D., & Tatari, O. (2013). Evaluating the use of neural networks and genetic algorithms for prediction of subgrade resilient modulus. *International Journal of Pavement Engineering*, *14*(4), 364-373.

127. Nikraz, H. (2004). *Geotechnical Engineering 262: Lecture notes: Curtin University of Technology*.Unpublished manuscript, Perth, Western Australia.

128. Nowamooz, H., Ho, X. N., Chazallon, C., & Hornych, P. (2013). The effective stress concept in the cyclic mechanical behavior of a natural compacted sand. *Engineering Geology*, *152*(1), 67-76.

129. Núñez, W. R., Malysz, R., Ceratti, J. A., & Gehling, W. Y. Y. (2014, September). Shear strength and permanent deformation of unbound aggregates used in Brazilian pavements. In *Pavements Unbound: Proceedings of the 6th International Symposium on Pavements Unbound (UNBAR 6), 6-8 July 2004,*

130. Ottino, J. M., & Khakhar, D. V. (2000). Mixing and segregation of granular materials. *Annual Review of Fluid Mechanics*, *32*(1), 55-91.

131. Ouf, M. E. S. A. R. (2001). *Stabilisation of clay subgrade soils using ground granulated blastfurnace slag* (Doctoral dissertation, University of Leeds).

132. Papp, W. J., Maher, M. H., & Baker, R. F. (1997). Use of shredded tires in the subbase layer of asphalt pavements. In *Testing Soil Mixed with Waste or Recycled Materials*. ASTM International.

133. Pappin, J. W. (1979). *Characteristics of a granular material for pavement analysis* (Doctoral dissertation, University of Nottingham).

134. Parakh, D., Harde, A., Naykodi, A., Kadam, R. and Shelke, P. (2016). Partial replacement of coarse aggregate by waste tyre rubber and fine aggregate by waste glass. *Imperial Journal of Interdisciplinary Research*, *2*(6).

135. Park, H. I., Kweon, G. C., & Lee, S. R. (2009). Prediction of resilient modulus of granular subgrade soils and subbase materials using artificial neural network. *Road Materials and Pavement Design*, *10*(3), 647-665.

136. Perlea, V. G. (2000). Liquefaction of cohesive soils. *Soil dynamics and liquefaction 2000. Proceedings of Sessions of Geo-Denver 2000, Denver, Colorado, USA, 5-8 August 2000*, 58-76.

137. Perlea, V. G., Koester, J. P., & Prakash, S. (1999, June). How liquefiable are cohesive soils? In *Proceedings of Second International Conference on Earthquake Geotechnical Engineering* (Vol. 2, pp. 611-618).

138. Poon, C. S., & Chan, D. (2006). Feasible use of recycled concrete aggregates and crushed clay brick as unbound road sub-base. *Construction and Building Materials*, *20*(8), 578-585.

139. Prasad, D. S. V., & Prasada Raju, G. V. R. (2009). Performance of waste tyre rubber on model flexible pavement. *ARPN Journal of Engineering and Applied Sciences*, *4*(6), 89-92.le

140. Pujades, E., Vàzquez-Suñé, E., Carrera, J., & Jurado, A. (2014). Dewatering of a deep excavation undertaken in a layered soil. *Engineering geology*, *178*, 15-27.

141. Rada, G., & Witczak, M. W. (1981). *Comprehensive evaluation of laboratory resilient moduli results for granular material* (No. 810).

142. Raghavan, D., Huynh, H., & Ferraris, C. F. (1998). Workability, mechanical properties, and chemical stability of a recycled tyre rubber-filled cementitious composite. *Journal of Materials Science*, *33*(7), 1745-1752.

143. Rahim, A. M., & George, K. P. (2004, January). Subgrade soil index properties to estimate resilient modulus. In *83rd Annual Meeting of Transportation Research Board, Washington DC*.

144. Rahman, M. S., & Erlingsson, S. (2016). Moisture influence on the resilient deformation behaviour of unbound granular materials. *International Journal of Pavement Engineering*, *17*(9), 763-775.

145. Rana, A. S. M. (2004). *Evaluation of recycled material performance in highway applications and optimization of their use* (Doctoral dissertation, Texas Tech University).

146. Rao, G. V., & Dutta, R. K. (2006). Compressibility and strength behaviour of sand-tyre chip mixtures. *Geotechnical & Geological Engineering*, *24*(3), 711724.

147. Reinhard, M., & Drefahl, A. (1999). Handbook for estimating physicochemical properties of organic compounds. *New York*, 39.

148. Ripley, B. D., & Hjort, N. L. (1996). *Pattern recognition and neural networks*. Cambridge university press.

149. Rodgers, G. A. (2006). *Resilient modulus predictions using engineering properties and neural networks* (Doctoral dissertation, Ohio State University).

150. Sabbar, A. S., Chegenizadeh, A., & Nikraz, H. (2017). Prediction of liquefaction susceptibility of clean sandy soils using artificial intelligence techniques. *Indian Geotechnical Journal*, 1-12.

151. Salgado, R., Yoon, S., & Siddiki, N. Z. (2003). Construction of tire shreds test embankment.

152. Seed, H. B., Chan, C. K., & Lee, C. E. (1962). Resilience characteristics of subgrade soils and their relation to fatigue failures in asphalt pavements. In *International Conference on the Structural Design of Asphalt Pavements. Supplement.* University of Michigan, Ann Arbor.

153. Senadheera, S., Nash, P., & Rana, A. (1995). Characterization of the behavior of granular road material containing glass cullet. *Department of Civil Engineering, Texas Tech University, Lubbock, Texas, USA*.

154. Senol, A., Bin-Shafique, M. S., Edil, T. B., & Benson, C. H. (2002, September). Use of class C fly ash for stabilization of soft subgrade. In *Proceedings of the 5th International Congress on Advances in Civil Engineering* (Vol. 53, pp. 89-95).

155. Shahin, M. A., Maier, H. R., & Jaksa, M. B. (2004). Data division for developing neural networks applied to geotechnical engineering. *Journal of Computing in Civil Engineering*, *18*(2), 105-114.

156. Sharp, K. G. (2005). *Guide to pavement technology: part 1: introduction to pavement technology* (No. AGPT01/05).

157. Signes, C. H., Fernández, P. M., Garzón-Roca, J., de la Torre, M. E. G., & Franco, R. I. (2016). An evaluation of the resilient modulus and permanent deformation of unbound mixtures of granular materials and rubber particles from scrap tyres to be used in subballast layers. *Transportation Research Procedia*, *18*, 384-391.

158. Signes, C. H., Fernández, P. M., Perallón, E. M., & Franco, R. I. (2015). Characterisation of an unbound granular mixture with waste tyre rubber for subballast layers. *Materials and Structures*, *48*(12), 3847-3861.

159. Siripun, K., Jitsangiam, P., & Nikraz, H. (2009). Characterization analysis and design of hydrated cement treated crushed rock base as a road base material in Western Australia. *International Journal of Pavement Research and Technology*, *2*(6), 257-263.

160. Smith, W. S., & Nair, K. (1973). Development of procedures for characterization of untreated granular base course and asphalt-treated base course materials.

161. Speir, R. H., & Witczak, M. W. (1996). Use of shredded rubber in unbound granular flexible pavement layers. *Transportation Research Record*, *1547*(1), 96106.

162. Standards Association of Australia (SAA). (2003). "Soil compaction and density tests-Determination of the dry density/moisture content relation of a soil using modified compactive effort." AS1289.5.2.1.

163. Standards Australia (1993), Geotechnical site investigation (AS 1726-1993), Standards Australia, Homebush, NSW, Australia.

164. Standards Australia. (1995a). Determination of the soil particle density of combined soil fraction-vacuum pycnometer method. *AS1289.3.5.2*, Australia.

165. Standards Australia. (1997a). Methods of testing soils for engineering purposes. Method 4.3.1: soil chemical tests-determination of the p_H value of a soil electrometric method. AS 1289.4.3.1-1997, Homebush, NSW, Australia.

166. Subramanian, R. M., & Jeyapriya, S. P. (2009). Study on Effect of Waste Tyres in Flexible Pavement System. *Indian Geotech. Soc. Chennai*, 19-24.

167. Sukumaran, B., Kyatham, V., Shah, A., & Sheth, D. (2002, May). Suitability of using California bearing ratio test to predict resilient modulus. In *Proceedings: Federal Aviation Administration Airport Technology Transfer Conference* (p. 9).

168. Sweere, G. T. (1990). Unbound granular bases for roads. Retrieved from http://resolver.tudelft.nl/uuid:1cc1c86a-7a2d-4bdc-8903-c665594f11eb.

169. Tchemou, G., Minsili, L. S., Mokotemapa, A. M., Eko, R. M., & Manguelle, J. H. (2011). Prediction of flexible pavement degradation: Application to rutting in Cameroonian highways. *Electronic Journal of Geotechnical Engineering*, *16*, 1301-1319.

170. Terzaghi, K., Peck, R. B., & Mesri, G. (1996). *Soil mechanics in engineering practice*. John Wiley & Sons.

171. Theyse, H. L. (2002). Stiffness, strength and performance of unbound aggregate material: Application of South African HVS and laboratory results to California flexible pavements. *Report produced under the auspices of the California Partnered Pavement Research Program for the California Department of Transportation. University of California*, *76*.

172. Thom, N. H., & Brown, S. F. (1987). *Effect of moisture on the structural performance of a crushed-limestone road base* (No. 1121).

173. Thom, N. H., & Brown, S. F. (1988). The effect of grading and density on the mechanical properties of a crushed dolomitic limestone. In *Australian Road Research Board (ARRB) Conference, 14th, 1988, Canberra* (Vol. 14, No. 7).

174. Thompson, M. R., & Robnett, Q. L. (1976). *Resilient properties of subgrade soils* (No. FHWA-IL-UI-160 Final Rpt.).

175. Uzan, J. (1985). Characterization of granular material. *Transportation research record*, *1022*(1), 52-59.

176. Van Niekerk, A. A., Molenaar, A. A. A., & Houben, L. J. M. (2002). Effect of material quality and compaction on the mechanical behaviour of base course materials and pavement performance. In *Proceedings of the 6th International Conference on the Bearing Capacity of Roads and Airfields, Lisbon, Portugal, 24-26 June 2002*. (Vol. 2).

177. VicRoads. (2010). Standard specifications for road works and bridge works, Section 812: Crushed rock for base and subbase pavement. Melbourne, Australia.

178. Viswanathan, K. (1996). *Characterization of waste recycled glass as a highway material* (Doctoral dissertation, Texas Tech University).

179. Vuong, B. (1992). Influence of density and moisture content on dynamic stress-strain behaviour of a low plasticity crushed rock. *Road and Transport Research*, *1*(2).

180. Wang, Y., Hu, Y., Wang, Y., Deng, H., Gong, X., Zhang, P., ... & Chen, Z. (2006). Magnetorheological elastomers based on isobutylene-isoprene rubber. *Polymer Engineering & Science*, *46*(3), 264-268.

181. Warith, M. A., & Rao, S. M. (2006). Predicting the compressibility behaviour of tire shred samples for landfill applications. *Waste Management*, *26*(3), 268276.

182. Wartman, J., Grubb, D. G., & Nasim, A. S. M. (2004). Select engineering characteristics of crushed glass. *Journal of Materials in Civil Engineering*, *16*(6), 526-539.

183. Watson, P. G. (1995). Stabilisation of crushed rock. *Materials Engineering Report*, (95/1).

184. Webb, W. M., & Campbell, B. E. (1986). Preliminary investigation into resilient modulus testing for new AASHTO pavement design guide. *Office of Materials and Research, Georgia Department of Transportation*.

185. Wei, Z., Yin, G., Li, G., Wang, J. G., Wan, L., & Shen, L. (2009). Reinforced terraced fields method for fine tailings disposal. *Minerals Engineering*, *22*(12), 1053-1059.

186. Werkmeister, S., Numrich, R., Dawson, A. R., & Wellner, F. (2003). Design of granular pavement layers considering climatic conditions. *Transportation Research Record*, *1837*(1), 61-70.

187. Witczak, M. W., Qi, X., & Mirza, M. W. (1995). Use of nonlinear subgrade modulus in AASHTO design procedure. *Journal of Transportation Engineering*, *121*(3), 273-282.

188. Wolff, H., & Visser, A. T. (1994, November). Incorporating elasto-plasticity in granular layer pavement design. In *Proceedings of the Institution of Civil Engineers-Transport* (Vol. 105, No. 4).

189. Xiangjun, C., & Zhanfeng, G. (2007, August). Applications of ANNs in geotechnical engineering. In *2007 8th International Conference on Electronic Measurement and Instruments* (pp. 3-656). IEEE.

190. Yamamuro, J. A., & Lade, P. V. (1998). Steady-state concepts and static liquefaction of silty sands. *Journal of geotechnical and geoenvironmental engineering*, *124*(9), 868-877.

191. Yang, S. R., Huang, W. H., & Tai, Y. T. (2005). Variation of resilient modulus with soil suction for compacted subgrade soils. *Transportation Research Record*, *1913*(1), 99-106.

192. Yang, Y., & Rosenbaum, M. S. (2002). The artificial neural network as a tool for assessing geotechnical properties. *Geotechnical & Geological Engineering*, *20*(2), 149-168.

193. Yoder, E. J., & Witczak, M. W. (1975). Principles of Pavement Design, John Wiley and Sons. *Inc., New York*, 150-155.

194. Zakaria, M., & Lees, G. (1996). Rutting characteristics of unbound aggregate layers. *Construction and Building Materials*, *10*(3), 185-189.

195. Zeng, P., Jimenez, R., & Jurado-Piña, R. (2015). System reliability analysis of layered soil slopes using fully specified slip surfaces and genetic algorithms. *Engineering Geology*, *193*, 106-117.

196. Zhang, Q., Yin, G., Wei, Z., Fan, X., Wang, W., & Nie, W. (2015). An experimental study of the mechanical features of layered structures in dam tailings from macroscopic and microscopic points of view. *Engineering Geology*, *195*, 142-154.

197. Zhou, Z. H., Cao, P., & Ye, Z. Y. (2014). Crack propagation mechanism of compression-shear rock under static-dynamic loading and seepage water pressure. *Journal of Central South University*, *21*(4), 1565-1570.

198. Zhu, W. C., & Tang, C. A. (2006). Numerical simulation of Brazilian disk rock failure under static and dynamic loading. *International Journal of Rock Mechanics and Mining Sciences*, *43*(2), 236-252.

199. Zurada, J. M. (1992). *Introduction to artificial neural systems* (Vol. 8). St. Paul: West Publishing Company.

Appendixes:

Laboratory data

Test Procedure: Study of the resilient behaviour
Project: 4R+BA+3R
Operator: Mustafa
Comments: 4R+BA+3R

Test Data

Start Date and Time: Thursday, August 27, 2015, at 2:46 PM

	Resilient Modulus (MPa)	Maximum Deviator Stress (kPa)	Minimum Deviator Stress (kPa)	Confining Stress (kPa)	Resilient Axial Strain (με)	Resilient Radial Strain (με)	Permanent Axial Strain (με)	Permanent Radial Strain (με)
Conditioning Cycles 1 to 10:	38.2	19.6	1.9	20.0	467	----	1026	----
Stress path 1:	27.8	20.0	2.1	20.0	644	----	2208	----
Stress path 2:	21.6	34.9	2.1	20.0	1525	----	6391	----
Stress path 3:	20.1	49.9	2.0	20.0	2381	----	10485	----
Stress path 4:	18.8	69.9	2.1	20.0	3609	----	17042	----
Stress path 5:	19.7	34.9	2.0	35.0	1671	----	16916	----
Stress path 6:	19.5	50.0	2.0	35.0	2459	----	17407	----
Stress path 7:	19.1	70.0	2.0	35.0	3565	----	19276	----
Stress path 8:	18.6	90.0	2.1	35.0	4735	----	24219	----
Stress path 9:	18.0	120.0	2.1	35.0	6537	----	39144	----
Stress path 10:	18.1	49.9	2.0	50.0	2653	----	39026	----
Stress path 11:	18.2	70.0	2.0	50.0	3731	----	39739	----
Stress path 12:	18.2	90.0	2.0	50.0	4822	----	41102	----
Stress path 13:	40.8	120.0	2.0	50.0	2900	----	47099	----
Stress path 14:	0.0	159.9	2.0	50.0	0	----	50000	----
Stress path 15:	0.0	70.0	2.1	70.0	0	----	50000	----
Stress path 16:	0.0	90.0	2.0	70.0	0	----	50000	----
Stress path 17:	0.0	120.0	2.0	70.0	0	----	50000	----
Stress path 18:	0.0	159.9	2.5	70.0	0	----	50000	----

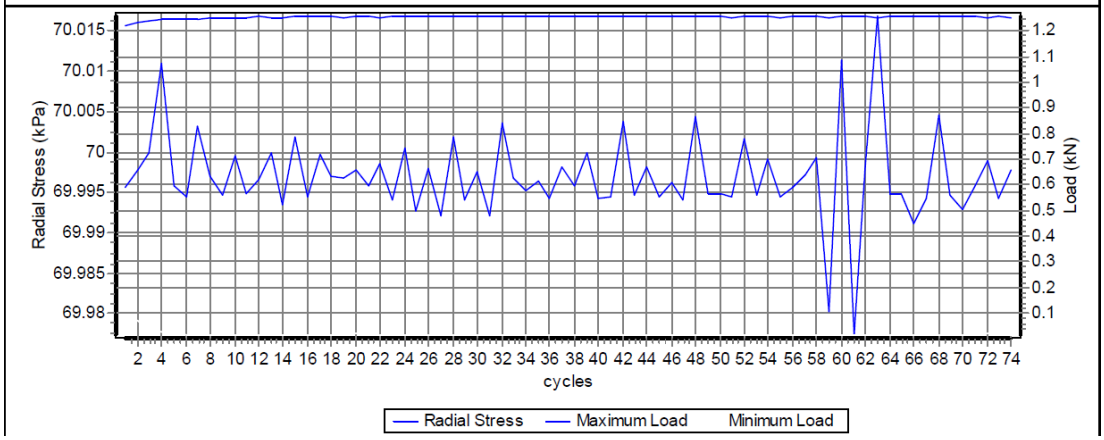

Test Data

Start Date and Time: Thursday, August 27, 2015, at 2:46 PM

	Resilient Modulus (MPa)	Maximum Deviator Stress (kPa)	Minimum Deviator Stress (kPa)	Confining Stress (kPa)	Resilient Axial Strain (με)	Resilient Radial Strain (με)	Permanent Axial Strain (με)	Permanent Radial Strain (με)
Conditioning Cycles 1 to 10:	38.2	19.6	1.9	20.0	467	----	1026	----
Stress path 1:	27.8	20.0	2.1	20.0	644	----	2208	----
Stress path 2:	21.6	34.9	2.1	20.0	1525	----	6391	----
Stress path 3:	20.1	49.9	2.0	20.0	2381	----	10485	----
Stress path 4:	18.8	69.9	2.1	20.0	3609	----	17042	----
Stress path 5:	19.7	34.9	2.0	35.0	1671	----	16916	----
Stress path 6:	19.5	50.0	2.0	35.0	2459	----	17407	----
Stress path 7:	19.1	70.0	2.0	35.0	3565	----	19276	----
Stress path 8:	18.6	90.0	2.1	35.0	4735	----	24219	----
Stress path 9:	18.0	120.0	2.1	35.0	6537	----	39144	----
Stress path 10:	18.1	49.9	2.0	50.0	2653	----	39026	----
Stress path 11:	18.2	70.0	2.0	50.0	3731	----	39739	----
Stress path 12:	18.2	90.0	2.0	50.0	4822	----	41102	----
Stress path 13:	40.8	120.0	2.0	50.0	2900	----	47099	----
Stress path 14:	0.0	159.9	2.0	50.0	0	----	50000	----
Stress path 15:	0.0	70.0	2.1	70.0	0	----	50000	----
Stress path 16:	0.0	90.0	2.0	70.0	0	----	50000	----
Stress path 17:	0.0	120.0	2.0	70.0	0	----	50000	----
Stress path 18:	0.0	159.9	2.5	70.0	0	----	50000	----

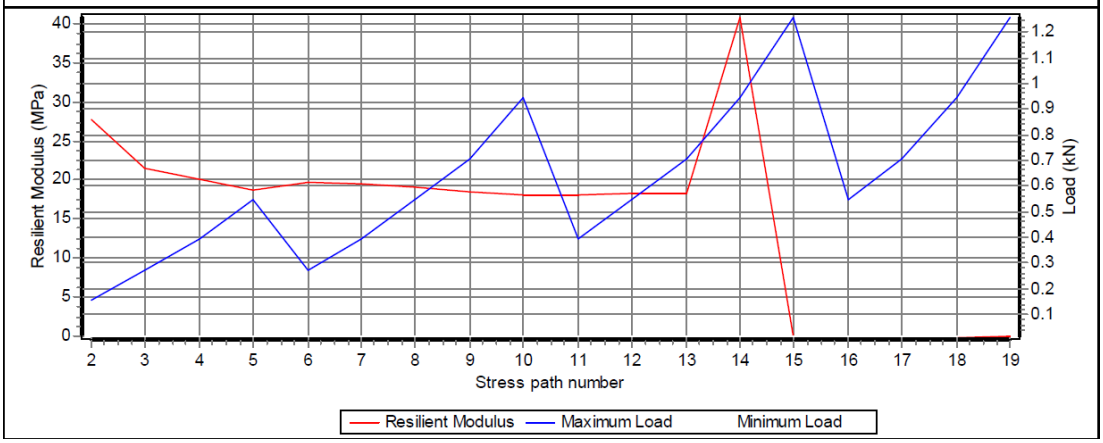

Test Parameters

Loading method: Constant confining pressure
Stress level: EN 13286-7 Low stress level

	Confining (kPa)	Deviator (kPa)
Conditioning:	70.0	200.0
Stress path 1:	20.0	20.0
	20.0	
	20.0	
	20.0	
	35.0	
	35.0	
	35.0	
	35.0	
	35.0	
	50.0	
	50.0	
	50.0	
	50.0	
	50.0	
	70.0	
	70.0	
	70.0	
	70.0	
	70.0	
	100.0	
	100.0	
	100.0	
	100.0	
	100.0	

Test Procedure: Study of the resilient behaviour
Project: B+10000 cyclec (2)
Operator: Mustafa
Comments: B+10000 cyclec (2)

Test Data

Start Date and Time: Monday, November 30, 2015, at 3:33 PM

	Resilient Modulus (MPa)	Maximum Deviator Stress (kPa)	Minimum Deviator Stress (kPa)	Confining Stress (kPa)	Resilient Axial Strain (µ€)	Resilient Radial Strain (µ€)	Permanent Axial Strain (µ€)	Permanent Radial Strain (µ€)
Conditioning Cycles 1 to 10:	20.4	18.9	2.4	20.0	819	----	728	----
Stress path 1:	23.7	19.9	2.0	20.0	753	----	4225	----
Stress path 2:	24.5	35.0	2.1	20.0	1346	----	8175	----
Stress path 3:	28.9	50.0	2.1	20.0	1656	----	11271	----
Stress path 4:	27.6	70.0	2.0	20.0	2466	----	14766	----
Stress path 5:	37.0	35.0	2.0	35.0	890	----	14447	----
Stress path 6:	41.1	50.0	2.1	35.0	1166	----	14767	----
Stress path 7:	30.7	70.0	2.0	35.0	2216	----	15116	----
Stress path 8:	28.7	89.8	2.3	35.0	3054	----	16882	----
Stress path 9:	75.5	119.7	2.2	35.0	1557	----	23443	----
Stress path 10:	33.7	50.0	2.1	50.0	1420	----	22978	----
Stress path 11:	35.1	69.9	2.0	50.0	1936	----	23064	----
Stress path 12:	41.0	89.7	2.5	50.0	2129	----	22871	----
Stress path 13:	397.1	119.6	2.0	50.0	304	----	24696	----
Stress path 14:	0.0	160.0	2.1	50.0	0	----	25000	----
Stress path 15:	0.0	70.1	2.0	70.0	0	----	25000	----
Stress path 16:	0.0	89.9	2.2	70.0	0	----	25000	----
Stress path 17:	0.0	119.9	2.1	70.0	0	----	25000	----
Stress path 18:	0.0	159.9	2.0	70.0	0	----	25000	----
Stress path 19:	0.0	199.9	2.7	70.0	0	----	25000	----

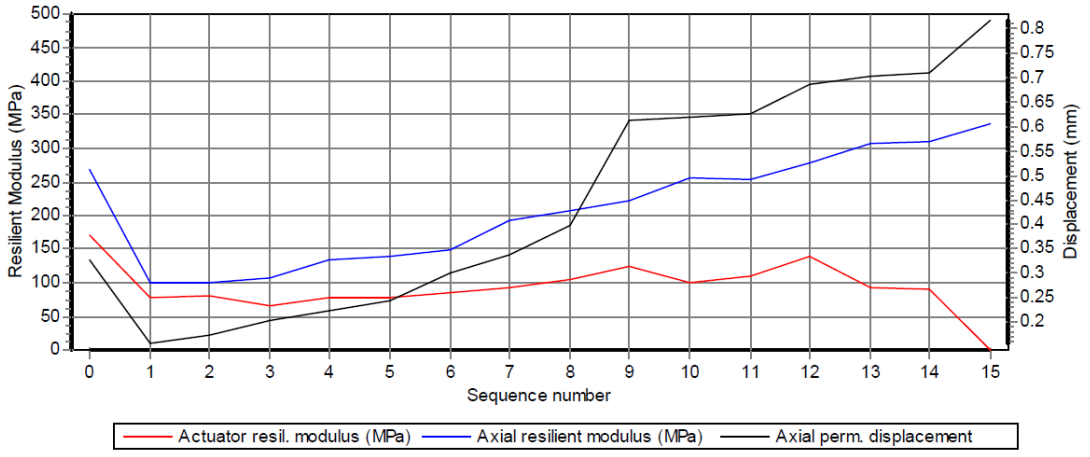

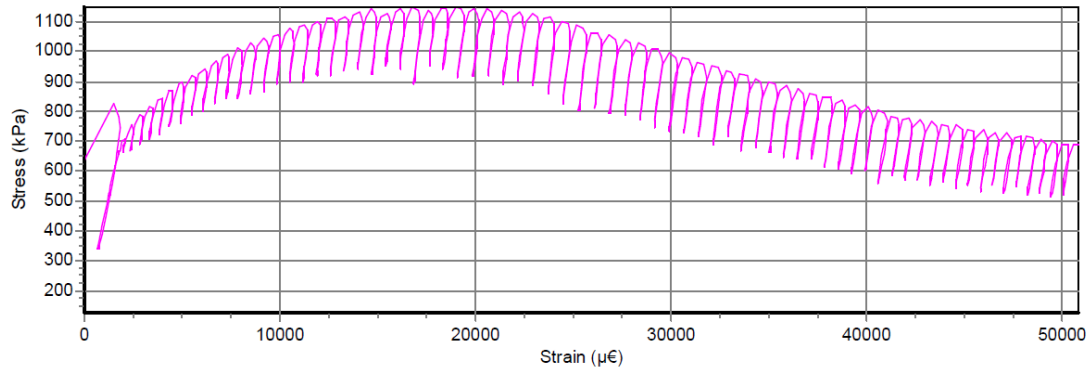

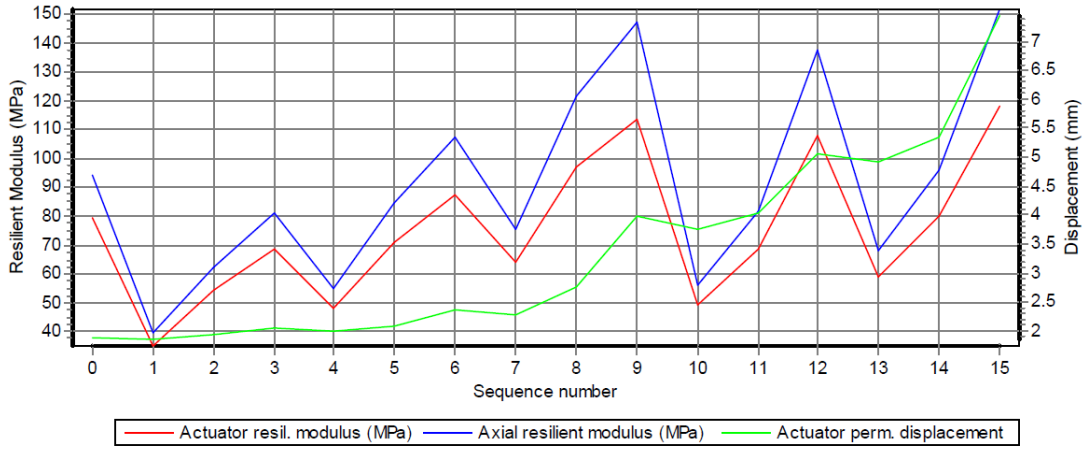
Resilient Modulus (MPa)
Displacement (mm)
Sequence number
Actuator resil. modulus (MPa)
Axial resilient modulus (MPa)
Actuator perm. displacement

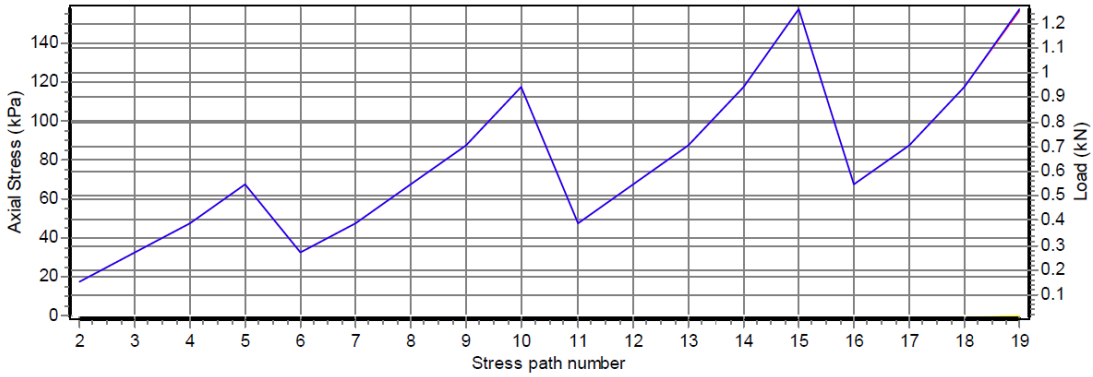
Axial Stress (kPa)
Load (kN)
Stress path number

Co-author attribution approval statement

School of Civil and Mechanical Engineering
Level 4, Building 204
GPO Box U1987

Hereby, I, Professor Hamid Nikraz, confirm that the following is my joint publication with Mustafa al-saedi. I, as a co-author, endorse that the level of all authors' contribution is accurately and appropriately addressed in the following table. I also consent this paper to be used in the thesis "Characterisation of Road Base Course Materials: The Effects of Waste Material Inclusion and Layering", submitted for the Degree of PhD in Civil Engineering of Curtin University.

Paper: Al-Saedi, M., Chegenizadeh, A., & Nikraz, H. (2018). Dynamic properties of crushed glass and tyre rubber in unbound pavement applications. *Australian Geomechanics Journal*, 53(4), 119-133.

Author's affiliation (in order of appearance in published version of paper):

1- Mustafa Al-saedi, Faculty of Science and Engineering, School of Civil and Mechanical Engineering, Curtin University, Perth, Australia.

2-Amin Chegenizadeh, Faculty of Science and Engineering, School of Civil and Mechanical Engineering, Curtin University, Perth, Australia.

3- Hamid Nikraz, Faculty of Science and Engineering, School of Civil and Mechanical Engineering, Curtin University, Perth, Australia.

		Conception and Design	Acquisition of method	Data manipulation	Interpretation & discussion	Paper drafting	Paper revising	Final approval
Authors	Mustafa Al-saedi	X	X	X	X	X	X	X
	Amin Chegenizadeh			X	X	X	X	X
	Hamid Nikraz			X	X	X	X	X
		I acknowledge that these represent my contribution to the above research output. Signed Date 30/08/2019						

School of Civil and Mechanical Engineering
Level 4, Building 204
GPO Box U1987

Hereby, I, Professor Hamid Nikraz, confirm that the following is my joint publication with Mustafa al-saedi. I, as a co-author, endorse that the level of all authors' contribution is accurately and appropriately addressed in the following table. I also consent this paper to be used in the thesis "Characterisation of Road Base Course Materials: The Effects of Waste Material Inclusion and Layering", submitted for the Degree of PhD in Civil Engineering of Curtin University.

Paper: Al-saedi, M., Chegenizadeh, A., & Nikraz, H. (2017). A Study on the Layered Structure of Bentonite, Crushed Rock and Sand under Repeated Triaxial Loading. *The Electronic Journal of Geotechnical Engineering*, *22*(4).

Author's affiliation (in order of appearance in published version of paper):

1- Mustafa Al-saedi, Faculty of Science and Engineering, School of Civil and Mechanical Engineering, Curtin University, Perth, Australia.

2-Amin Chegenizadeh, Faculty of Science and Engineering, School of Civil and Mechanical Engineering, Curtin University, Perth, Australia.

3- Hamid Nikraz, Faculty of Science and Engineering, School of Civil and Mechanical Engineering, Curtin University, Perth, Australia.

		Conception and Design	Acquisition of method	Data manipulation	Interpretation & discussion	Paper drafting	Paper revising	Final approval
Authors	Mustafa Al-saedi	X	X	X	X	X	X	X
	Amin Chegenizadeh			X	X	X	X	X
	Hamid Nikraz			X	X	X	X	X
		I acknowledge that these represent my contribution to the above research output. Signed … Date 30/08/2019						

Curtin University

School of Civil and Mechanical Engineering
Level 4, Building 204
GPO Box U1987

Hereby, I, Professor Hamid Nikraz, confirm that the following is my joint publication with Mustafa al-saedi. I, as a co-author, endorse that the level of all authors' contribution is accurately and appropriately addressed in the following table. I also consent this paper to be used in the thesis "Characterisation of Road Base Course Materials: The Effects of Waste Material Inclusion and Layering", submitted for the Degree of PhD in Civil Engineering of Curtin University.

Paper: Chegenizadeh, A. & Al-saedi, M. A. (2016, August 9-11). *Study on the Layered Structure of Crushed Rock and Sand under Repeated Triaxial Loading*. Paper presented at the Conference Program. Hawaii, USA.

Author's affiliation (in order of appearance in published version of paper):

1- Amin Chegenizadeh, Faculty of Science and Engineering, School of Civil and Mechanical Engineering, Curtin University, Perth, Australia.

2- Mustafa Al-saedi, Faculty of Science and Engineering, School of Civil and Mechanical Engineering, Curtin University, Perth, Australia.

3- Hamid Nikraz, Faculty of Science and Engineering, School of Civil and Mechanical Engineering, Curtin University, Perth, Australia.

		Conception and Design	Acquisition of method	Data manipulation	Interpretation & discussion	Paper drafting	Paper revising	Final approval
Authors	Amin Chegenizadeh	X	X	X	X	X	X	X
	Mustafa Al-saedi	X	X	X	X	X		
	Hamid Nikraz			X	X	X	X	X
		I acknowledge that these represent my contribution to the above research output. Signed Date 30/08/2019						

Curtin University

School of Civil and Mechanical Engineering
Level 4, Building 204
GPO Box U1987

Hereby, I, Professor Hamid Nikraz, confirm that the following is my joint publication with Mustafa al-saedi. I, as a co-author, endorse that the level of all authors' contribution is accurately and appropriately addressed in the following table. I also consent this paper to be used in the thesis "Characterisation of Road Base Course Materials: The Effects of Waste Material Inclusion and Layering", submitted for the Degree of PhD in Civil Engineering of Curtin University.

Paper: Al-Saedi, M., Chegenizadeh, A., & Nikraz, H. (2018, September 27 - 28). *Resilient Modulus and Deformation Responses of Waste Glass in Flexible Pavement System.* Paper presented at the 20th International Conference on Soil-Structure Interaction and Dynamics. London, United Kingdom.

Author's affiliation (in order of appearance in published version of paper):

1- Mustafa Al-saedi, Faculty of Science and Engineering, School of Civil and Mechanical Engineering, Curtin University, Perth, Australia.

2-Amin Chegenizadeh, Faculty of Science and Engineering, School of Civil and Mechanical Engineering, Curtin University, Perth, Australia.

3- Hamid Nikraz, Faculty of Science and Engineering, School of Civil and Mechanical Engineering, Curtin University, Perth, Australia.

Curtin University

School of Civil and Mechanical Engineering
Level 4, Building 204
GPO Box U1987
Perth Western Australia

Co-author Attribution Approval Statement

Hereby, I, Dr Amin Chegenizadeh, confirm that the following is my joint publication with Mustafa al-saedi. I, as a co-author, endorse that the level of all authors' contribution is accurately and appropriately addressed in the following table. I also consent this paper to be used in the thesis "Characterisation of Road Base Course Materials: The Effects of Waste Material Inclusion and Layering", submitted for the Degree of PhD in Civil Engineering of Curtin University.

Paper: Al-saedi, M., Chegenizadeh, A., & Nikraz, H. (2017). A Study on the Layered Structure of Bentonite, Crushed Rock and Sand under Repeated Triaxial Loading. *The Electronic Journal of Geotechnical Engineering*, *22*(4).

Author's affiliation (in order of appearance in published version of paper):

1- Mustafa Al-saedi, Faculty of Science and Engineering, School of Civil and Mechanical Engineering, Curtin University, Perth, Australia.

2-Amin Chegenizadeh, Faculty of Science and Engineering, School of Civil and Mechanical Engineering, Curtin University, Perth, Australia.

3- Hamid Nikraz, Faculty of Science and Engineering, School of Civil and Mechanical Engineering, Curtin University, Perth, Australia.

		Conception and Design	Acquisition of method	Data manipulation	Interpretation & discussion	Paper drafting	Paper revising	Final approval
Authors	Mustafa Al-saedi	X	X	X	X	X	X	X
	Amin Chegenizadeh	X		X	X	X	X	X
		I acknowledge that these represent my contribution to the above research output. Signed ..... Date 26/09/2019						
	Hamid Nikraz			X	X	X	X	X

Curtin University

School of Civil and Mechanical Engineering
Level 4, Building 204
GPO Box U1987
Perth Western Australia

Co-author Attribution Approval Statement

Hereby, I, Dr Amin Chegenizadeh, confirm that the following is my joint publication with Mustafa al-saedi. I, as a co-author, endorse that the level of all authors' contribution is accurately and appropriately addressed in the following table. I also consent this paper to be used in the thesis "Characterisation of Road Base Course Materials: The Effects of Waste Material Inclusion and Layering", submitted for the Degree of PhD in Civil Engineering of Curtin University.

Paper: Al-Saedi, M., Chegenizadeh, A., & Nikraz, H. (2018). Dynamic properties of crushed glass and tyre rubber in unbound pavement applications. *Australian Geomechanics Journal*, 53(4), 119-133.

Author's affiliation (in order of appearance in published version of paper):

1- Mustafa Al-saedi, Faculty of Science and Engineering, School of Civil and Mechanical Engineering, Curtin University, Perth, Australia.

2-Amin Chegenizadeh, Faculty of Science and Engineering, School of Civil and Mechanical Engineering, Curtin University, Perth, Australia.

3- Hamid Nikraz, Faculty of Science and Engineering, School of Civil and Mechanical Engineering, Curtin University, Perth, Australia.

		Conception and Design	Acquisition of method	Data manipulation	Interpretation & discussion	Paper drafting	Paper revising	Final approval
Authors	Mustafa Al-saedi	X	X	X	X	X	X	X
	Amin Chegenizadeh	X		X	X	X	X	X
		I acknowledge that these represent my contribution to the above research output. Signed Date 26/09/2019.						
	Hamid Nikraz			X	X	X	X	X

Curtin University

School of Civil and Mechanical Engineering
Level 4, Building 204
GPO Box U1987
Perth Western Australia

Co-author Attribution Approval Statement

Hereby, I, Dr Amin Chegenizadeh, confirm that the following is my joint publication with Mustafa al-saedi. I, as a co-author, endorse that the level of all authors' contribution is accurately and appropriately addressed in the following table. I also consent this paper to be used in the thesis "Characterisation of Road Base Course Materials: The Effects of Waste Material Inclusion and Layering", submitted for the Degree of PhD in Civil Engineering of Curtin University.

Paper: Al-Saedi, M., Chegenizadeh, A., & Nikraz, H. (2018, September 27 - 28). *Resilient Modulus and Deformation Responses of Waste Glass in Flexible Pavement System.* Paper presented at the 20th International Conference on Soil-Structure Interaction and Dynamics. London, United Kingdom.

Author's affiliation (in order of appearance in published version of paper):

1- Mustafa Al-saedi, Faculty of Science and Engineering, School of Civil and Mechanical Engineering, Curtin University, Perth, Australia.

2-Amin Chegenizadeh, Faculty of Science and Engineering, School of Civil and Mechanical Engineering, Curtin University, Perth, Australia.

3-Hamid Nikraz, Faculty of Science and Engineering, School of Civil and Mechanical Engineering, Curtin University, Perth, Australia.

		Conception and Design	Acquisition of method	Data manipulation	Interpretation & discussion	Paper drafting	Paper revising	Final approval
Authors	Mustafa Al-saedi	X	X	X	X	X	X	X
	Amin Chegenizadeh	X		X	X	X	X	X
		I acknowledge that these represent my contribution to the above research output. Signed ..... Date .....26/09/2019..						
	Hamid Nikraz			X	X	X	X	X